Diel and seasonal vertical migrations of high-latitude zooplankton: knowledge gaps and a high-resolution bridge

Kanchana Bandara

A thesis for the degree of Philosophiae Doctor (PhD)

PhD in Aquatic Biosciences (2017)

Faculty of Biosciences and Aquaculture, Nord University, Norway

dedicated to millions of zooplankton who sacrificed their lives for the advancement of science during the Billefjorden field campaign (2008-2009), the data of which fuels an integral part of this dissertation

Preface

This dissertation is submitted in partial fulfilment of the requirements for the degree of Philosophiae Doctor (PhD) at the Faculty of Biosciences and Aquaculture (FBA), Nord University, Bodø, Norway. The presented original research was carried out from 01.01.2015 to 29.12.2017, as a collaboration between the Nord University and the University Center in Svalbard, Norway. The PhD project (no. 6165) was funded by VISTA, a basic research program in collaboration between The Norwegian Academy of Science and Letters, and Statoil™.

The project team consisted of the following members:

Kanchana Bandara, MSc, Faculty of Biosciences and Aquaculture, Nord University & Department of Arctic Biology, University Center in Svalbard: PhD candidate

Ketil Eiane, Professor, Faculty of Biosciences and Aquaculture, Nord University: main supervisor

Øystein Varpe, Professor, Department of Arctic Biology, University Center in Svalbard & Senior researcher, Akvaplan-niva, Tromsø, Norway: co-supervisor

Rubao Ji, PhD, Associate Scientist, Biology Department, Woods Hole Oceanographic Institution, Woods Hole, MA, USA: co-supervisor

Kanchana Bandara

Bodø, December 29, 2017

Acknowledgements

The foremost appreciation should go to my main supervisor, Prof. Ketil Eiane for the support he rendered throughout this PhD program. Under your wings, I developed a substantial amount of skill, especially in the departments of writing and professional scientific thinking. Above all, I thank you for allowing me the freedom to do research on my own way. This independence will be the fuel that drives the rest of my career.

Gratitude should also extend to Prof. Øystein Varpe, who was the one that asked me to apply for VISTA PhD program. Moreover, it is the papers you authored that motivated me to pursue the life history theory and associated matters. Contributions of Dr. Rubao Ji are also mentioned with appreciation.

VISTA coordinator Håkon Sandbakken and PhD coordinator Jeanett Stegen, thank you for the helping me to drive through institutional and funding-related matters: you two are the best coordinators that I have known so far. Further, the support provided by Tormod Henry Skålsvik during purchasing of computers is mentioned with great appreciation.

I thank my family for the support extended during these three long-years (the way they say it), especially for understanding why their son/husband doesn't make phone calls regularly sometimes. Last, but not the least, if it wasn't for you—my friends, these three years in Bodø would have been so boring and lonely. You created a home away from home for me, for which, I am forever grateful to you.

List of abbreviations

1D	-	One-dimensional
2D	-	Two-dimensional
ADCP	-	Acoustic Doppler Current Profiler
AZFP	-	Acoustic Zooplankton and Fish Profiler
CPU	-	Central Processing Unit
D	-	Key discovery about vertical migration
DVM	-	Diel vertical migration
ES	-	Echosounder
GA	-	Genetic Algorithm
HAS	-	Hypothesis about adaptive significance
HPC	-	Hypothesis about proximate control
LX	-	Laplace Crossover
MPTM	-	Makinen, Periaux and Toivanen mutation
R	-	Selected major review
RCGA	-	Real-Coded Genetic Algorithm
RAM	-	Random Access Memory
SVM	-	Seasonal vertical migration

List of figures

List of tables

List of papers

Paper I **Bandara K**, Varpe Ø, Søreide JE, Wallenschus J, Berge J, Eiane K (2016) Seasonal vertical strategies in a high-Arctic coastal zooplankton community. Marine Ecology Progress Series 555:49-64

Paper II **Bandara K**, Varpe Ø, Ji R, Eiane K (2018) A high-resolution modeling study on diel and seasonal vertical migrations of high-latitude copepods. Ecological Modelling 368C:357-376

Paper III **Bandara K**, Varpe Ø, Ji R, Eiane K Artificial evolution of behavioral and life history strategies of Arctic *Calanus* spp. in response to bottom-up and top-down selection pressures. Manuscript

Table of contents

continued…

continued…

Abstract

Vertical migration is a widespread behavior among zooplankton. Based on the periodicity, two types of vertical migrations are described for high-latitude marine zooplankton: the diel vertical migration (DVM, periodicity < 24 h) and seasonal vertical migration (SVM, periodicity ca. 1 year). Despite ca. 200 years of research, questions still remain about the influence of environmental variability on vertical migrations, and the integrative effect of DVM and SVM on life history strategies and fitness of high-latitude zooplankton. As a first step toward addressing these knowledge gaps, we used year-round zooplankton net data collected in a high-Arctic fjord to describe seasonal vertical distributions of the dominant herbivore and carnivore taxa in association with the environmental variability. Results suggested that SVM of most carnivorous zooplankton studied was likely reflecting a tracking of the seasonal pattern of depth distributions in their herbivore prey. However, SVM of herbivore zooplankton could not be explained by any of the environmental variables used, probably due to the mismatch between the coarser spatio-temporal resolution of the deployed nets and finer spatio-temporal scales at which their vertical migrations occur. To study vertical migrations of high-latitude zooplankton and their environmental relations in higher spatio-temporal resolution, we developed a new computationally efficient strategy-oriented modeling framework. This model could simulate DVM and SVM throughout the entire life cycle of herbivorous zooplankton. Testing of this model, by simulating a generalized herbivorous copepod suggested that DVM and SVM can have profound and largely different effects on fitness and phenology. Hence these migratory behaviors should be studied in concert. Further, by developing the above modeling framework to allow for more species-specific parameterization, we found that top-down selection pressures mediated by the environment (i.e. predation risk) can have an overwhelming influence on the vertical migratory and life history strategies of Arctic herbivorous copepods (i.e. *Calanus* spp.). Altogether, these findings suggest that studying vertical migrations in higher spatial, temporal and biological resolution may contribute toward bridging the gaps of our understanding of the subject matter.

1. Introduction

1.1 Migration

While the interactions between organisms and their environment forms the foundation of Ecology, the mechanisms by which these interactions occur are studied as animal behavior. One particular case of animal behavior clearly sets apart from the rest in such a way that it involves movement of animals typically from one habitat to another, and is termed migration (Aidley 1981).

In an ecological perspective, migration is a widespread behavior that involves persistent and active movement of individuals often caused by spatial and temporal variation in resources and risks (Cresswell et al. 2011). Animals can migrate varying distances in search of better feeding (e.g. L'Abée-Lund & Vøllestad 1987, Williamson et al. 1988, Levey & Stiles 1992), survival (e.g. Werner et al. 1983, Hebblewhite & Merrill 2007, McKinnon et al. 2010) and reproductive opportunities (e.g. Hardy & Raymond 1980, Smith & Moore 2005, van Ginneken & Maes 2005). For example, among birds, the annual migration of North American blue grouse (*Dendeagapus obscurus*) ranges up to ca. 800–3000 body lengths (0.3–1 km, Hoffmann 1956, Cade & Hoffman 1993), while the annual transpolar migration of the Arctic tern (*Sterna paradisaea*) can extend up to ca. 2.5 x 10^8 body lengths (ca. 80000 km, Egevang et al. 2010). Irrespective of the distance travelled, migratory individuals will possess enhanced fitness compared to residents, given that the benefits of the migration overwhelm the costs (Aidley 1981). As a result, migration is seen as an adaptive strategy that enhances fitness.

1.2 Zooplankton migration: the concept of vertical migration

Migration is a common phenomenon in the realm of zooplankton. However, about a century ago, it was believed that zooplankton can only passively drift with water currents, but don't have a pronounced means of migration. Despite this early belief, it is well known today that they can actively migrate in the water column. Zooplankton

migrations are manifested through individual swimming movements brought about by rhythmical beating of flagella and cilia (e.g. Keller & Rubinow 1976, Matsumoto 1991), antennae, maxillae and pleopods (e.g. Strickler 1977, Kils 1983), or using fins and other modified muscular structures (e.g. Satterlie et al. 1985, Jordan 1992).

On a timescale ranging from a few seconds to minutes, most zooplankton swimming trajectories span over a three-dimensional space and are often described using diffusive motility models (e.g. Bundy et al. 1993, Schmitt & Seuront 2001). On a broader timescale (> 12 h), zooplankton vertical movements tend to be more pronounced compared to those in the horizontal dimension, and can span from a few meters in shallow freshwater bodies (Cerbin et al. 2003) to several kilometers in the open ocean (van Haren & Compton 2013). These vertical migrations are common among a wide range of zooplankton taxa, and probably represent the largest animal migration on earth in terms of biomass (Hays 2003, Williamson et al. 2011).

Vertical migrations are viewed as a type of commuting between shallow foraging habitats and a deep-water refugia (Dingle & Drake 2007). Depending on the frequency of commuting (periodicity), vertical migrations can be broadly categorized into diel and seasonal components. The shorter-term diel vertical migration (DVM) refers to a daily commuting of zooplankton between the foraging and refugial habitats, where the longer-term seasonal vertical migration (SVM) refers to an annual commuting. Despite the generality of this view, it has been used as the foundation of numerous theoretical studies on zooplankton vertical migrations.

1.3 Diel vertical migration of zooplankton

1.3.1 Brief history and present understanding

Historical observations of DVM dates ca. two centuries back to the records of Georges Cuvier (Cuvier 1817). These early observations were centered on the daily appearance and disappearance of microscopic crustaceans (the term plankton was not defined by

then) from the upper water layers of freshwater lakes. However, phenomenon of a vertical migration remained doubted until late 1800s, where Fuchs (1882) used depth-stratified net samples and described the differential day and night vertical distributions of numerous lifeforms including crustaceans. Fuchs's pioneering work echoed in numerous subsequent DVM studies on a wide range of taxonomic groups in both freshwater and marine realms. Consequently, by early 1900s, the term diel vertical migration was firmly established in the literature (see Russell 1927), and is currently understood as a geographically and taxonomically widespread behavior of zooplankton.

At present, two patterns of DVM are well known: the nocturnal DVM and the reverse DVM (reviewed in Bayly 1986). The nocturnal DVM, first documented by Cuvier (1817), is the most common diel vertical migratory behavior among zooplankton. It is characterized by an ascent from depths in the dusk and occupation of shallower waters during the night time, and a descent in the dawn and occupation of depths during the daytime (Fig. 1B). Early observations of what is now known as the reverse DVM dates back to Brook (1886), but the term was coined and brought into prominence following the work of Ohman et al. (1983). As the name implies, reverse DVM is the opposite of classic DVM, where zooplankton tend to occupy shallower waters during the daytime and deeper waters during the night (Fig. 1C).

1.3.2 Hypotheses about proximate control

Up to the mid-1900s, most DVM research was centered on describing its proximate control (how migration occurs, Fig. 2). Most such hypotheses on the proximate control of classic DVM were inspired by the observation that diel variability of zooplankton vertical behavior appear to correlate with those of irradiance and temperature (Russell 1927). It was thus suggested that zooplankton remain at depths during the daytime and migrate to near-surface waters during the night to avoid intense levels of irradiance or temperature (e.g. Cuvier 1817, Parker 1902, Michael 1911, Clarke 1934). The influence of irradiance on the proximate control of DVM was subjected to extensive field and laboratory testing especially during the first half of the 20th century (reviewed in Russell

1927, Cushing 1951). Consequently, by mid 1920s the relative change of irradiance during the diel cycle was considered as the main cue for zooplankton DVM (Rose 1925).

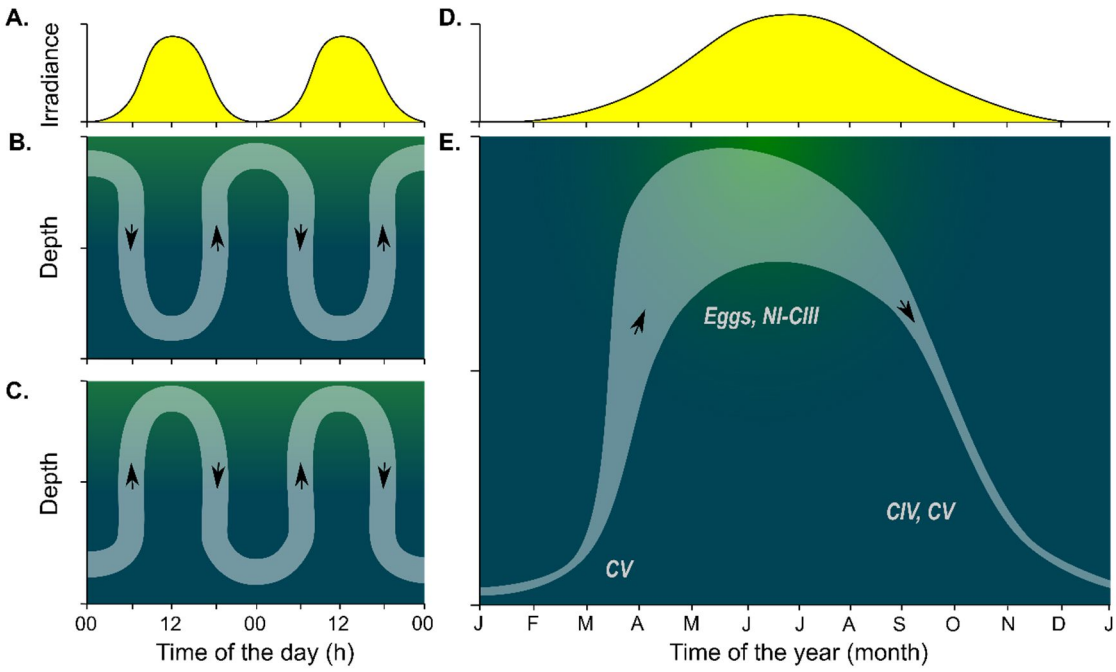

Fig. 1 Simplified conceptual models for DVM (A–C) and SVM (D, E). In nocturnal DVM, zooplankton tend to occupy shallower waters during the night and descends to depth during the daytime (B). The opposite happens in reverse DVM (C). Opaque white line represents the vertical trajectory of the population, and its thickness indicate the relative population size. Arrowheads point to the general direction of the vertical trajectory. Green color indicates productive vertical regions of the water column. Abscissae not to scale.

One main weakness of the irradiance intensity hypothesis is its inability to explain the reverse DVM. Although reverse DVM was iteratively reported following Brook (1886) (e.g. Herdman 1907, Tattersall 1911), these field observations did not receive a prominent attention and were sometimes criticized as sampling artifacts. Hypotheses-

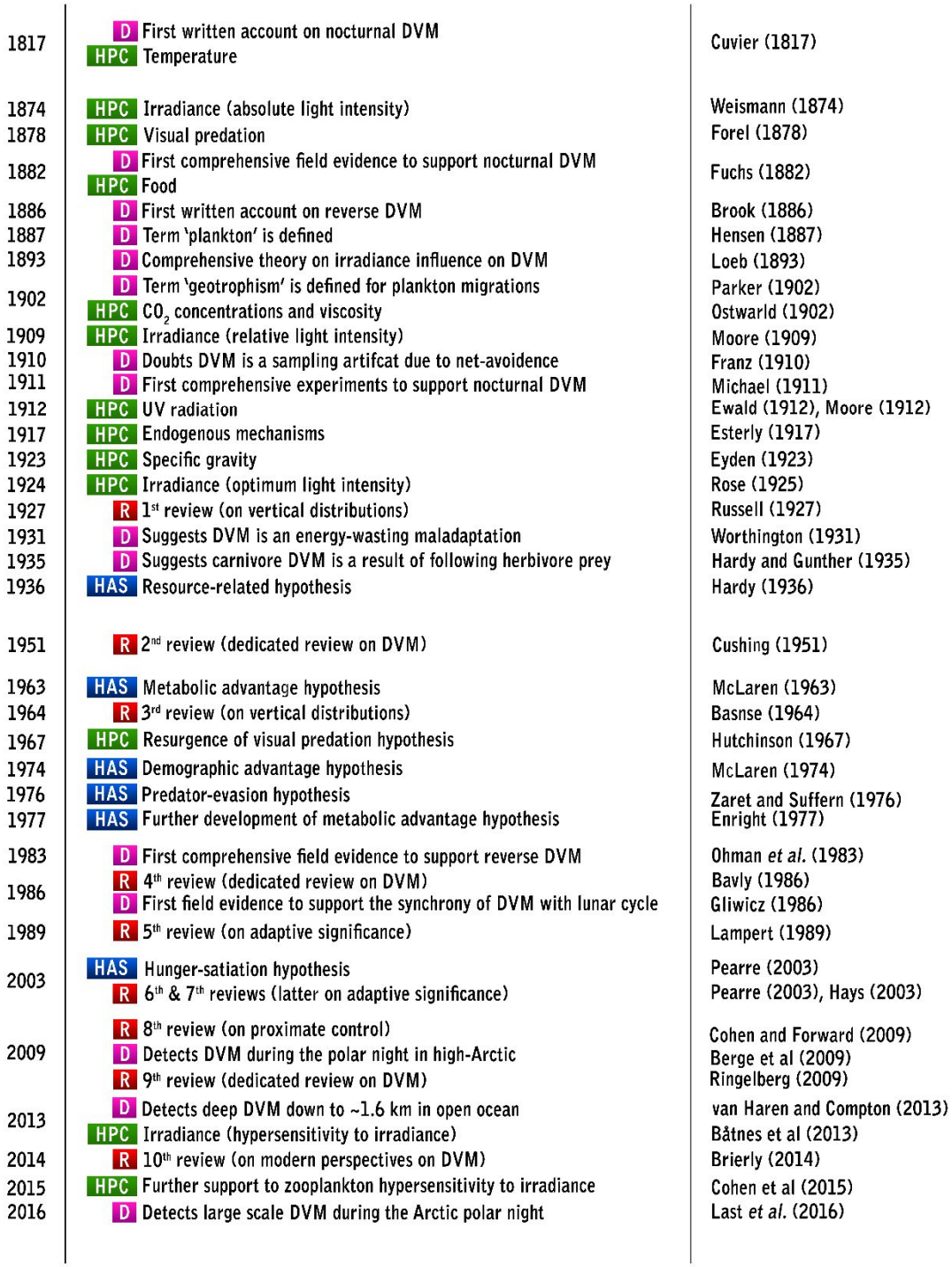

Fig. 2 Key discoveries (D) related to DVM of zooplankton that led to or has the potential of leading to hypotheses about proximate control (HPC) and hypotheses about adaptive significance (HAS), along with some selected major reviews (R). The list includes literature related to both freshwater and marine environments.

-that could provide a plausible explanation to both variants of DVM remained buried in the literature, perhaps overshadowed by extensive focus on irradiance intensity hypothesis. These include the early thoughts of Forel (1878) that avoidance of sun-lit waters by many pelagic crustaceans is due to the presence of pelagic fish, and Fuchs (1882) that DVM could be a feeding migration. These food- and predator-related control mechanisms of DVM did not receive a prominent scientific attention until the latter half of the 20th century (see below, and also Hutchinson 1967).

In the early 1900s, it was argued if DVM of zooplankton is behavior that minimizes exposure to harmful UV radiation (e.g. Ewald 1912, Moore 1912). However, this perspective was quickly criticized based on the observations on deep-water DVM (where ascent migration doesn't extend up to the surface) and reverse DVM. Few years later, Esterly (1917) observed persistent DVM behavior in copepods kept under continuous darkness, and hypothesized that DVM is regulated by an endogenous mechanism. However, even to date, evidence supporting this view remains elusive. Apart from these, salinity and density (e.g. Esterly 1919, Eyden 1923), and dissolved gases (e.g. Ostwald 1902) have also been viewed as proximate cues for DVM, but with little supporting evidence.

1.3.3 Hypotheses about adaptive significance

From mid-1960s, the focus on DVM research began to shift towards explaining its adaptive significance (also termed as ultimate causes, i.e. why migration occurs, Fig. 2). Pioneering work was done by Ian A. McLaren following his theoretical modeling work (McLaren 1963), possibly inspired by the earlier insights of George Evelyn Hutchinson (Hutchinson 1959). The field investigations, laboratory experiments, and modeling work conducted thenceforth have led to four well-established hypotheses regarding the adaptive significance of DVM (Table 1).

Table 1 Main hypotheses about the adaptive significance of DVM. Several additional hypotheses are reviewed in Lampert (1989) and Pearre (2003), but are not mentioned here due to its relatively less significance

Hypothesis	General description	Pioneering work
Metabolic advantage	Feeding in warm, food-rich surface waters at night and spending rest of the day in colder deeper waters possesses an energetic advantage.	McLaren (1963) Enright (1977)
Demographic advantage	Alike above, but posits that spending part of the day in colder deeper waters elevates the size at sexual maturity and ends up producing more offspring.	McLaren (1974)
Predator avoidance	Classic DVM: Zooplankton feed in food-rich surface waters during nighttime when visually orientating predators are least effective, and take refuge in deeper darker waters during the daytime.	Zaret and Suffern (1976)
	Reverse DVM: The above behavior is reversed in the case of non-visual (tactile) predators	Ohman et al. (1983)
Hunger/satiation	The daily ascent and descent migrations are driven by the nutritional state of the zooplankter. Where, hunger drives ascent migration and satiation causes descent (active downward swimming or passive sinking).	Pearre (2003)

Among hypotheses of adaptive significance, the predator avoidance hypothesis seems to be the most widely received: first, given the broad range of empirical evidence supporting it, and second, its ability to explain both the classic and the reverse variants of DVM (Bayly 1986, Lampert 1989, Hays 2003). Therefore, in a broader perspective, the diel vertical migration is generally seen as a strategy that trades off growth potential to

survival, by minimizing the time spent near food-rich surface waters during the time of the day that is most susceptible to visual (Loose & Dawidowicz 1994) or tactile predators (Ohman et al. 1983, Ohman 1990).

1.4 Seasonal vertical migration of zooplankton

1.4.1 Brief history and present understanding

In late 1800s, the seasonal appearance and disappearance of pelagic animals puzzled the marine scientists working in northerly latitudes (e.g. Schmidtlein 1879). Following the methods of Fuchs (1882), Chun (1888) used depth-stratified net samples and showed that the summertime disappearance of jellyfish and crustaceans from surface waters was due to their migration to depths exceeding 1000 m in the Mediterranean Sea. Although not geographically or taxonomically widespread, this behavior is common to many high-latitude zooplankton, and termed seasonal vertical migration (SVM).

SVM is generally characterized by a descent to deeper waters during summer and autumn, and ascent to near-surface waters by the spring of the following year (Fig. 1E). This pattern is common among most high-latitude herbivore zooplankton (reviewed in Conover 1988, Falk-Petersen et al. 2009, Varpe 2012), and carnivores that seasonally follow their herbivore prey (Hagen 1999). However, among omnivores, SVM may either be absent (Lischka & Hagen 2005) or sometimes reversed (Bandara 2014). In most cases, as the seasonal vertical distribution changes with the developmental stage (Fig. 1E) this is also termed as the ontogenetic vertical migration (Russell 1927, Banse 1964, Conover 1988, Falk-Petersen et al. 2009).

1.4.2 Hypotheses about proximate control

Hypotheses about proximate cues of SVM emerged since the time of its first introduction by Chun (1888), who suggested that warming of the surface waters in the

summer seasonally drives the pelagic species to deeper waters (Fig. 3). Birge (1904) considered both temperature and irradiance, and suggested the latter as a strong cue for the SVM of freshwater zooplankton and former is just a condition. In the marine realm however, the influence of irradiance on the SVM remained questionable, as the depth of the migration tend to extend well below the photic zone. However, by the end of the second decade of the 20th century, it was evident that irradiance could penetrate ocean depths greater than it was previously thought (Klugh 1925, Poole 1925, Atkins 1926, Poole & Atkins 1926). This likely have motivated the bloom of literature supporting the hypothesis regarding irradiance as a proximate cue for the SVM of marine herbivorous copepods (e.g. Bigelow 1926, Russell 1926, Nicholls 1933, Sømme 1934, Ussing 1938).

Alternative hypotheses on the proximate control of SVM began to surface by mid-1900s (Fig. 3). Based on the deep SVM depths (> 1000 m) of copepods in the Norwegian Sea, Østvedt (1955) doubted if neither irradiance nor temperature could act as proximate cues. Instead, he was the first to suggest endogenous regulation (i.e. endocrinal changes related with gonadal development) as a proximate cue for SVM. Despite the detailed studies conducted in the mid-20th century on endocrinal regulation of SVM (e.g. Carlisle & Pitman 1961, Harris 1963), conclusive evidence still remains elusive. A different endogenous regulation mechanism was suggested in In late 20th century, where it was hypothesized that the timing of SVM is regulated by an internal timer or a biological clock (Grigg & Bardwell 1982, Miller et al. 1991, Hirche 1996a). However, existence of such an endogenous timer is yet to be proven. Following a different line of reasoning, Kaartvedt (1996) suggested that the-timing and the depth dynamics of SVM may be regulated by the mortality risk imposed by planktivorous fish.

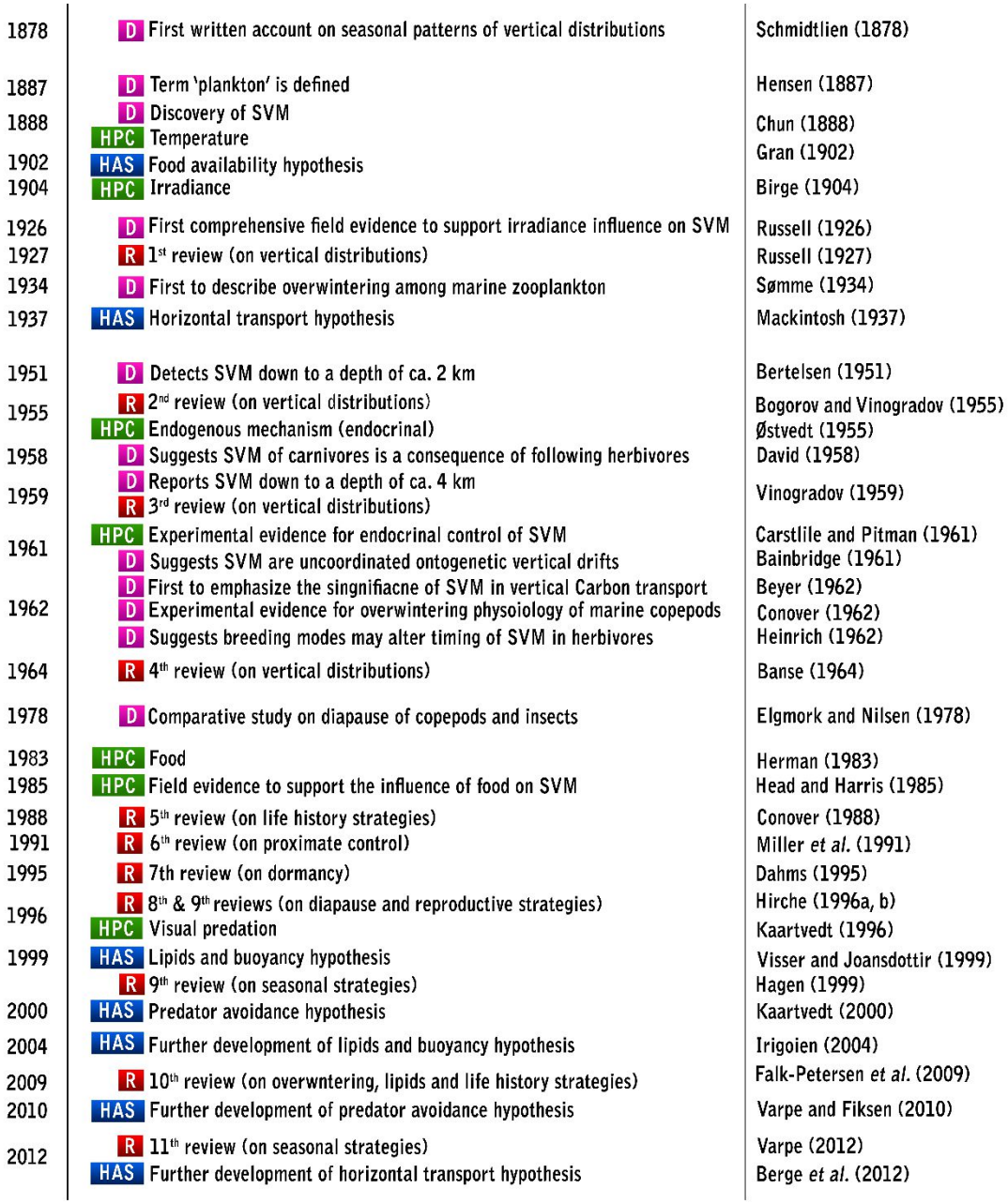

Fig. 3 Key discoveries (D) related to SVM of zooplankton that led to or has the potential of leading to hypotheses about proximate control (HPC) and hypotheses about adaptive significance (HAS), along with some selected major reviews (R).

Table 2 Main hypotheses that explain the adaptive significance of SVM.

Hypothesis	General description	Pioneering work
Food availability	SVM reflects adaptation to the seasonal changes of food availability, i.e. descent to depths for overwintering during the unproductive season and ascent to shallow productive waters at the onset of the productive season.	Gran (1902) Sømme (1934)
Predator avoidance	Generation length and hence the timing of the SVM is tuned to avoid seasonal peaks of visual predation risk, and depth of the SVM is determined by those with least visual predation risk.	Kaartvedt (1996) Kaartvedt (2000)
Lipids and buoyancy	Seasonal lipid stores play a central role in SVM by influencing the timing of the seasonal migration and the overwintering depth. This is controlled by the density of the stored lipids and the buoyancy effect it produces. The size of the lipid store is (locally) adapted to sink to a depth below the convective mixed layer during overwintering.	Visser and Jonasdottir (1999) Irigoien (2004)
Horizontal transport	Timing and depth of SVM allows zooplankton to be transported by water currents to regions with better feeding opportunities.	Mackintosh (1937)

1.4.3 Hypotheses about adaptive significance

Several key alternative views on adaptive significance of SVM are listed in Table 2. The food availability hypothesis seems to be more general and explains the seasonal migration patterns of zooplankton with different feeding strategies. Pioneering work was done by Gran (1902), who suggested that high-latitude herbivorous zooplankton descends to great depths to overwinter during the unproductive part of the year, and

ascend back to shallow waters as the primary production starts. However, Heinrich (1962) suggested that the timing of SVM in herbivorous zooplankton may be altered by different reproductive strategies (i.e. what is now known as capital and income breeding). David (1958) noted that the SVM of carnivorous zooplankton is a consequence of following their seasonally migrating herbivore-prey. SVM of omnivorous zooplankton seems to less pronounced, and usually related to the year-round abundance of food (e.g. Richter 1995, Falkenhaug et al. 1997, Lischka & Hagen 2005, Darnis & Fortier 2014). Compared to the food availability hypothesis, the rest are less well supported by literature. However, despite the generality of the food availability hypothesis, it is not clear if it is widely accepted among planktologists.

1.5 Knowledge gaps

Despite ca. 200 years of research, there are still gaps in our understanding about the causes and consequences of zooplankton vertical migrations. This knowledge gap appears to be wider regarding SVM compared to DVM. First, the proximate cues of SVM are poorly understood, mainly because there is often a spatial (i.e. vertical) mismatch between the depths of SVM and that at which the seasonal dynamics of physical environmental variables usually occur (Østvedt 1955). For example, it is commonly questioned that how a zooplankter overwintering several hundred meters would perceive spring–summer increase of irradiance or temperatures which are restricted to the shallow waters (Banse 1964). Alternative hypotheses, such as endogenous mechanisms, lipid level changes and predation risk appear to theoretically address these problems (Fig. 3), but are not satisfactorily supported by empirical evidence. Second, unlike DVM, there is no widely accepted hypothesis about the adaptive significance of SVM. This is because the timing and amplitude (the vertical extent) of SVM shows a profound variability between geographic locations (e.g. Russell 1927, Sømme 1934, Wiborg 1954, Daase et al. 2013, Melle et al. 2014), between different years within the same location (e.g. Kosobokova 1999, Pertsova & Kosobokova 2003), between species (e.g. Hirche 1991, Unstad & Tande 1991, Madsen et al. 2001, Lischka & Hagen 2005,

Hirche & Kosobokova 2011) and between individuals of the same species (Pearre 1979, Pedersen et al. 1995). However, none of the proposed hypotheses (Table 2) are capable providing a plausible explanation to this variability.

Despite extensive theoretical advancements on DVM, recent observations on high-amplitude DVM (van Haren & Compton 2013) and mid-winter DVM under the darkness of Arctic polar night (Berge et al. 2009, Hobbs 2016, Last et al. 2016) have challenged the current understanding of its proximate control. As with SVM, the question raised here is: how is it possible that animals residing at depths where irradiance-levels are extremely low, or in periods of the year with no sunlight use it as a proximate cue to perform DVM? A satisfactory explanation was provided to this problem in 2015, where detailed investigations of copepod and euphausiid zooplankton optical sensory mechanisms have revealed that zooplankton eyes are hypersensitive to irradiance, thus animals can show phototatic reactions to background irradiance sourced from moon, stars and aurora borealis (Båtnes et al. 2015, Cohen et al. 2015). Despite these explanations, the adaptive significance of mid-winter vertical migrations remains questioned. This is because most polar night diel migrants are predominantly herbivorous copepods or euphausiids (Berge et al. 2009, Daase et al. 2014, Błachowiak-Samołyk et al. 2015, Last et al. 2016), which are supposed to be in diapause in this time of the year. Although the reasons driving these migrations are not yet fully known, these motivate interactive research on DVM, SVM and overwintering strategies of high-latitude zooplankton.

2. Objectives

The main aim of this study is to improve our understanding of the influence of environmental variability on the diel and seasonal vertical migrations of high-latitude zooplankton, and to investigate the combined influence of DVM and SVM on their life history strategies and fitness. Here,

(i). Paper-I is aimed at investigating the influence of seasonal environmental variability on SVM of high-latitude zooplankton using field data,

(ii). Paper-II is aimed at addressing the key limitations of paper-I and developing a high-resolution modeling framework that allows studying the integrative effects DVM and SVM on the life history strategies and fitness of high-latitude zooplankton and,

(iii). Paper-III is aimed at further developing the above model to allow a detailed investigation that analyzes the relative contributions of bottom-up and top-down environmental variables (selection pressures) in shaping up of behavioral and life history strategies of several selected high-latitude zooplankton taxa with different body sizes, reproductive strategies and generation times.

3. General discussion

3.1 Paper-I: background and main findings

In Paper-I (Bandara et al. 2016), we attempted to describe the influences of seasonal environmental variability on zooplankton seasonal vertical migrations (SVM), using depth-stratified zooplankton abundance data collected in a high-Arctic fjord (Billefjorden, Svalbard, 78.40°N). The selection of this location was motivated by the limited advective influence (Nilsen et al. 2008), so that zooplankton vertical distributions could be interpreted largely as reflecting local behavior. The data set covered almost an annual cycle, including the winter months. Data were collected on a bi-weekly to monthly basis (i.e. 14–30 d temporal resolution) using a net with a relatively large mesh width, which provided an year-round time series of zooplankton vertical distributions across a broad range of taxonomic groups, including larger developmental stages of copepods, chaetognaths, hydromedusae and ctenophores. We interpreted the seasonal vertical distributions of these taxa as patterns of SVM, and related those to local environmental variability, and with each other through identifiable predator-prey interactions, which were termed seasonal vertical strategies.

According to our findings, it appeared that seasonal vertical strategies of most zooplankton taxa were linked through trophic interactions. We found statistically significant correlations between the vertical distributions of predators and prey taxa, which could be traced up to three trophic levels. Further, estimated correlation coefficients were highly significant for specific predators and prey. Therefore, we concluded that vertical strategies of predatory zooplankton were driven by those of their prey. However, we could not find any meaningful statistical associations between the vertical distributions of herbivore zooplankton (i.e. *Calanus finmarchicus*, *C. glacialis* and *C. hyperboreus*) and biotic or abiotic environmental parameters. All *Calanus* species descended to deeper waters before the pelagic bloom had terminated, and ascended back to near-surface waters in mid-winter. Although the reason behind this strong decoupling of herbivore SVM and food availability could not be derived from our data, this finding aligned with recent observations of *Calanus* spp. occurring closer to surface waters during the Arctic polar night (Daase et al. 2014, Błachowiak-Samołyk et al. 2015).

3.2 Paper-I: key limitations and motivation for Paper-II

Although Paper-I provided one of the best year-round evidence about how vertical migratory behavior can propagate through trophic levels, it was not an essentially novel observation. David (1958) was likely the first to suggest that Antarctic chaetognaths may seasonally follow their copepod prey to deeper waters. Similar seasonal prey-following strategies have been observed for numerous pelagic invertebrate (e.g. Torres et al. 1994, Kaartvedt et al. 2002) and vertebrate predators (e.g. Sims et al. 2003, Born et al. 2004, Laidre et al. 2007, Geoffroy et al. 2011).

Despite year-round coverage of the analyzed data, the means by which SVM of predominantly herbivorous *Calanus* species were controlled remained elusive. Two main factors could have affected this. First, our study did not focus on the seasonality of visual predation risk, which is a major influential factor for SVM (Kaartvedt 1996, Kaartvedt 2000, Varpe & Fiksen 2010). Second, the spatio-temporal scales at which the vertical migration had occurred in the fjord may have been finer than the coarse spatial (ca. 50 m vertical) and temporal (ca. 15–30 d) resolution employed in our study (e.g. Pearre 1979, Skjoldal et al. 2000). However, given the logistic challenges of sampling at high-latitudes, the year-round bi-weekly depth-stratified zooplankton data used in our study represent some of the best available zooplankton net samples yet.

Limitations of Paper-I provided the motivation to look for a sampling gear that could allow studying zooplankton vertical migrations in superior resolution. Beside plankton nets, there are numerous alternative techniques that facilitate *in-situ* observation of zooplankton populations in a superior spatio-temporal resolution (reviewed in Sameoto et al. 2000). However, zooplankton nets possess the advantage of having superior biological resolution (i.e. zooplankton can be identified to species and their developmental stages), which many of these novel techniques do not (Table 3). This suggest that all three aspects of resolution (i.e. spatial, temporal and biological) cannot be simultaneously maximized without compromising each other. However, the lack of a 'universal plankton sampler' that can optimize these resolution trade-offs presents the opportunity for developing a methodological framework for studying zooplankton vertical migrations in higher resolution.

Table 3: Some popular plankton sampling methods and their associated spatial (i.e. vertical), temporal and biological (i.e. species or developmental stage) resolution. Long-term deployment refers to the capability to deploy these devices affixed to ship-hulls or moorings to make continuous measurements. See Sameoto et al. (2000) for a detailed account.

Sampling method	Spatial resolution	Temporal resolution	Biological resolution	Long-term deployment
Plankton nets	low	low	high	no
Acoustic devices (ES, ADCP, AZFP)	high	high	low	yes
Optical plankton counters	high	high	low	yes
Video plankton recorders	high	high	high[a]	no

[a]Depends on the camera resolution, which largely doesn't allow for fine life-stage discrimination compared to that facilitated by plankton collecting devices.
ES: Echo-sounder, ADCP: Acoustic Doppler Current Profiler, AZFP: Acoustic Zooplankton and Fish Profiler

3.3 Paper-II: Background and main findings

3.3.1 Models; are they any good?

Mechanistic models offer a cost-effective means of studying zooplankton vertical migrations in higher spatial, temporal and biological resolution. Here, vertical migrations are modeled in a bottom-up fashion, i.e. based on the patterns described in the literature, relating associated traits that are manifested in the migration to internal states of the migrant and external environmental variables using mathematical functions (see Enquist & Ghirlanda 2005, Soetaert & Herman 2009, Grimm & Railsback 2013). Simulations are performed in artificial environments of varying spatial and temporal resolution to provide environment-specific predictions about migratory behavior, which are validated using field data or comparing with behavioral patterns described in the literature (Rykiel 1996).

Since the pioneering work of McLaren (1963), numerous models have been used to describe DVM, SVM and associated life history strategies of various marine and freshwater zooplankton taxa. These involve classic life history models (e.g. Fiksen & Giske 1995, Fiksen & Carlotti 1998, Ji 2011), individual based simulation models (e.g. Miller et al. 1998, Hjøllo et al. 2012, Ji et al. 2012), simulation models involving groups of individuals (e.g. Carlotti & Wolf 1998, Fiksen 2000) and process-oriented models (e.g. Enright 1977, Eiane & Parisi 2001). Models of DVM often possess the highest spatial (≤ 1 m) and temporal (≤ 1 h) resolution (e.g. Fiksen & Giske 1995, Eiane & Parisi 2001, Liu et al. 2003, Burrows & Tarling 2004, Hansen & Visser 2016). Models of SVM, diapause and associated seasonal strategies usually possess coarser spatio-temporal resolution, where vertical spatial elements range from 1 m depth bins to few vertical habitats, and time units ranging from 1 h pings to few seasons (e.g. Carlotti & Wolf 1998, Fiksen & Carlotti 1998, Hind et al. 2000, Ejsmond et al. 2015, Sainmont et al. 2015, Banas et al. 2016). These differences indicate the contrasting spatial and temporal scales that DVM and SVM occur, and as a result lifetime dynamics of DVM cannot be simulated in models of SVM without significantly elevating computer time. This most likely be the reason why models of SVM and associated seasonal strategies of high-latitude zooplankton either fully or partly (i.e. of younger developmental stages) disregard DVM. However, since DVM is a geographically, taxonomically and ontogenetically widespread behavior (Huntley & Brooks 1982, Osgood & Frost 1994, Hays 1995, Bianchi & Mislan 2016, Gjøsæter et al. 2017, Knutsen et al. 2017), prudence of such simplifications and its potential influence on model predictions remains questionable. Therefore, to test this further, and to see if the elevation of computer time by modeling lifetime dynamics of DVM and SVM in concert is a favorable trade-off for biological information ensued, we developed a novel, computationally efficient modeling framework.

3.3.2 The strategy-oriented modeling framework

The strategy-oriented modeling framework was built around three core arguments. First, DVM and SVM are adaptive strategies that enhance opportunities of feeding, growth, survival and reproduction, and hence fitness (Aidley 1981, Alerstam et al. 2003, Cresswell et al. 2011, Litchman et al. 2013). Second, DVM and SVM predominantly occur as responses to spatio

temporal variability of resources and risks (e.g. Huntley & Brooks 1982, Bollens & Frost 1989, Kaartvedt 1996, Dingle & Drake 2007, Bandara et al. 2016). Third, vertical migration is not itself a trait that can be modelled, but is manifested by several underlying morphological, physiological and behavioral attributes, and their size-age-or stage-specific variability (reviewed in, Zink 2002, Cresswell et al. 2011).

Based on the above arguments, in paper-II (Bandara et al. 2018), we defined an entity termed 'vertical strategy', which represents a unique timing and amplitude of DVM and SVM and its ontogenetic trajectory. Vertical strategies were manifested using multiple (six) evolvable proxies. Payoffs rendered by vertical strategies hardwired to copepods born in different times of the year were assessed by their growth, survival and reproductive performances, which we termed fitness. For a given model environment, fitness was heuristically maximized using a Genetic Algorithm (GA: Holland 1975) to derive environment-specific optimal estimates of the vertical strategy, time of birth and several other associated life history traits. A graphical summary of this modeling framework is given in the Fig. 2 of Bandara et al. (2018).

In the model, six evolvable proxies of vertical strategies together with the time of birth (see Table 2 in Paper-II) produced a complex, seven-dimensional optimization problem, which could be efficiently solved using heuristic techniques (Zanakis & Evans 1981). Further, to improve the accuracy and efficiency of the optimization process, we used a Real-Coded Genetic Algorithm (RCGA: Davis 1989, Lucasius & Kateman 1989, Herrera et al. 1998), with pre-benchmarked selection, recombination and mutation operators that are known to perform well with multi-dimensional optimization problems. However, as there is no guarantee that the GA would converge on the globally optimal solution (Zanakis & Evans 1981, Rardin & Uzsoy 2001, Strand et al. 2002), we performed 10 replicate simulations of each scenario modelled (cf. Record et al. 2010, Maps et al. 2011).

We developed, executed and analyzed the model using R™ v.3.3.1 (R Core Team 2016) in the RStudio™ v. 1.0.136 (RStudio Team 2016) integrated development environment. As execution rates of even the most well-optimized code in R™ can be inherently slower compared to most low-level computing platforms, such as C++ and FORTRAN (Wickham

2015), we used the high performance computing package *Rcpp* (Eddelbuettel et al. 2011) to speed-up simulations.

In the trials, we estimated that a typical model run (i.e. from the seeding of 10^6 strategies to converging on an optimal strategy) takes on average ca. 18.3 hours to complete on sequential basis (single-threaded operation) using an Intel® Core™ i7-7700K central processing unit (CPU) running at an overclocked turbo speed at ca. 4.9 GHz. A parallelization trial using a loop-level construct (e.g. Larus 1993, Oplinger et al. 1999, Yu 2002) was shown to be ca. 3.6 times faster on the same CPU, which possesses four processor cores (workers). However, since we did not have access to a supercomputer with numerous processor cores, the efficiency of the above parallel execution could not be properly utilized. Further, given the high number of replicate model runs to be executed (410 model runs in total, Table 4) we decided to execute the model on a sequential basis, while running up to six instances (replicates) of the model on the same 4-core CPU without significantly reducing performance. This created an excessive memory (random access memory, RAM) demand, which was addressed using memory-efficient data objects manifested by the high-performance computing package *bigmemory* (Kane et al. 2013). We halved the total computational time by using a second CPU (with same configuration) to run the model (Table 4). Through this, we demonstrated that this model can be executed with reasonable efficiency even with the limited computational resources at hand.

3.3.3 Model predictions

Through the establishment of the strategy-oriented modeling framework, we could efficiently model both DVM and SVM in higher spatial (1 m vertical) and temporal (1 h) resolution covering the entire annual life cycle of the modelled copepods. Model runs along a latitudinal gradient under variable levels of visual predation risk have shown how differential patterns of DVM, SVM and other life history traits, such as birth times, sizes of overwintering stages and breeding modes would emerge in response to both bottom-up (i.e. temperature and food availability) and top-down (predation risk) environmental drivers. In the model, DVM emerged as a response to elevated visual predation risk, through which survival was enhanced at the cost of growth potential. Thus, it appeared that at higher levels

of visual predation risk, the modelled copepods cannot not perform SVM earlier in the year, as the DVM-induced loss of growth potential yields more time to develop to overwintering stages. However, by delaying their birth times, copepods could use higher summertime temperatures to attain higher growth, which was efficiently traded off for survival through pronounced DVM, while performing SVM more or less at the same time of the year predicted for lower visual predation risk. These findings indicated that new noteworthy information can be extracted from modelling DVM and SVM of high-latitude zooplankton in concert.

Table 4: Management of computer time (Paper-II). Executing up to six instances of the model (replicates) sequentially on two CPUs produced the lowest computer time. The two CPUs used here were identical (Intel® Core™-i7 7700K).

Attribute	Sequential single execution	Parallel execution	Sequential multiple execution
Unique model runs	41[a]	41[a]	41[a]
Total model runs (x 10 replicates)	410	410	410
CPU clock speed (overclocked turbo)	ca. 4.9 GHz	ca. 4.6 GHz[b]	ca. 4.6 GHz[b]
No. of cores	4	4	4
Unit run time	18.3 h	5.1 h	18.8 h
No. of simultaneous executions possible	1	1	6
Total predicted run time (one CPU)	7503 h (ca. 312 d)	2091 h (ca. 87 d)	1285 h (ca. 53 d)
Total predicted run time (two CPUs)	3752 h (ca. 157 d)	1046 h (ca. 44 d)	643 h (ca. 27 d)

[a]Includes one basic run, 28 runs for sensitivity analysis and 12 runs along the modeled latitudinal gradient under variable levels of visual predation risk
[b]CPU speed reduces due to increased thermal throttling at higher workloads

3.4. Paper-II: key limitations and motivation for Paper-III

The strategy-oriented modeling framework has three major limitations. First, since the strategies hold the primus over individuals (i.e. strategies are hardwired to individuals), the biological resolution tend to contrast the higher spatio-temporal resolution. In nature, individual personalities and motivation (Kralj-Fišer & Schuett 2014) can often override behavioral decisions, such as timing and amplitude of vertical migration (Hays et al. 2001, Pearre 2003). Although this can be easily built into the model as state-dependent processes of decision reversal (e.g. Houston & McNamara 1992, McNamara & Houston 1996), we did not implement these changes to the current iteration of the model (both in Paper-II and -III) for simplicity. The second limitation is lack of quantitative feedbacks between strategies and the model environment, such as the impact of grazing on the duration of the productive season. Consequently, competition for resources in the form of density-dependent games between strategies (e.g. Fiksen 2000) are not present in this model. Finally, the implemented 1 m spatial and 1 h temporal resolution can overlook zooplankton behavior occurring in finer spatio-temporal scales (Visser 2001, Seuront et al. 2003). However, such finer resolutions were not adopted in this study to keep computer time under manageable limits.

In addition to the above, the most important limitation of the Paper-II (Bandara et al. 2018) in the context of this study was that the modelled copepod does not fully represent the life strategies of Arctic *Calanus* species. The fixed generation time (i.e. one year) and body mass (maximum ≈ 333 µg C) used in Bandara et al. (2018) did not fully represent those observed for *C. finmarchicus*, *C. glacialis* and *C. hyperboreus* (e.g. Conover 1988, Unstad & Tande 1991, Hirche et al. 1994, Falk-Petersen et al. 2009). Therefore, there was a general need for relaxing the generation time and body size assumptions, and modeling three different species rather than a generalized model copepod. Further, there was also a need of extending the modelled latitudinal gradient in Bandara et al. (2018) beyond 75°N, possibly toward ca. 80°N to represent seasonally ice-covered waters of the high-Arctic.

3.5 Paper-III: background and main findings

3.5.1 An improved model

In Paper-III (unpublished manuscript), we relaxed the generation time and body size restrictions implemented by Paper-II (Bandara et al. 2018) and adopted species-specific parameterization to develop three model-species representing the behavioral and life history strategies of *C. finmarchicus*, *C. glacialis* and *C. hyperboreus*. Here, apart from the vertical strategy, we introduced two evolvable parameters to represent the plasticity of body sizes and generation times observed for above species. The modelled latitudinal gradient was also extended toward ca. 80°N, but for simplicity, we did not model the seasonal sea-ice cover. By adopting these modifications, we attempted to answer the important question that remain unanswered in Paper-I (Bandara et al. 2016), i.e. how vertical migrations and associated life history strategies of Arctic *Calanus* spp. are influenced by environmental variability?

The model was based on the same strategy-oriented construct (Bandara et al. 2018), but with few modifications. First, to adopt the two additional evolvable parameters we removed two least influential evolvable parameters used in the first model (Paper-II), i.e. the size-specificity of light sensitivity parameter and the overwintering depth parameter (cf. Table 2 of Paper-II with that of Paper-III). Here, the former represented the ontogenetic DVM trajectory and the latter allowed overwintering depth to evolve in response to external environmental variability. In Paper III, we implemented general rules (based on literature) to describe these behavioral patterns. The second major modification was the adoption of a novel growth sub-model to allow species-specific patterns of growth. The growth sub-model presented in Paper-III was based on the parameters calculated from Maps et al. (2011), and was designed to address some practical concerns of the above (see Appendix S2 of Paper-III for a detailed account). The third major modification was the implementation of exponential size-dependent visual predation risk function to replace the more conservative linear function used in Paper-II (cf. Fig. 4a of Paper-II with Fig. 5a of Paper-III).

Apart from these improvements of parameterization, the RCGA was also reinforced with novel recombination and mutation operators, i.e. Laplace crossover operator (LX: Deep & Thakur 2007) for recombination, and Makinen, Periaux and Toivanen method (MPTM:

Toivanen et al. 1999) for mutation. Further, the number of seeds (strategies) were increased up to 2.5 x 10^6.

Table 5: Management of computer time (Paper-III). Executing up to 16 instances of the model (replicates) sequentially on a single Intel® Core™-i9 7920X CPU produced the lowest computer time.

Attribute	Sequential single execution	Parallel execution	Sequential multiple execution
Unique model runs	96[a]	96[a]	96[a]
Total model runs (x 10 replicates)	960	960	960
CPU clock speed (turbo)	ca. 4.3 GHz	ca. 4.3 GHz	ca. 4.3 GHz
No. of cores	12	12	12
Unit run time	29.4 h	2.8 h	29.4 h
No. of simultaneous executions possible	1	1	16
Total predicted run time	28224 h (ca. 1176 d)	2688 h (ca. 112 d)	1764 h (ca. 74 d)

[a]Includes three basic runs, 12 runs for sensitivity analysis and 81 runs along the modeled latitudinal gradient under variable levels of visual predation risk

The 2.5-fold increase in the number of strategies simulated in the model had a significant influence on the model performance. To reduce computer time, we made some performance tweaks to the code, and removed the semi-stochastic predictive algorithm (see Appendix S2 in Paper-II) for copepod vertical search behavior. With these changes, we could adopt the increased number of strategies without significantly elevating the computer time. In the new model, the estimated average computer time needed to complete a single sequential model run (i.e. from the seeding of 2.5 x 10^6 strategies to converging on an optimal strategy) was ca. 29.4 hours, for an Intel® Core™ i9 7920X CPU running at a turbo clock speed

at ca. 4.3 GHz. In this 12-core CPU, the loop-level parallel execution trial on *RMPI* (Yu 2002) was ca. 10.7 times faster than the sequential execution. However, given the higher number of replicate model runs that had to be performed (960 model runs in total), we executed the model on sequential basis, while running up to 16 instances of the model on the above 12-core CPU (Table 5).

3.5.2 Model predictions

In Paper-III, we found that when top-down selection pressures were insignificant (i.e. low visual predation risk), there were obvious inter-specific south to north (ca. 60°N–80°N) trends in the predicted behavioral and life history strategies of *Calanus* spp., driven predominantly by the both bottom-up environmental selection pressures (i.e. temperature and food availability). However, increasing visual predation risk caused the top-down selection pressures to become predominant, and the three model-species employed largely similar tactics to counter the threat of visual predation. As a result, the influence of bottom-up selection pressures became diminished, where the predicted latitudinal and species-specific differences of birth times, timing of SVM, timing of reproduction, size of overwintering stages, size at sexual maturity, breeding modes and fecundity became less pronounced. Here, modest elevations of visual predation risk were countered with the manifestation of DVM behavior. However, at the point where this growth potential to survival trade-off became unfavorable, further increase of visual predation risk was countered with the plasticity of body sizes, which affected numerous allometric processes of growth, reproduction and survival, and created a significant impact on the observed behavior and life history patterns. We used these findings to conclude that top-down selection pressures serve a more significant role in shaping up of behavioral and life history strategies of Arctic *Calanus* species.

3.6 Paper III: key limitations and motivation for a follow-up paper

Although several assumptions of the model were relaxed from Paper-II to Paper-III, we still feel the need to relax some key assumptions for the next iteration of this model. First is the assumption of semelparity, which holds well for *C. finmarchicus* and to some extent *C.*

glacialis (but see Kosobokova 1999). However, our findings showed that species-CH (i.e. the model-species representing *C. hyperboreus*) had the potential for an iteroparous breeding strategy, which is well-documented for this species (Hirche 2013). Second, to represent the full spectrum of generation times exhibited by Arctic *Calanus* species, the model should allow life cycles with < 1 year generation times. In both the Paper-II and -III, the model hinted the possibility of some copepods (species-CF in Paper-III) to produce more than one generations per year, which is a common observation made for *C. finmarchicus* in many lower-latitude locations (e.g. Fish 1936, Lie 1965, Matthews et al. 1978, McLaren et al. 2001, Bagøien et al. 2012). However, this modification cannot be harbored without modifying the fitness function, which at its current formulation, does not allow to estimate fitness of < 1 year generation time. The third limitation of this model is the lack of flexible feeding behavior among the modelled species. In nature, all *Calanus* spp. have shown the ability to switch to alternative food sources in the absence of phytoplankton (Runge & Ingram 1991, Plourde & Runge 1993, Søreide et al. 2008, Campbell et al. 2016). We believe that investigating the adaptive significance of this omnivores feeding strategy may hold the key to answer the question why *Calanus* spp. in the high-Arctic are active during the polar night. Finally, none of the above modifications would make complete sense unless the model is run in a stochastic model environment. Although timing of pelagic bloom is more or less predictable at ice-free lower latitudes, if the model is to run at ice-covered waters of the High-Arctic, we believe that year-to-year unpredictability in bottom-up and top-down environmental drivers should be allowed. This will enable us to check how model predicted optimal strategies would be robust to spatio temporal heterogeneity of environment (e.g. Fiksen 2000, Eiane & Parisi 2001, Ji 2011).

4. Concluding remarks and outlook

The strategy-oriented modeling framework employed in this study could efficiently simulate both DVM and SVM in higher spatio-temporal resolution, and predicted how environmental variability influences vertical migrations, and the influence of the latter on fitness and phenology of high-latitude herbivorous zooplankton (Paper-II and -III). Such predictions could not be derived from the year-round field data used in this study (Paper-I), likely because its lower spatio-temporal resolution did not match the spatio-temporal scales at which the vertical migrations usually occur. Therefore, these findings highlight the importance of future field and modeling studies to investigate DVM and SVM in concert.

To model DVM and SVM in concert, prospective modeling studies should focus on innovative ways of improving spatial and temporal resolution without significantly elevating computer time (e.g. Carlotti & Wolf 1998, Huse et al. 1999, Eiane & Parisi 2001). Coupling such high-resolution 1D models with 2D ocean circulation models would allow accurate predictions about the robustness of behavioral and life history strategies of high-latitude zooplankton over space and time. Nonetheless, due to the scarcity of high-resolution field data, validating these models would remain challenging. To facilitate model validation with existing data, we encourage building of spatially explicit models to represent locations where long-term zooplankton data are available (e.g. White Sea and weather-ship M).

Mechanistic models are useful tools to develop understanding about complex biological processes or behavioral patterns where empirical data are scarce (Kiørboe 2008, Bauer & Klaassen 2013). Nonetheless, all models are simplifications of the real world, and thus do not render a complete picture about the questions under investigation. Similarly, the strategy oriented high-resolution models that were employed in this study only provide a temporary bridge to span the current knowledge gaps of zooplankton diel and seasonal vertical migrations. A thorough build-up of our understanding on the subject matter relies on the development of empirical research toward year-round monitoring of individual zooplankters in higher spatial and temporal resolution (Davis et al. 1996). Until those glory-days arrive, findings of high-resolution models of zooplankton vertical behavior would resonate in the field of plankton ecology.

5. References

Aidley D (1981) Questions about migration. In: Aidley D (ed) Animal migration. Press Syndicae of the University of Cambridge, New York, USA, p 1-9

Alerstam T, Hedenström A, Åkesson S (2003) Long-Distance Migration: Evolution and Determinants. Oikos 103:247-260

Atkins W (1926) A quantitative consideration of some factors concerned in plant growth in water. ICES Journal of Marine Science 1:99-126

Bagøien E, Melle W, Kaartvedt S (2012) Seasonal development of mixed layer depths, nutrients, chlorophyll and *Calanus finmarchicus* in the Norwegian Sea – A basin-scale habitat comparison. Progress in Oceanography 103:58-79

Bainbridge R (1961) Migrations. In: Waterman TH (ed) The physiology of Crustacea. Academic Press, New York, USA

Banas NS, Møller EF, Nielsen TG, Eisner LB (2016) Copepod life strategy and population viability in response to prey timing and temperature: Testing a new model across latitude, time, and the size spectrum. Frontiers in Marine Science 3:225

Bandara K (2014) Mesozooplankton community dynamics in a high arctic fjord. Universitetet i Nordland

Bandara K, Varpe Ø, Ji R, Eiane K (2018) A high-resolution modeling study on diel and seasonal vertical migrations of high-latitude copepods. Ecological Modelling 368C:357-376

Bandara K, Varpe Ø, Søreide JE, Wallenschus J, Berge J, Eiane K (2016) Seasonal vertical strategies in a high-Arctic coastal zooplankton community. Marine Ecology Progress Series 555:49-64

Banse K (1964) On the vertical distribution of Zooplankton in the sea. Progress in Oceanography 2:53-125

Båtnes AS, Miljeteig C, Berge J, Greenacre M, Johnsen G (2015) Quantifying the light sensitivity of Calanus spp. during the polar night: potential for orchestrated migrations conducted by ambient light from the sun, moon, or aurora borealis? Polar Biology 38:51-65

Bauer S, Klaassen M (2013) Mechanistic models of animal migration behaviour – their diversity, structure and use. The Journal of animal ecology 82:498-508

Bayly I (1986) Aspects of diel vertical migration in zooplankton, and its enigma variations. In: Deckker P, Williams WD (eds) Limnology in Australia. Kluwer Academic Publishers Group, Dordrecht, The Netherlands, p 349-368

Berge J, Cottier F, Last KS, Varpe Ø and others (2009) Diel vertical migration of Arctic zooplankton during the polar night. Biology letters 5:69-72

Berge J, Varpe Ø, Moline MA, Wold A, Renaud PE, Daase M, Falk-Petersen S (2012) Retention of ice-associated amphipods: possible consequences for an ice-free Arctic Ocean. Biology Letters 8:1012-1015

Bertelsen E (1951) The Ceratioid Fishes: Ontogeny, Taxonomy, Distribution and Biology. Dana-Report 39:1-276

Beyer F (1962) Absorption of water in crustaceans and the standing crop of zooplankton. Rapports et Proces-Verbaux des Reunions Conseil permanent International pour I'Exploration de la Mer 153:79-85

Bianchi D, Mislan KAS (2016) Global patterns of diel vertical migration times and velocities from acoustic data. Limnology and Oceanography 61:353-364

Bigelow HB (1926) Plankton of the offshore waters of the Gulf of Maine. Bulletin of United States Fisheries Beureau 40:1-509

Birge EA (1904) The Annual Address of the President: The Thermocline and Its Biological Significance. Transactions of the American Microscopical Society 25:5-33

Błachowiak-Samołyk K, Wiktor JM, Hegseth EN, Wold A, Falk-Petersen S, Kubiszyn AM (2015) Winter Tales: the dark side of planktonic life. Polar Biology 38:23-36

Bogorov V, Vinogradov M (1955) Some essential features of zooplankton distribution in the Northwestern Pacific Ocean. Trans Institutional Marine Fisheries and Oceanography of USSR 18:113-123

Bollens SM, Frost BW (1989) Predator-induced diet vertical migration in a planktonic copepod. Journal of Plankton Research 11:1047-1065

Born EW, Teilmann J, Acquarone M, Riget FF (2004) Habitat use of ringed seals (*Phoca hispida*) in the North Water area (North Baffin Bay). Arctic 57:129-142

Brierley AS (2014) Diel vertical migration. Current Biology 24:R1074-R1076

Brook G (1886) Report on the herring fishery of Loch Fyne and the adjacent districts during 1885. Fourth annual report of the Fishery Board for Scotland 4:47-60

Bundy MH, Gross TF, Coughlin DJ, Strickler JR (1993) Quantifying Copepod Searching Efficiency Using Swimming Pattern and Perceptive Ability. Bulletin of Marine Science 53:15-28

Burrows MT, Tarling G (2004) Effects of density dependence on diel vertical migration of populations of northern krill: a genetic algorithm model. Marine Ecology Progress Series 277:209-220

Cade BS, Hoffman RW (1993) Differential Migration of Blue Grouse in Colorado. The Auk 110:70-77

Campbell RG, Ashjian CJ, Sherr EB, Sherr BF and others (2016) Mesozooplankton grazing during spring sea-ice conditions in the eastern Bering Sea. Deep Sea Research Part II: Topical Studies in Oceanography 134:157-172

Carlisle D, Pitman W (1961) Diapause, neurosecretion and hormones in Copepoda. Nature 190:827-828

Carlotti F, Wolf KU (1998) A Lagrangian ensemble model of *Calanus finmarchicus* coupled with a 1D ecosystem model. Fisheries Oceanography 7:191-204

Cerbin S, Balayla DJ, Van de Bund WJ (2003) Small-scale distribution and diel vertical migration of zooplankton in a shallow lake (Lake Naardermeer, the Netherlands). Hydrobiologia 491:111-117

Chun C (1888) The pelagic animal world in greater depths of the sea and their relationships with the surface fauna (*in German*). In: Bibliotheca Zoologica. Cassel (verlag von Theodor Fischer), Munich, Germany, p 1-106

Clarke GL (1934) Further observations on the diurnal migration of copepods in the gulf of maine. The Biological Bulletin 67:432-455

Cohen EB, Forward RB (2009) Zooplankton diel vertical migration—a review of proximate control. In: Gibson R, Atkinson R, Gordon J (eds) Oceanography and marine biology: an annual review, p 77-110

Cohen JH, Berge J, Moline MA, Sørensen AJ and others (2015) Is ambient light during the high Arctic polar night sufficient to act as a visual cue for zooplankton? PloS one 10:e0126247

Conover RJ (1962) Metabolism and growth in *Calanus hyperboreus* in relation to its life cycle. Rapports et Proces-Verbaux des Reunions Conseil permanent International pour l'Exploration de la Mer 153:190-197

Conover RJ (1988) Comparative life histories in the genera *Calanus* and *Neocalanus* in high latitudes of the northern hemisphere. In: Boxshall GA, Schminke HK (eds) Biology of Copepods: Proceedings of the Third International Conference on Copepoda. Springer Netherlands, Dordrecht, p 127-142

Cresswell K, William H, Sword G (2011) Understanding the evolution of migration through empirical examples. In: Milner-Gulland E, Mryxell JM, Sinclair A (eds) Animal migration: a synthesis. Oxford University Press, Oxford, England, p 7-16

Cushing DH (1951) The vertical migration of planktonic crustacea. Biological Reviews 26:158-192

Cuvier G (1817) The animal kingdom; Crustaceans, Arachnids and Insects (*in French*). Chez Deterville, Paris, France

Daase M, Falk-Petersen S, Varpe Ø, Darnis G and others (2013) Timing of reproductive events in the marine copepod *Calanus glacialis*: a pan-Arctic perspective. Canadian Journal of Fisheries and Aquatic Sciences 70:871-884

Daase M, Varpe Ø, Falk-Petersen S (2014) Non-consumptive mortality in copepods: occurrence of *Calanus* spp. carcasses in the Arctic Ocean during winter. Journal of Plankton Research 36:129-144

Dahms H-U (1995) Dormancy in the Copepoda—an overview. Hydrobiologia 306:199-211

Darnis G, Fortier L (2014) Temperature, food and the seasonal vertical migration of key arctic copepods in the thermally stratified Amundsen Gulf (Beaufort Sea, Arctic Ocean). Journal of Plankton Research 36:1092-1108

David PM (1958) The distribution of the *Chaetognatha* of the Southern Ocean. Discovery Reports 29:199-228

Davis CS, Gallager SM, Marra M, Stewart WK (1996) Rapid visualization of plankton abundance and taxonomic composition using the Video Plankton Recorder. Deep Sea Research Part II: Topical Studies in Oceanography 43:1947-1970

Davis L (1989) Adapting operator probabilities in genetic algorithms Proceedings of the third international conference on Genetic algorithms, p 61-69

Deep K, Thakur M (2007) A new crossover operator for real coded genetic algorithms. Applied Mathematics and Computation 188:895-911

Dingle H, Drake VA (2007) What is migration? Bioscience 57:113-121

Eddelbuettel D, François R, Allaire J, Chambers J, Bates D, Ushey K (2011) Rcpp: Seamless R and C++ integration. Journal of Statistical Software 40:1-18

Egevang C, Stenhouse IJ, Phillips RA, Petersen A, Fox JW, Silk JRD (2010) Tracking of Arctic terns *Sterna paradisaea* reveals longest animal migration. Proceedings of the National Academy of Sciences 107:2078-2081

Eiane K, Parisi D (2001) Towards a robust concept for modelling zooplankton migration. Sarsia 86:465-475

Ejsmond MJ, Varpe Ø, Czarnoleski M, Kozłowski J (2015) Seasonality in offspring value and trade-offs with growth explain capital breeding. The American Naturalist 186:E111-E125

Elgmork K, Nilssen J (1978) Equivalence of copepod and insect diapause. Verhandlungen des Internationalen Verein Limnologie 20:2511-2517

Enquist M, Ghirlanda S (2005) Neural Networks and Animal Behavior. Princeton University Press, Princeton, NJ, USA

Enright JT (1977) Diurnal vertical migration: Adaptive significance and timing. Part 1. Selective advantage: A metabolic model. Limnology and Oceanography 22:856-872

Esterly CO (1917) The occurrence of a rhythm in the geotropism of two species of plankton copepods when certain recurring external conditions are absent. University of California Publications of Zoology 8:1-7

Esterly CO (1919) Reactions of various plankton animals with reference to their diurnal migrations. University of California Publications of Zoology 19:1-83

Ewald WF (1912) On artificial modification of light reactions and the influence of electrolytes on phototaxis. Journal of Experimental Zoology 13:591-612

Eyden D (1923) Specific gravity as a factor in the vertical distribution of plankton. Biological Reviews 1:49-55

Falk-Petersen S, Mayzaud P, Kattner G, Sargent JR (2009) Lipids and life strategy of Arctic *Calanus*. Marine Biology Research 5:18-39

Falkenhaug T, Tande KS, Semenova T (1997) Diel, seasonal and ontogenetic variations in the vertical distributions of four marine copepods. Marine Ecology Progress Series 149:105-119

Fiksen Ø (2000) The adaptive timing of diapause–a search for evolutionarily robust strategies in *Calanus finmarchicus*. ICES Journal of Marine Science 57:1825-1833

Fiksen Ø, Carlotti F (1998) A model of optimal life history and diel vertical migration in *Calanus finmarchicus*. Sarsia 83:129-147

Fiksen Ø, Giske J (1995) Vertical distribution and population dynamics of copepods by dynamic optimization. ICES Journal of Marine Science 52:483-503

Fish CJ (1936) The Biology of *Calanus finmarchicus* in the Gulf of Maine and Bay of Fundy. Biological Bulletin 70:118-141

Forel FA (1878) Faunistic studies in the freshwater lakes of Switzerland (*in German*). Zeitschrift Wissenschaftliche Zooloogie 30:383-391

Franz V (1910) Phototaxis and migration. Following experiments with juveniles and fish larvae (*in German*). International Review of Hydrobiology 3:306-334

Fuchs TH (1882) About the pelagic flora and fauna: what do we understand by the deep sea fauna and by why physical moment is occurring under same conditions? (*in German*). Verhandlungen der Kaiserlich-Königlichen Geologischen Reichsanstalt 7:49-70

Geoffroy M, Robert D, Darnis G, Fortier L (2011) The aggregation of polar cod (*Boreogadus saida*) in the deep Atlantic layer of ice-covered Amundsen Gulf (Beaufort Sea) in winter. Polar Biology 34:1959-1971

Gjøsæter H, Wiebe P, Knutsen T, Ingvaldsen RB (2017) Evidence of diel vertical migration of mesopelagic sound-scattering organisms in the Arctic. Frontiers in Marine Science 4:332

Gliwicz ZM (1986) A lunar cycle in zooplankton. Ecology 67:883-897

Gran HH (1902) The plankton of the Norwegian Sea is treated from a biological and hydrographic point of view (*in German*). Report on Norwegian Fishery and Marine Investigations 2:1-219

Grigg H, Bardwell SJ (1982) Seasonal observations on moulting and maturation in Stage V copepodites of *Calanus finmarchicus* from the Firth of Clyde. Journal of the Marine Biological Association of the United Kingdom 62:315-327

Grimm V, Railsback SF (2013) Individual-based Modeling and Ecology. Princeton University Press, Princeton, NJ, USA

Hagen W (1999) Reproductive strategies and energetic adaptations of polar zooplankton. Invertebrate Reproduction & Development 36:25-34

Hansen AN, Visser AW (2016) Carbon export by vertically migrating zooplankton: an optimal behavior model. Limnology and Oceanography 61:701-710

Hardy AC (1936) Plankton ecology and the hypothesis of animal exclusion Proceedings of the Linnean Society of London. Wiley Online Library, p 64-70

Hardy AC, Gunther ER (1935) The plankton of the South Georgia whaling grounds and adjacent waters, 1926-1927. Discovery Reports 11:1-456

Hardy LM, Raymond LR (1980) The Breeding Migration of the Mole Salamander, *Ambystoma talpoideum*, in Louisiana. Journal of Herpetology 14:327-335

Harris JE (1963) The Role of Endogenous Rhythms in Vertical Migration. Journal of the Marine Biological Association of the United Kingdom 43:153-166

Hays GC (1995) Ontogenetic and seasonal variation in the diel vertical migration of the copepods *Metridia lucens* and *Metridia longa*. Limnology and Oceanography 40:1461-1465

Hays GC (2003) A review of the adaptive significance and ecosystem consequences of zooplankton diel vertical migrations. In: Jones MB, Ingólfsson A, Ólafsson E, Helgason GV, Gunnarsson K, Svavarsson J (eds) Migrations and Dispersal of Marine Organisms: Proceedings of the 37th European Marine Biology Symposium held in Reykjavík, Iceland, 5–9 August 2002. Springer Netherlands, Dordrecht, p 163-170

Hays GC, Kennedy H, Frost BW (2001) Individual variability in diel vertical migration of a marine copepod: Why some individuals remain at depth when others migrate. Limnology and Oceanography 46:2050-2054

Head EJH, Harris LR (1985) Physiological and biochemical changes in *Calanus hyperboreus* from Jones Sound NWT during the transition from summer feeding to overwintering condition. Polar Biology 4:99-106

Hebblewhite M, Merrill EH (2007) Multiscale wolf predation risk for elk: does migration reduce risk? Oecologia 152:377-387

Heinrich A (1962) The life histories of plankton animals and seasonal cycles of plankton communities in the oceans. ICES Journal of Marine Science 27:15-24

Hensen V (1887) On the determination of plankton and marine matter in plants and animals (*in German*). In: Jahresbericht der Kommission zur Wissenschaftlichen Untersuchung der deutschen Meere für die Jahre 1882 bis 1886. Paul Parey, Berlin, Germany, p 1-109

Herdman W (1907) Plankton fishing off the Isle of Man. Science 26:551-554

Herman AW (1983) Vertical distribution patterns of copepods, chlorophyll, and production in northeastern Baffin Bay. Limnology and oceanography 28:709-719

Herrera F, Lozano M, Verdegay JL (1998) Tackling real-coded genetic algorithms: Operators and tools for behavioural analysis. Artificial intelligence review 12:265-319

Hind A, Gurney WSC, Heath MR, Bryant A (2000) Overwintering strategies in *Calanus finmarchicus*. Marine Ecology Progress Series 193:95-107

Hirche H-J (1991) Distribution of dominant calanoid copepod species in the Greenland Sea during late fall. Polar Biology 11:351-362

Hirche H-J (1996a) Diapause in the marine copepod, *Calanus finmarchicus* — A review. Ophelia 44:129-143

Hirche H-J (1996b) The reproductive biology of the marine copepod, *Calanus finmarchicus*— a review. Ophelia 44:111-128

Hirche H-J (2013) Long-term experiments on lifespan, reproductive activity and timing of reproduction in the Arctic copepod *Calanus hyperboreus*. Marine Biology 160:2469-2481

Hirche H-J, Hagen W, Mumm N, Richter C (1994) The Northeast Water Polynya, Greenland Sea. Polar Biology 14:491-503

Hirche H-J, Kosobokova K (2011) Winter studies on zooplankton in Arctic seas: the Storfjord (Svalbard) and adjacent ice-covered Barents Sea. Marine Biology 158:2359-2376

Hjøllo SS, Huse G, Skogen MD, Melle W (2012) Modelling secondary production in the Norwegian Sea with a fully coupled physical/primary production/individual-based *Calanus finmarchicus* model system. Marine Biology Research 8:508-526

Hobbs L (2016) Winter vertical migration of Arctic zooplankton. University of Aberdeen

Hoffmann RS (1956) Observations on a Sooty Grouse Population at Sage Hen Creek, California. The Condor 58:321-337

Holland JH (1975) Adaptation in natural and artificial systems. An introductory analysis with application to biology, control, and artificial intelligence. Ann Arbor, MI: University of Michigan Press, Michigan, USA

Houston AI, McNamara JM (1992) Phenotypic plasticity as a state-dependent life-history decision. Evolutionary Ecology 6:243-253

Huntley M, Brooks E (1982) Effects of age and food availability on diel vertical migration of *Calanus pacificus*. Marine Biology 71:23-31

Huse G, Strand E, Giske J (1999) Implementing behaviour in individual-based models using neural networks and genetic algorithms. Evolutionary Ecology 13:469-483

Hutchinson GE (1959) Homage to Santa Rosalia or Why Are There So Many Kinds of Animals? The American Naturalist 93:145-159

Hutchinson GE (1967) A treatise on limnology. Volume II. Introduction to lake biology and the limnoplankton. John Wiley and Sons, New York, USA

Irigoien X (2004) Some ideas about the role of lipids in the life cycle of *Calanus finmarchicus*. Journal of Plankton Research 26:259-263

Ji R (2011) *Calanus finmarchicus* diapause initiation: new view from traditional life history-based model. Marine Ecology Progress Series 440:105-114

Ji R, Ashjian CJ, Campbell RG, Chen C and others (2012) Life history and biogeography of *Calanus* copepods in the Arctic Ocean: An individual-based modeling study. Progress in Oceanography 96:40-56

Jordan CE (1992) A model of rapid-start swimming at intermediate reynolds number: Undulatory locomotion in the chaetognath *Sagitta elegans*. Journal of Experimental Biology 163:119-137

Kaartvedt S (1996) Habitat preference during overwintering and timing of seasonal vertical migration of *Calanus finmarchicus*. Ophelia 44:145-156

Kaartvedt S (2000) Life history of Calanus finmarchicus in the Norwegian Sea in relation to planktivorous fish. ICES Journal of Marine Science 57:1819-1824

Kaartvedt S, Larsen T, Hjelmseth K, Onsrud MS (2002) Is the omnivorous krill *Meganyctiphanes norvegica* primarily a selectively feeding carnivore? Marine Ecology Progress Series 228:193-204

Kane MJ, Emerson JW, Weston S (2013) Scalable Strategies for Computing with Massive Data. Journal of Statitical Software 55:1-19

Keller JB, Rubinow SI (1976) Swimming of flagellated microorganisms. Biophysical Journal 16:151-170

Kils U (1983) Swimming and feeding of Antarctic krill, *Euphausia superba*—some outstanding energetics and dynamics—some unique morphological details. Berichte zur Polarforschung 4:130-155

Kiørboe T (2008) A mechanistic approach to plankton ecology. Princeton University Press, New Jersey, USA

Klugh AB (1925) Ecological photometry and a new instrument for measuring light. Ecology 6:203-237

Knutsen T, Wiebe P, Gjøsæter H, Ingvaldsen RB, Lien G (2017) High Latitude epipelagic and mesopelagic scattering layers—a reference for future Arctic ecosystem change. Frontiers in Marine Science 4:334

Kosobokova K (1999) The reproductive cycle and life history of the Arctic copepod *Calanus glacialis* in the White Sea. Polar Biology 22:254-263

Kralj-Fišer S, Schuett W (2014) Studying personality variation in invertebrates: why bother? Animal Behaviour 91:41-52

L'Abée-Lund JH, Vøllestad LA (1987) Feeding migration of roach, *Rutilus rutilus* (L.), in Lake Arungen, Norway. Journal of Fish Biology 30:349-355

Laidre KL, Heide-Jørgensen MP, Nielsen TG (2007) Role of the bowhead whale as a predator in West Greenland. Marine Ecology Progress Series 346:285-297

Lampert W (1989) The adaptive significance of diel vertical migration of zooplankton. Functional Ecology 3:21-27

Larus JR (1993) Loop-level parallelism in numeric and symbolic programs. IEEE Transactions on Parallel and Distributed Systems 4:812-826

Last KS, Hobbs L, Berge J, Brierley AS, Cottier F (2016) Moonlight drives ocean-scale mass vertical migration of zooplankton during the Arctic winter. Current Biology 26:244-251

Levey DJ, Stiles FG (1992) Evolutionary Precursors of Long-Distance Migration: Resource Availability and Movement Patterns in Neotropical Landbirds. The American Naturalist 140:447-476

Lie U (1965) Quantities of zooplankton and propagation of *Calanus finmarchicus* at permanent stations on the Norwegian coast and at Spitsbergen, 1959 1962. Fiskeridirektoratets skrifter, Serie Havundersøkelser 13:5-19

Lischka S, Hagen W (2005) Life histories of the copepods *Pseudocalanus minutus*, *P. acuspes* (Calanoida) and *Oithona similis* (Cyclopoida) in the Arctic Kongsfjorden (Svalbard). Polar Biology 28:910-921

Litchman E, Ohman MD, Kiørboe T (2013) Trait-based approaches to zooplankton communities. Journal of Plankton Research 35:473-484

Liu S-H, Sun S, Han B-P (2003) Diel vertical migration of zooplankton following optimal food intake under predation. Journal of Plankton Research 25:1069-1077

Loeb J (1893) On artificial transformation of positive heliotropic animals into negative heliotropism and vice versa (*in German*). Archiv für die gesamte Physiologie des Menschen und der Tiere 54:81-107

Loose CJ, Dawidowicz P (1994) Trade-offs in diel vertical migration by zooplankton: the costs of predator avoidance. Ecology 75:2255-2263

Lucasius CB, Kateman G (1989) Application of genetic algorithms in chemometrics Proceedings of the third international conference on Genetic algorithms. Morgan Kaufmann Publishers Inc., p 170-176

Mackintosh NA (1937) The seasonal circulation of the Antarctic macroplankton. Discovery Reports 16:365-412

Madsen S, Nielsen TG, Hansen BW (2001) Annual population development and production by *Calanus finmarchicus*, *C. glacialis* and *C. hyperboreus* in Disko Bay, western Greenland. Marine Biology 139:75-93

Maps F, Pershing AJ, Record NR (2011) A generalized approach for simulating growth and development in diverse marine copepod species. ICES journal of marine science 69:370-379

Matsumoto GI (1991) Swimming movements of ctenophores, and the mechanics of propulsion by ctene rows. Hydrobiologia 216:319-325

Matthews JBL, Hestad L, Bakke JLW (1978) Ecological-studies in korsfjorden, western norway-generations and stocks of *Calanus hyperboreus* and *Calanus finmarchicus* in 1971-1974. Oceanologica acta 1:277-284

McKinnon L, Smith PA, Nol E, Martin JL and others (2010) Lower Predation Risk for Migratory Birds at High Latitudes. Science 327:326-327

McLaren IA (1963) Effects of Temperature on Growth of Zooplankton, and the Adaptive Value of Vertical Migration. Journal of the Fisheries Research Board of Canada 20:685-727

McLaren IA (1974) Demographic Strategy of Vertical Migration by a Marine Copepod. The American Naturalist 108:91-102

McLaren IA, Head EJH, Sameoto DD (2001) Life cycles and seasonal distributions of *Calanus finmarchicus* on the central Scotian Shelf. Canadian Journal of Fisheries and Aquatic Sciences 58:659-670

McNamara JM, Houston AI (1996) State-dependent life histories. Nature 380:215-221

Melle W, Runge J, Head EJH, Plourde S and others (2014) The North Atlantic Ocean as habitat for *Calanus finmarchicus*: Environmental factors and life history traits. Progress in Oceanography 129:244-284

Michael ELR (1911) Classification and Vertical Distribution of the *Chaetognatha* of the San Diego Region: Including Redescriptions of Some Doubtful Species of the Group. The University Press, California, USA

Miller CB, Cowles TJ, Wiebe PH, Copley NJ, Grigg H (1991) Phenology in *Calanus finmarchicus*; hypotheses about control mechanisms. Marine Ecology Progress Series 72:79-91

Miller CB, Lynch DR, Carlotti F, Gentleman W, Lewis CV (1998) Coupling of an individual-based population dynamic model of *Calanus finmarchicus* to a circulation model for the Georges Bank region. Fisheries Oceanography 7:219-234

Moore AR (1912) Concerning negative phototropism in *Daphnia pulex*. Journal of Experimental Zoology 13:573-575

Moore B (1909) Reactions of marine organisms in relation to light and phosphorescence Proceedings and Transactions of the Liverpool Biological Society, p 1-34

Nicholls A (1933) On the biology of *Calanus finmarchicus*. I. Reproduction and seasonal distribution in the Clyde Sea area during 1932. Journal of the Marine Biological Association of the United Kingdom 19:83-110

Nilsen F, Cottier F, Skogseth R, Mattsson S (2008) Fjord–shelf exchanges controlled by ice and brine production: the interannual variation of Atlantic Water in Isfjorden, Svalbard. Continental Shelf Research 28:1838-1853

Ohman MD (1990) The demographic benefits of diel vertical migration by zooplankton. Ecological Monographs 60:257-281

Ohman MD, Frost BW, Cohen EB (1983) Reverse diel vertical migration: an escape from invertebrate predators. Science 220:1404-1407

Oplinger JT, Heine DL, Lam MS (1999) In search of speculative thread-level parallelism Parallel Architectures and Compilation Techniques, 1999 Proceedings 1999 International Conference on. IEEE, p 303-313

Osgood KE, Frost BW (1994) Ontogenetic diel vertical migration behaviors of the marine planktonic copepods *Calanus pacificus* and *Metridia lucens*. Marine Ecology Progress Series 104:13-25

Østvedt OJ (1955) Zooplankton investigations from weather ship M in the Norwegian Sea, 1948-49. Hvalrådets Skrifter 40:1-93

Ostwald W (1902) The theory of plankton (*in German*). Biologisches Zentralblatt 22:596-605

Parker GH (1902) The reactions of copepods to various stimuli and the bearing of this on daily depth-migrations. Bulletin of United States Fish Commission 22:103-123

Pearre S (1979) Problems of detection and interpretation of vertical migration. Journal of Plankton Research 1:29-44

Pearre S (2003) Eat and run? The hunger/satiation hypothesis in vertical migration: history, evidence and consequences. Biological Reviews 78:1-79

Pedersen G, Tande KS, Ottesen G (1995) Why does a component of *Calanus finmarchicus* stay in the surface waters during the overwintering period in high latitudes? ICES Journal of marine Science 52:523-531

Pertsova N, Kosobokova K (2003) Zooplankton of the White Sea: features of the composition and structure, seasonal dynamics, and the contribution to the formation of matter fluxes. Oceanology 43:S108-S122

Plourde S, Runge J (1993) Reproduction of the planktonic copepod *Calanus finmarchicus* in the Lower St. Lawrence Estuary: relation to the cycle of phytoplankton production and evidence for a *Calanus* pump. Marine Ecology Progress Series:217-227

Poole H (1925) On the photo-electric measurement of submarine illumination Scientific Proceedings of the Royal Dublin Society, p 99-115

Poole H, Atkins W (1926) On the Penetration of Light into Sea Water. Journal of the Marine Biological Association of the United Kingdom 14:177-198

R Core Team (2016) R: A Language and Environment for Statistical Computing 3.3.1 https://www.R-project.org/

Rardin RL, Uzsoy R (2001) Experimental evaluation of heuristic optimization algorithms: A tutorial. Journal of Heuristics 7:261-304

Record NR, Pershing AJ, Runge J, Mayo C, Monger BC, Chen C (2010) Improving ecological forecasts of copepod community dynamics using genetic algorithms. Journal of Marine Systems 82:96-110

Richter C (1995) Seasonal changes in the vertical distribution of mesozooplankton in the Greenland Sea Gyre (75°N): distribution strategies of calanoid copepods. ICES Journal of Marine Science 52:533-539

Ringelberg J (2009) Diel vertical migration of zooplankton in lakes and oceans: causal explanations and adaptive significances. Springer Science & Business Media, Dordrecht, The Netherlands

Rose M (1925) Contribution to the study of plankton biology: the problem of diel vertical migration (*in French*). Archives de zoologie expérimentale et générale 64:387-401

RStudio Team (2016) RStudio: Integrated Development Environment for R 1.0.136 http://www.rstudio.com/

Runge J, Ingram RG (1991) Under-ice feeding and diel migration by the planktonic copepods *Calanus glacialis* and *Pseudocalanus minutus* in relation to the ice algal production cycle in southeastern Hudson Bay, Canada. Marine Biology 108:217-225

Russell FS (1926) The Vertical Distribution of Marine Macroplankton IV. The Apparent Importance of Light Intensity as a Controlling Factor in the Behaviour of Certain Species in the Plymouth Area. Journal of the Marine Biological Association of the United Kingdom 14:415-440

Russell FS (1927) The vertical distribution of plankton in the sea. Biological Reviews 2:213-262

Rykiel EJ (1996) Testing ecological models: the meaning of validation. Ecological Modelling 90:229-244

Sainmont J, Andersen KH, Thygesen UH, Fiksen Ø, Visser AW (2015) An effective algorithm for approximating adaptive behavior in seasonal environments. Ecological Modelling 311:20-30

Sameoto DD, Wiebe PH, Runge J, Postel L, Dunn J, Miller CB, Coombs S (2000) Collecting Zooplankton. In: Harris R, Wiebe PH, Lenz J, Skjoldal HR, Huntley M (eds) ICES Zooplankton Methodology Manual. Adademic Press, San Diego, CA, USA, p 55-83

Satterlie RA, Labarbera M, Spencer AN (1985) Swimming in the Pteropod Mollusc, *Clione limacina* I. Behaviour and Morphology. Journal of Experimental Biology 116:189-204

Schmidtlein R (1879) Comparative survey of the appearance of larger pelagic animals during the years 1875/77 (*in German*). Mittheilungen aus der Zoologischen Station zu Neapel 2:162-175

Schmitt FG, Seuront L (2001) Multifractal random walk in copepod behavior. Physica A: Statistical Mechanics and its Applications 301:375-396

Seuront L, Brewer MC, Strickler JR (2003) Quantifying zooplankton swimming behavior: the question of scale. In: Seuront L, Strutton PG (eds) Handbook of scaling methods in aquatic ecology: measurement, analysis, simulation. CRC Press, Boca Raton, FL, USA, p 333-360

Sims DW, Southall EJ, Richardson AJ, Reid PC, Metcalfe JD (2003) Seasonal movements and behaviour of basking sharks from archival tagging: no evidence of winter hibernation. Marine Ecology Progress Series 248:187-196

Skjoldal HR, Wiebe PH, Foote KG (2000) Sampling and Experimental Design. In: Harris R, Wiebe PH, Lenz J, Skjoldal HR, Huntley M (eds) ICES Zooplankton Methodology Manual. Adademic Press, San Diego, CA, USA, p 33-49

Smith RJ, Moore FR (2005) Arrival timing and seasonal reproductive performance in a long-distance migratory landbird. Behavioral Ecology and Sociobiology 57:231-239

Soetaert K, Herman PMJ (2009) A Practical Guide to Ecological Modelling Using R as a Simulation Platform. Springer Science and Business Media, Yerseke, The Netherlands

Sømme JD (1934) Animal plankton of the Norwegian coast waters and the open sea. I. Production of *Calanus finmarchicus* (Gunner) and *Calanus hyperboreus* (Krøyer) in the Lofoten Area. Fiskeridirektoratets skrifter, Serie Havundersøkelser 4:1-163

Søreide JE, Falk-Petersen S, Hegseth EN, Hop H, Carroll ML, Hobson KA, Błachowiak-Samołyk K (2008) Seasonal feeding strategies of *Calanus* in the high-Arctic Svalbard region. Deep Sea Research Part II: Topical Studies in Oceanography 55:2225-2244

Strand E, Huse G, Giske J (2002) Artificial evolution of life history and behavior. The American Naturalist 159:624-644

Strickler JR (1977) Observation of swimming performances of planktonic copepods. Limnology and Oceanography 22:165-170

Tattersall WM (1911) *Schizopodous* Crustacea from the North-east Atlantic Slope: Second Supplement. Department of agriculture and technical instruction for Ireland, Harward, UK

Toivanen J, Makinen RE, Périaux J, Cloud Cedex F (1999) Multidisciplinary shape optimization in aerodynamics and electromagnetics using genetic algorithms. International Journal of Numerical Methods in Fluids 30:149-159

Torres JJ, Aarset A, Donnelly J, Hopkins TL, Lancraft T, Ainley D (1994) Metabolism of Antarctic micronektonic Crustacea as a function of depth of occurrence and season. Marine Ecology Progress Series 113:207-219

Unstad KH, Tande KS (1991) Depth distribution of *Calanus finmarchicus* and *C. glacialis* in relation to environmental conditions in the Barents Sea. Polar Research 10:409-420

Ussing HH (1938) The biology of some important plankton animals in the fjords of East Greenland: treaarsexpeditionen til Christian den X's Land 1931-34. Reitzel, Copenhagen, Denmark

van Ginneken VJT, Maes GE (2005) The European eel (*Anguilla anguilla*, Linnaeus), its Lifecycle, Evolution and Reproduction: A Literature Review. Reviews in Fish Biology and Fisheries 15:367-398

van Haren H, Compton TJ (2013) Diel Vertical Migration in Deep Sea Plankton Is Finely Tuned to Latitudinal and Seasonal Day Length. PloS one 8:e64435

Varpe Ø (2012) Fitness and phenology: annual routines and zooplankton adaptations to seasonal cycles. Journal of Plankton Research 34:267-276

Varpe Ø, Fiksen Ø (2010) Seasonal plankton–fish interactions: light regime, prey phenology, and herring foraging. Ecology 91:311-318

Vinogradov M (1959) Vertical migration of deep sea zooplankton (*translated from Russian*). Science summaries: Achievements in Oceanography 1:111-140

Visser AW (2001) Hydromechanical signals in the plankton. Marine Ecology Progress Series 222:1-24

Visser AW, Jonasdottir S (1999) Lipids, buoyancy and the seasonal vertical migration of *Calanus finmarchicus*. Fisheries Oceanography 8:100-106

Weismann A (1874) Animal life in Lake Constance (*in German*). Zeitschrift Fur Wissenschartliche Zoologie 24:404-435

Werner EE, Gilliam JF, Hall DJ, Mittelbach GG (1983) An Experimental Test of the Effects of Predation Risk on Habitat Use in Fish. Ecology 64:1540-1548

Wiborg KF (1954) Investigations on Zooplankton in Coastal and Offshore Waters of Western and Northwestern Norway-With Special Reference to the Copepods. Fiskeridirektoratets skrifter, Serie Havundersøkelser 11:1-244

Wickham H (2015) Advanced R. CRC Press, New York, USA

Williamson CE, Fischer JM, Bollens SM, Overholt EP, Breckenridge JK (2011) Toward a more comprehensive theory of zooplankton diel vertical migration: Integrating ultraviolet radiation and water transparency into the biotic paradigm. Limnology and Oceanography 56:1603-1623

Williamson D, Williamson J, Ngwamotsoko KT (1988) Wildebeest migration in the Kalahari. African Journal of Ecology 26:269-280

Worthington EB (1931) Vertical movements of fresh-water Macroplankton. Internationale Revue der gesamten Hydrobiologie und Hydrographie 25:394-436

Yu H (2002) Rmpi: parallel statistical computing in R. R News 2:10-14

Zanakis SH, Evans JR (1981) Heuristic “optimization”: Why, when, and how to use it. Interfaces 11:84-91

Zaret TM, Suffern JS (1976) Vertical migration in zooplankton as a predator avoidance mechanism. Limnology and Oceanography 21:804-813

Zink RM (2002) Towards a framework for understanding the evolution of avian migration. Journal of Avian Biology 33:433-436

Paper-I

Vol. 555: 49–64, 2016
doi: 10.3354/meps11831

MARINE ECOLOGY PROGRESS SERIES
Mar Ecol Prog Ser

Published August 18

Seasonal vertical strategies in a high-Arctic coastal zooplankton community

Kanchana Bandara[1,*], Øystein Varpe[2,3], Janne E. Søreide[2], Jago Wallenschus[2], Jørgen Berge[2,4], Ketil Eiane[1]

[1]Faculty of Biosciences and Aquaculture, Nord University, 8049 Bodø, Norway
[2]The University Centre in Svalbard (UNIS), 9171 Longyearbyen, Norway
[3]Akvaplan-niva, Fram Centre, 9296 Tromsø, Norway
[4]Faculty of Biosciences, Fisheries and Economics, UiT The Arctic University of Norway, 9037 Tromsø, Norway

ABSTRACT: We studied the larger (>1000 µm) size fraction of zooplankton in an Arctic coastal water community in Billefjorden, Svalbard (78° 40′ N), Norway, in order to describe seasonal vertical distributions of the dominant taxa in relation to environmental variability. *Calanus* spp. numerically dominated the herbivores; *Aglantha digitale*, *Mertensia ovum*, *Beroë cucumis*, and *Parasagitta elegans* were the dominant carnivores. Omnivores and detritivores were numerically less important. Descent to deeper regions of the water column (>100 m) between August and October, and ascent to the shallower region (<100 m) between November and May was the overall seasonal pattern in this zooplankton community. In contrast to other groups, *P. elegans* did not exhibit pronounced vertical migrations. Seasonal vertical distributions of most species showed statistical associations with the availability of their main food source. The vertical distribution of later developmental stages of *Calanus* spp. was inversely associated with fluorescence, indicating that they descended from the shallower region while it was still relatively productive, and ascended before the primary production had started to increase. Strong associations between the vertical distributions of secondary consumer *M. ovum* and *Calanus* spp., and tertiary consumer *B. cucumis* and *M. ovum* indicated that these carnivores seasonally followed their prey through the water column. We conclude that seasonal vertical migrations are a widespread trait in the high Arctic community studied, and predator–prey interactions seem particularly central in shaping the associations between the seasonal vertical strategies of adjacent trophic levels.

KEY WORDS: Seasonal vertical migration · Food availability · Trophic interactions · Pelagic environments · Predator–prey interactions

INTRODUCTION

Pronounced seasonal oscillations in abiotic (e.g. solar radiation, temperature, sea ice) and biotic (e.g. food availability, predation pressure) environments offer challenges to zooplankton in high latitudes. In particular, seasonality in food availability is believed to be a significant challenge (Clarke & Peck 1991, Conover & Huntley 1991, Hagen 1999, Varpe 2012). Arctic zooplankton possess adaptations to counter a seasonally variable food supply, such as energy storage (Lee et al. 2006, Varpe et al. 2009), diapause (Carlisle 1961, Hirche 1996), and seasonal vertical migrations (Conover 1988). Zooplankton seasonal vertical migrations are understood as an adaptive behavior that optimizes their position in the water column in response to seasonal variability in the environment (Werner & Gilliam 1984). We refer to this behavior as their 'seasonal vertical strategy'. Seasonal vertical strategies of some high-latitude herbivorous zooplankton are well-documented (e.g. Conover 1988, Falk-Petersen et al. 2009), and their adap-

*Corresponding author: kanchana.bandara@nord.no

Publisher: Inter-Research · www.int-res.com

tive value has also been analyzed in modeling studies (e.g. Fiksen 2000, Varpe et al. 2007).

The underlying regulation of zooplankton seasonal vertical strategies has been a subject of interest since early 1900s (Russell 1927, Banse 1964). Seasonal variability in hydrography (Hirche 1991), photoperiod (Sømme 1934, Miller et al. 1991), and visual predation (Kaartvedt 1996, Dale et al. 1999, Kaartvedt 2000) are some external environmental cues that are thought to regulate seasonal vertical strategies. Internal (endogenous) regulation through seasonal changes in gonad development (Østvedt 1955), lipids and buoyancy (Visser & Jónasdóttir 1999), and long-term endogenous timers (Miller et al. 1991, Hirche 1996) have also been suggested.

Many components of zooplankton life strategies are viewed as adaptations to seasonal variations in food supply (Ji et al. 2010, Varpe 2012), but the influence of food availability on seasonal vertical strategies remains poorly understood, particularly for carnivorous species. As the seasonal food supply is more pronounced for Arctic herbivorous zooplankton (Conover & Huntley 1991, Hagen 1999), whose energetic demands mainly depend on a short period of annual primary production (Falk-Petersen et al. 2009), it can be argued that their seasonal vertical strategies are tightly coupled with food availability. Although vertical distributions of *Calanus* spp. appear to be associated with food availability (chlorophyll *a* distributions) in spring (Herman 1983, Søreide et al. 2008, Basedow et al. 2010), it is less well-studied for the rest of the year. Compared to herbivores, Arctic carnivorous and omnivorous zooplankton rely to a greater extent on a year-round food supply (Hagen 1999). Therefore, it has been suggested that their seasonal adaptations are less pronounced compared to herbivores (Ji et al. 2010, Varpe 2012). As vertical distributions vary seasonally in a number of carnivorous hydromedusae (e.g. Pertsova et al. 2006), ctenophores (e.g. Siferd & Conover 1992), chaetognaths (e.g. Grigor et al. 2014), euphausiids (e.g. Lass et al. 2001), and copepods (e.g. Vestheim et al. 2005), it appears that seasonal vertical strategies of Arctic carnivorous zooplankton are more diverse than previously thought. Since many carnivores rely on herbivores as their main food source, the potential influence of the vertical strategies of herbivorous zooplankton on their predators may be ecologically significant. This is portrayed in the findings of Nelson et al. (1997) and Sims et al. (2005), where a close resemblance between the vertical behavior of planktivorous sharks and the diel vertical migration (DVM) of herbivorous zooplankton were reported. Whether such relationships exist on seasonal timescales is not known, and open for investigation.

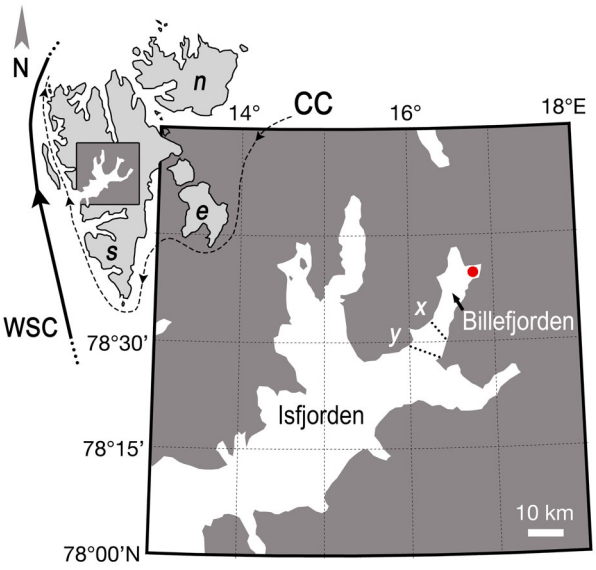

Fig. 1. Study area; sampling site is indicated by the red dot. *x* and *y* indicate coarse locations of the inner and outer sills of Billefjorden respectively. Positions of the west Spitsbergen current (WSC) and the coastal current (CC) were adopted from Svendsen et al. (2002). *s*: Spitsbergen, *n*: Nordaustlandet, *e*: Edgeøya

Investigating the seasonality of zooplankton strategies and interactions requires studying pelagic communities over the course of an annual cycle. Apart from a few studies (e.g. Hop et al. 2006), year-round zooplankton community investigations are rare in the Arctic. Here, we investigated seasonal vertical distributions of the dominant herbivore and carnivore zooplankton in a high-latitude coastal zooplankton community during a 10-month period in 2008 and 2009. We studied the extent to which the seasonal vertical distributions of the above zooplankton could be explained by the seasonal dynamics of their primary food source, or physical environmental variables such as temperature, salinity, and irradiance.

MATERIALS AND METHODS

Study site

Environmental variables and zooplankton samples were collected monthly between August 2008 and May 2009 at a 189 m deep station (78° 39.72′ N, 16° 44.34′ E) within the inner basin of Billefjorden, located at the west coast of Spitsbergen, the largest island in the Svalbard archipelago (Fig. 1). The inner basin of Billefjorden remains ice-covered from ca.

December to June (Arnkværn et al. 2005). Two 50 to 70 m deep sills located near the mouth of the fjord (Fig. 1) act as a topographical barrier that hinders the advection of the Atlantic water masses into Billefjorden (Cottier et al. 2005, Nilsen et al. 2008). Because of this, Arnkværn et al. (2005) argued that zooplankton population dynamics in Billefjorden are influenced more by internal processes than by advection.

Environmental variables

Temperature and salinity were profiled *in situ* using either a CTD/STD model DS 204 (SAIV) or a Seabird™ CTD (Sea-Bird Electronics). Since no CTDs were deployed on 27 August and 07 September 2008, and 23 March 2009 (Table 1), we obtained temperature and salinity data for these dates from a moored instrument series (www.sams.ac.uk/oceans-2025/arctic-mooring) deployed <0.5 nautical miles away (78° 39.76′ N, 16° 11.24′ E) from the sampling site (see Supplement 1 at www.int-res.com/articles/suppl/m555p049_supp.pdf). We measured photosynthetically active radiation (PAR) from a QSP 2300 log quantum scalar irradiance sensor (Biospherical Instruments), and fluorescence from a Seapoint™ chlorophyll fluorometer (Seapoint Sensors) affixed to the above mooring at 29 m. Fluorescence could not be accurately estimated due to the lack of fluorometer calibration coefficients for most of the year. Therefore, raw voltage outputs of the fluorometer were presented as normalized values between 0 and 1 after removing some extreme readings (sensor noise). This provided an approximate variation of the fluorescence during the study, because according to the calibration equation (Seapoint Sensors; data not shown), fluorescence is estimated as a linear function of the voltage outputs.

Raw voltage outputs (O_i) of the irradiance sensor were converted to PAR by applying a wet calibration factor ($C = 5.05 \times 10^{12}$), and a dark voltage of 0.0130 V (Biospherical Instruments) as:

$$\mathrm{PAR} = C(10^{O_i} - 10^{0.0130}) \quad (1)$$

Temperature and salinity measurements were visualized using the Spatial Analyst™ extension of ArcGIS™ version 9.3 (ESRI). Here, the data were interpolated temporally over the depth range using the natural neighbor method (Sibson 1981). Fluorescence and PAR data are presented as daily means. Sea ice charts developed by the Ice Information Portal of the Norwegian Metrological Institute (http://polarview.met.no/) were used to describe the sea ice extent in Billefjorden during the study period.

Table 1. Zooplankton samples and CTD casts collected during the study. A sample is a depth-stratified 0–180 m net haul. Day samples (D) were collected between 11:00 and 17:00 h; night samples (N), between 23:00 and 04:00 h local time (UTC + 1). Note that the lack of CTD data in August, September, and March (dashes in the rightmost column) were compensated by the data of the mooring (see Supplement 1 at www.int-res.com/articles/suppl/m555p049_supp.pdf)

Date (dd/mm/yyyy)	No. of Samples	Time of collection	CTD casts
27/08/2008	1	N	–
07/09/2008	2	D + N	–
23/09/2008	2	D + N	x
17/10/2008	3	D + N	x
04/11/2008	2	D + N	x
03/12/2008	2	D + N	x
14/01/2009	1	D + N	x
26/02/2009	3	D + N	x
23/03/2009	1	N	–
30/03/2009	1	D	x
20/04/2009	1	D	x
27/04/2009	1	D	x
04/05/2009	1	D	x

Zooplankton

Zooplankton were sampled by vertical hauls using a WP-3 net (area of the opening: 1 m^2; mesh size: 1 mm) fitted with a Nansen-type messenger-operated closing device. Samples were taken from the vessel, or with a tetrapod-mounted cable towed by a snowmobile at ca. 1 m s^{-1} when sampling from sea ice. Three depth strata were sampled (0–50, 50–100, and 100–180 m), excluding the bottommost 10 m. Larger (>10 mm) gelatinous zooplankton that could dissolve upon formaldehyde preservation were identified, and their body lengths were measured immediately after collection. The rest of the samples were preserved in a borax-buffered 4% formaldehyde-in-seawater solution.

In the laboratory, the larger specimens were counted from the entire samples. The smaller and more numerous individuals (predominantly copepods) were counted in subsamples obtained using a box splitter (Motoda 1985) until a minimum of 100 individuals were counted per sample. On average, ~24% (range: 0.15 to 100%) of the total sample volume was used. Zooplankton were identified to the lowest possible taxonomic level, and classified into trophic groups according to the literature (see Table 2).

Prosome lengths (PL) of copepods were measured to the nearest 0.1 mm using a stereomicroscope (Leica Microsystems). We measured bell heights (BH) of hydromedusae and total lengths (TL) of other zooplankton. The copepodite stage 4 (CIV) and older developmental stages of *Calanus hyperboreus* (which were the only stages captured in this species) were identified by the presence of an acute spine on their fifth thoracic segment (e.g. Parent et al. 2011). The rest of the *Calanus* spp. were identified by a length frequency analysis following Arnkværn et al. (2005) using the R (R Core Team 2013) package 'mixdist' v.0.5-4 (Macdonald & Du 2012). We used the PLs of 3908 CVs, 1409 adult females, and 387 adult males of *Calanus* spp. pooled over the study period for the analysis. PL boundaries derived by the length frequency analysis were evaluated against those published in relevant literature to distinguish species. We also used this method on monthly pooled length measurements (BH or TL) of other taxa to identify any size groups.

Zooplankton abundances (ind. m^{-3}) were estimated assuming 100% filtration efficiency of the WP-3 net. Monthly mean abundances were used in data presentation and analyses. This was estimated by averaging the total abundance of a given taxon in a given month over the number of samples (i.e. net hauls) collected in that month (Table 1).

Seasonal vertical distributions of the dominant zooplankton species (i.e. those that contributed >0.1% of the total numerical abundance [corresponding to 5 ind. m^{-3}], and were captured more or less throughout the investigation) were presented as monthly mean abundances in each depth stratum. Since the relative abundance of dominant taxa in each depth stratum in day and night replicate samples (Table 1) varied <9%, the mean abundances of the replicates were used in the presentation and analyses of seasonal vertical distributions.

Seasonal vertical strategies

In order to describe zooplankton seasonal vertical distributions as seasonal vertical strategies, we described the water column in 2 regions: a shallower region (0 to 100 m), and a deeper region (100 to 180 m). We considered the maximum sill depth of the fjord (~70 m), maximum thermohaline stratification depth (~80 m) recorded in the study, and the vertical resolution of our sampling design (minimum 50 m) in making the above discrimination. We estimated a vertical distribution index (V) for each species by taking the difference between the population proportions of the 2 vertical regions in each month as:

$$V = \frac{(N_{0-100} - N_{100-180})}{(N_{0-100} + N_{100-180})} \quad (2)$$

where N_{0-100} and $N_{100-180}$ represent the monthly mean abundance of the shallow and deeper regions of the water columns, respectively. V ranges between −1 and 1, in which the upper limit represents the entire population distributed in the shallower region of the water column, and the lower limit represents the opposite scenario. Here we assumed the influences of zooplankton advection in and out of this community to be negligible (see Supplement 2 at www.int-res.com/articles/suppl/m555p049_supp.pdf), and therefore, the dynamics of V over the time series is primarily due to the vertical migration of zooplankton across the 2 vertical regions.

We used correlation analyses to describe the association between the monthly vertical distribution indices of the dominant taxa and physical (i.e. mean temperature, salinity, and PAR) and biological (availability of the main food source) environmental variables, assuming a linear association between the above. We tested the above variables for normality (Shapiro-Wilk test; Shapiro & Wilk 1965), and homoscedasticity (2-sample Levene's test; Levene 1960), and found that most variables violated the assumptions of parametric correlation tests. Therefore, we used the nonparametric Kendall's rank correlation test with adjustment to tied ranks (coefficient = τ_b) (Kendall 1938, 1945) in the analyses.

RESULTS

Environmental variables

The inner basin of Billefjorden was covered with land-fast sea ice from late December 2008 until the end of the investigation in May 2009 (Fig. 2a). Maximum PAR and fluorescence values were recorded between August and September, and decreased to 0.2 µmol m^{-2} s^{-1} and 0.10 units respectively after November (Fig. 2a,b). Pronounced thermo-haline stratifications observed in the early part of the study broke down between November and January, and resulted in a well-mixed, cold (<−1.0°C), and relatively high saline (>34 PSU) water column (Fig. 2c,d). This lack of stratification persisted until the end of sampling.

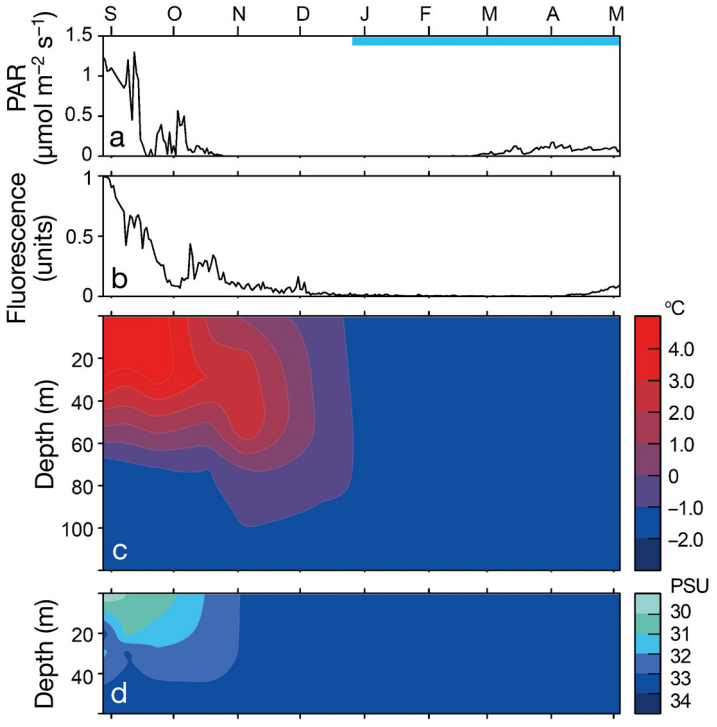

Fig. 2. Seasonal variability in (a) photosynthetically active radiation (PAR), (b) fluorescence (normalized between 0 and 1 unit), (c) temperature, and (d) salinity during the study. The blue bar in (a) indicates the period of land-fast sea ice cover. The ordinates of (c) and (d) are cropped at 120 and 60 m respectively due to the prevailing homogeneity of those parameters. Note that the abscissa extends from 27 August 2008 to 04 May 2009

Zooplankton community composition and trophic relationships

A total of 8 herbivores, 8 omnivores, 4 detritivores, and 17 carnivores comprised the 37 zooplankton taxa captured in this study (Table 2). The PL boundaries derived from the length–frequency analysis of *Calanus* spp. (Table 3) were in accordance with those published for *C. finmarchicus* and *C. glacialis* (see Supplement 3 at www.int-res.com/articles/suppl/m555p049_supp.pdf). Numerically, *C. glacialis* dominated the herbivore community (relative abundance ~77.6%; Table 2) alongside *C. finmarchicus* (~17%) and *C. hyperboreus* (~2%). Carnivores accounted for ~2.5% of the total numerical abundance (Table 2), and were dominated by the chaetognath *Parasagitta elegans* (~1.2%), the ctenophores *Mertensia ovum* (~0.5%) and *Beroë cucumis* (~0.4%), and the hydromedusa *Aglantha digitale* (~0.2%). Omnivorous and detritivorous zooplankton only contributed to ~1% of the total numerical abundance (Table 2).

Table 2. Zooplankton taxa captured in this study, their relative abundances, and feeding modes (references given as numbers in superscript). Indet.: indeterminate

Taxon	Feeding mode	Relative abundance (%)
Bougainvillia spp.	Carnivore[02, 42]	0.02
Halitholus spp.	Carnivore[18]	0.01
Sarsia spp.	Carnivore[42]	<0.01
Aglantha digitale	Carnivore[05, 27, 42]	0.21
Mertensia ovum	Carnivore[35, 39]	0.45
Beroë cucumis	Carnivore[22, 31]	0.36
Clione limacina	Carnivore[04, 23]	0.02
Limacina helicina	Omnivore[17, 21]	0.03
L. retroversa	Herbivore[40], omnivore[17]	<0.01
Gastropoda indet.	–	0.01
Parasagitta elegans	Carnivore[16, 24]	1.18
Eukrohnia hamata	Carnivore[07, 20]	0.08
Anonyx nugax	Scavenger[14, 19]	<0.01
Themisto abyssorum	Carnivore[16]	<0.01
T. libellula	Carnivore[32]	<0.01
Amphipoda indet.	–	<0.01
Munnopsis spp.	Herbivore/detritivore[28]	<0.01
Isopoda indet.	–	<0.01
Mysidae indet.	–	0.03
Meganyctiphanes norvegica	Carnivore[03, 10]	<0.01
Thysanoessa inermis	Herbivore[03, 19]	0.11
T. longicaudata	Omnivore[11, 36]	<0.01
T. raschii	Omnivore[09, 10]	<0.01
Eualus gaimardii	Carnivores[29, 37]	<0.01
Pandalus borealis	Omnivore[15]	<0.01
Necora puber	Carnivore[26, 41]	<0.01
Hyas spp.	Carnivore/scavenger[43]	<0.01
Calanus sp.	–	0.11
Calanus finmarchicus	Herbivore[25, 38]	16.92
C. glacialis	Herbivore[25, 38]	77.56
C. hyperboreus	Herbivore[25, 38]	2.02
Microcalanus spp.	Herbivore/detritivore[13]	<0.01
Pseudocalanus spp.	Herbivore[34]	<0.01
Paraeuchaeta norvegica	Carnivore[30, 33]	<0.01
Metridia longa	Omnivore[01]	0.86
Oikopleura spp.	Particle feeder/omnivore[06]	<0.01
Leptoclinus spp. (larvae)	Carnivore[12]	<0.01

References (in chronological order): [01]Haq (1967); [02]Fraser (1969); [03]Ackman et al. (1970); [04]Conover & Lalli (1972); [05]Smedstad (1972); [06]Alldredge (1976); [07]Sullivan (1980); [08]Falk-Petersen et al. (1981); [09]Sargent & Falk-Petersen (1981); [10]Falk-Petersen et al. (1982); [11]: Williams & Lindley (1982); [12]Eschmeyer et al. (1983); [13]Hopkins (1985); [14]Sainte-Marie & Lamarche (1985); [15]Shumway et al. (1985); [16]Falk-Petersen et al. (1987); [17]Lalli & Gilmer (1989); [18]Larson & Harbison (1989); [19]Sainte-Marie et al. (1989); [20]Øresland (1990); [21]Gilmer & Harbison (1991); [22]Purcell (1991); [23]Hermans & Satterlie (1992); [24]Alvarez-Cadena (1993); [25]Graeve et al. (1994); [26]Freire & Gonzalez-Gurriaran (1995); [27]Pagès et al. (1996); [28]Brusca (1997); [29]Graeve et al. (1997); [30]Olsen et al. (2000); [31]Falk-Petersen et al. (2002); [32]Auel & Werner (2003); [33]Skarra & Kaartvedt (2003); [34]Lischka & Hagen (2005); [35]Lundberg et al. (2006); [36]Blachowiak-Samolyk et al. (2007); [37]Nygård et al. (2007); [38]Falk-Petersen et al. (2009); [39]Graeve et al. (2008); [40]Bernard & Froneman (2009); [41]Silva et al. (2010); [42]Prudkovsky (2013); [43]Boxshall et al. (2015)

Table 3. Prosome length boundaries (mm) used to separate the 2 *Calanus* taxa, with their % composition within each developmental stage in parentheses. The rightmost column presents chi-squared statistic of the fitted model with the degrees of freedom in parentheses. $^{*}p < 0.05; ^{**}p < 0.01; ^{***}p < 0.001$

Developmental stage	Prosome length (% composition) *C. finmarchicus*	*C. glacialis*	χ^2 (df)
CV	2.45–2.98 (38.96)	≥2.98 (59.74)	187.97** (11)
Adult females	2.38–2.92 (16.64)	≥2.92 (83.24)	54.47** (13)
Adult males	≤3.04 (7.20)	>3.04 (92.08)	19.55* (10)

Based on the literature, we considered fluorescence as an indicator of the primary food source for herbivorous zooplankton, and identified *Calanus* spp. as the main prey of the secondary consumers *A. digitale*, *M. ovum*, and *P. elegans*, and *M. ovum* as that of the tertiary consumer *B. cucumis* (see references in Table 2).

Seasonal variability in abundance of the dominant zooplankton

Herbivores

The highest mean abundances of *C. finmarchicus* (~100 ind. m^{-3}), *C. glacialis* (~430 ind. m^{-3}), and *C. hyperboreus* (~13 ind. m^{-3}) were recorded between August and November (Fig. 3a–c). During this period, CV was the dominant developmental stage of *C. finmarchicus* and *C. glacialis* (>95%: Fig. 3d,e). After November, relative abundance of CV decreased, and adult male and female copepodites increased. In *C. hyperboreus*, CIV was the dominant developmental stage throughout the study (Fig. 3f).

Carnivores

The mean abundances of *A. digitale* and *M. ovum* peaked at ~4 ind. m^{-3} in October (Fig. 4a,b). *B. cucumis* was captured in relatively large numbers (mean abundance: ~2.5 ind. m^{-3}) in October and May (Fig. 4c). We could not identify any size groups of the 3 above species from length–frequency analyses. However, their abundance peaks were dominated by relatively small individuals (mean ± SD body length: 6.6 ± 1.5 mm for *A. digitale*, 6.7 ± 5.3 mm for *M. ovum*, and 2.9 ± 1.6 mm for *B. cucumis*; Fig. 4 e–g). The mean body lengths of *A. digitale* and *M. ovum* increased throughout the study period, while that of *B. cucumis* decreased after reaching a maximum (9.31 ± 6.4 mm) in November. *P. elegans* was captured in higher numbers in September (~5.5 ind. m^{-3}), December (~4.5 ind. m^{-3}), and between April and May

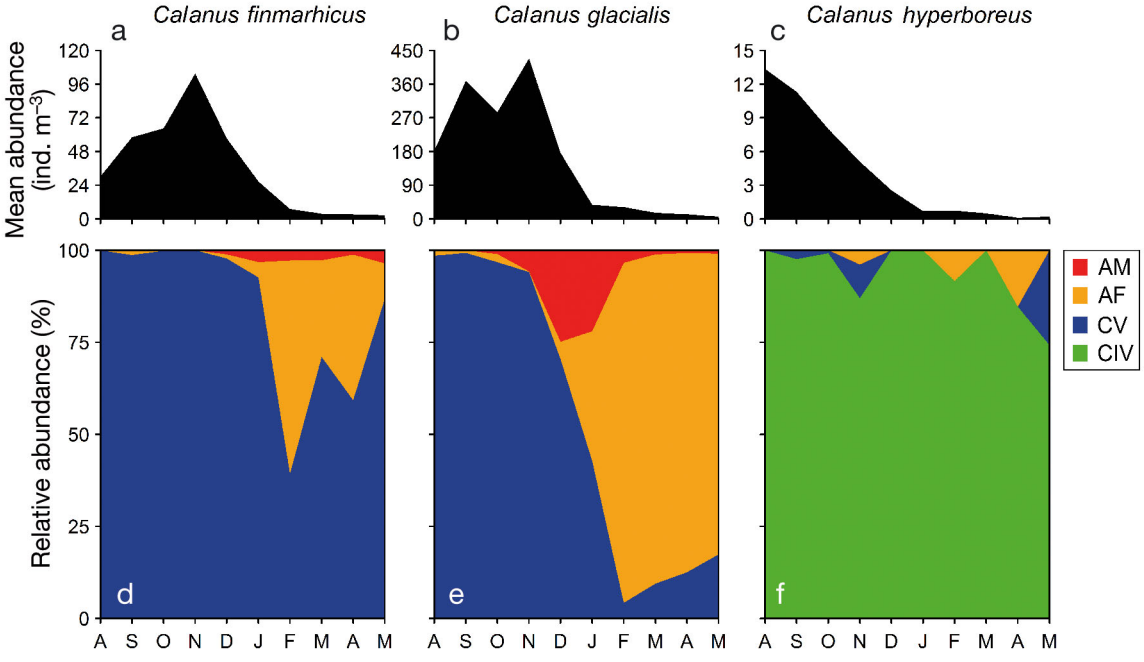

Fig. 3. Seasonal variability in (a–c) mean abundance and (d–f) relative developmental stage composition of dominant herbivores during the study. AM: adult males; AF: adult females; CV and CIV: copepodite stage 5 and 4, respectively

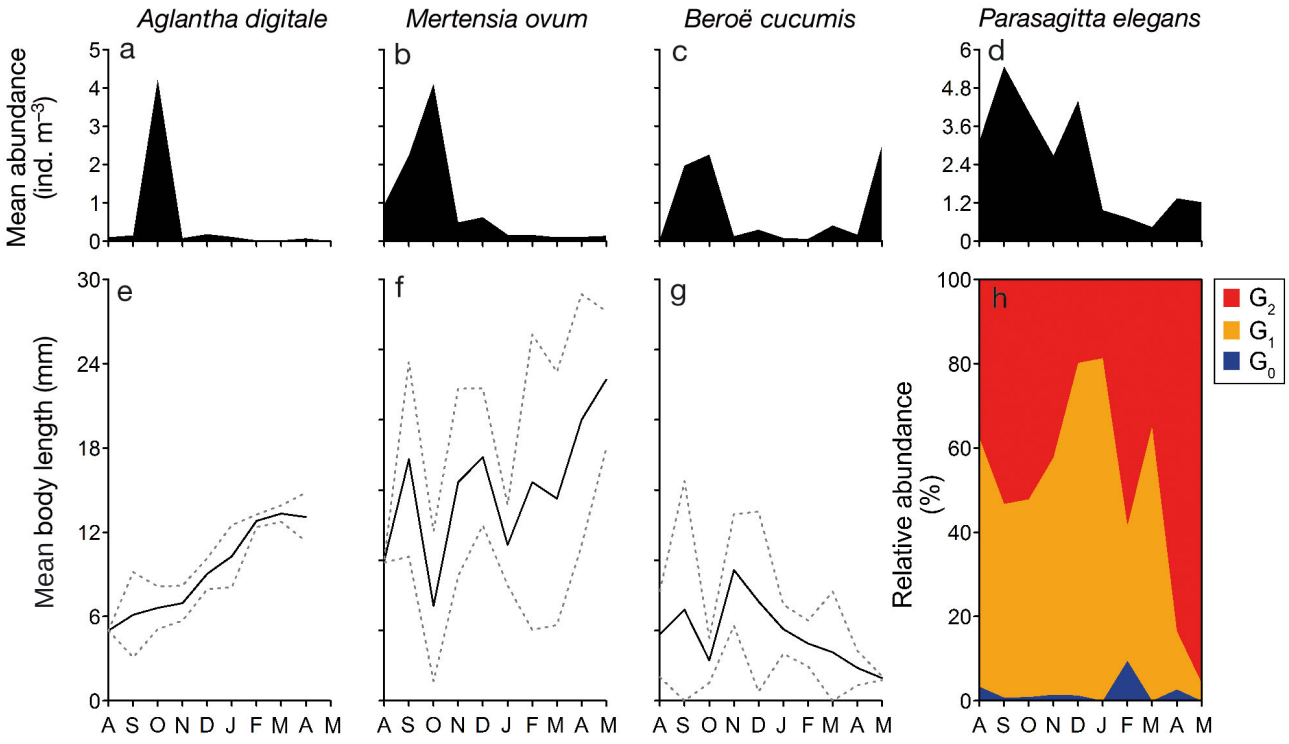

Fig. 4. Seasonal variability in (a–d) mean abundance and (e–h) mean body length of dominant carnivores during the study. Body lengths are presented as bell height for *A. digitale* and total length (TL) for other species. The TL dynamics of *P. elegans* in (h) is presented as variation in relative abundance of the 3 size groups. Dashed lines in (e–g) denote standard deviation of body length (mm)

(~1.5 ind. m^{-3}) (Fig. 4d). We derived 3 size groups for *P. elegans* from the length–frequency analysis (G_0, G_1, and G_2: see Supplement 4 at www.int-res.com/articles/suppl/m555p049_supp.pdf). The first abundance peak was composed of more or less equal proportions of the 2 relatively large size groups (G_1: mean ± SD TL: 23.4 ± 1.8 mm; G_2: 34.2 ± 1.4 mm), with G_1 dominating ~80% of the second abundance peak (Fig. 4h). The relative abundance of G_2 increased from January to >80% in April and May, while the smallest size group (G_0: 14.7 ± 1.2 mm) remained less prominent (<10%) throughout the investigation.

Seasonal variability in vertical distribution of the dominant zooplankton

Herbivores

Between August and November, the mean abundance of *C. finmarchicus* (CV) and *C. glacialis* (CV and adult females) in the lower 80 m of the water column gradually increased (Fig. 5a,b). Conversely, the mean abundance of these 2 species in the upper 100 m decreased from August, and reached a minimum in October, during which their vertical distribution indices were at the lowest (V ~ –0.9; Fig. 6a,b). From November onwards, *C. finmarchicus* and *C. glacialis* CVs had relocated to the upper 100 m along with adult copepodites. By February, the vertical distribution indices of these 2 species reached the maximum (V ~ 0.6 for *C. finmarchicus* and V ~ 0.8 for *C. glacialis*). Thereafter, the mean abundance of CV and adult copepodites of the above species in the upper 100 m decreased, and by the end of the investigation in May, their vertical distribution indices remained around zero. The mean abundance of CIV *C. hyperboreus* in the lower 80 m progressively decreased from August, and was only distributed in the upper 100 m between November and January (Figs. 5c & 6c). From February onwards, a few *C. hyperboreus* CIV, CV and adult female copepodites (mean abundance <1 ind. m^{-3} mo^{-1}) were relocated in the lower 80 m.

Carnivores

The mean abundance of *A. digitale*, *M. ovum*, and *B. cucumis* in the upper 100 m gradually

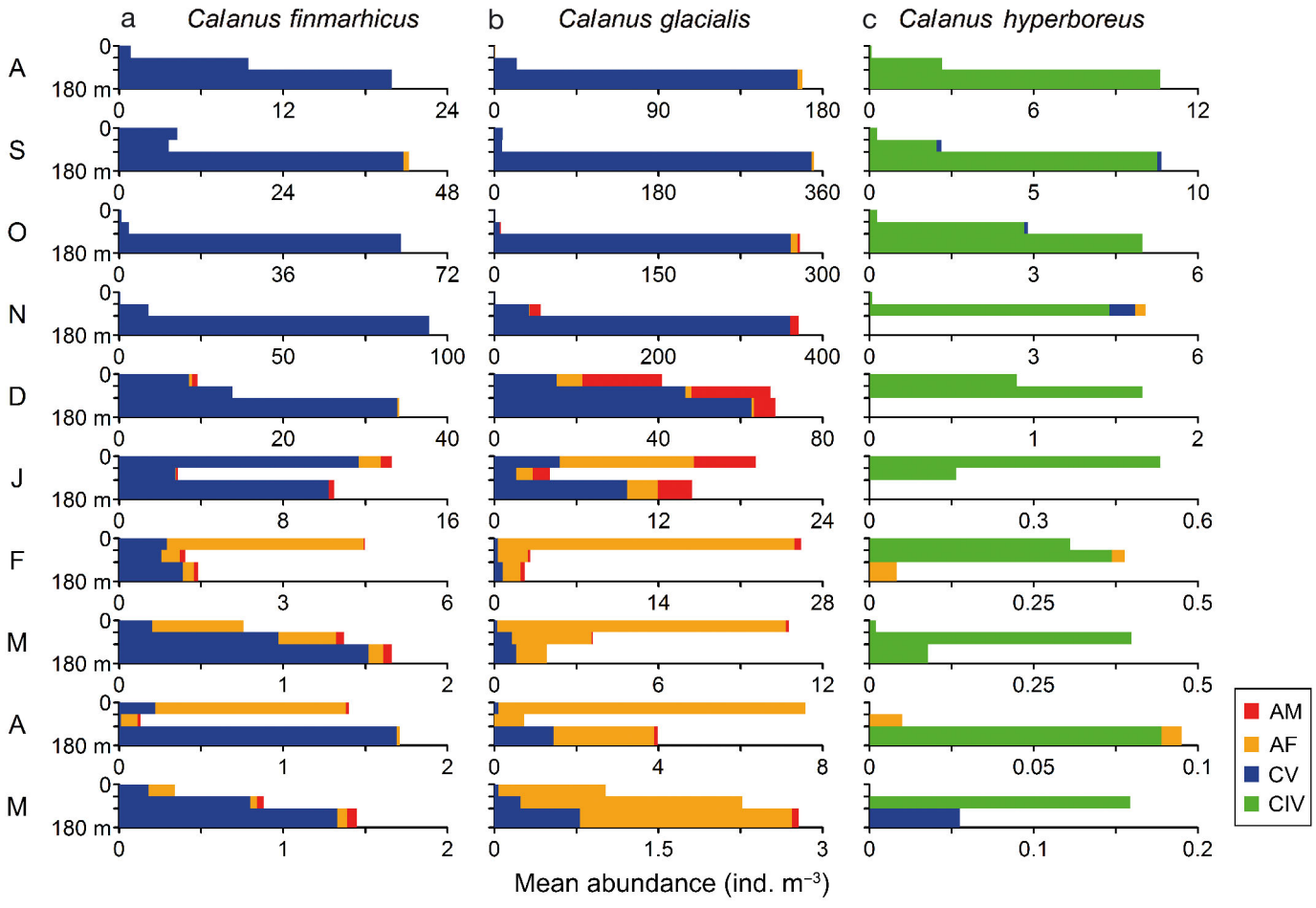

Fig. 5. Seasonal vertical distributions of dominant herbivores during the study. Ordinates represent depth (0–50, 50–100, and 100–180 m). AM: adult males, AF: adult females; CV and CIV: copepodite stage 5 and 4, respectively

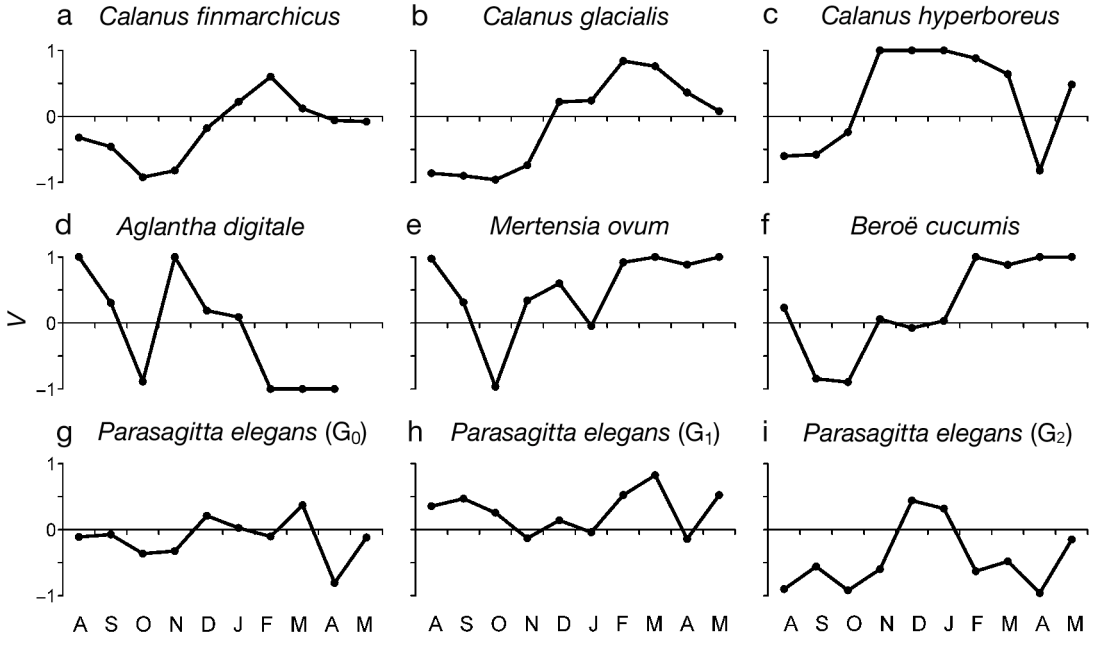

Fig. 6. Seasonal variability in the vertical distribution indices (V) of the dominant zooplankton taxa during the study. V ranges from −1 to 1, in which the latter represents the entire population distributed in the shallower region, and the latter represents the opposite scenario. *A. digitale* was not captured to compute its V in May. See Supplement 5 for more information

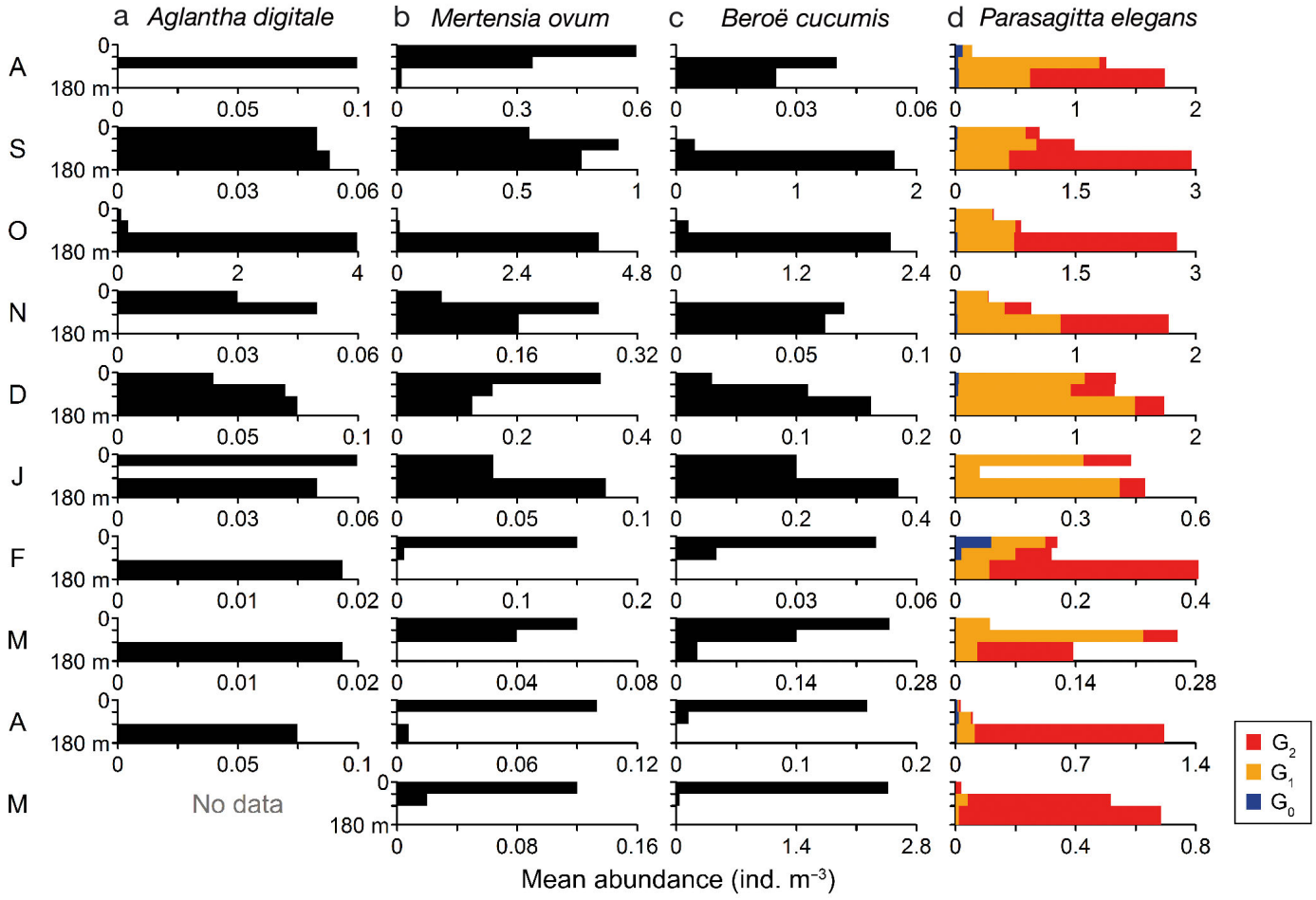

Fig. 7. Seasonal vertical distributions of dominant carnivores during the study. Ordinates represent depth (0–50, 50–100, and 100–180 m). Note that *Aglantha digitale* was not captured in May 2009

decreased from August (Fig. 7a–c), and their vertical distribution indices gradually decreased to ~–0.9 in October (Fig. 6d–f). From November onwards, the mean abundance of *M. ovum* and *B. cucumis* in the upper 100 m, and their vertical distribution indices gradually increased, and the latter remained ~1 from February until the end of sampling in May (Fig. 6e, f). Although *A. digitale* had relocated to the upper 100 m between November and January, it was captured in the lower 80 m after February (Fig. 7a). Throughout this study, *P. elegans* was captured in all 3 depth strata (Fig. 7d). The vertical distribution index of the G_2 size group of *P. elegans* remained <–0.5 for most of the time series (Fig. 6i), indicating that >75% of its population was distributed in the lower 80 m throughout the study. Conversely, the G_0 and G_1 size groups were distributed across the entire depth range (Fig. 6g,h).

Seasonal vertical distributions and environmental variables

The vertical distribution index (V) of *Calanus* spp. (all species and developmental stages combined; see Table S5 in Supplement 5 at www.int-res.com/articles/suppl/m555p049_supp.pdf) showed a strong negative association with mean fluorescence (τ_b = –0.72, $p < 0.01$, n = 10), and a weak negative association with mean temperature (τ_b = –0.49, $p = 0.05$, n = 10) (Table 4, Fig. 8a). While the vertical distribution index of *M. ovum* showed a moderate positive association with that of *Calanus* spp. (τ_b = 0.51, $p = 0.04$, n = 10), we found a strong positive association between the vertical distribution indices of *B. cucumis* and *M. ovum* (τ_b = 0.71, $p < 0.01$, n = 10) (Table 4, Fig. 8b,c). The vertical distribution index of *A. digitale* showed a moderate negative association with mean temperature (τ_b = –0.57, $p = 0.04$, n = 9). Vertical distribution indices of *P. elegans* were not significantly associ-

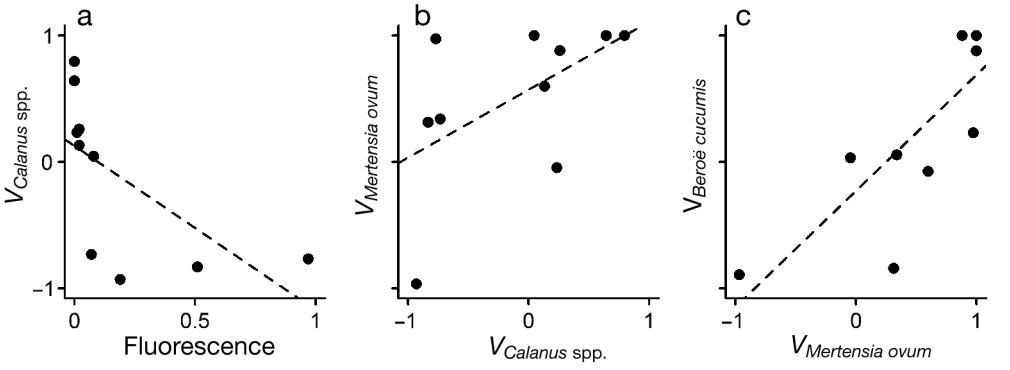

Fig. 8. Representation of statistically significant relationships between the vertical distribution indices (V) of dominant taxa and the availability of their main food source (cf. Table 4). Trend lines (dashed) were estimated by linear regression, and are solely for visualization of patterns in the data

Table 4. Associations between the vertical distribution indices (V) of dominant taxa and environmental variables presented as Kendall's rank correlation coefficients (τ_b). See Fig. 8 for additional information. PAR: photosynthetically active radiation; G_0, G_1, G_2: size groups based on length–frequency analysis; $^*p < 0.05$; $^{**}p < 0.01$

Species	Temperature	Salinity	PAR	Availability of the main food source			n
				Fluorescence	$V_{Calanus\ spp.}$	$V_{M.\ ovum}$	
Calanus spp.	−0.49*	0.31	−0.30	−0.72**	–	–	10
Aglantha digitale	−0.57*	−0.21	0.06	–	−0.53	–	9
Mertensia ovum	−0.30	0.12	0.14	–	0.51*	–	10
Beroë cucumis	−0.44	0.21	0.05	–	–	0.71**	10
Parasagitta elegans (G_0)	−0.13	0.09	−0.26	–	0.24	–	10
P. elegans (G_1)	−0.02	−0.11	0.14	–	0.04	–	10
P. elegans (G_2)	−0.13	0.27	−0.44	–	0.16	–	10

ated with any physical or biological environmental parameters that were used in our analyses (Table 4).

DISCUSSION

Seasonal patterns in vertical distributions and their relation to environmental variability

A gradual decrease in the vertical distribution index from August to October, and an increase from November to May were common to most of the investigated herbivorous (*Calanus* spp.) and carnivorous (*Aglantha digitale*, *Mertensia ovum* and *Beroë cucumis*) zooplankton taxa (Fig. 6a–f). Descent to the deeper region (>100 m) of the water column in early autumn, and ascent to the shallower region (<100 m) from late autumn to early spring was hence the overall seasonal pattern in this high Arctic zooplankton community. During their descent in the autumn, large numbers of zooplankton appeared to migrate from the warmer, sunlit, and productive shallow waters of this fjord (Fig. 2). Zooplankton abundances sharply declined during the winter (Figs. 3 & 4), and during the spring, most of the remaining individuals had ascended to a colder, darker, and unproductive water mass. As an exception, *Parasagitta elegans* did not show seasonal migrations (Fig. 6g–i).

Seasonal vertical distributions of most zooplankton taxa showed statistical associations with the availability of their main food source (Table 4, Fig. 8). The inverse association between the vertical distribution index of *Calanus* spp. and mean fluorescence indicates that they descended from the shallower region while it was relatively productive, and ascended before the primary production had started to increase (Figs. 2b & 6a–c). Therefore, it seems that the seasonal vertical strategies of the dominant herbivorous zooplankton in this study were not regulated by food (phytoplankton) availability. As vertical distribution indices of the secondary consumer *M. ovum* and *Calanus* spp., and the tertiary consumer *B. cucumis* and *M. ovum* were positively associated, we argue that these predatory zooplankton seasonally followed their prey (e.g. Fraser & David 1959, Torres et al. 1994, Hagen 1999). The seasonal vertical strategies of the above carnivores were likely regulated by seasonality in food availability (i.e. seasonal vertical strategies of their main prey), and further indicates that seasonal vertical strategies of zooplankton in lower trophic levels influence those in higher levels through trophic interactions. Still, we observed con-

siderable variability, and a lack of seasonal migrations in *P. elegans*. Consequently, numerous other factors, such as the timing and trade-offs between feeding and other life cycle events (Heath 1999, Varpe 2012), differences in prey selection (Greene 1986), feeding on alternative food sources (Hirche & Kwasniewski 1997, Søreide et al. 2006, Casanova et al. 2012), and predation risk (Kaartvedt 1996, Dale et al. 1999, Varpe & Fiksen 2010) may also have contributed to the regulation of the observed seasonal vertical strategies.

Seasonal vertical strategies of the dominant zooplankton

Herbivores

The CVs of *Calanus finmarchicus*, CVs and adult females of *C. glacialis*, and CIVs of *C. hyperboreus* likely resided in the deeper region until November (e.g. Conover 1988, Falk-Petersen et al. 2009, our Fig. 5). The gradually decreasing vertical distribution indices of *C. finmarchicus* and *C. glacialis* until October (Fig. 6a,b), and simultaneous increase in their mean abundances in the deeper region (Fig. 5a,b) indicate that a considerable fraction of the CVs of these 2 species descended and recruited to their deep water populations in the autumn. Conversely, the vertical distribution data of *C. hyperboreus* indicate neither a descent (which may have occurred prior to the commencement of sampling), nor recruitment to its deep water population (Figs. 5c & 6c). In order to build up energy reserves, a fraction of the *C. finmarchicus* and *C. glacialis* CVs may have grazed in the shallower region relatively late into the productive season prior to their descent (Fig. 2b). These CVs may have been the *Calanus* spp. reported by Berge et al. (2014) that contributed to the acoustic backscattering detected near a chlorophyll maximum in this fjord in late September. Østvedt (1955), Pedersen et al. (1995) and Hirche (1996) also oberved a part of the summer–autumn *C. finmarchicus* population feeding in surface waters, while the rest resided in deep waters.

The gradually increasing vertical distribution indices indicate an ascent of *Calanus* spp. between November and February (Fig. 6a–c). By February, a maximum of ~80% of the *Calanus* community had ascended to the shallower region (Fig. 5). Similar to our findings, Daase et al. (2014) and Blachowiak-Samolyk et al. (2015) reported shallow vertical distributions (<100 m) of *Calanus* spp. in January from ~81° N in Rijpfjorden, Svalbard. However, the timing of the ascent we report here is earlier than the March to June period reported in most high-latitude investigations (e.g. Heath 1999, Gislason & Astthorsson 2000, Hirche & Kosobokova 2011, Melle et al. 2014).

As the vertical strategy of *Calanus* spp. was inversely related to fluorescence, it is unlikely that food availability served as a primary cue for their descent and ascent. However, a definitive conclusion on this matter cannot be made since vertical fluorescence profiles were not used in our study. We suggest that these herbivores, dominated by *C. glacialis*, ascended early as a part of a capital breeding strategy or to feed on ice algae, which were not detected by our fluorescence measurements (e.g. Varpe et al. 2009, Søreide et al. 2010). *Calanus* spp. use ice algae as an alternative food source to spawn prior to the phytoplankton bloom (Runge & Ingram 1991, Hirche & Kwasniewski 1997, Søreide et al. 2010). A summer–autumn descent while there is still food available near the surface, and ascent to shallow waters during the dark, unproductive winter (Fig. 2a,b) suggest a migration driven by processes other than the availability of food. The negative association between the *Calanus* vertical distribution index and mean temperature (Table 4) reflects the tendency of the seasonal descent and subsequent induction of diapause in *C. glacialis* to occur in relation to the summer–autumn warming of the surface waters (Niehoff & Hirche 2005, Pertsova & Kosobokova 2010). The overwintering depth and timing of the seasonal migration of *Calanus* spp. can also be influenced by planktivorous fish (Kaartvedt 1996, Dale et al. 1999, Kaartvedt 2000, Varpe & Fiksen 2010). Although we did not sample fish populations in this investigation, trawl samples collected in Billefjorden in August 2008 showed that ~60% of the stomach contents of polar cod *Boreogadus saida* consisted of *Calanus* spp. (Renaud et al. 2012). Therefore, the potential influence of visual predation on the seasonal vertical strategies of *Calanus* spp. in this fjord should not be ruled out.

Carnivores

Vertical distribution data of *A. digitale*, *M. ovum*, and *B. cucumis* indicate that these carnivores descended to the deeper region between August and October (Fig. 6d–f). From November onwards, *M. ovum* and *B. cucumis* gradually ascended and remained in the shallower region from February to the end of this investigation in May. Unlike the 2 cteno-

phore species, the ascent of *A. digitale* is not clearly evident (Fig. 6d). It should be noted that the vertical distribution data of this species after November may not be accurate due to its low numerical abundance (Fig. 4a). Descent to deeper waters in autumn, and ascent to shallower waters between spring and summer has been reported for *A. digitale*, *M. ovum*, and *B. cucumis* from ~59° N in the Northeast Atlantic (Williams & Conway 1981), ~62.5° N in Frobisher Bay (Percy 1989), ~67° N in White Sea (Pertsova et al. 2006), and ~74° N in Resolute Passage (Siferd & Conover 1992). In addition, shallow spring–summer vertical distributions of *M. ovum* and *B. cucumis* have been reported from ~55.5° N in the Bornholm basin of the Baltic Sea (Lehtiniemi et al. 2013), between 68 and 80° N in the Barents Sea and Fram Strait, (Swanberg & Båmstedt 1991a), and between 72 and 75° N in the western Arctic Ocean (Purcell et al. 2010).

Based on the positive association between the vertical distribution indices (Table 4, Fig. 8b), we argue that *M. ovum* seasonally followed *Calanus* spp. *M. ovum* is a secondary consumer that feeds on *Calanus* spp., and specifically on their older developmental stages (Greene 1986, Purcell 1991, Swanberg & Båmstedt 1991b). In the winter, *M. ovum* feeds on overwintering *Calanus* populations (Larson & Harbison 1989, Siferd & Conover 1992) and accumulates lipids (Percy 1989, Lundberg et al. 2006). Therefore, the older developmental stages (CIV, CV, and adult copepodites) of *Calanus* spp. sampled in this study may have served as a main prey source for *M. ovum*, and this predator–prey relationship is reflected by their similar vertical strategies. However, it should be noted that younger developmental stages of *Calanus* spp. which occupy shallower waters between March and May in this fjord (e.g. Arnkværn et al. 2005, Bailey 2010) may also have been a potential source of prey for *M. ovum*. Although *A. digitale* is a secondary consumer that primarily feed on copepods (see references in Table 2), its vertical distribution was not significantly associated with that of *Calanus* spp. (Table 4). Despite the similarities in the vertical strategies of *A. digitale* and *M. ovum* until October (Fig. 6d,e), the low numerical abundances of the former may have inaccurately represented its vertical distribution thereafter, and probably affected the results of the correlation analyses.

The positively associated vertical distribution indices suggest that the predatory ctenophore *B. cucumis* seasonally followed *M. ovum* (Table 4, Fig. 8c). *B. cucumis* is a tertiary consumer that specifically feeds on *M. ovum* (see references in Table 2). Therefore, it is likely that the strong predator–prey relationship between these 2 ctenophores were reflected in their markedly similar vertical strategies (Fig. 6e,f). Similar spatial associations between these 2 species have been reported from ~74° N in Resolute Passage (Siferd & Conover 1992), and between 75 and 79° N in the Barents Sea (Swanberg & Båmstedt 1991a, Søreide et al. 2003). Although the mean TL of *M. ovum* became substantially larger than that of *B. cucumis* after November (Fig. 4f,g), it may not have affected their predator–prey relationship as *Beroë* can feed on prey larger than itself (Tamm & Tamm 1991), or on body parts of the prey (Swanberg 1974).

The accuracy of interpreting statistical associations between predator and prey zooplankton, as their trophic relationships can be hampered by the coarse vertical resolution of our samples (e.g. Pearre 1979). It is possible for predator and prey zooplankton to coexist in a depth stratum of 50 m (the vertical sampling resolution of this study) without encountering each other. As this bias tends to be pronounced in periods with low predator and/or prey abundances (e.g. Greene 1986), we did not interpret the vertical strategies of *A. digitale* (after November), or the G_0 size group of *P. elegans* in detail (Fig. 4a,d,h). Therefore, further analyses (e.g. gut content analyses and dietary lipid analyses) would be required in order to verify whether the associations between the vertical strategies of predators and prey zooplankton observed in this study truly reflect their trophic interactions.

The 3 size groups of *P. elegans* did not show pronounced seasonal migrations (Fig. 6g–i) irrespective of the seasonal oscillations of the environmental parameters observed in this study (Table 4). However, the largest size group (G_2) occupied the deeper region for most of the study, while the smaller G_0 and G_1 size groups were distributed throughout the water column. Deep water residence of larger individuals of *P. elegans* has been documented from 50° N at 'Ocean Station P' (Sullivan 1980, Terazaki & Miller 1986), ~75° N in Baffin Bay (Samemoto 1987), and ~78° N from our study location in Billefjorden (Grigor et al. 2014). The vertical strategy of the smallest size group (G_0) may not be accurate because our samples did not capture sufficient numbers of those sizes Grigor et al. (2014) reported from this fjord (sampled by nets with finer mesh size and documented as cohort–0 of their study: cf. length data in Table S4 in Supplement 4).

As larger chaetognaths prefer larger prey, such as the older development stages of *Calanus* (Greene 1986, Falkenhaug 1991, Saito & Kiørboe 2001), it is

likely that the G_2 size group of *P. elegans* fed on *Calanus* copepodites occupying the deeper regions of the water column. Despite the ascent of *Calanus* spp. between November and February, a fraction of the *C. finmarchicus* and *C. glacialis* population was observed in the deeper region throughout this study (Fig. 5a,b), and may have served as a year-round prey source for the largest *P. elegans* size group. In support of this view, gut content and lipid analyses of *P. elegans* collected from Billefjorden and other adjacent fjords by Grigor et al. (2015) suggests that *P. elegans* primarily feed on *Calanus* spp. It remains unclear why the relatively small size fraction of *P. elegans* population remained in the shallower region throughout this investigation (Fig. 7d). One possibility is that they may have preyed on smaller developmental stages of *Calanus* spp. and smaller copepod species, such as *Oithona similis*, *Microcalanus* spp., *Pseudocalanus* spp., and *Metridia longa* (Falkenhaug 1991, Walkusz et al. 2003, Grigor et al. 2015), prey categories which were undersampled by the large mesh width of the WP-3 net used in our investigation.

CONCLUSIONS

This study is one of few that have investigated seasonal vertical distributions of multiple members of a zooplankton community in the Arctic over a near-annual, high-resolution time series. Our findings suggest that seasonal vertical migrations are a widespread trait in the community, and that seasonality in food availability relates to seasonal vertical strategies of zooplankton in different trophic levels. This relationship was positive and strongest for the associations between herbivores and secondary consumers, and between secondary consumers and tertiary consumers. Further year-round field investigations that can combine high-resolution sampling methods with high spatial resolution (e.g. Norrbin et al. 2009), information on individual variability in size and energy reserves (e.g. Vogedes et al. 2010), accurate species determination (e.g. Parent et al. 2011, Gabrielsen et al. 2012), and year-round, mooring-based monitoring of the environment would be necessary to test the generality of our findings.

Acknowledgements. This work was carried out as part of the ConocoPhillip-funded project Arctic Sea in Winter Time (ArcWin) and the Cleopatra I project (178766/S30) funded by the Norwegian Research Council. The authors are thankful to the many students and staff at UNIS who helped during the fieldwork. Particular thanks to Allison Bailey for her considerable contribution in the field. The authors also thank Dr. F. Cottier and C. Griffiths (Scottish Association of Marine Science) for providing data from the joint SAMS-UNIS moored observatory in Billefjorden. Financial support during the period of data analyses was provided by VISTA, a basic research program in collaboration between The Norwegian Academy of Science and Letters, and Statoil™. The authors are also thankful to the 3 anonymous reviewers for critically reading earlier drafts of the manuscript and suggesting substantial improvements.

LITERATURE CITED

Ackman RG, Eaton CA, Sipos JC, Hooper SN, Castell JD (1970) Lipids and fatty acids of two species of North Atlantic krill (*Meganyctiphanes norvegica* and *Thysanoëssa inermis*) and their role in the aquatic food web. J Fish Res Board Can 27:513–533

Alldredge AL (1976) Field behavior and adaptive strategies of appendicularians (Chordata: Tunicata). Mar Biol 38:29–39

Alvarez-Cadena JN (1993) Feeding of the chaetognath *Sagitta elegans* Verrill. Estuar Coast Shelf Sci 36:195–206

Arnkværn G, Daase M, Eiane K (2005) Dynamics of coexisting *Calanus finmarchicus*, *Calanus glacialis*, and *Calanus hyperboreus* populations in a high-Arctic fjord. Polar Biol 28:528–538

Auel H, Werner I (2003) Feeding, respiration and life history of the hyperiid amphipod *Themisto libellula* in the Arctic marginal ice zone of the Greenland Sea. J Exp Mar Biol Ecol 296:183–197

Bailey AM (2010) Lipids and diapause in *Calanus* spp. in a high-Arctic fjord: state-dependent strategies? Tracking lipids through the polar night. MSc thesis, University of Tromsø

Banse K (1964) On the vertical distribution of Zooplankton in the sea. Prog Oceanogr 2:53–125

Basedow SL, Tande KS, Stige LC (2010) Habitat selection by a marine copepod during the productive season in the Subarctic. Mar Ecol Prog Ser 416:165–178

Berge J, Cottier FR, Varpe Ø, Renaud PE and others (2014) Arctic complexity: a case study on diel vertical migration of zooplankton. J Plankton Res 36:1279–1297

Bernard KS, Froneman PW (2009) The sub-Antarctic euthecosome pteropod, *Limacina retroversa*: distribution patterns and trophic role. Deep-Sea Res I 56:582–598

Blachowiak-Samolyk K, Kwasniewski S, Dmoch K, Hop H, Falk-Petersen S (2007) Trophic structure of zooplankton in the Fram Strait in spring and autumn 2003. Deep-Sea Res II 54:2716–2728

Blachowiak-Samolyk K, Wiktor JM, Hegseth EN, Wold A, Falk-Petersen S, Kubiszyn AM (2015) Winter tales: the dark side of planktonic life. Polar Biol 38:23–36

Boxshall GA, Mees J, Costello MJ, Hernandez F and others (2015) World register of marine species (WoRMS). www.marinespecies.org (accessed 11 Mar 2015)

Brusca R (1997) Isopoda. Version 06 August 1997. Tree of Life web project. http://tolweb.org/Isopoda (accessed 11 Mar 2015)

Carlisle DB (1961) Diapause, neurosecretion and hormones in Copepoda. Nature 190:827–828

Casanova JP, Barthelemy R, Duvert M, Faure E (2012) Chaetognaths feed primarily on dissolved and fine particulate organic matter, not on prey: implications for marine food webs. Hypo Life Sci 2:20–29

Clarke A, Peck LS (1991) The physiology of polar marine zooplankton. Polar Res 10:355–370

Conover RJ (1988) Comparative life histories in the genera

Calanus and *Neocalanus* in high latitudes of the northern hemisphere. Hydrobiologia 167:127–142

Conover RJ, Huntley M (1991) Copepods in ice-covered seas — distribution, adaptations to seasonally limited food, metabolism, growth patterns and life cycle strategies in polar seas. J Mar Syst 2:1–41

Conover RJ, Lalli CM (1972) Feeding and growth in *Clione limacina* (Phipps), a pteropod mollusc. J Exp Mar Biol Ecol 9:279–302

Cottier FR, Tverberg V, Inall M, Svendsen H, Nilsen F, Griffiths C (2005) Water mass modification in an Arctic fjord through cross-shelf exchange: the seasonal hydrography of Kongsfjorden, Svalbard. J Geophys Res 110:C12005

Daase M, Varpe Ø, Falk-Petersen S (2014) Non-consumptive mortality in copepods: occurrence of *Calanus* spp. carcasses in the Arctic Ocean during winter. J Plankton Res 36:129–144

Dale T, Bagøien E, Melle W, Kaartvedt S (1999) Can predator avoidance explain varying overwintering depth of *Calanus* in different oceanic water masses? Mar Ecol Prog Ser 179:113–121

Eschmeyer WN, Herald ES, Hammann H (1983) A field guide to Pacific coast fishes of North America. Houghton Mifflin Company, Boston, MA

Falk-Petersen S, Gatten RR, Sargent JR, Hopkins CCE (1981) Ecological investigations on the zooplankton community in Balsfjorden, northern Norway: seasonal changes in the lipid class composition of *Meganyctiphanes norvegica* (M. Sars), *Thysanoessa raschii* (M. Sars), and *T. inermis* (Krøyer). J Exp Mar Biol Ecol 54:209–224

Falk-Petersen S, Sargent JR, Hopkins CCE, Vaja B (1982) Ecological investigations on the zooplankton community of Balsfjorden, northern Norway: lipids in the euphausiids *Thysanoessa raschi* and *T. inermis* during spring. Mar Biol 68:97–102

Falk-Petersen S, Sargent JR, Tande KS (1987) Lipid composition of zooplankton in relation to the sub-Arctic food web. Polar Biol 8:115–120

Falk-Petersen S, Dahl TM, Scott CL, Sargent JR and others (2002) Lipid biomarkers and trophic linkages between ctenophores and copepods in Svalbard waters. Mar Ecol Prog Ser 227:187–194

Falk-Petersen S, Mayzaud P, Kattner G, Sargent JR (2009) Lipids and life strategy of Arctic *Calanus.* Mar Biol Res 5: 18–39

Falkenhaug T (1991) Prey composition and feeding rate of *Sagitta elegans* var. *arctica* (Chaetognatha) in the Barents Sea in early summer. Polar Res 10:487–506

Fiksen Ø (2000) The adaptive timing of diapause – a search for evolutionarily robust strategies in *Calanus finmarchicus.* ICES J Mar Sci 57:1825–1833

Fraser J (1969) Experimental feeding of some medusae and Chaetognatha. J Fish Res Board Can 26:1743–1762

Fraser J, David PM (1959) The distribution of the Chaetognatha of the Southern Ocean. Discov Rep 29:200–229

Freire J, Gonzalez-Gurriaran E (1995) Feeding ecology of the velvet swimming crab *Necora puber* in mussel raft areas of the Ría de Arousa (Galicia, NW Spain). Mar Ecol Prog Ser 119:139–154

Gabrielsen TM, Merkel B, Søreide JE, Johansson-Karlsson and others (2012) Potential misidentifications of two climate indicator species of the marine arctic ecosystem: *Calanus glacialis* and *C. finmarchicus.* Polar Biol 35: 1621–1628

Gilmer RW, Harbison GR (1991) Diet of *Limacina helicina* (Gastropoda: Thecosomata) in Arctic waters in midsummer. Mar Ecol Prog Ser 77:125–134

Gislason A, Astthorsson OS (2000) Winter distribution, ontogenetic migration, and rates of egg production of *Calanus finmarchicus* southwest of Iceland. ICES J Mar Sci 57:1727–1739

Graeve M, Kattner G, Hagen W (1994) Diet-induced changes in the fatty acid composition of Arctic herbivorous copepods: experimental evidence of trophic markers. J Exp Mar Biol Ecol 182:97–110

Graeve M, Kattner G, Piepenburg D (1997) Lipids in Arctic benthos: Does the fatty acid and alcohol composition reflect feeding and trophic interactions? Polar Biol 18:53–61

Graeve M, Lundberg M, Böer M, Kattner G, Hop H, Falk-Petersen S (2008) The fate of dietary lipids in the Arctic ctenophore *Mertensia ovum* (Fabricius 1780). Mar Biol 153:643–651

Greene CH (1986) Patterns of prey selection: implications of predator foraging tactics. Am Nat 128:824–839

Grigor JJ, Søreide JE, Varpe Ø (2014) Seasonal ecology and life-history strategy of the high-latitude predatory zooplankter *Parasagitta elegans.* Mar Ecol Prog Ser 499: 77–88

Grigor JJ, Marais AE, Falk-Petersen S, Varpe Ø (2015) Polar night ecology of a pelagic predator, the chaetognath *Parasagitta elegans.* Polar Biol 38:87–98

Hagen W (1999) Reproductive strategies and energetic adaptations of polar zooplankton. Invertebr Reprod Dev 36:25–34

Haq SM (1967) Nutritional physiology of *Metridia lucens* and *M. longa* from the Gulf of Maine. Limnol Oceanogr 12:40–51

Heath MR (1999) The ascent migration of *Calanus finmarchicus* from overwintering depths in the Faroe–Shetland Channel. Fish Oceanogr 8:84–99

Herman AW (1983) Vertical distribution patterns of copepods, chlorophyll, and production in northeastern Baffin Bay. Limnol Oceanogr 28:709–719

Hermans CO, Satterlie RA (1992) Fast-strike feeding behavior in a pteropod mollusk, *Clione limacina* Phipps. Biol Bull (Woods Hole) 182:1–7

Hirche HJ (1991) Distribution of dominant calanoid copepod species in the Greenland Sea during late fall. Polar Biol 11:351–362

Hirche HJ (1996) Diapause in the marine copepod, *Calanus finmarchicus* — a review. Ophelia 44:129–143

Hirche HJ, Kosobokova KN (2011) Winter studies on zooplankton in Arctic seas: the Storfjord (Svalbard) and adjacent ice-covered Barents Sea. Mar Biol 158:2359–2376

Hirche HJ, Kwasniewski S (1997) Distribution, reproduction and development of *Calanus* species in the northeast water in relation to environmental conditions. J Mar Syst 10:299–317

Hop H, Falk-Petersen S, Svendsen H, Kwasniewski S, Pavlov V, Pavlova O, Søreide JE (2006) Physical and biological characteristics of the pelagic system across Fram Strait to Kongsfjorden. Prog Oceanogr 71:182–231

Hopkins TL (1985) Food web of an Antarctic midwater ecosystem. Mar Biol 89:197–212

Ji R, Edwards M, Mackas DL, Runge JA, Thomas AC (2010) Marine plankton phenology and life history in a changing climate: current research and future directions. J Plankton Res 32:1355–1368

Kaartvedt S (1996) Habitat preference during overwintering and timing of seasonal vertical migration of *Calanus finmarchicus.* Ophelia 44:145–156

Kaartvedt S (2000) Life history of *Calanus finmarchicus* in the Norwegian Sea in relation to planktivorous fish. ICES J Mar Sci 57:1819–1824

Kendall MG (1938) A new measure of rank correlation. Biometrika 30:81–93

Kendall MG (1945) The treatment of ties in ranking problems. Biometrika 33:239–251

Lalli CM, Gilmer RW (1989) Pelagic snails: the biology of holoplanktonic gastropod mollusks. Stanford University Press, Stanford, CA

Larson RJ, Harbison GR (1989) Source and fate of lipids in polar gelatinous zooplankton. Arctic 42:339–346

Lass S, Tarling GA, Virtue P, Matthews JBL, Mayzaud P, Buchholz F (2001) On the food of northern krill *Meganyctiphanes norvegica* in relation to its vertical distribution. Mar Ecol Prog Ser 214:177–200

Lee RF, Hagen W, Kattner G (2006) Lipid storage in marine zooplankton. Mar Ecol Prog Ser 307:273–306

Lehtiniemi M, Gorokhova E, Bolte S, Haslob H and others (2013) Distribution and reproduction of the Arctic ctenophore *Mertensia ovum* in the Baltic Sea. Mar Ecol Prog Ser 491:111–124

Levene H (1960) Robust tests for equality. In: Olkin I, Ghurye SG, Hoeffding W, Madow WG, Mann HB (eds) Contributions to probability and statistics — essays in honor of Harold Hotelling. Stanford University Press, Stanford, CA, p 278–292

Lischka S, Hagen W (2005) Life histories of the copepods *Pseudocalanus minutus*, *P. acuspes* (Calanoida) and *Oithona similis* (Cyclopoida) in the Arctic Kongsfjorden (Svalbard). Polar Biol 28:910–921

Lundberg M, Hop H, Eiane K, Gulliksen B, Falk-Petersen S (2006) Population structure and accumulation of lipids in the ctenophore *Mertensia ovum.* Mar Biol 149:1345–1353

Macdonald P, Du J (2012) mixdist: finite mixture distribution models. R package version 0.5-4. http://CRAN.R-project.org/package=mixdist

Melle W, Runge JA, Head EJH, Plourde S and others (2014) The North Atlantic Ocean as habitat for *Calanus finmarchicus*: environmental factors and life history traits. Prog Oceanogr 129:244–284

Miller CB, Cowles TJ, Wiebe PH, Copley NJ, Grigg H (1991) Phenology in *Calanus finmarchicus*; hypotheses about control mechanisms. Mar Ecol Prog Ser 72:79–91

Motoda S (1985) Devices of simple plankton apparatus VII. Bull Mar Sci 37:776–777

Nelson DR, McKibben JN, Strong WR Jr, Lowe CG, Sisneros JA, Schroeder DM, Lavenberg RJ (1997) An acoustic tracking of a megamouth shark, *Megachasma pelagios*: a crepuscular vertical migrator. Environ Biol Fishes 49: 389–399

Niehoff B, Hirche HJ (2005) Reproduction of *Calanus glacialis* in the Lurefjord (western Norway): indication for temperature-induced female dormancy. Mar Ecol Prog Ser 285:107–115

Nilsen F, Cottier FR, Skogseth R, Mattsson S (2008) Fjord-shelf exchanges controlled by ice and brine production: the interannual variation of Atlantic Water in Isfjorden, Svalbard. Cont Shelf Res 28:1838–1853

Norrbin F, Eilertsen HC, Degerlund M (2009) Vertical distribution of primary producers and zooplankton grazers during different phases of the Arctic spring bloom. Deep-Sea Res II 56:1945–1958

Nygård H, Berge J, Gulliksen B, Camus L (2007) The occurrence of *Eualus gaimardii gibba* Krøyer 1841 (Crustacea, Decapoda) in the sympagic habitat: an example of bentho-sympagic coupling. Polar Biol 30:1351–1354

Olsen EM, Jørstad T, Kaartvedt S (2000) The feeding strategies of two large marine copepods. J Plankton Res 22: 1513–1528

Øresland V (1990) Feeding and predation impact of the chaetognath *Eukrohnia hamata* in Gerlache Strait, Antarctic Peninsula. Mar Ecol Prog Ser 63:201–209

Østvedt OJ (1955) Zooplankton investigations from weather ship M in the Norwegian Sea, 1948-49. Hvalrad Skr 40: 1–93

Pagès F, González HE, González SR (1996) Diet of the gelatinous zooplankton in Hardangerfjord (Norway) and potential predatory impact by *Aglantha digitale* (Trachymedusae). Mar Ecol Prog Ser 139:69–77

Parent GJ, Plourde S, Turgeon J (2011) Overlapping size ranges of *Calanus* spp. off the Canadian Arctic and Atlantic coasts: impact on species' abundances. J Plankton Res 33:1654–1665

Pearre S Jr (1979) Problems of detection and interpretation of vertical migration. J Plankton Res 1:29–44

Pedersen G, Tande KS, Ottesen GO (1995) Why does a component of *Calanus finmarchicus* stay in the surface waters during the overwintering period in high latitudes? ICES J Mar Sci 52:523–531

Percy JA (1989) Abundance, biomass, and size frequency distribution of an Arctic ctenophore, *Mertensia ovum* (Fabricius) from Frobisher Bay, Canada. Sarsia 74:95–105

Pertsova N, Kosobokova K (2010) Interannual and seasonal variation of the population structure, abundance, and biomass of the Arctic copepod *Calanus glacialis* in the White Sea. Oceanology (Mosc) 50:531–541

Pertsova NM, Kosobokova KN, Prudkovsky AA (2006) Population size structure, spatial distribution, and life cycle of the hydromedusa *Aglantha digitale* (OF Müller, 1766) in the White Sea. Oceanology (Mosc) 46:228–237

Prudkovsky AA (2013) Trophic role of ambush-foraging hydromedusae in the White Sea. Mar Ecol (Berl) 34: 153–164

Purcell JE (1991) A review of cnidarians and ctenophores feeding on competitors in the plankton. In: Williams RB, Cornelius PFS, Hughes RG, Robson EA (eds) Coelenterate biology: recent research on Cnidaria and Ctenophora. Springer, Dordrecht, p 335–342

Purcell JE, Hopcroft RR, Kosobokova KN, Whitledge TE (2010) Distribution, abundance, and predation effects of epipelagic ctenophores and jellyfish in the western Arctic Ocean. Deep-Sea Res II 57:127–135

R Core Team (2013) R: a language and environment for statistical computing. R Foundation for Statistical Computing, Vienna

Renaud PE, Berge J, Varpe Ø, Lønne OJ, Nahrgang J, Ottesen C, Hallanger I (2012) Is the poleward expansion by Atlantic cod and haddock threatening native polar cod, *Boreogadus saida?* Polar Biol 35:401–412

Runge JA, Ingram RG (1991) Under-ice feeding and diel migration by the planktonic copepods *Calanus glacialis* and *Pseudocalanus minutus* in relation to the ice algal production cycle in southeastern Hudson Bay, Canada. Mar Biol 108:217–225

Russell FS (1927) The vertical distribution of plankton in the sea. Biol Rev Camb Philos Soc 2:213–262

Sainte-Marie B, Lamarche G (1985) The diets of six species of the carrion-feeding lysianassid amphipod genus *Anonyx* and their relation with morphology and swimming behaviour. Sarsia 70:119–126

Sainte-Marie B, Percy JA, Shea JR (1989) A comparison of meal size and feeding rate of the lysianassid amphipods *Anonyx nugax*, *Onisimus* (=*Pseudalibrotus*) *litoralis* and *Orchomenella pinguis.* Mar Biol 102:361–368

Saito H, Kiørboe T (2001) Feeding rates in the chaetognath *Sagitta elegans*: effects of prey size, prey swimming

behaviour and small-scale turbulence. J Plankton Res 23: 1385–1398

Samemoto DD (1987) Vertical distribution and ecological significance of chaetognaths in the Arctic environment of Baffin Bay. Polar Biol 7:317–328

Sargent JR, Falk-Petersen S (1981) Ecological investigations on the zooplankton community in Balsfjorden, northern Norway: lipids and fatty acids in *Meganyctiphanes norvegica*, *Thysanoessa raschi* and *T. inermis* during mid-winter. Mar Biol 62:131–137

Shapiro SS, Wilk MB (1965) An analysis of variance test for normality (complete samples). Biometrika 52:591–611

Shumway SE, Perkins HC, Schick DF, Stickney AP (1985) Synopsis of biological data on the pink shrimp, *Pandalus borealis* Kroyer, 1838. FAO Fisheries Synopsis No. 144. NOAA Tech Rep NMFS 30, US Department of Commerce, Washington, DC

Sibson R (1981) A brief description of natural neighbour interpolation. In: Barnett V (ed) Interpreting multivariate data. John Wiley & Sons, New York, NY, p 21–36

Siferd TD, Conover RJ (1992) Natural history of ctenophores in the Resolute Passage area of the Canadian High Arctic with special reference to *Mertensia ovum.* Mar Ecol Prog Ser 86:133–144

Silva AC, Hawkins SJ, Clarke KR, Boaventura DM, Thompson RC (2010) Preferential feeding by the crab *Necora puber* on differing sizes of the intertidal limpet *Patella vulgata.* Mar Ecol Prog Ser 416:179–188

Sims DW, Southall EJ, Tarling GA, Metcalfe JD (2005) Habitat specific normal and reverse diel vertical migration in the plankton feeding basking shark. J Anim Ecol 74: 755–761

Skarra H, Kaartvedt S (2003) Vertical distribution and feeding of the carnivorous copepod *Paraeuchaeta norvegica.* Mar Ecol Prog Ser 249:215–222

Smedstad OM (1972) On the biology of *Aglantha digitale rosea* (Forbes) (Coelenterata: Trachymedusea) in the Inner Oslofjord. Nor J Zool 20:111–135

Sømme JD (1934) Animal plankton of the Norwegian coast waters and the open sea. I. Production of *Calanus finmarchicus* (Gunner) and *Calanus hyperboreus* (Krøyer) in the Lofoten Area. Fiskeridir Skr (Havunders) 4:1–163

Søreide JE, Hop H, Falk-Petersen S, Gulliksen B, Hansen E (2003) Macrozooplankton communities and environmental variables in the Barents Sea marginal ice zone in late winter and spring. Mar Ecol Prog Ser 263:43–64

Søreide JE, Hop H, Carroll ML, Falk-Petersen S, Hegseth EN (2006) Seasonal food web structures and sympagic–pelagic coupling in the European Arctic revealed by stable isotopes and a two-source food web model. Prog Oceanogr 71:59–87

Søreide JE, Falk-Petersen S, Hegseth EN, Hop H, Carroll ML, Hobson KA, Blachowiak-Samolyk K (2008) Seasonal feeding strategies of *Calanus* in the high-Arctic Svalbard region. Deep-Sea Res II 55:2225–2244

Søreide JE, Leu E, Berge J, Graeve M, Falk-Petersen S (2010) Timing of blooms, algal food quality and *Calanus glacialis* reproduction and growth in a changing Arctic. Glob Change Biol 16:3154–3163

Sullivan BK (1980) In situ feeding behavior of *Sagitta elegans* and *Eukrohnia hamata* (Chaetognatha) in relation to the vertical distribution and abundance of prey at Ocean Station 'P'. Limnol Oceanogr 25:317–326

Svendsen H, Beszczynska Møller A, Hagen JO, Lefauconnier B and others (2002) The physical environment of Kongsfjorden–Krossfjorden, an Arctic fjord system in Svalbard. Polar Res 21:133–166

Swanberg N (1974) The feeding behavior of *Beroe ovata.* Mar Biol 24:69–76

Swanberg N, Båmstedt U (1991a) Ctenophora in the Arctic: the abundance, distribution and predatory impact of the cydippid ctenophore *Mertensia ovum* (Fabricius) in the Barents Sea. Polar Res 10:507–524

Swanberg N, Båmstedt U (1991b) The role of prey stratification in the predation pressure by the cydippid ctenophore *Mertensia ovum* in the Barents Sea. Hydrobiologia 216-217:343–349

Tamm SL, Tamm S (1991) Reversible epithelial adhesion closes the mouth of *Beroë*, a carnivorous marine jelly. Biol Bull (Woods Hole) 181:463–473

Terazaki M, Miller CB (1986) Life history and vertical distribution of pelagic chaetognaths at Ocean Station P in the subarctic Pacific. Deep-Sea Res A, Oceanogr Res Pap 33: 323–337

Torres JJ, Aarset A, Donnelly J, Hopkins TL, Lancraft T, Ainley D (1994) Metabolism of Antarctic micronektonic Crustacea as a function of depth of occurrence and season. Mar Ecol Prog Ser 113:207–219

Varpe Ø (2012) Fitness and phenology: annual routines and zooplankton adaptations to seasonal cycles. J Plankton Res 34:267–276

Varpe Ø, Fiksen Ø (2010) Seasonal plankton-fish interactions: light regime, prey phenology, and herring foraging. Ecology 91:311–318

Varpe Ø, Jørgensen C, Tarling GA, Fiksen Ø (2007) Early is better: seasonal egg fitness and timing of reproduction in a zooplankton life history model. Oikos 116:1331–1342

Varpe Ø, Jørgensen C, Tarling GA, Fiksen Ø (2009) The adaptive value of energy storage and capital breeding in seasonal environments. Oikos 118:363–370

Vestheim H, Kaartvedt S, Edvardsen B (2005) State-dependent vertical distribution of the carnivore copepod *Pareuchaeta norvegica.* J Plankton Res 27:19–26

Visser AW, Jónasdóttir SH (1999) Lipids, buoyancy and the seasonal vertical migration of *Calanus finmarchicus.* Fish Oceanogr 8:100–106

Vogedes D, Varpe Ø, Søreide JE, Graeve M, Berge J, Falk-Petersen S (2010) Lipid sac area as a proxy for individual lipid content of Arctic calanoid copepods. J Plankton Res 32:1471–1477

Walkusz W, Storemark K, Skau T, Gannefors C, Lundberg M (2003) Zooplankton community structure; a comparison of fjords, open water and ice stations in the Svalbard area. Pol Polar Res 24:149–165

Werner EE, Gilliam JF (1984) The ontogenetic niche and species interactions in size-structured populations. Annu Rev Ecol Syst 15:393–425

Williams R, Conway DVP (1981) Vertical distribution and seasonal abundance of *Aglantha digitale* (OF Müller) (Coelenterata: Trachymedusae) and other planktonic coelenterates in the northeast Atlantic Ocean. J Plankton Res 3:633–643

Williams R, Lindley JA (1982) Variability in abundance, vertical distribution and ontogenetic migrations of *Thysanoessa longicaudata* (Crustacea: Euphausiacea) in the north-eastern Atlantic Ocean. Mar Biol 69:321–330

Editorial responsibility: Anna Pasternak, Moscow, Russian Federation

Submitted: November 16, 2015; Accepted: July 7, 2016
Proofs received from author(s): August 9, 2016

The following supplements accompany the article

Seasonal vertical strategies in a high-Arctic coastal zooplankton community

Kanchana Bandara*, Øystein Varpe, Janne E. Søreide, Jago Wallenschus, Jørgen Berge, Ketil Eiane

*Corresponding author: kanchana.bandara@nord.no

Marine Ecology Progress Series 555: 49–64 (2016)

Supplement 1. Sources of additional hydrographic data

Table S1. Sensors of the mooring from which temperature and salinity data were obtained for August 27 and September 07, 2008, and March 23, 2009

Parameter	Sensor	Moored depth(s) (m)
Temperature	Seabird 16plus SeaCAT recorder	30
	VEMCO minilog-II-T thermal logger	43, 53, 63, 73, 111, 126, 152
	SBE 37-SM MicroCAT recorder	20, 88.5, 186
Salinity	Seabird 16plus SeaCAT recorder	30
	SBE 37-SM MicroCAT recorder	20, 88.5, 186

Supplement 2. Potential influences of Atlantic Water (AW) advection during the study

We used the temperature and salinity data measured in the study and identified different water masses that prevailed in Billefjorden. However, we didn't find any signatures of AW in during the study (see Fig. S1 below). Other investigations conducted in Billefjorden in the same period (e.g. Bailey 2010, Grigor et al. 2014) have also suggested that the influence of AW advection was negligible.

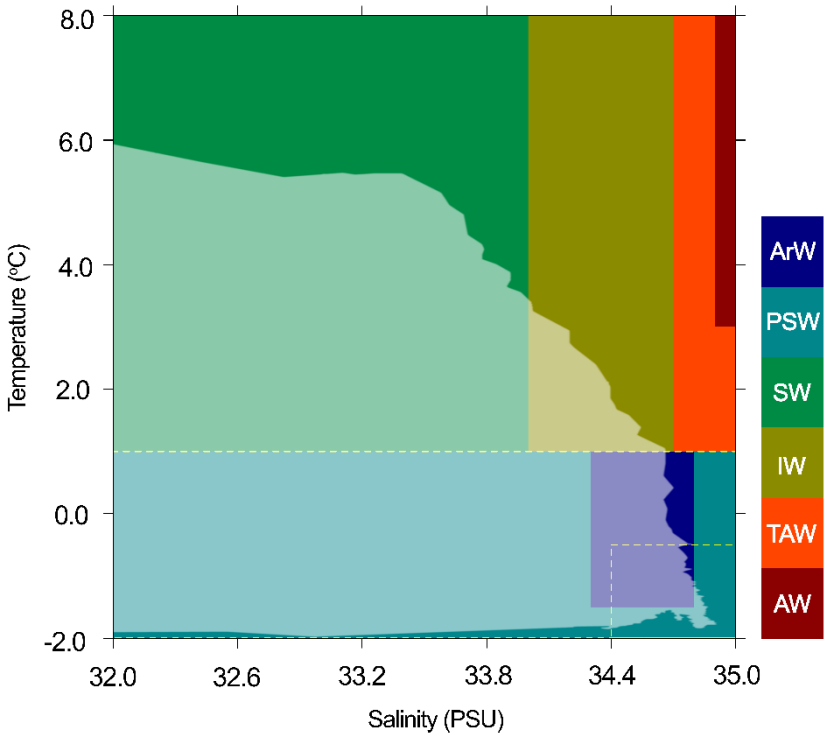

Fig. S1. The range of temperature and salinity measurements recorded in the study (opaque white polygon), and their water mass associations (colored polygons). The abscissa is cropped at 32 PSU. ArW: Arctic water, PSW: polar surface water, SW: surface water, IW: intermediate water, (T)AW: (transformed) Atlantic water. Dashed line: local water (LW, above), and winter cooled water (WCW, below). Water mass associations were adopted from Swift (1986), Hopkins (1991), Svendsen et al. (2002), and Nilsen et al. (2008)

Supplement 3. The PL based separation of *Calanus* taxa

We observed three components in CV and adult female *Calanus* PL distributions (Fig. S2a, b), and two components in that of adult males (Fig. S2c). Although we fitted normal distribution models for all the components, the fraction of the *Calanus* community represented by the smallest component (*Calanus* sp. in Table 2 in the text) was not used in the analyses because the PL boundaries separating it from the other two did not match any literature in Table S3, and its abundance was extremely low. These may be mis-staged smaller copepodites.

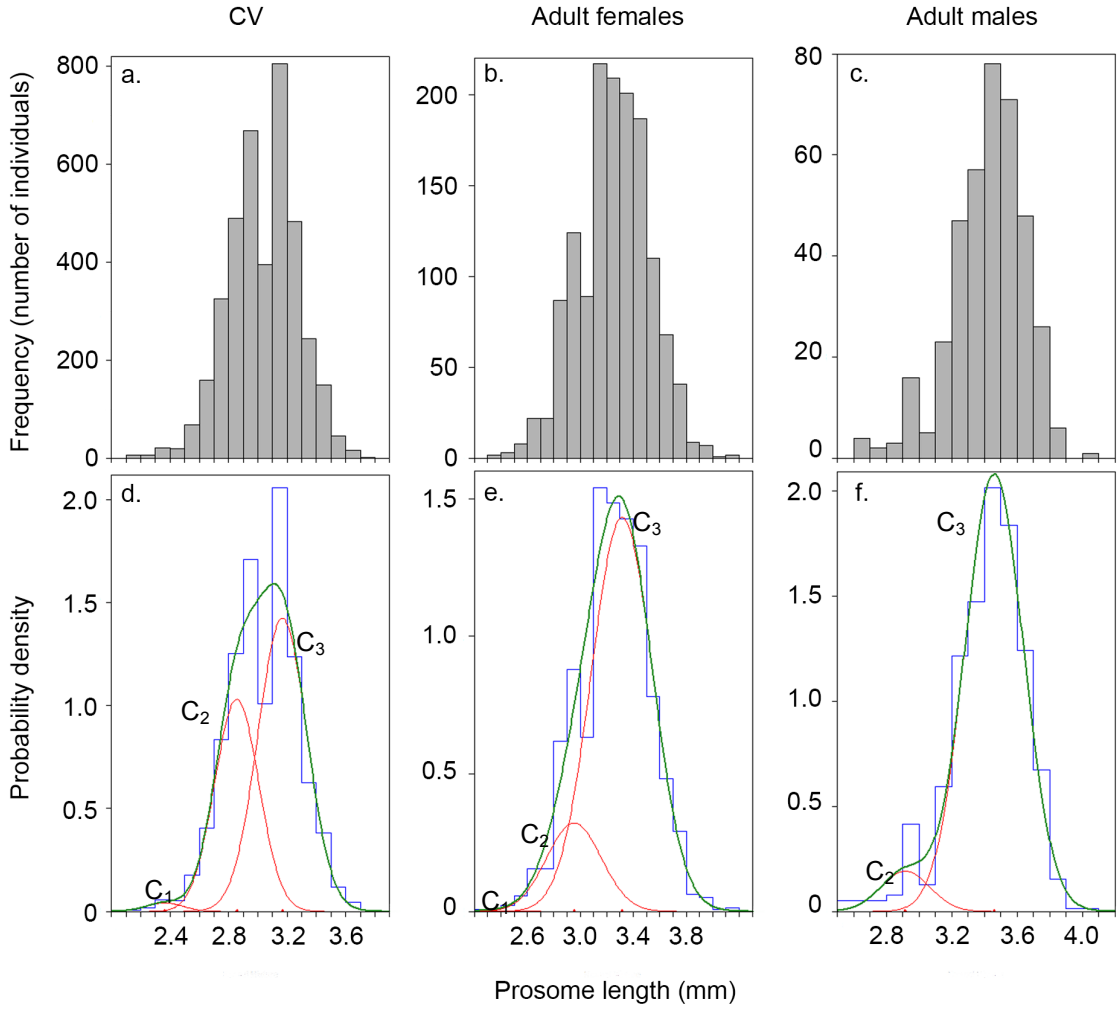

Fig. S2. Overlapped components within the PL distributions of *Calanus* spp. (a–c), and normal distribution models fitted to represent each component (d–f). The means of each fitted normal component model are presented by red ticks on the abscissae of the bottom panels

Table S2. The % overlap between the fitted normal components (C_i) in the *Calanus* spp. PL distributions (see Fig. S2 for reference) estimated by numerical integration

Component	C_1 & C_2	C_1 & C_3	C_2 & C_3
CV	6.36	1.26	33.17
Adult females	12.20	0.00	39.97
Adult males	–	–	10.12

Table S3. PL boundaries (mm) used in some high latitude investigations for separation of coexisting *C. finmarchicus* (CF) and *C. glacialis* (CG) populations. These PL boundaries are comparable with those derived in the present investigation (cf. Table 3 in the text). However, note that the mesh widths of the nets/filters used in these investigations are lesser (50–300 μm) than that of our investigation (1000 μm)

Authors	CV		Adult females		Adult males	
	CF	CG	CF	CG	CF	CG
Jaschnov (1972)	–	–	2.20–3.00	3.60–4.50	–	–
Hirche (1991)	< 3.10	> 3.10	< 3.10	> 3.20	–	–
Unstad and Tande (1991)	< 3.00	3.00–3.40	< 3.20	3.20–4.50	–	–
Koszteyn and Kwasniewski (1992)	< 3.05	3.05–3.95	2.85–3.00	3.50–4.40	–	–
Hirche et al. (1994)	1.95–3.05	2.95–3.90	2.35–3.20	3.20–4.60	–	–
Madsen et al. (2001)	1.75–2.70	2.73–3.90	< 3.00	> 3.00	–	–
Kwasniewski et al. (2003)	< 2.90	≥ 2.90	< 3.20	≥ 3.20	–	–
Daase and Eiane (2007)	< 2.94	> 2.94	< 3.24	> 3.24	–	–
Hirche and Kosobokova (2011)	1.70–2.85	2.90–3.50	2.90–3.15	3.20–4.60	1.85–2.90	2.95–3.60

Supplement 4. The TL based separation of *P. elegans* size groups

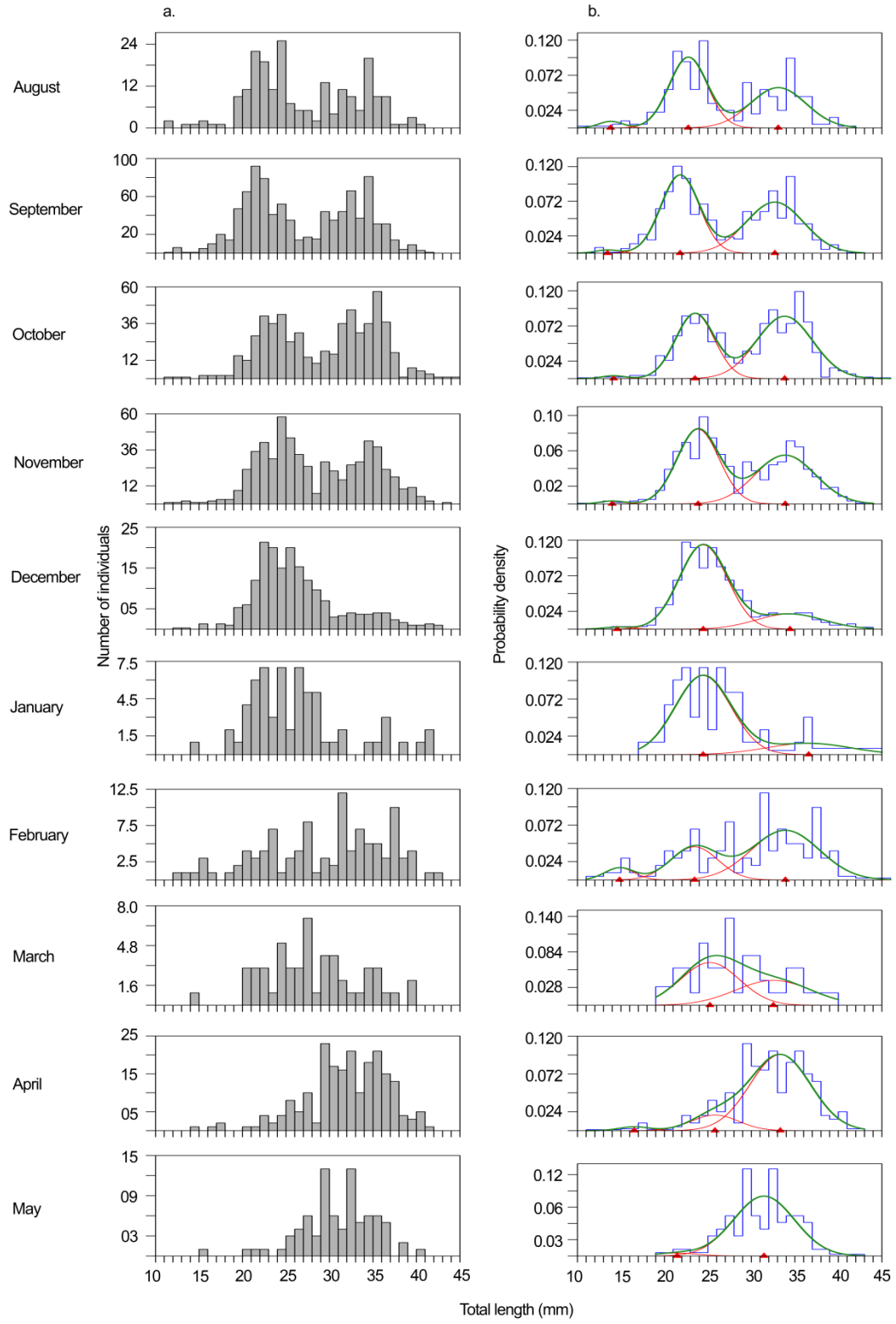

Fig. S3. Overlapped components within monthly TL distributions of *P. elegans* (a), and normal distribution models fitted to represent each component (b). The mean PLs of each fitted component model are presented as red ticks on abscissae of the right panels

Table S4. The number individuals (n) used in the length frequency analysis, and the chi-square statistics (χ^2) with the degrees of freedom (df) of the fitted component distribution models for monthly TL distributions of *P. elegans* (see Fig. S3 for reference). The monthly mean TLs (mm) of each size group is given in the three right columns

Month	n	df	χ^2	Mean TL ± SD		
				G_0	G_1	G_2
August	210	21	47.55***	14.16 ± 1.83	23.18 ± 2.04	33.62 ± 3.04
September	915	24	91.37***	13.22 ± 0.83	22.21 ± 2.27	33.30 ± 3.01
October	574	26	63.52***	14.20 ± 1.79	23.79 ± 2.19	34.28 ± 3.11
November	589	25	42.89**	14.00 ± 1.41	24.27 ± 2.38	34.60 ± 3.08
December	546	22	20.54	15.17 ± 1.33	24.97 ± 2.70	35.60 ± 3.19
January	63	16	17.95	–	24.69 ± 3.31	37.27 ± 3.52
February	105	22	33.72*	15.28 ± 1.38	23.45 ± 2.31	34.30 ± 3.86
March	52	15	14.25	–	24.87 ± 3.11	33.77 ± 3.24
April	208	18	36.26**	17.00 ± 1.41	25.04 ± 1.72	33.84 ± 3.33
May	82	14	26.07*	–	19.67 ± 2.38	31.92 ± 3.59

* $p < 0.05$, ** $p < 0.01$, *** $p < 0.001$

A note on the *P. elegans* size groups

The mean TLs of each size group we derived for *P. elegans* from the length frequency analysis matched those described by Grigor et al. (2014) for this species in this fjord following the same time series. We termed the three size groups as G_0, G_1, and G_2 in comparison with the cohorts 0, 1, and 2 of their investigation. As a WP-2 net was used in their study, they captured higher numbers of G_0 (cohort 0) individuals. See the above work for a detailed account of the population dynamics of this species.

Supplement 5. The vertical distribution index: additional data

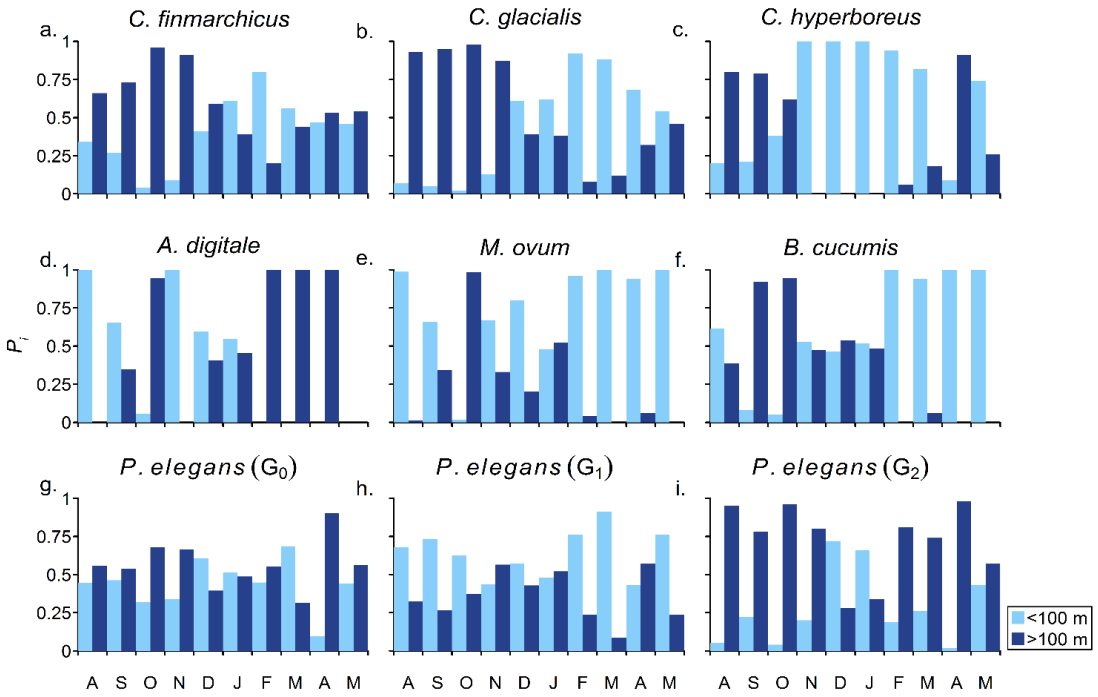

Fig. S4. Proportion of the population (P_i of dominant taxa) distributed in the two vertical regions of the water column during the study. For a given species in a given month, the difference between its population proportions of the shallower region and the deeper region was calculated as the vertical distribution index (V: See Table S5 below).

Table S5. Seasonal variability in vertical distribution index (V) of the dominant zooplankton taxa during the study. V ranges from -1 to 1, in which the former represents the entire population distributed in the shallower region, and latter represents the opposite scenario. *A. digitale* was not captured to compute its V in May

Species	Aug	Sep	Oct	Nov	Dec	Jan	Feb	Mar	Apr	May
C. finmarchicus	-0.32	-0.46	-0.91	-0.82	-0.19	0.21	0.59	0.12	-0.06	-0.08
C. glacialis	-0.86	-0.90	-0.95	-0.73	0.22	0.23	0.84	0.77	0.35	0.09
C. hyperboreus	-0.59	-0.57	-0.24	1.00	1.00	1.00	0.89	0.64	-0.81	0.48
Calanus spp.	-0.77	-0.83	-0.93	-0.73	0.13	0.23	0.79	0.64	0.26	0.04
A. digitale	1.00	0.31	-0.89	1.00	0.19	0.09	-1.00	-1.00	-1.00	–
M. ovum	0.97	0.31	-0.97	0.34	0.60	-0.04	1.00	1.00	0.88	1.00
B. cucumis	0.23	-0.84	-0.89	0.06	-0.07	0.03	1.00	0.88	1.00	1.00
P. elegans (G_0)	-0.11	-0.07	-0.36	-0.32	0.21	0.03	-0.10	0.37	-0.81	-0.12
P. elegans (G_1)	0.35	0.47	0.25	-0.13	0.14	-0.04	0.52	0.82	-0.14	0.52
P. elegans (G_2)	-0.90	-0.56	-0.92	-0.60	0.44	0.32	-0.63	-0.48	-0.96	-0.15

LITERATURE CITED

Bailey AM (2010) Lipids and diapause in *Calanus* spp. in a high-Arctic fjord: state-dependent strategies? Tracking lipids through the polar night. MSc thesis, University of Tromsø, Tromsø, Norway

Daase M, Eiane K (2007) Mesozooplankton distribution in northern Svalbard waters in relation to hydrography. Polar Biol 30:969-981

Grigor JJ, Søreide JE, Varpe Ø (2014) Seasonal ecology and life-history strategy of the high-latitude predatory zooplankter *Parasagitta elegans*. Mar Ecol Prog Ser 499:77-88

Hirche H-J (1991) Distribution of dominant calanoid copepod species in the Greenland Sea during late fall. Polar Biol 11:351-362

Hirche H-J, Hagen W, Mumm N, Richter C (1994) The Northeast Water polynya, Greenland Sea. Polar Biol 14:491-503

Hirche H-J, Kosobokova KN (2011) Winter studies on zooplankton in Arctic seas: the Storfjord (Svalbard) and adjacent ice-covered Barents Sea. Mar Biol 158:2359-2376

Hopkins TS (1991) The GIN Sea—A synthesis of its physical oceanography and literature review 1972–1985. Earth-Sci Rev 30:175-318

Jaschnov WA (1972) On the Systematic Status of *Calanus glacialis*, *Calanus finmarchicus* and *Calanus helgolandicus*. Crustaceana 22:279-284

Koszteyn J, Kwasniewski S (1992) The near shore zooplankton of the Tikhaia Bay (Franz Josef Land) in August 1991. Norsk Polarinst Medd 120:23-33

Kwasniewski S, Hop H, Falk-Petersen S, Pedersen G (2003) Distribution of *Calanus* species in Kongsfjorden, a glacial fjord in Svalbard. J Plankton Res 25:1-20

Madsen SJ, Nielsen TG, Hansen BW (2001) Annual population development and production by *Calanus finmarchicus*, *C. glacialis* and *C. hyperboreus* in Disko Bay, western Greenland. Mar Biol 139:75-83

Nilsen F, Cottier FR, Skogseth R, Mattsson S (2008) Fjord–shelf exchanges controlled by ice and brine production: the interannual variation of Atlantic Water in Isfjorden, Svalbard. Cont Shelf Res 28:1838-1853

Svendsen H, Beszczynska□Møller A, Hagen JO, Lefauconnier B and others (2002) The physical environment of Kongsfjorden–Krossfjorden, an Arctic fjord system in Svalbard. Polar Res 21:133-166

Swift JH (1986) The Arctic Waters. In: Hurdle BG (ed) The Nordic Seas. Springer New York, New York, NY, p 129-154

Unstad KH, Tande KS (1991) Depth distribution of *Calanus finmarchicus* and *C. glacialis* in relation to environmental conditions in the Barents Sea. Polar Res 10:409-420

Paper-II

Ecological Modelling 368 (2018) 357–376

Contents lists available at ScienceDirect

Ecological Modelling

journal homepage: www.elsevier.com/locate/ecolmodel

A high-resolution modeling study on diel and seasonal vertical migrations of high-latitude copepods

Kanchana Bandara[a,b,*], Øystein Varpe[b,c], Rubao Ji[d], Ketil Eiane[a]

[a] Faculty of Biosciences and Aquaculture, Nord University, 8049, Bodø, Norway
[b] The University Centre in Svalbard, 9171, Longyearbyen, Norway
[c] Akvaplan-niva, Fram Centre, 9296, Tromsø, Norway
[d] Woods Hole Oceanographic Institution, Redfield 2-14, Woods Hole, MA 02543, USA

ARTICLE INFO

Article history:
Received 20 September 2017
Received in revised form
12 December 2017
Accepted 12 December 2017

Keywords:
Vertical migration
Seasonality
Phenology
Optimization model
Genetic algorithm
Habitat choice

ABSTRACT

Despite diel and seasonal vertical migrations (DVM and SVM) of high-latitude zooplankton have been studied since the late-19th century, questions still remain about the influence of environmental seasonality on vertical migration, and the combined influence of DVM and SVM on zooplankton fitness. Toward addressing these, we developed a model for simulating DVM and SVM of high-latitude herbivorous copepods in high spatio-temporal resolution. In the model, a unique timing and amplitude of DVM and SVM and its ontogenetic trajectory were defined as a vertical strategy. Growth, survival and reproductive performances of numerous vertical strategies hardwired to copepods spawned in different times of the year were assessed by a fitness estimate, which was heuristically maximized by a Genetic Algorithm to derive the optimal vertical strategy for a given model environment. The modelled food concentration, temperature and visual predation risk had a significant influence on the observed vertical strategies. Under low visual predation risk, DVM was less pronounced, and SVM and reproduction occurred earlier in the season, where capital breeding played a significant role. Reproduction was delayed by higher visual predation risk, and copepods that spawned later in the season used the higher food concentrations and temperatures to attain higher growth, which was efficiently traded off for survival through DVM. Consequently, the timing of SVM did not change much from that predicted under lower visual predation risk, but the body and reserve sizes of overwintering stages and the importance of capital breeding diminished. Altogether, these findings emphasize the significance of DVM in environments with elevated visual predation risk and shows its contrasting influence on the phenology of reproduction and SVM, and moreover highlights the importance of conducting field and modeling work to study these migratory strategies in concert.

1. Introduction

Vertical migration is a common behavior of many zooplankton taxa. Based on the periodicity, vertical migrations of high-latitude zooplankton are classified into diel and seasonal components, which have been studied since the late-19th century (reviewed in Russell, 1927; Cushing, 1951; Banse, 1964). The short-term diel vertical migration (DVM) has a periodicity of up to 24 h, and is understood as a strategy that trades off growth potential to reduce the mortality risk imposed by visual predators (Lampert, 1989; Ohman, 1990; Loose and Dawidowicz, 1994). The long-term seasonal vertical migration (SVM) has a periodicity of up to one year, and reflects adaptations to seasonal extremities of food availability (Head and Harris, 1985; Hind et al., 2000; Bandara et al., 2016), temperature (Hirche, 1991; Astthorsson and Gislason, 2003) and predation risk (Kaartvedt, 1996; Bagøien et al., 2000; Varpe and Fiksen, 2010). In either case, since both DVM and SVM can alter feeding, growth, survival and reproduction, and ultimately affect fitness (Aidley, 1981; Alerstam et al., 2003; Cresswell et al., 2011; Litchman et al., 2013), these migratory strategies are termed vertical strategies (Bandara et al., 2016).

Empirical knowledge on zooplankton vertical strategies largely comes from studying the dynamic vertical positioning of populations in a water column, and are often rather coarse in spatial (vertical) and temporal resolution (Pearre, 1979). This can undermine the key concept that such migrations are individual responses

* Corresponding author at: Faculty of Biosciences and Aquaculture, Nord University, 8049, Bodø, Norway.
E-mail addresses: kanchana.bandara@nord.no, kanchana_bandara@live.com (K. Bandara).

https://doi.org/10.1016/j.ecolmodel.2017.12.010

Table 1
Some endogenous and exogenous cues that are believed to proximately or ultimately regulate diel and seasonal vertical migrations of marine and freshwater zooplankton. Literature do not come from an exhaustive review and only serve as examples.

Cue	DVM	SVM
Temperature	McLaren (1963), Enright (1977)	Hirche (1991), Heath and Jónasdóttir (1999), Astthorsson and Gislason (2003)
Light (absolute or relative irradiance from sun, moon, stars, or aurora borealis, photoperiod, spectral quality, polarization etc.)	Clarke (1933), Gliwicz (1986), Frank and Widder (1997), Berge et al. (2009), Båtnes et al. (2015), Cohen et al. (2015), Bianchi and Mislan (2016), Bozman et al. (2017)	Sømme (1934), Ussing (1938), Miller et al. (1991)
Dissolved oxygen	Devol (1981), Bianchi et al. (2013)	–
Water depth, transparency and UV radiation	Rhode et al. (2001), Williamson et al. (2011), Ekvall et al. (2015)	Dupont and Aksnes (2012)
Tides, currents and advective transport	Hardy (1935), Wroblewski (1982), Kimmerer and McKinnon (1987)	Berge et al. (2012), Irigoien (2004)
Food availability	Hardy and Gunther (1935), Huntley and Brooks (1982), George (1983), Johnsen and Jakobsen (1987)	Herman (1983), Hind et al. (2000), Head and Harris (1985), Bandara et al. (2016)
Visual and tactile predation	Zaret and Suffern (1976), Iwasa (1982), Ohman (1990), Bollens et al. (1992), Loose and Dawidowicz (1994)	Kaartvedt (1996), Kaartvedt (2000), Dale et al. (1999), Bagøien et al. (2000), Varpe and Fiksen (2010)
Body size, ontogeny and pigmentation	Zaret and Kerfoot (1975), Uye et al. (1990), Hays et al. (1994), Dale and Kaartvedt (2000)	Østvedt (1955), Hind et al. (2000)
Nutritional state and lipid reserves	Fiksen and Carlotti (1998), Sekino and Yamamura (1999)	Visser and Jónasdóttir (1999), Thorisson (2006)
Endogenous rhythms and internal biological clocks	Cohen and Forward (2009), van Haren and Compton (2013)	Carlisle and Pitman (1961), Miller et al. (1991), Hirche (1996)

to certain cues or stimuli and not a property of the population (Zink, 2002), and may complicate the understanding of the relationships between vertical strategies and environmental variables (see Table 1 for examples). Moreover, since diel and seasonal vertical migrations occur on different spatial and temporal scales, studying these migrations together in the field in adequate resolution remains a major challenge. Although novel optical and acoustic methods of *in-situ* observation offer a solution to some of these problems (e.g. Basedow et al., 2010; Sainmont et al., 2014b; Bozman et al., 2017; Darnis et al., 2017), long-term deployment and accurately resolving the identity of the migrants remain as key challenges.

Mechanistic models offer an alternative means of studying zooplankton vertical strategies in higher resolution. Models related to DVM usually encompass the highest spatial (≤1 m), temporal (≤1 h) and biological (=individual) resolution (e.g. Fiksen and Giske, 1995; Eiane and Parisi, 2001; Liu et al., 2003; Burrows and Tarling, 2004; Hansen and Visser, 2016). Models related to SVM and diapause (i.e. hibrnation in deeper waters, e.g. Hirche, 1996) encompass the same biological resolution, but are usually coarse in spatio-temporal resolution. Here, the time intervals range from 1 h to 1d and vertical spatial elements are usually resolved to either absolute depth units (e.g. 1 m bins) or segregated habitats (e.g. Fiksen and Carlotti, 1998; Miller et al., 1998; Hind et al., 2000; Ji, 2011; Ji et al., 2012; Sainmont et al., 2015; Banas et al., 2016). The choice of a coarser spatio-temporal resolution of these models reflects the broader space and time scales at which the SVM and diapause occurs. This contrasting spatio-temporal scale makes it difficult to harbor lifetime dynamics of DVM to be simulated in SVM models without significantly increasing computer time. Consequently, most models that simulate SVM tend to either fully (e.g. Hind et al., 2000) or partly (i.e. of younger developmental stages, e.g. Fiksen and Carlotti, 1998) disregard DVM. However, the validity of such simplifications are questionable, given the geographically and taxonomically widespread nature of zooplankton DVM behavior and its ontogenetic patterns (Huntley and Brooks, 1982; Huang et al., 1993; Osgood and Frost, 1994; Hays, 1995). It is thus interesting to investigate whether the extra biological information resulting from modeling DVM and SVM in concert is a worthy trade-off for the elevated computer time. If so, such models may lead to improvements of the current understanding about how environmental seasonality shapes up vertical strategies, and the means of which the latter influences life histories of high latitude zooplankton.

Table 2
Evolvable (soft) parameters optimized in the model. The first six are proxies that define the vertical strategy. Vertical strategies of copepods spawned in different times of the year (t_B) are optimized using the GA.

Term	Definition	Range	Interval	Unit
α	Light sensitivity parameter	0–I_{max}[a]	1	$\mu mol\, m^{-2}\, s^{-1}$
β	Size-specificity of light sensitivity parameter	0–10	1	dim.less
γ	Growth allocation parameter	0–1	0.01	dim.less
δ	Seasonal descent parameter	0–1	0.01	dim.less
ζ	Overwintering depth	1–500	10	m
ε	Seasonal ascent parameter	0–1	0.01	dim.less
t_B	Time of birth[b]	1–8760	1	h

[a] The upper limit of α changes with the maximum surface irradiance of the model environment, i.e. I_{max} = 1500 $\mu mol\, m^{-2}\, s^{-1}$ for Environment-L, 1300 $\mu mol\, m^{-2}\, s^{-1}$ for Environment-M and 1100 $\mu mol\, m^{-2}\, s^{-1}$ for Environment-H (cf. Fig. 1).
[b] Time of being spawned.

In this study, we present a model of zooplankton vertical strategies. The model operates in a high-latitude setting and simulates both DVM and SVM of a herbivorous copepod with an annual life cycle in high spatial (vertical) and temporal resolution. Using this model, we aim to investigate the influence of environmental variables on vertical strategies, and how vertical strategies affect fitness and phenology in seasonal environments. We further discuss how short-term behavior (DVM) influences and interacts in the longer-term and shape-up different life history components of copepod strategies.

2. Materials and methods

Although the model is not strictly individual-based, it is described following the Overview, Design concepts and Details (ODD) protocol (Grimm et al., 2006, 2010) to improve reproducibility.

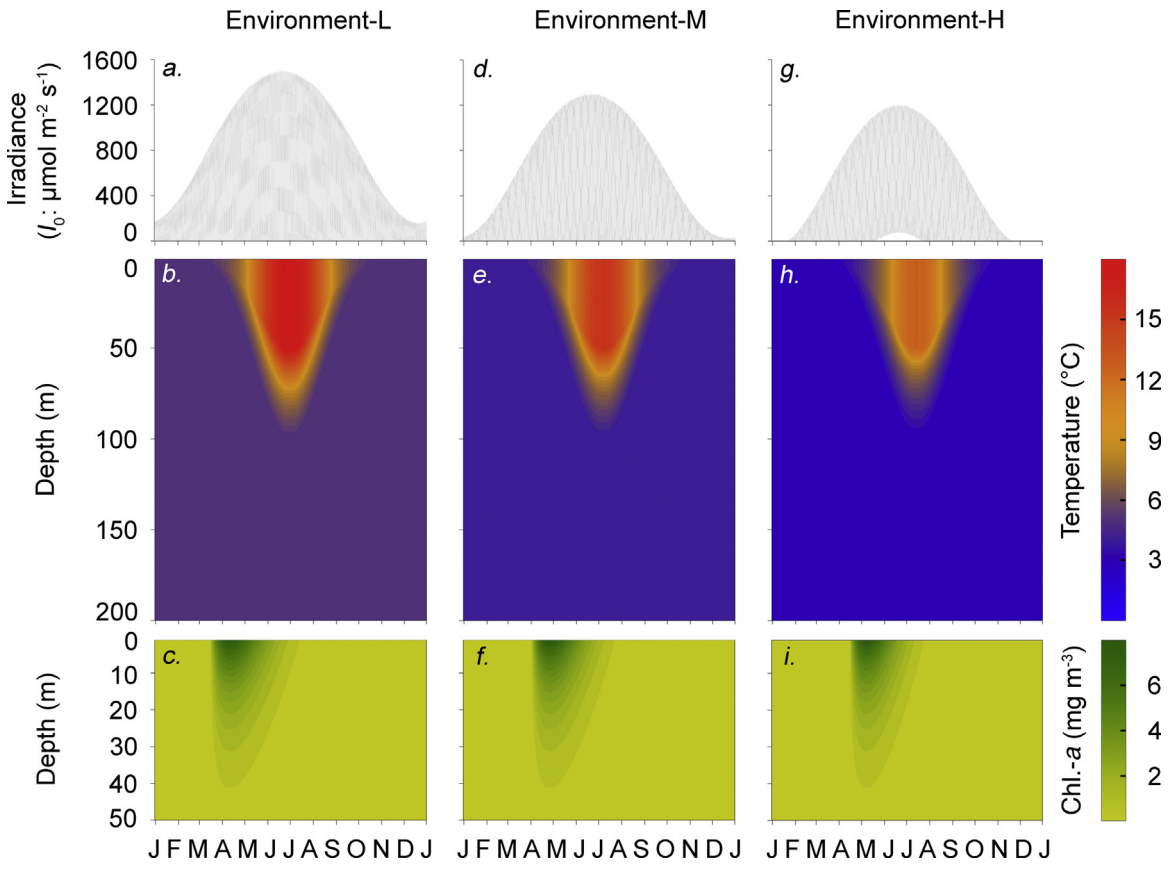

Fig. 1. The modelled dynamics of irradiance incident on the sea surface (hourly estimates; a, d, g), temperature (b, e, h) and food availability (c, f, i, expressed as Chlorophyll-*a* biomass) in the three model environments. See Appendix A1 in Supplementary material for a detailed comparison.

2.1. Purpose

The purpose of the model is to investigate the bottom-up and top-down influences of environmental variability (i.e. irradiance, temperature, food-availability and predation risk) on vertical strategies of a high-latitude herbivorous copepod, and to understand the influences of vertical strategies on its fitness and phenology.

2.2. Entities, state variables and scales

The model consists of three entities: vertical strategies, model organism and the model environment. Vertical strategies define the timing, amplitude and the ontogenetic trajectories of DVM and SVM, and are described using six evolvable (soft) parameters (Table 2). These are hardwired to the model organism, i.e. copepods spawned in different times of the year.

The model organism is a hypothetical herbivorous semelparous female copepod (hereafter, the copepod) with an annual life cycle that resembles *Calanus finmarchicus* and *C. glacialis* in terms of body size, behavior and life history strategies (Conover, 1988). These two species often dominate the copepod biomass in the North Atlantic and most Eurasian sub-Arctic and Arctic seas and shelves (Falk-Petersen et al., 2009). Their life cycle consists of an embryonic stage (egg), six naupliar stages (NI–NVI), five copepodite stages (CI–CV) and an adult. Eggs that are released in near-surface waters in the spring usually develop into CIV or CV stages toward the end of the productive season. As further development is typically constrained by the duration of the productive season and seasonal peaks of visual predation risk, CIVs and CVs descend into deeper waters and remain in a state of diapause/dormancy with minimal physiological activity (Hirche, 1996). Overwintering stages ascend to near-surface waters as the primary production commences in the following year, molt into adults and start to reproduce (Conover, 1988; Varpe, 2012). The life cycle of the two species is usually completed within one year in most sub-Arctic and Arctic locations (Falk-Petersen et al., 2009; Daase et al., 2013), within which reside the model environments of this study.

The model runs in three 500-m deep artificial seasonal environments that represent three high-latitude locations along the southern and southeastern coast of Norway (60–70°N). These environments do not point to specific geographic locations, but the modelled environmental dynamics were adopted from field measurements from the above region (Appendix A1 in Supplementary material). The baseline model simulation (hereafter, the basic run) runs in Environment-L, representing the lower end (ca. 60°N) of the selected geographical range. Here, the modelled irradiance, temperature and food availability are highly seasonal and vertically structured (Fig. 1a–c), but are assumed constant between years. The irradiance incident on the sea surface follows the global clear-sky horizontal irradiance model of Robledo and Soler (2000), and peaks at ca. 1500 µmol m^{-2} s^{-1} (Fig. 1a, Appendix A1 in Supplementary material). The sea surface temperature reaches a maximum of 18 °C in the summer (e.g. Bagøien et al., 2000), and distributes evenly in the surface mixed layer (Fig. 1b). Below this, the temperature decreases with depth and converges to a minimum of 4 °C at ca. 100 m (e.g. Ingvaldsen and Loeng, 2009). The pelagic productive season extends ca. 180 days, with a chlorophyll-*a* peak at 8 mg m^{-3} in mid-April (Fig. 1c: Sakshaug et al., 2009; Daase et al., 2013). We manipulated the environmental parameters of Environment-L to formulate two additional artificial environments: Environment-M (ca. 65°N, Fig. 1d–f) and Environment-H (ca. 70°N, Fig. 1g–i),

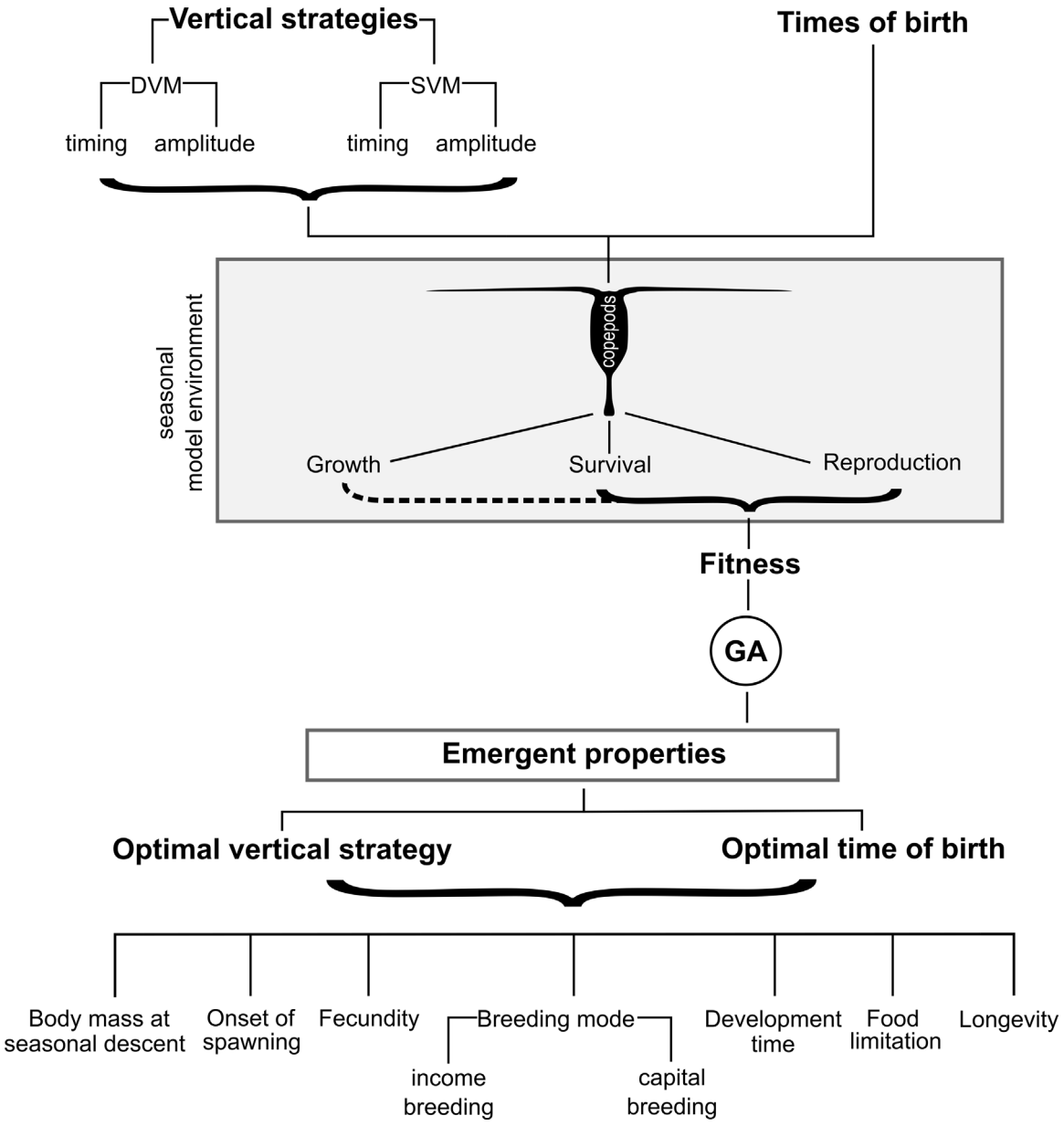

Fig. 2. The model overview. Vertical strategies that define the timing and amplitude of DVM and SVM are hardwired to copepods born in different times of the year. Growth, survival and reproduction of these copepods are simulated in a seasonal environment to derive a fitness estimate that is heuristically maximized by the GA to derive the optimal vertical strategy, time of birth and several associated life history traits emerging from the model. Dashed line represents the indirect dependency of the fitness estimate on growth (Section 2.6.4).

representing the mid-point and the higher end of the selected geographical range (Appendix A1 in Supplementary material).

Copepods are characterized by six states: vertical location (depth), structural body mass, energetic reserve, reproductive output (fecundity), survivorship and developmental stage. The model has a temporal coverage of an annual cycle and a unidimensional (vertical) spatial coverage of 500 m. The time and space consist of 1 h and 1 m discreet intervals.

2.3. Process overview and scheduling

At each timestep, the model follows vertical strategies hardwired to copepods born in different times of the year and simulates their growth, survival and reproduction. State variables are updated simultaneously. Vertical strategies are evaluated using a fitness function based on the expected survival and reproductive performances. The fitness is heuristically maximized using a Genetic Algorithm (GA, Holland, 1975) to estimate the optimal vertical strategy and optimal time of birth for a given set of environmental conditions (Fig. 2).

2.4. Design concepts

2.4.1. Basic principles

The high spatial and temporal resolution implemented in the model allow both DVM and SVM to be simulated over the entire annual life cycle of the copepod. Carlotti and Wolf (1998) have implemented a similar construct, but the SVM of their model was constrained by fixing the timing of ascent and descent to match the field observations of the region of interest. In contrast, the timing and the amplitude of DVM and SVM of our model are flexible and allowed to evolve according to the environmental conditions. To

Table 3
Emergent properties of the model. The timing and amplitude and of DVM and SVM altogether forms the vertical strategy of a copepod.

Trait/attribute	Units	Description
Time of birth	Day of the year	Time of being spawned
Surface time	h	Unified estimate representing the timing of DVM, i.e. the stage-specific mean no. of hours per day occupied in waters with highest growth potential (usually the surface waters)
Amplitude of diel vertical migration	m	The vertical range corresponding to the above
Time of seasonal descent and ascent	Day of the year	Separate estimates representing the timing of SVM (ascent and descent)
Amplitude of seasonal vertical migration	m	Overwintering depth
Body mass at seasonal descent	μg C	Structural and energetic reserve mass at the onset of diapause
Onset of egg production	Day of the year	–
Fecundity	No. of eggs	No. of eggs produced during the lifetime
Breeding mode index	dim.less	Proportion of capital breeding eggs (0 = pure income breeding, 1 = pure capital breeding)
Food limitation index	dim.less	Stage-specific total no. hours with food-limited growth (Eq. (3)) as a fraction of stage duration (0 = no food limitation, 1 = total food limitation)
Development time	d	From egg to a given stage
Longevity	d	Duration of the life cycle, from birth to death

achieve this level of flexibility, we used multiple evolvable proxies to represent vertical migration (Table 2). This resulted in a complex seven-dimensional optimization problem that can be efficiently solved using heuristic techniques (Zanakis and Evans, 1981). As evolutionary algorithms provide an efficient means of solving multi-dimensional optimization problems (Deb, 2001; Eiben and Smith, 2003), we used a GA as the optimization platform of this model. Further, to increase the precision of the evolvable parameters and that of the behavioral strategies and life history traits ensued (Fig. 2), we used a GA variant with floating point representation (i.e. a Real-Coded Genetic Algorithm, Davis, 1989; Lucasius and Kateman, 1989; Herrera et al., 1998).

The strategy-oriented construct of this model contrasts classic individual-based models of zooplankton life history and behavior in two main ways: first, trading off of biological resolution (strategies vs. individuals) to accommodate higher spatio-temporal resolution, and second, the lack of population-level responses such as density dependence. As a result, modelled vertical strategies do not interact with each other and show no quantitative feedbacks with the model environment (e.g. impact of grazing on food concentration and duration of the productive season).

2.4.2. Emergence

The behavioral strategies and life history traits emerging from the model are presented in Fig. 2 and described in Table 3.

2.4.3. Adaptation and sensing

Copepods are sensitive to their internal states (i.e. structural body mass, mass of the energetic reserve and developmental stage) and external stimuli (i.e. irradiance, temperature, food concentration and depth). Altogether, these determine the size- or stage-specific patterns of growth, metabolism, reproduction and vertical behavior (Section 2.6).

2.4.4. Objectives

The model uses a fitness estimate that evaluates the expected reproduction and survival performances rendered by different vertical strategies (Section 2.6.4).

2.4.5. Prediction and stochasticity

The vertical search pattern of copepod behavior is based on a semi-stochastic predictive algorithm (Section 2.6.2.2 and Appendix A2 in Supplementary material). Stochasticity plays a central role in the model initialization (Section 2.5) and selection, recombination and mutation operators of the GA (Section 2.6.4).

2.4.6. Observations

For a given model environment, the model produces heuristic estimates of the optimal vertical strategy and optimal time of birth, along with a range of associated life history traits (Fig. 2, Table 3).

2.5. Initialization

The model initializes with seeding of N (=10^6) eggs at random times of the year to random depths (<50 m) of the water column. Each seed represents an embryonic stage of a copepod with a specific vertical strategy, which is determined by randomly assigning values to the evolvable proxies. The ranges (bounds) and resolutions of these proxies are listed in Table 2.

2.6. Submodels

2.6.1. Growth and development

We modelled somatic growth in Carbon units (μg C) according to the growth model of Huntley and Boyd (1984) (Eqs. (1)–(8) below), using a Chlorophyll-a/C ratio of 0.030 (Båmstedt et al., 1991; Sakshaug et al., 2009). This growth sub-model was used due to its simplicity and general applicability, which are shown by its utility to model several different copepod taxa with varying body sizes representing a wide range of geographical locations (e.g. Robinson, 1994; Fiksen and Giske, 1995; Roman et al., 2000). Definitions and units of all the terms described henceforth are listed in Table 4.

For ambient food concentrations (F: μg C ml^{-1}) above a specific saturation concentration (f), growth is food-independent, and occurs at a maximum rate (G_T: μg C ind^{-1} h^{-1}) dependent only on the ambient temperature (T) as;

$$(G_T)_{i,t,z} = \left(G'_{max}\right)_{t,z} \cdot W_{i,t} \quad (1)$$

Here, i represents individual, t time and z is depth, where $G'_{\max}$ (μg C mg dry mass h^{-1}) is the maximum temperature-dependent mass-specific growth rate, assuming a Carbon: dry body mass (W, mg) ratio of 0.40 (Huntley and Boyd, 1984), defined as;

$$\left(G'_{\max}\right)_{t,z} = 0.903 \cdot \exp(0.110 \cdot T_{t,z}) \quad (2)$$

If the ambient food concentration drops below the saturation concentration, the growth occurs at a rate limited by food availability (G_F) as;

$$(G_F)_{i,t,z} = a \cdot b_{t,z} \cdot W_{i,t}^{n_{t,z}} \cdot F_{t,z} - k \cdot W_{i,t}^{m_{t,z}} \quad (3)$$

Table 4
Definitions, values and units of the terms used in the model.

Term	Definition	Value/formula	Units
a	Assimilation coefficient	0.70[b]	–
$b_{t,z}$	Clearance coefficient	Eq. (4)[a]	ml mg dry mass h^{-1}
E	Egg development parameter	717[e,f]	–
$f_{i,t,z}$	Saturation food concentration	Eq. (8)[a]	μg C ml^{-1}
$F_{t,z}$	Ambient food concentration	Section 2.2	μg C ml^{-1}
$(Gi_{max})_{t,z}$	Maximum mass-specific growth rate	Eq. (2)[a]	μg C mg dry mass h^{-1}
$(G_F)_{i,t,z}$	Food-limited growth rate	Eq. (3)[a]	μg C ind^{-1} h^{-1}
$(G_T)_{i,t,z}$	Non food-limited growth rate	Eq. (1)[a]	μg C ind^{-1} h^{-1}
$H_{i,t,z}$	Survivorship	Eq. (15)	–
i	Individual	–	–
$Ii_{t,z}$	Remapped $I_{t,z}$	$0.9 \geq Ii \geq 0.1$	–
$I_{t,0}$	Irradiance incident on sea surface	Appendix A1 in Supplementary material[c]	μmol m^{-2} s^{-1}
$I_{t,z}$	Downwelling irradiance at depth z	Eq. (9)	μmol m^{-2} s^{-1}
j	Developmental stage	0–12 (Egg–Adult)	–
$K_{i,t}$	Scalar for visual predation risk	$1 > K > 0$	–
$k_{t,z}$	Respiratory coefficient	Eq. (5)[a]	μg C mg dry mass h^{-1}
$(M_n)_{t,z}$	Non-visual predation risk	Section 2.6.2.1	–
$(M_s)_{i,t,z}$	Starvation risk	Eq. (12)	–
$m_{t,z}$	Exponent (respiration)	Eq. (6)[a]	–
$(M_v)_{i,t,z}$	Visual predation risk	Eq. (10)	–
N	No. of initial seeds	1,000,000	–
$n_{t,z}$	Exponent (clearance)	Eq. (7)[a]	–
R_i	Fecundity	Eq. (13)	no. of eggs
t	Time	1–8760	h
$T_{t,z}$	Ambient temperature	Section 2.2	°C
$U_{i,t}$	Cruising velocity	Eq. (11)	m h^{-1}
$(W_c)_{i,t}$	Structural mass	–	μg C
W_E	Unit egg mass	0.55[d]	μg C
$W_{i,t}$	Dry body mass (assuming 40% C)	–	mg
$(W_q)_{i,t}$	Catabolized structural mass (proportion to the maximum lifetime structural mass)	$0 \geq W_q \geq 0.5$	–
$(W_R)_{i,t,z}$	Matter allocated for egg production	–	μg C
$(W_s)_{i,t}$	Storage (energetic reserve) mass	–	μg C
W_x	Stage-specific critical molting mass	Table 5	μg C
z	Depth	0–500	m
Φ	Termination condition of the RCGA	Section 2.6.4	–
ψ	Light attenuation coefficient	0.06[g]	m^{-1}
ω	Parameter for weighing fitness	0 or 1	–
Ω_i	Fitness	Eq. (14)	–

[a] Huntley and Boyd (1984).
[b] Fiksen and Giske (1995).
[c] Robledo and Soler (2000).
[d] Calculated from Salzen (1956).
[e] Campbell et al. (2001).
[f] Ji et al. (2012).
[g] Eiane and Parisi (2001).

where two terms of the right-hand side of the equation refer to the assimilation and respiratory rates respectively. The assimilation coefficient (a) is assumed to be constant (Table 4), but Huntley and Boyd (1984) found that the coefficients of clearance (b) and respiration (k), and the exponents (n and m) vary with ambient temperature as;

$$b_{t,z} = 1.777 \cdot \exp(0.234 \cdot T_{t,z}) \quad (4)$$

$$k_{t,z} = 0.375 \cdot \exp(0.0546 \cdot T_{t,z}) \quad (5)$$

$$n_{t,z} = 0.671 \cdot \exp(0.0199 \cdot T_{t,z}) \quad (6)$$

$$m_{t,z} = 0.858 \cdot \exp(-0.008 \cdot T_{t,z}) \quad (7)$$

At the point where F reaches f, Eqs. (1) and (3) balance out, and the f becomes;

$$f_{i,t,z} = \frac{\left[\left(G'_{max}\right)_{t,z} \cdot W_{i,t} + k_{t,z} \cdot W_{i,t}^{m_{t,z}}\right]}{a \cdot b_{t,z} \cdot W_{i,t}^{n_{t,z}}} \quad (8)$$

This growth sub-model is not applicable to the first two nauplii stages, which do not feed (Fig. 3a, Marshall and Orr, 1972; Mauchline, 1998). For simplicity, we assumed the growth of NI and NII stages to occur at a temperature-dependent rate (Eqs. (1) and (2)). The growth of early developmental stages (NI–CIII) is solely allocated to the building up of structural mass (W_c, μg C, Fig. 3a, b and Table 5).

The embryonic development follows a Bělehrádek temperature function (Campbell et al., 2001; Ji et al., 2012). The post-embryonic development (from stage j to $j+1$) occurs only if W_c exceeds a stage-specific critical molting mass (W_x, μg C, Table 5). However, for simplicity, we did not model the dependence of molting process on the physiological state (Nival et al., 1988) and the limitation of growth by the exoskeleton (Mauchline, 1998).

2.6.2. Survival

2.6.2.1. Predation risk. Visual (v) and non-visual (n) predators induce mortality, which is estimated as a probability following Eiane and Parisi (2001) as;

$$I_{t,z} = I_{t,0} \cdot \exp\left(-\psi \cdot z\right) \quad (9)$$

where I_z and I_0 are irradiance at depth z and surface at a given time, and ψ (=0.06 m^{-1}) is the attenuation coefficient for downwards directed irradiance in the water column. We remapped irradiance (I) between 0.1–0.9 (I') so that visual predation risk is not nullified even at the lowest levels of irradiance, and the copepod has some chance of survival even at highest levels of irradiance.

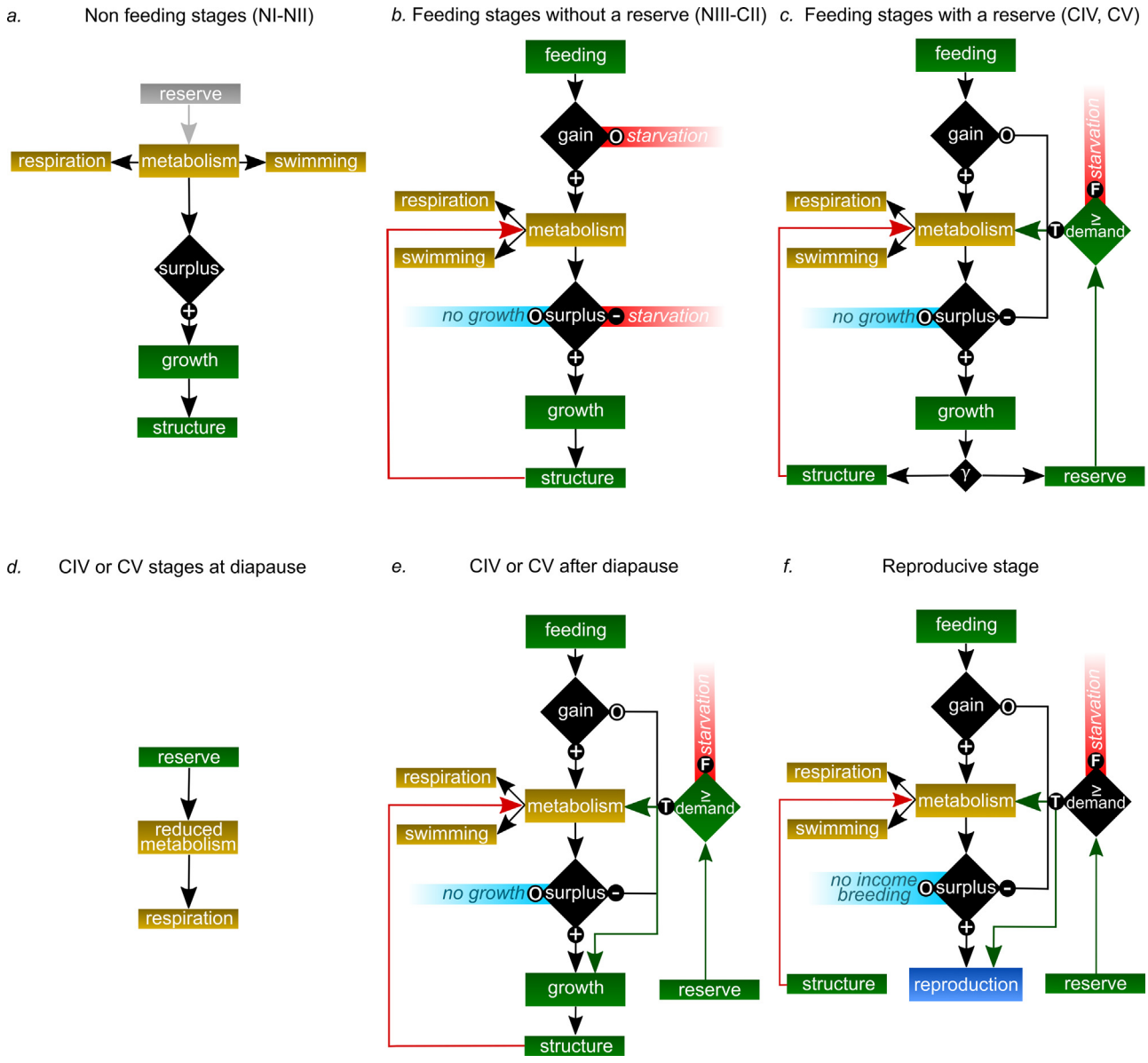

Fig. 3. Simplified physiological pathways modelled in this study. Some life stages are grouped together due to their similarities in energy allocation patterns (a–f). Starvation (highlighted in red) triggers catabolic pathways marked in red. T and F are Boolean values true and false. γ is the growth allocation parameter (Table 2). A comparative summary is given in Table 5.

The detection efficiency of visually orientating planktivores increases with the size of their prey (Brooks and Dodson, 1965; Batty et al., 1990). For simplicity, we modelled the size-dependent visual predation risk using a linear model, assuming that the largest developmental stage is ca. 10 times more vulnerable to visual predators compared to the smallest developmental stage (Fig. 4a, Table 5, De Robertis, 2002). This was implemented using the scalar K ($1 > K > 0$) as;

$$(M_v)_{i,t,z} = I'_{t,z} \cdot K_{i,t} \quad (10)$$

The initial value of K (i.e. K value at the embryonic stage, range = 1×10^{-4}–1.5×10^{-2}) was decided so that it produces hourly estimates of visual predator-induced mortality.

We assumed the mortality risk caused by non-visual predators (non-visual predation risk, M_n) to be 1% of the maximum visual predation risk and constant over time and depth (Eiane and Parisi, 2001).

2.6.2.2. Diel vertical migration. The copepod may perform DVM to trade off growth potential to minimize the visual predation risk. We used the photoreactive behavior as a proxy to estimate the timing and amplitude of DVM (e.g. Kerfoot, 1970; Carlotti and Wolf, 1998). Here, α, an evolvable light sensitivity parameter (Table 2) was used to define an irradiance threshold above which induces a negative phototatic response in the vertical swimming behavior (Båtnes et al., 2015; Cohen et al., 2015). At any given time, the copepod occupies a depth with an irradiance level ($I_{t,z}$) below α. From a series of possible depth bins that satisfy the $I_{t,z} < \alpha$ condition, we assumed that the copepod searches and occupies the depth that maximizes its growth potential. For simplicity, we further assumed that internal state-dependent factors, such as hunger and satiation have a negligible influence on the modelled DVM. The vertical search pattern was predicted using a biased random walk algorithm (Codling, 2003, Appendix A2 in Supplementary material), assuming that the copepod is neutrally buoyant and vertically moves in the water column at a maximum velocity (hereafter cruising veloc-

Table 5
Developmental stages, their maximum structural body masses (W_x) and stage-specific variability in several biological processes modelled in this study (cf. Fig. 3). Dashes indicate non-applicability.

Stage	W_x (μgC)	Feeding	Structural growth	Energetic Reserve	Respiration	Swimming	Egg production
Egg	0.55	–	–	–	–	–	–
NI	0.55	–	x	–	x	x	–
NII	0.68	–	x	–	x	x	–
NIII	0.91	x	x	–	x	x	–
NIV	1.84	x	x	–	x	x	–
NV	2.72	x	x	–	x	x	–
NVI	3.92	x	x	–	x	x	–
CI	6.01	x	x	–	x	x	–
CII	9.84	x	x	–	x	x	–
CIII	17.58	x	x	–	x	x	–
CIV	36.42	x[a]	x[d]	x	x[c]	x[d]	–
CV	110.03	x[a]	x[d]	x	x[c]	x[d]	–
Adult	332.27	x	–	x[b]	x	x	x

W_x values resemble those published for *C. finmarchicus* and *C. glacialis* by Båmstedt et al. (1991); and Campbell et al. (2001).
[a] Feeding ceases during diapause.
[b] Does not allocate surplus growth to develop the energetic reserve, but inherit the reserves from its developmental progression.
[c] Reduces during diapause.
[d] Not relevant during diapause.

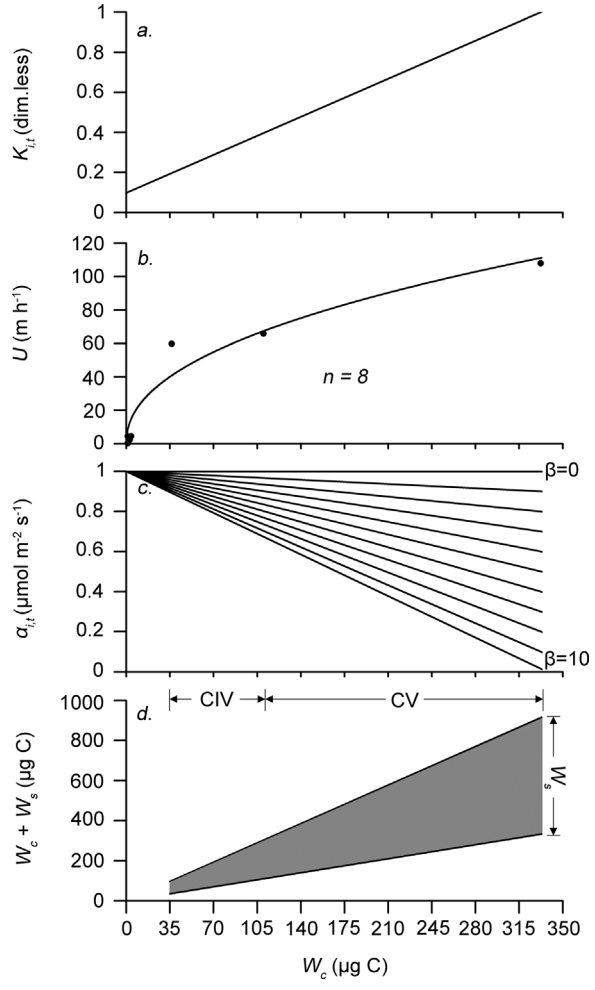

Fig. 4. Relationships of (a) visual predation risk scalar, (b) cruising velocity, (c) light sensitivity parameter and (d) the total body mass of the copepod with its structural mass (W_c). The cruising velocity (U) model was fitted using laboratory and field estimates of *Calanus* spp. from Hardy and Bainbridge (1954), Greene and Landry (1985) and Heywood (1996) (points in panel b). The different linear models for β, that scale the light sensitivity parameter (α) are optimized in the model (Table 2). The lower and upper border of the shaded polygon (panel d) represent the total body mass for growth allocation parameter (γ) = 0 and 1 respectively.

ity, U). We used several stage-specific cruising velocity estimates of *Calanus* spp. available in the literature (Fig. 4b), and related those to body mass as;

$$U_{i,t} = 8.0116 \cdot (W_c)_{i,t}^{0.4531} \quad (11)$$

We considered the size- or stage-specific variability of DVM as a response to size-dependent visual predation risk (Zaret and Kerfoot, 1975; Uye et al., 1990; Hays et al., 1994; Eiane and Ohman, 2004) and modelled it by scaling the light sensitivity parameter (α) with the body mass (W_c). As data on the light sensitivity of younger developmental stages (NI–CIII) of *Calanus* spp. is rare, we could not derive a general relationship between W_c and α. To address this, we defined an evolvable parameter β that describes the size specificity of α, which, at its maximum ($\beta = 10$) downscales α of the adult female to 10% of that of the egg/NI (Fig. 4c). Higher trajectories than $\beta = 10$ were not used, as it was shown in the trial runs that the model always converges on $\beta < 10$ even at highest levels of visual predation risk.

2.6.2.3. Energy storage. CIV and CV stages can allocate a specific fraction from surplus growth (evolvable growth allocation parameter: γ, Table 2) to build up an energy reserve (Fig. 3c) that possesses a maximum size of 70% of the total body mass (Fig. 4d, Fiksen and Carlotti, 1998).

2.6.2.4. Seasonal vertical migration. Similar to most high-latitude marine zooplankton, which descend to depths during the unproductive part of the year (reviewed in Conover, 1988; Hagen and Auel, 2001; Falk-Petersen et al., 2009), the copepod may perform SVM. We used the state of the energetic reserve as a proxy of timing of the SVM (cf. Visser and Jónasdóttir, 1999). Here, the copepod descends to a specific depth (evolvable overwintering depth ζ, Table 2) when the stores account for a specific fraction of the total body mass (evolvable seasonal descent parameter: δ, Table 2). Upon reaching the overwintering depth, the copepod remains stagnant at a diapause state (Hirche, 1996) with its metabolic rate reduced by 90% from that under normal conditions (Fig. 3d, Table 5, Pasternak et al., 1994; Varpe et al., 2007). The overwintering period terminates when a specific fraction (evolvable seasonal ascent parameter: ε, Table 2) of the energetic reserve is exhausted. After the overwintering period, surplus gains are not allocated to develop further energetic reserves, but may be used for structural growth and reproduction (Fig. 3e and f, Table 5).

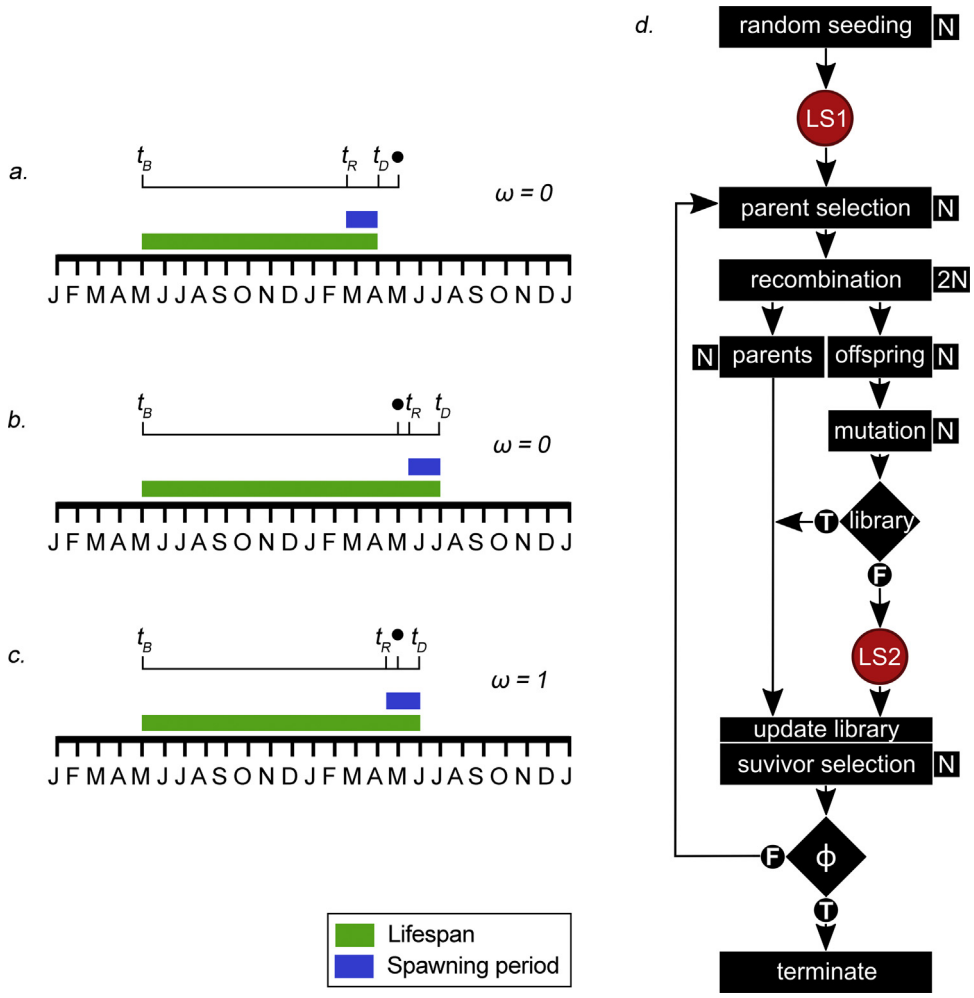

Fig. 5. (a–c) Mechanism of weighing fitness. Fitness of a copepod is multiplied by a binary weight $\omega = 0$ if its egg production season ($t_D - t_R$) does not overlap the time of birth (t_B, May 1 in this example, denoted by a black dot) and vice versa. (d) Simplified workflow of initialization and optimization steps of the model. The initial set of strategies enter the optimization loop after going through the first life cycle simulation (LS1). The GA optimizes seven evolvable (soft) parameters (Table 2) by repeatedly applying selection, recombination and mutation operators until a termination condition (φ) is satisfied. T and F are Boolean true and false conditions. No. of strategies (i.e. size of the GA-population, *N* or *2N*) at each operation is indicated to the right.

2.6.2.5. Metabolism. The basal metabolic cost relates with the body mass and ambient temperature, expressed as $k{\cdot}W^m$ in Eq. (3) (terms as defined above and in Table 4). The metabolic cost of zooplankton vertical movements can account for 0–300% of the basal metabolic demand (Vlymen, 1970; Foulds and Roff, 1976; Morris et al., 1985; Dawidowicz and Loose, 1992). For simplicity, we assumed the cost of vertical movement to be 150% of the basal metabolic cost (mid-point of the above range). This additional cost is subtracted from the growth Eqs. (1) or (3). The energy reserve is used to balance the metabolic demands that cannot be sustained under low ambient food concentrations (Fig. 3c–f).

2.6.2.6. Starvation risk. When energy reserves are depleted, the metabolic demands that cannot be balanced by food intake are met by catabolizing structural body mass (Fig. 3b–f). This elevates the mortality risk due to starvation (starvation risk, M_s), which is defined as a probability that increases as a linear function of catabolized structural mass as;

$$(M_s)_{i,t} = 2 \cdot \left(W_q\right)_{i,t} \tag{12}$$

Here, W_q is the catabolized structural mass expressed as a proportion of the maximum structural mass prior to structural catabolization. W_q can reach a maximum of 0.5, during which M_s peaks following Eq. (12), and the copepod dies according the Chossat's rule (Chossat, 1843), which posits that starving animals may catabolize about half of their body weight before death. Irrespective of the age of this generalized rule, it has been used as a constraint in starvation studies of many vertebrate and invertebrate taxa (e.g. Threlkeld, 1976; Spencer, 1997; Costello, 1998; Loos et al., 2010).

2.6.3. Reproduction

We assumed that somatic growth ceases after the final molt, and all adults become sexually mature at a constant structural body mass (Fig. 3f, Table 5). Energetic input to egg production may be sourced from food intake (income breeding) or allocating a specific amount of matter (C) equivalent to the maximum growth rate (G_T: Eqs. (1) and (2)) from the remaining energetic reserve (capital breeding, cf. Varpe et al., 2009). The fecundity (R) from the time of sexual maturity (t_R = time of final molt) to a given time horizon (t_X) is estimated using the matter allocated to egg production (W_R) and the unit egg mass (W_E = 0.55 μg C) as;

$$R_i = \sum_{t_R}^{t_X} \frac{(W_R)_{i,t,z}}{W_E} \tag{13}$$

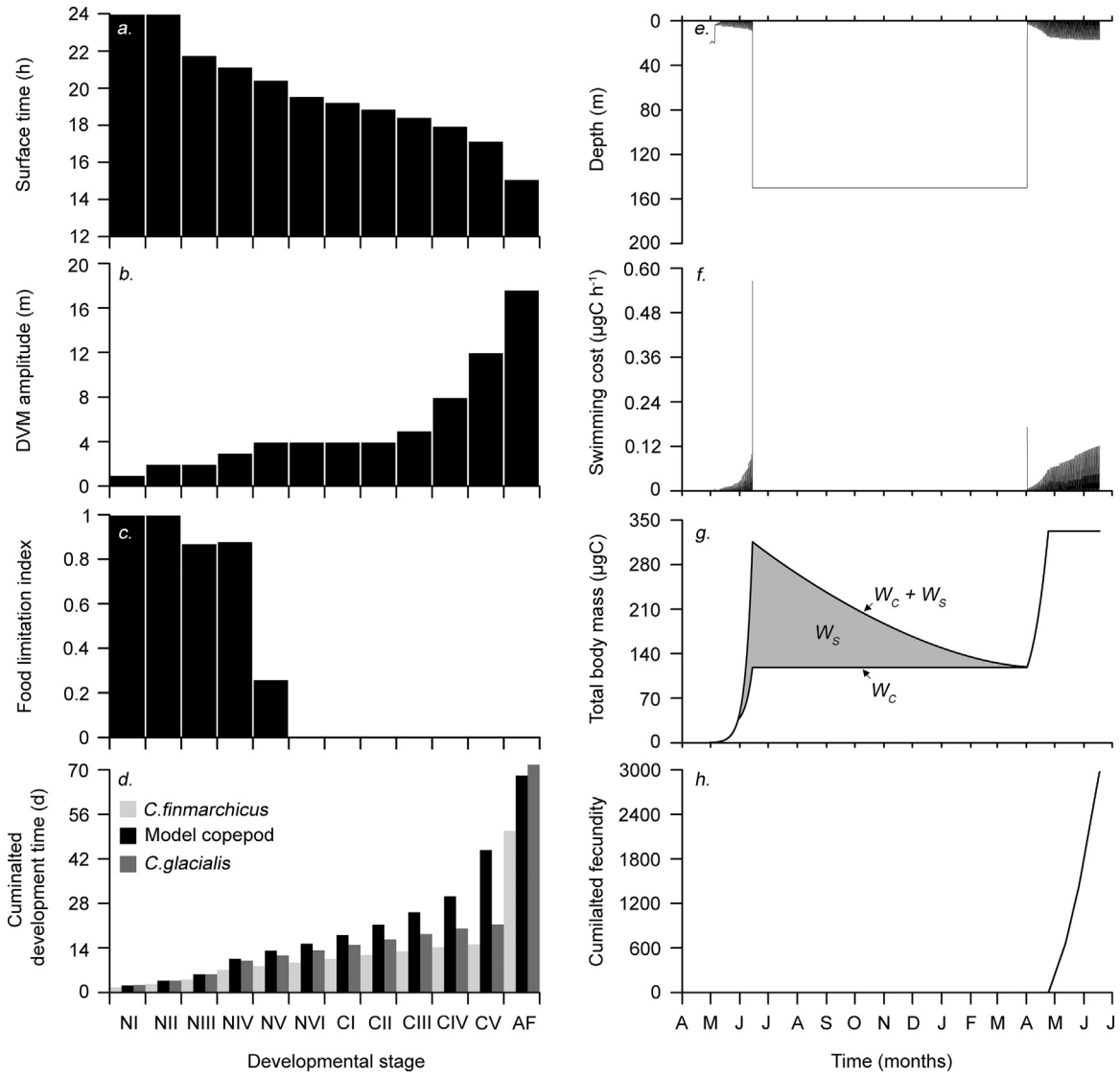

Fig. 6. Predicted optimal vertical strategy and associated growth and reproductive performances of the copepod in the basic run at Environment-L (cf. Fig. 1a–c). The surface time (a) is the stage-specific mean no. of hours per day that the copepod occupies food-rich surface waters, and amplitude (b) is its vertical range. Panel d compares predicted development times (excluding overwintering duration) to those estimated for *C. finmarchicus* and *C. glacialis* following Bělehrádek functions parameterized by Campbell et al. (2001) and Ji et al. (2012). W_c and W_s refer to structural body mass and size of the energetic reserve respectively.

2.6.4. Fitness function and optimization

To evaluate the performance of a vertical strategy, we derived a fitness estimate (Ω) as a function of survivorship and fecundity as;

$$\Omega_i = \left(\sum_{t_B}^{t_X} H_{i,t,z} \cdot R_{i,t,z} \right) \cdot \omega \tag{14}$$

Here, ω is a weight that adjusts fitness (see below) and H is the survivorship, i.e. the probability of survival from birth (t_B) to a given time horizon (t_X) estimated as a function of visual, non-visual and starvation risks (M_v, M_n and M_s) as;

$$H_{i,t,z} = \prod_{t_B}^{t_X} 1 - \left[(M_v)_{i,t,z} + (M_n)_{t,z} + (M_s)_{i,t} \right] \tag{15}$$

The term Ω technically resembles the net reproductive rate (e.g. Stearns, 1992), and is used in some optimization models (e.g. Kiørboe and Hirst, 2008) but may not bare the same interpretation given the strategy-oriented construct of this model. When the model predicts an optimal vertical strategy and time of birth for a particular environment, we can assume that those predicted optima should persist from one generation to the next if the environment remains constant. If a copepod's spawning period lasts from time t_R to t_D (time of death) we assumed that it produces a series of offspring with the same vertical strategy, but born at different times of the year (ranging from t_R to t_D). However, only the offspring with a time of birth matching that of the mother can represent the entire evolvable (soft) parameter set of the mother, and guarantee its persistence from one generation to another (Fig. 5a–c). Therefore, we adjusted the fitness using a binary weight (ω) by setting $\omega = 0$ if the copepod's spawning season does not overlap its time of birth (Fig. 5a and b) and vice versa (Fig. 5c).

We used a Real-Coded Genetic Algorithm (RCGA) to derive heuristic estimates of optimal vertical strategy and time of birth that maximizes fitness in a given model environment (Fig. 5d). In the RCGA, six proxies of vertical strategies and the time of birth of the copepod that those are hardwired to (Table 2) are considered as genes on a single chromosome. The RCGA begins by selecting a mating pool of N chromosomes (=parents, i.e. N vertical strategies seeded in different times of the year) from the initial

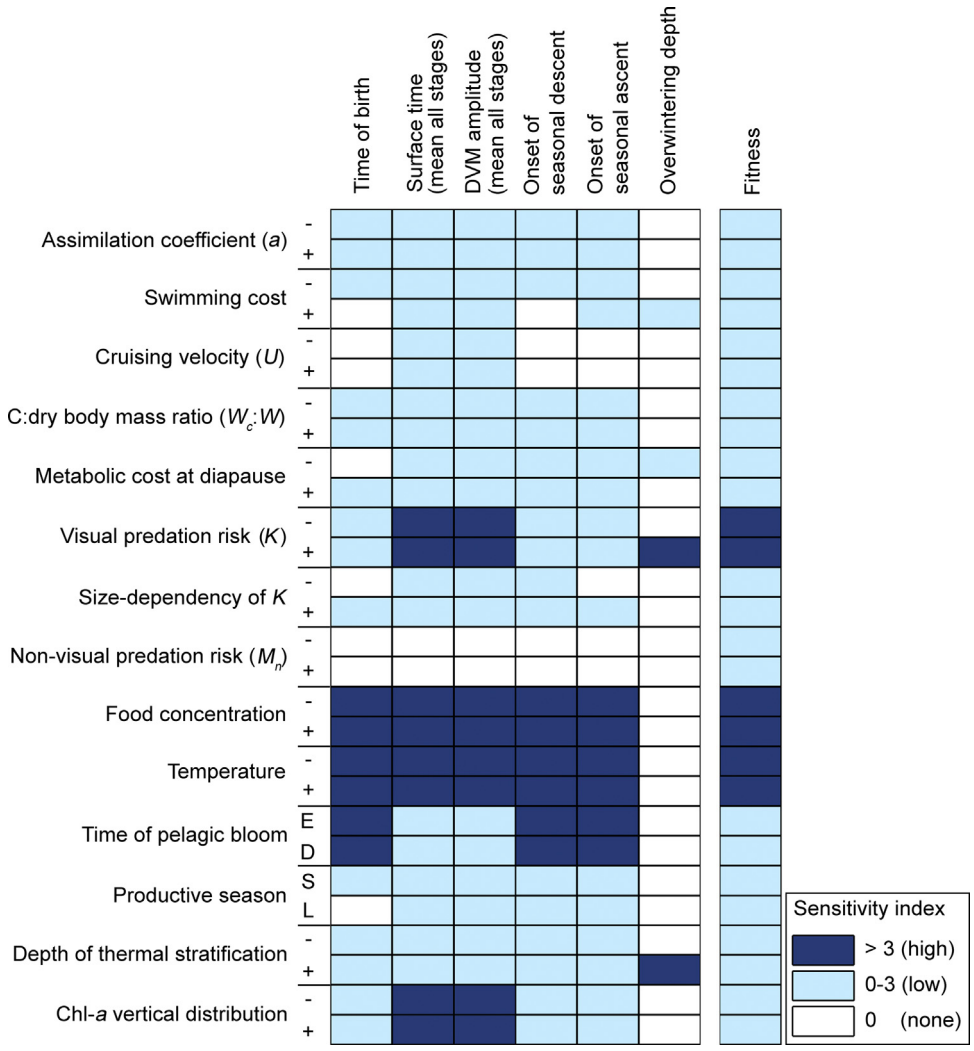

Fig. 7. Graphical summary of the sensitivity analysis. Model parameters and environmental variables tested for sensitivity are presented on the vertical dimension, and the model-predicted optima of time of birth and vertical strategy, and the associated fitness on the horizontal dimension. +/−: 25% increase/decrease in the parameter value, E/D: 15-d earlier/delayed and S/L: 15-d shorter/longer scenarios regarding timing and duration of the productive season (see Appendix A3 in Supplementary material).

seeds using a binary (two-way) deterministic tournament selection (Goldberg and Deb, 1991; Miller and Goldberg, 1995). Genes of two randomly selected parents from the mating pool are recombined through blend crossover following the BLX-α method (Eshelman and Schaffer, 1993), which produces two offspring (recombinants). Genes of the recombinants are mutated at a probability of 0.02 by random replacement (uniform mutation: Eiben and Smith, 2003; Haupt and Haupt, 2004). The population of strategies resulting from these operations comprises of N parents, whose fitness is known and N offspring, whose fitness is not yet known. Parents with unique gene combinations are selected to construct a library (hereafter, the reference library), which is updated at each iteration. Each offspring is compared with those in the reference library to assess their fitness. Fitness of the offspring with similar gene combination to those in the library are assigned *in-situ*, while the rest goes through the life cycle simulation to determine fitness (LS-2 in Fig. 5d). Once the fitness of all $2N$ individuals are known, N survivors are selected following a round-robin (all-play-all) tournament of size 10 (Harik et al., 1997; Eiben and Smith, 2003). This process is repeated for a minimum of 100 iterations, and terminated when the mean fitness of the population shows no improvement for 25 consecutive iterations (ϕ in Fig. 5d, Eiben and Smith, 2003).

2.7. Programming, execution and analysis of the model

We used R version 3.3.1 (R Core Team, 2016) and R Studio integrated development environment (IDE) version 1.0.136 (RStudio Team, 2016) along with the high-performance computing packages Rcpp (Eddelbuettel et al., 2011) and bigmemory (Kane et al., 2013) to construct, simulate and analyze the model.

A basic run was performed in the Environment-L using default values for model parameters (Table 4). In order to test the influence of model parameters and environmental variables on model-predicted vertical strategies and fitness, we performed a sensitivity analysis following (Jørgensen and Bendoricchio, 2001). Here, we calculated a sensitivity score (S_x) as;

$$S_x = \frac{(X_{BR} - X_M)/X_{BR}}{(P_{BR} - P_M)/P_{BR}} \tag{16}$$

where X is the predicted model output of the basic run (X_{BR}) and the modified run (X_M) for a given change (±25%) of input parameter value between the basic run (P_{BR}) and the modified run (P_M). We tested the sensitivity of vertical strategies and fitness for 13 different input parameters (Appendix A3 in Supplementary material). For the convenience of interpretation of these results, we presented the sensitivity scores under three categories: no-sensitivity ($S_x = 0$), low sensitivity ($0 < S_x \leq 3$) and high sensitivity ($S_x > 3$). Finally, we

Table 6
Predicted variability of emergent behavioral strategies and life history traits (Fig. 2, Table 3) induced by model parameters and environmental variables analyzed for sensitivity (Fig. 7, Appendix A3 in Supplementary material). Only the input parameters with highest influence on fitness (sensitivity index >3) are tabulated.

Parameter	Variation	Time of birth (day)	Surface time[a] (h)	DVM amplitude[a] (m)	Onset of seasonal descent (day)	Onset of seasonal ascent (day)	Overwintering depth (m)	Development time[b] (d)	Food limitation index[a]	Body mass at seasonal descent (μgC)		Onset of egg production (day)	Fecundity	Breeding mode index	Longevity (d)	Absolute fitness
										W_c	W_s					
Basic run	0%	120	20.5	5	166	92	150	68.1	0.33	120.4	195.7	114	2972	0.000	414	4.10
Visual predation risk (K)	−25%	118	22.7	3	163	91	150	65.2	0.38	127.0	203.2	111	3834	0.000	430	21.2
	+25%	123	19.8	7	168	90	170	69.4	0.29	116.0	185.6	114	1446	0.000	389	0.90
Food concentration (F)	−25%	105	22.9	3	183	85	150	98.4	0.25	221.1	342.7	105	415	0.018	384	1.00
	+25%	122	19.8	6	157	99	150	59.5	0.63	120.8	196.3	123	3957	0.000	424	8.70
Temperature	−25%	103	23.0	2	181	82	150	99.1	0.21	229.7	346.3	103	654	0.022	387	1.20
	+25%	127	19.7	7	160	107	150	47.0	0.68	124.4	202.5	121	5285	0.000	412	16.1

W_c = structural mass, W_s = mass of energetic reserve.
[a] Mean of all stages.
[b] From egg to adult excluding the overwintering period.

studied the changes of heuristically optimized vertical strategies by performing model simulations in the three model environments at different levels of visual predation risk, while maintaining the rest of the parameter values at its default levels.

As GAs produce heuristic estimates of the maximum fitness, there is no guarantee that it would converge on the global maximum given a potentially diverse fitness landscape (Record et al., 2010). Therefore, we replicated each model run 10 times with different starting values assigned to the soft parameters (Table 2) to check if the algorithm converges on the same set of solutions. As the optimized parameter values showed little variability between replicate runs (<5%), we used the mean of the replicates for each parameter for analyses.

3. Results

3.1. The basic run

In the basic run, the life cycle emerging from the model began as an egg spawned at 20 m depth in late-April. The first two nauplii stages did not perform DVM, but DVM and the associated metabolic cost (swimming cost) increased ontogenetically from NIII onwards (Fig. 6a, b, e and f). The somatic growth of all developmental stages beyond NV occurred under food limitation (Fig. 6c), and because of reduced growth rates, their predicted development times were higher than those estimated from Bělehrádek temperature functions (Fig. 6d). As the energetic reserve reached 65% of the total body mass ($W_s \approx 196$ μgC, Fig. 6g), the developmental stage CV descended to an overwintering depth of 150 m in mid-June, ca. 2 months before the pelagic primary production had terminated (Fig. 6e). It remained there for ca. 290 days, and ascended into near-surface waters again in early-April of the following year, ca. 10 days after the pelagic primary production had commenced (Fig. 1c), with fully depleted energetic reserves. Although the energetic cost of seasonal migration was quite high, the cost of ascent was ca. ¼ of that of the descent due to the loss of body mass during overwintering (Fig. 6f and g). The copepod developed to an adult female in mid-April, and thenceforth produced eggs (ca. 3000) via income breeding until mid-June and then died (Fig. 6h).

3.2. Sensitivity analysis

The model-predicted fitness was highly sensitive to visual predation risk, food concentration and temperature (Fig. 7). A 25% change in the visual predation risk ($K = 7.5 \times 10^{-3}$ and 1.25×10^{-2}) influenced the DVM, which intensified at the higher-end of K and vice versa (Table 6). Although the overwintering depth deepened by ca. 13% under higher visual predation risk, it did not change under lower visual predation risk. Furthermore, higher visual predation risk lowered the fecundity and longevity, and vice versa (Table 6).

A 25% change in food concentration ($F = 10$ and 6 mg m^{-3} Chl.-a) notably influenced the DVM, timing of SVM and time of birth, but not the overwintering depth (Fig. 7). Under low food concentration, the DVM was less pronounced and the seasonal descent was delayed ca. 15 d compared to the basic run, possibly because of foraging later into the feeding season due to lower growth potential sustained under increased food limitation (Table 6). However, the copepod overwintered as a significantly large CV with elevated energetic reserves, and made ca. 7-d earlier spring ascent (late March), followed by spawning that preceded the pelagic bloom by ca. 2 days (cf. Fig. 1c). Here, ca. 2% of the total egg production was sourced from capital breeding (Table 6). Early seasonal ascent, capital breeding and early spawning thus appear as strategies employed to avoid seasonal peak in visual predation risk (cf. Fig. 1a, Eqs. (9) and (10)) when foraging efforts are elevated to cope with lower

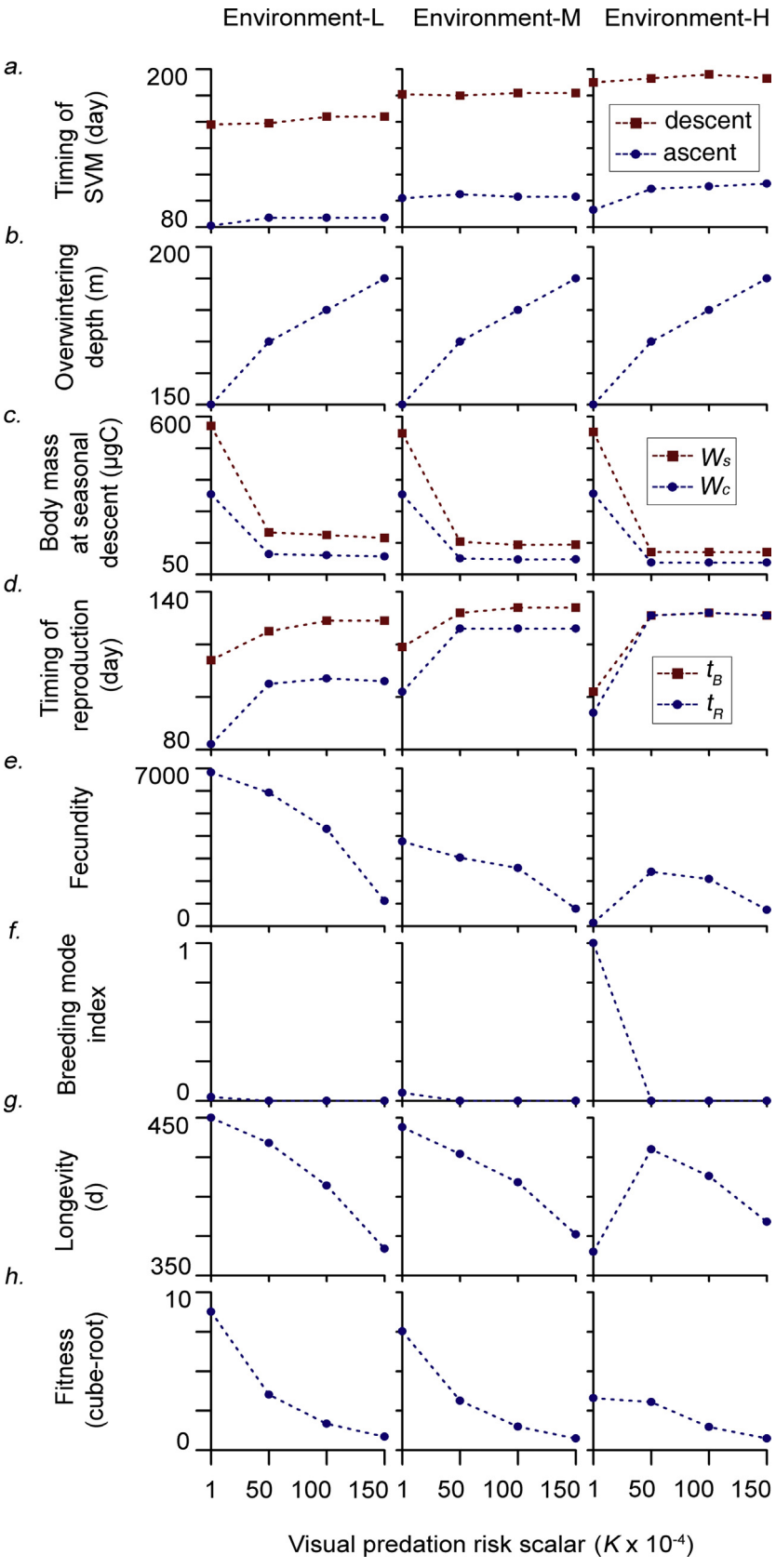

Fig. 8. Predicted optima of time of birth (t_B), vertical strategy and associated life history traits of the copepod in the three model environments under variable levels of visual predation risk. Visual predation risk is scaled by varying the parameter K in a range of $1–150 \times 10^{-4}$. The fitness is cube-root transformed for the convenience of visualization. Time is presented as day of the year, where day 1 = 1 January. W_c and W_s are structural and energy reserve masses, and t_R is time of first reproduction.

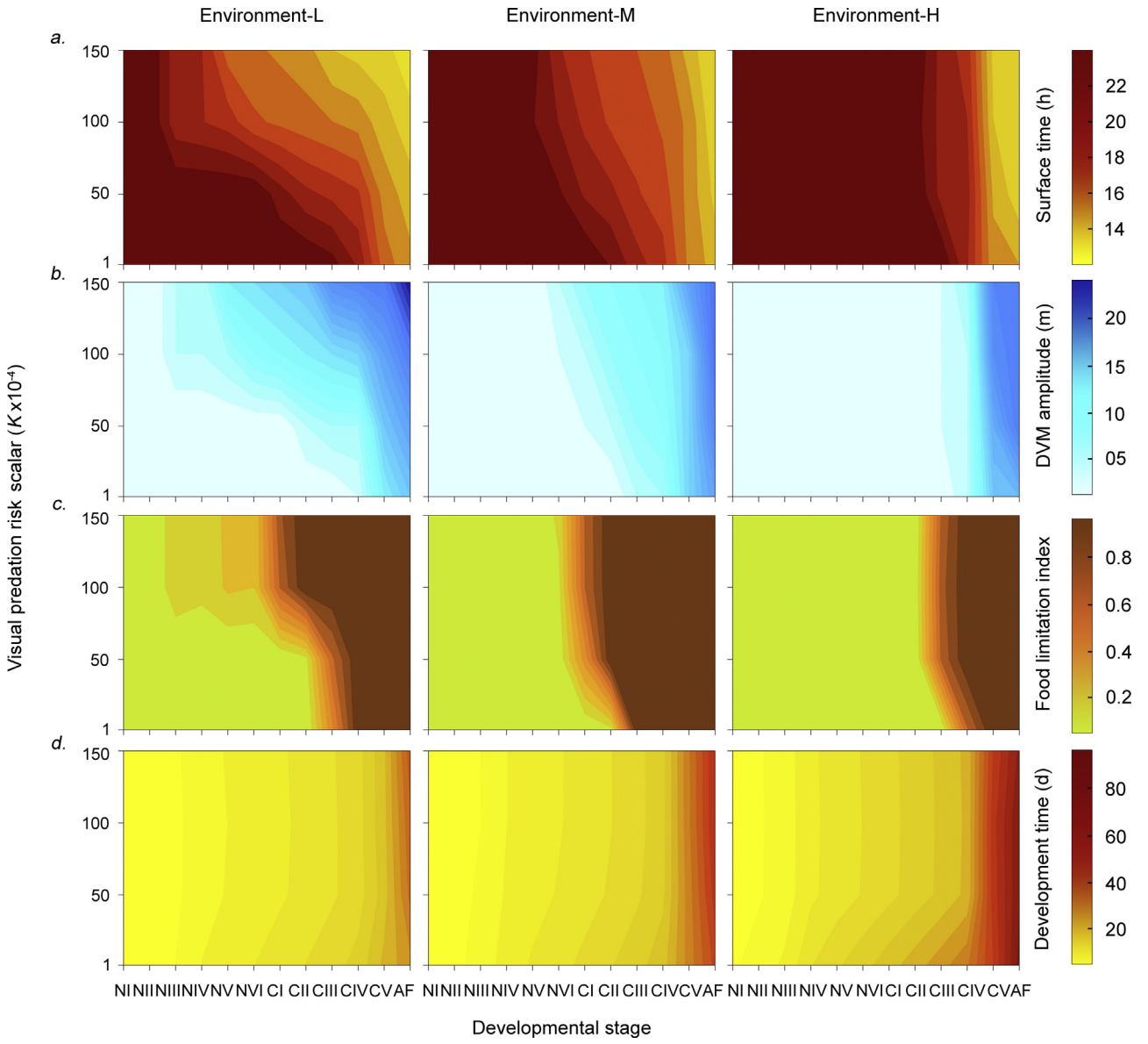

Fig. 9. Predicted stage-specific surface time (a), DVM amplitude (b), food limitation index (c) and the development times (egg to a given stage excluding the overwintering period, d) of the copepod in the three model environments under variable levels of visual predation risk.

growth potential. However, this came with a cost of decreased fecundity (80%) and longevity (7%) (Fig. 7, Table 6). Increased food concentration had the opposing effects on the predicted behavioral strategies and life history traits described above (Fig. 7, Table 6).

The influence of 4.5 °C change in temperature (T = 22.5 and 13.5 °C) on copepod's behavior and life history followed the same general trends described for food concentration (Fig. 7, Table 6), and highlight the equally important roles played by food availability and temperature in growth and development.

3.3. Latitudinal environmental variability and visual predation risk

Model-predicted optimal time of birth, body mass (W_c and W_s) at seasonal descent, overwintering depth and longevity changed with visual predation risk (K), but showed less variability along the modelled latitudinal environmental gradient (Fig. 8b–d and g). The predicted optimal time of birth changed from late-April to mid-May with increasing visual predation risk, and was constant across the three model environments, with the exception that it occurred the earliest in mid-April at Environment-H under the lowest visual predation risk ($K = 10^{-4}$, Fig. 8d). At lower levels of visual predation risk, the copepod overwintered as relatively large CVs with elevated energetic reserves at relatively shallow depths (Fig. 8b and c). However, as the visual predation risk increased, the copepod overwintered as smaller CVs or CIVs with relatively less energetic reserves at greater depths. Although the predicted longevity decreased by ca. 80 d along the modelled visual predation risk gradient (Fig. 8g), longevity at Environment-H under $K = 10^{-4}$ was lower (365 d) compared to those predicted under higher visual predation risk levels (384–430 d).

The predicted timing of SVM showed significant variability across the three model environments, but was less affected by visual predation risk (Fig. 8a). Both the descent and ascent occurred earliest at the lowest latitude environment, but happened later in the season at higher-latitude environments, with a shift of about a month. Although this reflects the delayed occurrence of the pelagic bloom along the modelled latitudinal gradient (Fig. 1c, f

and i, Appendix A1 in Supplementary material), the seasonal ascent at Environment-H under lowest visual predation risk ($K = 10^{-4}$) occurred ca. 25 days before the pelagic primary production had commenced (Figs. 1i and 8a).

The predicted onset of spawning, fecundity and breeding mode index (Fig. 8d–f), along with the predicted timing and amplitude of DVM, food limitation index and development time (Fig. 9) varied with both the visual predation risk and latitudinal environmental gradient. In all model environments, the spawning started earliest under the lowest visual predation risk ($K = 10^{-4}$, Fig. 8d). Here, spawning commenced ca. 5–7 days earlier than the onset of spring primary production in lower latitude environments (Fig. 1c and f), and ca. 2.5–5% of the total egg production were sourced from capital breeding (Fig. 8f). Spawning at Environment-H commenced ca. 25 d prior to the pelagic bloom, but lasted only for ca. 10 days (Figs. 1i, 8d and g). Consequently, the expected fecundity was the lowest (ca. 145 eggs, Fig. 8e) and all eggs were sourced from capital breeding (Fig. 8f). The onset of spawning shifted later into the season at higher latitude model environments at higher levels of visual predation risk, and occurred after the commencement of the pelagic primary production (Figs. 1c, f, i and 8d). Here, all eggs were produced via income breeding (Fig. 8f). At lower levels of visual predation risk ($10^{-4} \leq K \leq 5 \times 10^{-3}$), the predicted DVM pattern was similar across the three model environments, where developmental stages until early copepodites did not perform DVM (Fig. 9a and b). Although the model predicted the younger developmental stages (NIII onwards) to perform DVM under elevated visual predation risk at Environment-L, this effect gradually waned in higher-latitude model environments. The food limitation index strongly followed the DVM pattern, where developmental stages that performed DVM suffered from increased food limitation (Fig. 9c). Food limitation significantly reduced the growth rates (cf. Eqs. (1)–(3), see also Appendix A4 in Supplementary material), and consequently, the development times increased along the modelled environmental gradient (Fig. 9d). Further, in each model environment, lowest development times were predicted under the lowest level of visual predation risk.

4. Discussion

4.1. Influence of environmental variables on vertical strategies

4.1.1. Diel vertical migration

In this model, visual predation risk had the highest influence on the DVM, which diminished under low visual predation risk (Figs. 7 and 9, Table 6) and completely ceased when visual predation was removed from the model ($K = 0$, data not presented). Conversely, under high visual predation risk, also younger developmental stages reduced the time spent in food-rich surface waters by performing low-amplitude (shallow) DVM (Fig. 9a and b). Food concentration and temperature also influenced the DVM (Fig. 7, Table 6). Lower food concentrations or temperatures produced low-amplitude DVM, possibly due the low growth potential attained in cold, food-limited conditions (Fig. 9, Eqs. (1)–(8), Appendix A4 in Supplementary material). Under these conditions, it appears that modelled copepods do not possess sufficient growth potential to trade off for survival and perform high-amplitude (deep) DVM, a conclusion also drawn in empirical work (e.g. Huntley and Brooks, 1982; Loose and Dawidowicz, 1994). Reduced or absence of DVM under low food concentrations and temperatures are reported from several other modeling studies on copepods and euphausiids (e.g. Andersen and Nival, 1991; Fiksen and Giske, 1995; Fiksen and Carlotti, 1998; Tarling et al., 2000) and from empirical work on marine copepods and freshwater cladocerans (e.g. Hardy and Gunther, 1935; Huntley and Brooks, 1982; Johnsen and Jakobsen, 1987). However, the largely exogenous-regulated DVM behavior emerging from this model does not render a complete view on the subject matter, as DVM can also be sensitive to internal (physiological) states of zooplankton (e.g. hunger and satiation, Hays et al., 2001; Pearre, 2003).

The effect of temperature on growth potential further explains the diminished influence of visual predation risk on the timing and amplitude of DVM predicted at higher latitude model environments (Fig. 9). Albeit similar food concentrations, the modelled temperatures decreased from lower- to higher-latitude model environments, reflecting a decreasing gradient of growth potential (Fig. 1, Appendix A4 in Supplementary material). Consequently, the model-predicted optimal DVM strategy for higher-latitude environments was to elevate the growth potential by spending more time foraging in near-surface waters (Fig. 9a and b). This effect was most pronounced among younger developmental stages (NIII–CI), whose DVM reduced from environment-L to -M, and completely ceased at environment-H. DVM of younger developmental stages (NIII onwards) are most commonly reported from lower latitudes for *Calanus* spp. (e.g. Huntley and Brooks, 1982; Uye et al., 1990; Huang et al., 1993; Osgood and Frost, 1994; Zakardjian et al., 1999) and *Metridia* spp. (e.g. Hays, 1995). While some field studies failed to detect notable DVM in high-latitudes (e.g. Blachowiak-Samolyk et al., 2006; Basedow et al., 2010), others reported ontogenetic increase of DVM (CI onwards, e.g. Dale and Kaartvedt, 2000; Daase et al., 2008) in *Calanus* spp. However, empirical data with high spatial, temporal and biological (i.e. developmental stage) resolution is needed to test the ontogenetic and latitudinal patterns of DVM predicted by our model.

The predicted DVM amplitudes spanned across the productive part of the water column (i.e. upper 30 m, cf. Figs. 1, 6 and 9), and showed a positive relationship with the vertical extent of food availability (Fig. 7). Moreover, strategies that involve higher-amplitude DVM lead to increased food-limitation, where younger developmental stages with no energetic reserves tend to suffer from starvation risk due to low temperatures and food concentrations that prevail in deeper parts of the model environments (Fig. 1). Therefore, low-amplitude DVM appears to be a strategy that efficiently trades off growth potential for survival, by balancing both the visual predation and starvation risks (Kerfoot, 1970; Fiksen and Giske, 1995; De Robertis, 2002). Although higher-amplitude DVM can be predicted either by not modeling starvation risk or imposing starvation tolerance (e.g. Andersen and Nival, 1991; Carlotti and Wolf, 1998; Zakardjian et al., 1999; Tarling et al., 2000), we did not follow these approaches because our model sufficiently represents the relative importance of DVM across the modelled environmental gradients.

4.1.2. Seasonal vertical migration

Food availability and temperature had the most notable influence on the model-predicted timing of SVM (Fig. 7, Table 6). The predicted shift in timing of seasonal descent and ascent coincided with those of the pelagic algal bloom and thermal stratification along the modelled latitudinal gradient (Figs. 1 and 8a). This agrees with the argument that food availability is the ultimate factor influencing the timing of seasonal vertical migration of *Calanus* spp. (Herman, 1983; Head and Harris, 1985; Hind et al., 2000). However, field estimates of timing of SVM of *Calanus* spp. from low to high latitudes do not point to a simple south–north gradient as predicted in our model (Table 7, see also Melle et al., 2014). This discrepancy of model predictions and field estimates underlies the differences between location-specific variability in hydrography, algal bloom dynamics and species composition (e.g. Hirche, 1991; Daase et al., 2013), diversity of generation lengths and breeding strategies (e.g. Conover, 1988; Falk-Petersen et al., 2009) and climate-driven and other stochastic oscillations of environmental

Table 7
Timing of seasonal ascent and descent of *Calanus* spp. estimated by several high-latitude field investigations. These estimates are based on observation of zooplankton populations oftentimes containing various combinations of *C. helgolandicus*, *C. finmarchicus*, *C. glacialis* and *C. hyperboreus*. Geographical location is approximate. Data for North-Atlantic are available in Melle et al. (2014).

Study	Lat.	Lon.	Onset of descent	Onset of ascent
Hirche (1984)	58° N	11° E	mid-October	mid-May
Bagøien et al. (2000)	59° N	10° E	July–August	March
Heath (1999)	61° N	4° W	–	May
Gislason and	62° N	20° W	–	April
Astthorsson (2000)	64° N	28° W	–	April
Østvedt (1955)	66° N	2° E	July	April
Kosobokova (1999)	66° N	35° E	mid-July	mid-May
Astthorsson and Gislason (2003)	68° N	13° E	–	May
Madsen et al. (2001)	69° N	54° W	–	mid-April
Madsen et al. (2008)	69° N	54° W	late-September	early-April
Hirche (1997)	71° N	4° E	July–August	April
	74° N	1° E	July–August	April
Unstad and Tande (1991)	75° N	30° E	–	May
Arashkevich et al. (2002)	76° N	33° E	July	May
Hirche and Kosobokova (2011)	77° N	25° E	–	March
Hirche and Kosobokova (2003)	78° N	82.5° E	–	mid-May
Bandara et al. (2016)	78° N	16° E	July–August	mid-February
Dawson (1978)	84° N	112° W	August	June

conditions (e.g. Reid et al., 1998; Eiane and Parisi, 2001; Ji, 2011). However, direct comparisons between vertical migratory patterns predicted by a strategy-oriented model and field estimates should be done with caution, as an environment-specific optimal vertical strategy predicted by the model contrasts the diversity of vertical behavior exhibited by individuals of a zooplankton population.

Visual predation risk and depth of thermal stratification (summer–autumn) were the only environmental variables that influenced the model-predicted overwintering depth (Figs. 7 and 8b, Table 6). The overwintering depth deepened at higher levels of visual predation risk and deeper thermal stratification depths, and agrees with Hirche (1991), Kaartvedt (1996), Dale et al. (1999), Bagøien et al. (2000) and Astthorsson and Gislason (2003) that *Calanus* spp. prefer colder water masses with low predator abundance for overwintering. However, the overwintering depths predicted by or model underestimate those of field observations, which can extend well below 1000 m (e.g. Østvedt, 1955). Apart from the shallow bottom depths modelled, this discrepancy largely reflects how overwintering habitat selection of *Calanus* spp. is influenced by the buoyancy-effect of stored lipid reserves (Visser and Jónasdóttir, 1999), convective mixing of surface waters (Irigoien, 2004) and vertical distribution of water masses and predator populations, such as mesopelagic fish, predatory ctenophores and krill (Hirche, 1991; Kaartvedt 1996; Bagøien et al., 2000; Bandara et al., 2016).

4.2. Influence of vertical strategies on fitness and phenology

4.2.1. Diel vertical migration

In the model, high-amplitude DVM caused increased food limitation that led to slow growth and development and reduced fecundity (Figs. 7 and 9, Table 6). This ultimately resulted in lower fitness relative to that predicted for low-amplitude DVM. It is therefore apparent that decisions to fully or partly disregard DVM in models focusing SVM and other seasonal strategies should be made with caution, as our findings indicate that DVM can have a notable negative influence on growth and development of younger developmental stages, especially at lower latitudes.

At higher levels of visual predation risk, the model predicted up to a one month delay in the onset of spawning (Fig. 8d), and highlights the influence of predation risk on the reproductive phenology (Magnhagen, 1991; Stibor, 1992; Varpe et al., 2007). These late-spawned copepods appeared to possess higher fitness compared to those spawned earlier (Fig. 8h). This seems counterintuitive as zooplankton are more vulnerable to visual predation risk later in the season due to the higher irradiance levels that persist in late-spring and summer. In this model, the early feeding season (i.e. until the time of peak pelagic bloom) is characterized by higher food concentrations and lower temperatures (Fig. 1). Although the food concentration decreases by ca. 20% by late spring or early-summer, the ambient temperature increases by ca. 2–4 times. Further, even at the onset of the productive season, the visual predation risk had reached ca. 70% of its maximum in all model environments (Fig. 1a, d and g). Therefore, it is likely that copepods born relatively later in the season use the higher temperatures to attain a higher growth (Eqs. (1)–(8), Appendix A4 in Supplementary material), which is then efficiently traded off for survival through DVM to counter the risk of increasing visual predation risk (Fig. 9). Conversely, due to lower temperatures, copepods born earlier in the season must elevate the time spent foraging in near-surface waters to attain higher growth rates, and become more vulnerable to visual predation risk. However, it should be noted that our model does not consider the ability of *Calanus* spp. to use the darker and seasonally ice-covered period of the year to attain growth with minimal influence from visual predators by feeding on alternative food sources, such as ice algae and microzooplankton (Conover and Siferd, 1993; Søreide et al., 2010).

Compared to the phenology of reproduction, the elevated visual predation risk had little influence on the timing of seasonal migration (Fig. 8a). The SVM strategy predicted by the model was to descend to overwintering depth approximately at the same period of the year (mid–late summer), but with ca. $^1/_3$ lesser the body mass (both structural and energetic reserve mass) compared to that under the lowest visual predation risk (Fig. 8a and c). As higher visual predation risk tends to intensify DVM in this model (Fig. 9a and b), it appears that trading off growth potential for survival makes an earlier seasonal descent unfavorable, as food-limitation and slower growth rates (Fig. 9c and d) demands more time to acquire sufficient energy reserves to overwinter, despite the smaller body mass of the overwintering stage. Further, as the model-predicted body mass of the overwintering stage reaches a lower threshold at $K > 10^{-4}$ (Fig. 8c), it is likely that modelled copepods overwintered with minimum reserves to last the overwintering duration, and therefore makes an earlier descent (with lesser energy reserves) nearly impossible. In the contrary, occupying near-surface waters later into the season and descend to

overwintering depths with elevated energetic reserves is also unfavorable as the visual predation risk in this model is not nullified even at the deepest parts of the water column (Eq. (10)). The lesser influence of visual predation risk on the timing of SVM does not align with Kaartvedt (2000) and Varpe and Fiksen (2010) who view predation by planktivorous fish as a key driver of generation lengths and timing of seasonal descent in *C. finmarchicus* in the Norwegian Sea. However, the consequences of DVM on the timing of seasonal descent presented here may diminish if there is an energetic benefit of DVM (e.g. McLaren, 1963; Enright, 1977), if copepods are capable of utilizing alternative food sources (e.g. Runge and Ingram, 1991; Hirche and Kwasniewski, 1997) or if there is a strong size selection against larger developmental stages by visual predators than the linear relationship applied in our model (cf. Fig. 4a with Brooks and Dodson, 1965; Batty et al., 1990; Langbehn and Varpe, 2017).

4.2.2. Seasonal vertical migration

SVM was essential for the wintertime survival of the modelled copepods, given its food source is only available during the primary production season (spring–autumn, Fig. 1). Different combinations of proxies (Table 2) yielded non-seasonally migrating strategies, in which the copepods developed to adults and reproduced within the same productive season. Although this strategy had the potential to produce more than one generation per year (especially in the relatively lower-latitude environment-L, Fig. 1a–c), we did not peruse this further, as our focus was on an annual life cycle (see the fitness weighing process, Eq. (14), Fig. 5a–c).

The body mass and the size of energetic reserve at seasonal descent together with the timing of seasonal ascent had a profound influence on the predicted timing of reproduction, breeding strategy and fecundity (Fig. 8). Overwintering as large CVs with elevated energetic reserves at lower visual predation risk enabled the copepod to allocate the post-overwintering surplus energetic reserves to capital breeding in the following year (Fig. 8c and f, and see also Sainmont et al., 2014a; Ejsmond et al., 2015; Halvorsen, 2015). As capital breeding emerged in environments with lower temperatures and food concentrations (Fig. 7, Table 6), it appears as a strategy that allows the new generation to feed from the very start of the feeding season, while avoiding the seasonal peak in visual predation risk later in the year (Fig. 1, see also Varpe et al., 2009). The proportional increase of capital breeding eggs from relatively lower-latitude environment-L to higher-latitude environment-H reflects the decreasing temperature gradient that occur at overwintering depths of these environments (Figs. 1, 8b and f). Overwintering in colder water masses reduces the metabolic costs and conserves the energetic reserve, which ultimately boosts the fecundity through capital breeding (Hirche, 1991; Hirche, 1996; Astthorsson and Gislason, 2003). The pure capital breeding strategy predicted at environment-H under the lowest visual predation risk more resembles the spawning strategy of *C. hyperboreus* than *C. finmarchicus* and *C. glacialis* (Conover, 1988; Falk-Petersen et al., 2009). The sensitivity of the model-predicted breeding strategy to visual predation risk indicates an extensive pre-breeding cost of capital breeding imposed by the size-dependent visual predation risk and acquisition and carriage of energy reserves (Jönsson, 1997; Varpe et al., 2009). Moreover, excess energy storage (i.e. more than to overwinter) and capital breeding do not emerge as dominant strategies in this model as the environmental parameters are modelled in a perfectly predictable manner, without any year-to-year variability. However, capital breeding and energy storage may possess a much larger adaptive significance in nature, where spatio-temporal environmental heterogeneity and unpredictability are more pronounced compared to our model (e.g. Jönsson, 1997; Fischer et al., 2009).

4.3. Concluding remarks

Findings of this study highlight the influence of environmental variables on vertical strategies, and suggest that in seasonal environments, DVM and SVM should be studied in concert, as these behavioral strategies can have profound and largely different effects on fitness and phenology of herbivorous zooplankton. Therefore, given the significance of biological information ensued, sacrificing computer time to adopt higher spatio-temporal resolution in behavioral and life-history models seems to be an appealing practice. However, strong recommendations should only be made after testing our model predictions further, especially, through improvements to cope with environmental stochasticity (e.g. Eiane and Parisi, 2001; Ji, 2011), and to incorporate the plasticity of feeding strategies, generation times and body sizes of *Calanus* spp. (e.g. Broekhuizen et al., 1995; Fuchs and Franks, 2010; Ji et al., 2012; Banas et al., 2016).

Acknowledgements

This project was funded by VISTA (project no. 6165), a basic research program in collaboration between The Norwegian Academy of Science and Letters and Statoil. ØV received funding from the Fulbright Arctic Initiative and thanks the Woods Hole Oceanographic Institution for hosting during the Fulbright exchange. Authors are also thankful to the two anonymous reviewers for critically reading the earlier draft of the manuscript and suggesting substantial improvements.

Appendix A. Supplementary data

Supplementary data associated with this article can be found, in the online version, at https://doi.org/10.1016/j.ecolmodel.2017.12.010.

References

Aidley, D., 1981. Questions about migration. In: Aidley, D. (Ed.), Animal Migration, vol. 2. Press Syndicae of the University of Cambridge, New York, USA, pp. 1–9.
Alerstam, T., Hedenström, A., Åkesson, S., 2003. Long-distance migration: evolution and determinants. Oikos 103, 247–260, http://dx.doi.org/10.1034/j.1600-0706.2003.12559.x.
Andersen, V., Nival, P., 1991. A model of the diel vertical migration of zooplankton based on euphausiids. J. Mar. Res. 49, 153–175, http://dx.doi.org/10.1357/002224091784968594.
Arashkevich, E., Wassmann, P., Pasternak, A., Riser, C.W., 2002. Seasonal and spatial changes in biomass, structure, and development progress of the zooplankton community in the Barents Sea. J. Mar. Syst. 38, 125–145, http://dx.doi.org/10.1016/S0924-7963(02)00173-2.
Astthorsson, O.S., Gislason, A., 2003. Seasonal variations in abundance, development and vertical distribution of *Calanus finmarchicus*, *C. hyperboreus* and *C. glacialis* in the East Icelandic Current. J. Plankton Res. 25, 843–854, http://dx.doi.org/10.1093/plankt/25.7.843.
Båmstedt, U., Eilertsen, H.C., Tande, K.S., Slagstad, D., Skjoldal, H.R., 1991. Copepod grazing and its potential impact on the phytoplankton development in the Barents Sea. Polar Res. 10, 339–354, http://dx.doi.org/10.1111/j.1751-8369.1991.tb00658.x.
Båtnes, A.S., Miljeteig, C., Berge, J., Greenacre, M., Johnsen, G.H., 2015. Quantifying the light sensitivity of *Calanus* spp. during the polar night: potential for orchestrated migrations conducted by ambient light from the sun, moon, or aurora borealis? Polar Biol. 38, 51–65, http://dx.doi.org/10.1007/s00300-013-1415-4.
Bagøien, E., Kaartvedt, S., Øverås, S., 2000. Seasonal vertical migrations of *Calanus* spp. in Oslofjorden. Sarsia 85, 299–311, http://dx.doi.org/10.1080/00364827.2000.10414581.
Banas, N.S., Møller, E.F., Nielsen, T.G., Eisner, L.B., 2016. Copepod life strategy and population viability in response to prey timing and temperature: testing a new model across latitude, time, and the size spectrum. Front. Mar. Sci. 3, 225, http://dx.doi.org/10.3389/fmars.2016.00225.
Bandara, K., Varpe, Ø., Søreide, J.E., Wallenschus, J., Berge, J., Eiane, K., 2016. Seasonal vertical strategies in a high-Arctic coastal zooplankton community. Mar. Ecol. Prog. Ser. 555, 49–64, http://dx.doi.org/10.3354/meps11831.
Banse, K., 1964. On the vertical distribution of zooplankton in the sea. Prog. Oceanogr. 2, 55–125, http://dx.doi.org/10.1016/0079-6611(64)90003-5.

Basedow, S.L., Tande, K.S., Stige, L.C., 2010. Habitat selection by a marine copepod during the productive season in the Subarctic. Mar. Ecol. Prog. Ser. 416, 165–178, http://dx.doi.org/10.3354/meps08754.
Batty, R., Blaxter, J., Richard, J., 1990. Light intensity and the feeding behaviour of herring, *Clupea harengus*. Mar. Biol. 107, 383–388, http://dx.doi.org/10.1007/BF01313419.
Berge, J., et al., 2009. Diel vertical migration of Arctic zooplankton during the polar night. Biol. Lett. 5, 69–72, http://dx.doi.org/10.1098/rsbl.2008.0484.
Berge, J., Varpe, Ø., Moline, M.A., Wold, A., Renaud, P.E., Daase, M., Falk-Petersen, S., 2012. Retention of ice-associated amphipods: possible consequences for an ice-free Arctic Ocean. Biol. Lett. 8, 1012–1015, http://dx.doi.org/10.1098/rsbl.2012.0517.
Bianchi, D., Mislan, K., 2016. Global patterns of diel vertical migration times and velocities from acoustic data. Limnol. Oceanogr. 61, 353–364, http://dx.doi.org/10.1002/lno.10219.
Bianchi, D., Galbraith, E.D., Carozza, D.A., Mislan, K., Stock, C.A., 2013. Intensification of open-ocean oxygen depletion by vertically migrating animals. Nat. Geosci. 6, 545–548, http://dx.doi.org/10.1038/ngeo1837.
Blachowiak-Samolyk, K., et al., 2006. Arctic zooplankton do not perform diel vertical migration (DVM) during periods of midnight sun. Mar. Ecol. Prog. Ser. 308, 101–116, http://dx.doi.org/10.3354/meps308101.
Bollens, S.M., Frost, B.W., Thoreson, D.S., Watts, S.J., 1992. Diel vertical migration in zooplankton: field evidence in support of the predator avoidance hypothesis. Hydrobiologia 234, 33–39, http://dx.doi.org/10.1007/bf00010777.
Bozman, A., Titelman, J., Kaartvedt, S., Eiane, K., Aksnes, D.L., 2017. Jellyfish distribute vertically according to irradiance. J. Plankton Res. 39, 280–289, http://dx.doi.org/10.1093/plankt/fbw097.
Broekhuizen, N., Heath, M.R., Hay, S.J., Gurney, W.S.C., 1995. Modelling the dynamics of the North Sea's Mesozooplankton. Neth. J. Sea Res. 33, 381–406, http://dx.doi.org/10.1016/0077-7579(95)90054-3.
Brooks, J.L., Dodson, S.I., 1965. Predation, body size, and composition of plankton. Science 150, 28–35, http://dx.doi.org/10.1126/science.150.3692.28.
Burrows, M.T., Tarling, G., 2004. Effects of density dependence on diel vertical migration of populations of northern krill: a genetic algorithm model. Mar. Ecol. Prog. Ser. 277, 209–220, http://dx.doi.org/10.3354/meps277209.
Campbell, R.G., Wagner, M.M., Teegarden, G.J., Boudreau, C.A., Durbin, E.G., 2001. Growth and development rates of the copepod *Calanus finmarchicus* reared in the laboratory. Mar. Ecol. Prog. Ser. 221, 161–183, http://dx.doi.org/10.3354/meps221161.
Carlisle, D.B., Pitman, W.J., 1961. Diapause, neurosecretion and hormones in copepoda. Nature 190, 827–828, http://dx.doi.org/10.1038/190827b0.
Carlotti, F., Wolf, K.U., 1998. A Lagrangian ensemble model of *Calanus finmarchicus* coupled with a 1D ecosystem model. Fish Oceanogr. 7, 191–204, http://dx.doi.org/10.1046/j.1365-2419.1998.00085.x.
Chossat, C., 1843. Recherches expérimentales sur l'inanition. Imprimerie Royale, Paris, France.
Clarke, G.L., 1933. Diurnal migration of plankton in the Gulf of Maine and its correlation with changes in submarine irradiation. Biol. Bull. 65, 402–436, http://dx.doi.org/10.2307/1537215.
Codling, E.A., 2003. Biased Random Walks in Biology. Master Thesis. The University of Leeds.
Cohen, J., Forward, R., 2009. Zooplankton Diel Vertical Migration? A review of proximate control. In: Oceanography and Marine Biology. Oceanography and Marine Biology—An Annual Review. CRC Press, pp. 77–109, http://dx.doi.org/10.1201/9781420094220.ch2.
Cohen, J., et al., 2015. Is ambient light during the high Arctic polar night sufficient to act as a visual cue for zooplankton? PLoS One 10, e0126247, http://dx.doi.org/10.1371/journal.pone.0126247.
Conover, R., Siferd, T.D., 1993. Dark-season survival strategies of coastal zone zooplankton in the Canadian Arctic. Arctic, 303–311, http://dx.doi.org/10.14430/arctic1357.
Conover, R., 1988. Comparative life histories in the genera *Calanus* and *Neocalanus* in high latitudes of the northern hemisphere. In: Biology of Copepods. Springer, pp. 127–142, http://dx.doi.org/10.1007/BF00026299.
Costello, J., 1998. Physiological response of the hydromedusa *Cladonema californicum* Hyman (Anthomedusa: Cladonemidae) to starvation and renewed feeding. J. Exp. Biol. Ecol. 225, 13–28, http://dx.doi.org/10.1016/S0022-0981(97)00204-9.
Cresswell, K.A., Satterthwaite, W.H., Sword, G.A., 2011. Understanding the evolution of migration through empirical examples. In: Milner-Gulland, E.J., Fryxell, J.M., Sinclair, A.R.E. (Eds.), Animal Migration a Synthesis, vol. 1. Oxford University Press, Oxford, U.K, pp. 7–17.
Cushing, D.H., 1951. The vertical migration of planktonic crustacea. Biol. Rev. 26, 158–192, http://dx.doi.org/10.1111/j.1469-185X.1951.tb00645.x.
Daase, M., Eiane, K., Aksnes, D.L., Vogedes, D., 2008. Vertical distribution of *Calanus* spp. and *Metridia longa* at four Arctic locations. Mar. Biol. Res. 4, 193–207, http://dx.doi.org/10.1080/17451000801907948.
Daase, M., et al., 2013. Timing of reproductive events in the marine copepod *Calanus glacialis*: a pan-Arctic perspective. Can. J. Fish. Aquat. Sci. 70, 871–884, http://dx.doi.org/10.1139/cjfas-2012-0401.
Dale, T., Kaartvedt, S., 2000. Diel patterns in stage-specific vertical migration of *Calanus finmarchicus* in habitats with midnight sun. ICES J. Mar. Sci. 57, 1800–1818, http://dx.doi.org/10.1006/jmsc.2000.0961.
Dale, T., Bagøien, E., Melle, W., Kaartvedt, S., 1999. Can predator avoidance explain varying overwintering depth of *Calanus* in different oceanic water masses? Mar. Ecol. Prog. Ser. 179, 113–121, http://dx.doi.org/10.3354/meps179113.
Darnis, G., et al., 2017. From polar night to midnight sun: Diel vertical migration, metabolism and biogeochemical role of zooplankton in a high Arctic fjord (Kongsfjorden, Svalbard). Limnol. Oceanogr. 57, 1800–1818, http://dx.doi.org/10.1006/jmsc.2000.0961.
Davis, L., 1989. Adapting operator probabilities in genetic algorithms. Proceedings of the Third International Conference on Genetic Algorithms, 61–69.
Dawidowicz, P., Loose, C.J., 1992. Cost of swimming by *Daphnia* during diel vertical migration. Limnol. Oceanogr. 37, 665–669, http://dx.doi.org/10.4319/lo.1992.37.3.0665.
Dawson, J.K., 1978. Vertical distribution of Calanus hyperboreus in the central Arctic Ocean. Limnol. Oceanogr. 23, 950–957, http://dx.doi.org/10.4319/lo.1978.23.5.0950.
De Robertis, A., 2002. Size-dependent visual predation risk and the timing of vertical migration: an optimization model. Limnol. Oceanogr. 47, 925–933, http://dx.doi.org/10.4319/lo.2000.45.8.1838.
Deb, K., 2001. Multi-objective Optimization Using Evolutionary Algorithms, vol. 16. John Wiley & Sons, New York, USA.
Devol, A.H., 1981. Vertical distribution of zooplankton respiration in relation to the intense oxygen minimum zones in two British Columbia fjords. J. Plankton Res. 3, 593–602, http://dx.doi.org/10.1093/plankt/3.4.593.
Dupont, N., Aksnes, D.L., 2012. Effects of bottom depth and water clarity on the vertical distribution of *Calanus* spp. J. Plankton Res. 34, 263–266, http://dx.doi.org/10.1093/plankt/fbr096.
Eddelbuettel, D., François, R., Allaire, J., Chambers, J., Bates, D., Ushey, K., 2011. Rcpp: seamless R and C++ integration. J. Stat. Softw. 40, 1–18, http://dx.doi.org/10.18637/jss.v040.i08.
Eiane, K., Ohman, M.D., 2004. Stage-specific mortality of *Calanus finmarchicus*, *Pseudocalanus elongatus* and *Oithona similis* on Fladen Ground, North Sea, during a spring bloom. Mar. Ecol. Prog. Ser. 268, 183–193, http://dx.doi.org/10.3354/meps268183.
Eiane, K., Parisi, D., 2001. Towards a robust concept for modelling zooplankton migration. Sarsia 86, 465–475, http://dx.doi.org/10.1080/00364827.2001.10420486.
Eiben, A.E., Smith, J.E., 2003. Introduction to Evolutionary Computing, vol. 53. Springer, Berlin, Germany.
Ejsmond, M.J., Varpe, Ø., Czarnoleski, M., Kozłowski, J., 2015. Seasonality in offspring value and trade-offs with growth explain capital breeding. Am. Nat. 186, E111–E125, http://dx.doi.org/10.1086/683119.
Ekvall, M.T., Hylander, S., Walles, T., Yang, X., Hansson, L.A., 2015. Diel vertical migration, size distribution and photoprotection in zooplankton as response to UV-A radiation. Limnol. Oceanogr. 60, 2048–2058, http://dx.doi.org/10.1002/lno.10151.
Enright, J., 1977. Diurnal vertical migration: adaptive significance and timing. Part 1. Selective advantage: a metabolic model. Limnol. Oceanogr. 22, 856–872, http://dx.doi.org/10.4319/lo.1977.22.5.0856.
Eshelman, L.J., Schaffer, J.D., 1993. Real-coded genetic algorithms and interval-schemata. Found. Genet. Algorithm 2, 187–202, http://dx.doi.org/10.1016/B978-0-08-094832-4.50018-0.
Falk-Petersen, S., Mayzaud, P., Kattner, G., Sargent, J.R., 2009. Lipids and life strategy of Arctic *Calanus*. Mar. Biol. Res. 5, 18–39, http://dx.doi.org/10.1080/17451000802512267.
Fiksen, Ø., Carlotti, F., 1998. A model of optimal life history and diel vertical migration in *Calanus finmarchicus*. Sarsia 83, 129–147, http://dx.doi.org/10.1080/00364827.1998.10413678.
Fiksen, Ø., Giske, J., 1995. Vertical distribution and population dynamics of copepods by dynamic optimization. ICES J. Mar. Sci. 52, 483–503, http://dx.doi.org/10.1016/1054-3139(95)80062-X.
Fischer, B., Taborsky, B., Dieckmann, U., 2009. Unexpected patterns of plastic energy allocation in stochastic environments. Am. Nat. 173, E108–E120, http://dx.doi.org/10.1086/596536.
Foulds, J., Roff, J.C., 1976. Oxygen consumption during simulated vertical migration in *Mysis relicta* (Crustacea, Mysidacea). Can. J. Zool. 54, 377–385, http://dx.doi.org/10.1139/z76-042.
Frank, T.M., Widder, E.A., 1997. The correlation of downwelling irradiance and staggered vertical igration patterns of zooplankton in Wilkinson Basin, Gulf of Maine. J. Plankton Res. 19, 1975–1991, http://dx.doi.org/10.1093/plankt/19.12.1975.
Fuchs, H.L., Franks, P.J., 2010. Plankton community properties determined by nutrients and size-selective feeding. Mar. Ecol. Prog. Ser. 413, 1–15, http://dx.doi.org/10.3354/meps08716.
George, D., 1983. Interrelations between the vertical distribution of *Daphnia* and chlorophyll a in two large limnetic enclosures. J. Plankton Res. 5, 457–475, http://dx.doi.org/10.1093/plankt/5.4.457.
Gislason, A., Astthorsson, O.S., 2000. Winter distribution, ontogenetic migration, and rates of egg production of *Calanus finmarchicus* southwest of Iceland. ICES J. Mar. Sci. 57, 1727–1739, http://dx.doi.org/10.1006/jmsc.2000.0951.
Gliwicz, Z.M., 1986. A lunar cycle in zooplankton. Ecology 67, 883–897, http://dx.doi.org/10.2307/1939811.
Goldberg, D.E., Deb, K., 1991. A comparative analysis of selection schemes used in genetic algorithms. In: Rawlins, G. (Ed.), Foundations of Genetic Algorithms, vol. 1. Morgan Kaufmann Publishers, San Mateo, California, USA, pp. 69–93.
Greene, C.H., Landry, M.R., 1985. Patterns of prey selection in the cruising calanoid predator *Euchaeta elongata*. Ecology 66, 1408–1416, http://dx.doi.org/10.2307/1938003.

Grimm, V., et al., 2006. A standard protocol for describing individual-based and agent-based models. Ecol. Model. 198, 115–126, http://dx.doi.org/10.1016/j.ecolmodel.2006.04.023.
Grimm, V., Berger, U., DeAngelis, D.L., Polhill, J.G., Giske, J., Railsback, S.F., 2010. The ODD protocol: a review and first update. Ecol. Model. 221, 2760–2768, http://dx.doi.org/10.1016/j.ecolmodel.2010.08.019.
Hagen, W., Auel, H., 2001. Seasonal adaptations and the role of lipids in oceanic zooplankton. Zoology 104, 313–326, http://dx.doi.org/10.1078/0944-2006-00037.
Halvorsen, E., 2015. Significance of lipid storage levels for reproductive output in the Arctic copepod *Calanus hyperboreus*. Mar. Ecol. Prog. Ser. 540, 259–265, http://dx.doi.org/10.3354/meps11528.
Hansen, A.N., Visser, A.W., 2016. Carbon export by vertically migrating zooplankton: an optimal behavior model. Limnol. Oceanogr. 61, 701–710, http://dx.doi.org/10.1002/lno.10249.
Hardy, A., Bainbridge, R., 1954. Experimental observations on the vertical migrations of plankton animals. J. Mar. Biolog. Assoc. U. K. 33, 409–448, http://dx.doi.org/10.1017/S0025315400008456.
Hardy, A.C., Gunther, E.R., 1935. The Plankton of the South Georgia Whaling Grounds and Adjacent Waters, 1926–1927. The University Press, Cambridge, UK.
Hardy, A., 1935. The plankton community, the whale fisheries and the hypothesis of animal exclusion. Discov. Rep. 11, 273–360.
Harik, G.R., Lobo, F.G., Goldberg, D.E., 1997. The compact genetic algorithm. Urbana 51, 61801, http://dx.doi.org/10.1109/4235.797971.
Haupt, R.L., Haupt, S.E., 2004. Practical Genetic Algorithms. John Wiley & Sons, New Jersey, USA.
Hays, G., Proctor, C., John, A., Warner, A., 1994. Interspecific differences in the diel vertical migration of marine copepods: the implications of size, color, and morphology. Limnol. Oceanogr. 39, 1621–1629, http://dx.doi.org/10.4319/lo.1994.39.7.1621.
Hays, G.C., Kennedy, H., Frost, B.W., 2001. Individual variability in diel vertical migration of a marine copepod: why some individuals remain at depth when others migrate. Limnol. Oceanogr. 46, 2050–2054, http://dx.doi.org/10.4319/lo.2001.46.8.2050.
Hays, G., 1995. Ontogenetic and seasonal variation in the diel vertical migration of the copepods *Metridia lucens* and *Metridia longa*. Limnol. Oceanogr. 40, 1461–1465, http://dx.doi.org/10.4319/lo.1995.40.8.1461.
Head, E.J.H., Harris, L.R., 1985. Physiological and biochemical changes in *Calanus hyperboreus* from Jones Sound NWT during the transition from summer feeding to overwintering condition. Polar Biol. 4, 99–106, http://dx.doi.org/10.1007/BF00442907.
Heath, M.R., Jónasdóttir, S.H., 1999. Distribution and abundance of overwintering *Calanus finmarchicus* in the Faroe–Shetland Channel. Fish. Oceanogr. 8, 40–60, http://dx.doi.org/10.1046/j.1365-2419.1999.00012.x.
Heath, M.R., 1999. The ascent migration of *Calanus finmarchicus* from overwintering depths in the Faroe–Shetland Channel. Fish. Oceanogr. 8, 84–99, http://dx.doi.org/10.1046/j.1365-2419.1999.00013.x.
Herman, A.W., 1983. Vertical distribution patterns of copepods, chlorophyll, and production in northeastern Baffin Bay. Limnol. Oceanogr. 28, 709–719, http://dx.doi.org/10.4319/lo.1983.28.4.0709.
Herrera, F., Lozano, M., Verdegay, J.L., 1998. Tackling real-coded genetic algorithms: operators and tools for behavioural analysis. Artif. Intell. Rev. 12, 265–319, http://dx.doi.org/10.1023/A:1006504901164.
Heywood, K.J., 1996. Diel vertical migration of zooplankton in the Northeast Atlantic. J. Plankton Res. 18, 163–184, http://dx.doi.org/10.1093/plankt/18.2.163.
Hind, A., Gurney, W.S.C., Heath, M.R., Bryant, A., 2000. Overwintering strategies in *Calanus finmarchicus*. Mar. Ecol. Prog. Ser., 95–107, http://dx.doi.org/10.3354/meps193095.
Hirche, H.-J., Kosobokova, K., 2003. Early reproduction and development of dominant calanoid copepods in the sea ice zone of the Barents Sea—need for a change of paradigms? Mar. Biol. 143, 769–781, http://dx.doi.org/10.1007/s00227-003-1122-8.
Hirche, H.-J., Kosobokova, K., 2011. Winter studies on zooplankton in Arctic seas: the Storfjord (Svalbard) and adjacent ice-covered Barents Sea. Mar. Biol. 158, 2359–2376, http://dx.doi.org/10.1007/s00227-011-1740-5.
Hirche, H.-J., Kwasniewski, S., 1997. Distribution, reproduction and development of *Calanus* species in the Northeast water in relation to environmental conditions. J. Mar. Syst. 10, 299–317, http://dx.doi.org/10.1016/S0924-7963(96)00057-7.
Hirche, H.-J., 1984. Seasonal distribution of *Calanus finmarchicus* (Gunnerus) and *C. helgolandicus* (Claus) in a Swedish fjord. Crustaceana, 233–241.
Hirche, H.-J., 1991. Distribution of dominant calanoid copepod species in the Greenland Sea during late fall. Polar Biol. 11, 351–362, http://dx.doi.org/10.1007/BF00239687.
Hirche, H.-J., 1996. Diapause in the marine copepod, *Calanus finmarchicus*—a review. Ophelia 44, 129–143, http://dx.doi.org/10.1080/00785326.1995.10429843.
Hirche, H.-J., 1997. Life cycle of the copepod *Calanus hyperboreus* in the Greenland Sea. Mar. Biol. 128, 607–618, http://dx.doi.org/10.1007/s002270050.
Holland, J.H., 1975. Adaptation in Natural and Artificial Systems. An Introductory Analysis with Application to Biology, Control, and Artificial Intelligence. University of Michigan Press, Ann Arbor, MI.
Huang, C., Uye, S., Onbé, T., 1993. Ontogenetic diel vertical migration of the planktonic copepod *Calanus sinicus* in the Inland Sea of Japan. Mar. Biol. 117, 289–299, http://dx.doi.org/10.1007/BF00345674.
Huntley, M., Boyd, C., 1984. Food-limited growth of marine zooplankton. Am. Nat. 124, 455–478, http://dx.doi.org/10.1086/284288.
Huntley, M., Brooks, E., 1982. Effects of age and food availability on diel vertical migration of *Calanus pacificus*. Mar. Biol. 71, 23–31, http://dx.doi.org/10.1007/BF00396989.
Ingvaldsen, R., Loeng, H., 2009. Physical oceanography. In: Sakshaug, E., Johnsen, G.H., Kovacs, K. (Eds.), Ecosystem Barents Sea. Tapir Academic Press, Trondheim, Norway, pp. 33–64.
Irigoien, X., 2004. Some ideas about the role of lipids in the life cycle of *Calanus finmarchicus*. J. Plankton Res. 26, 259–263, http://dx.doi.org/10.1093/plankt/fbh030.
Iwasa, Y., 1982. Vertical migration of zooplankton: a game between predator and prey. Am. Nat. 120, 171–180, http://dx.doi.org/10.1086/283980.
Jönsson, K.I., 1997. Capital and income breeding as alternative tactics of resource use in reproduction. Oikos, 57–66, http://dx.doi.org/10.2307/3545800.
Jørgensen, S.E., Bendoricchio, G., 2001. Fundamentals of Ecological Modelling, vol. 21. Elsevier Science Ltd., Oxford, UK.
Ji, R., et al., 2012. Life history and biogeography of *Calanus* copepods in the Arctic Ocean: an individual-based modeling study. Prog. Oceanogr. 96, 40–56, http://dx.doi.org/10.1016/j.pocean.2011.10.001.
Ji, R., 2011. *Calanus finmarchicus* diapause initiation: new view from traditional life history-based model. Mar. Ecol. Prog. Ser. 440, 105–114, http://dx.doi.org/10.3354/meps09342.
Johnsen, G.H., Jakobsen, P.J., 1987. The effect of food limitation on vertical migration in *Daphnia longispina*. Limnol. Oceanogr. 32, 873–880, http://dx.doi.org/10.4319/lo.1987.32.4.0873.
Kaartvedt, S., 1996. Habitat preference during overwintering and timing of seasonal vertical migration of *Calanus finmarchicus*. Ophelia 44, 145–156, http://dx.doi.org/10.1080/00785326.1995.10429844.
Kaartvedt, S., 2000. Life history of *Calanus finmarchicus* in the Norwegian Sea in relation to planktivorous fish. ICES J. Mar. Sci. 57, 1819–1824, http://dx.doi.org/10.1006/jmsc.2000.0964.
Kane, M.J., Emerson, J.W., Weston, S., 2013. Scalable strategies for computing with massive data. J. Stat. Softw. 55, 1–19, http://dx.doi.org/10.18637/jss.v055.i14.
Kerfoot, W.B., 1970. Bioenergetics of vertical migration. Am. Nat. 104, 529–546, http://dx.doi.org/10.1086/282688.
Kiørboe, T., Hirst, A.G., 2008. Optimal development time in pelagic copepods. Mar. Ecol. Prog. Ser. 367, 15–22, http://dx.doi.org/10.3354/meps07572.
Kimmerer, W., McKinnon, A., 1987. Zooplankton in a marine bay. II. Vertical migration to maintain horizontal distributions. Mar. Ecol. Prog. Ser., 53–60.
Kosobokova, K., 1999. The reproductive cycle and life history of the Arctic copepod *Calanus glacialis* in the White Sea. Polar Biol. 22, 254–263, http://dx.doi.org/10.1007/s003000050418.
Lampert, W., 1989. The adaptive significance of diel vertical migration of zooplankton. Funct. Ecol. 3, 21–27, http://dx.doi.org/10.2307/2389671.
Langbehn, T.J., Varpe, Ø., 2017. Sea-ice loss boosts visual search: fish foraging and changing pelagic interactions in polar oceans. Glob. Change Biol. 12, 5318–5330, http://dx.doi.org/10.1111/gcb.13797.
Litchman, E., Ohman, M.D., Kiørboe, T., 2013. Trait-based approaches to zooplankton communities. J. Plankton Res. 35, 473–484, http://dx.doi.org/10.1093/plankt/fbt019.
Liu, S.-H., Sun, S., Han, B.-P., 2003. Diel vertical migration of zooplankton following optimal food intake under predation. J. Plankton Res. 25, 1069–1077, http://dx.doi.org/10.1093/plankt/25.9.1069.
Loos, M., Ragas, A.M., Plasmeijer, R., Schipper, A.M., Hendriks, A.J., 2010. Eco-SpaCE: an object-oriented, spatially explicit model to assess the risk of multiple environmental stressors on terrestrial vertebrate populations. Sci. Total Environ. 408, 3908–3917, http://dx.doi.org/10.1016/j.scitotenv.2009.11.045.
Loose, C.J., Dawidowicz, P., 1994. Trade-offs in Diel vertical migration by zooplankton: the costs of predator avoidance. Ecology 75, 2255–2263, http://dx.doi.org/10.2307/1940881.
Lucasius, C.B., Kateman, G., 1989. Application of genetic algorithms in chemometrics. In: Proceedings of the Third International Conference on Genetic Algorithms. Morgan Kaufmann Publishers Inc., pp. 170–176.
Madsen, S., Nielsen, T.G., Hansen, B.W., 2001. Annual population development and production by *Calanus finmarchicus*, *C. glacialis* and *C. hyperboreus* in Disko Bay, western Greenlan. Mar. Biol. 139, 75–93, http://dx.doi.org/10.1007/s002270100552.
Madsen, S., Nielsen, T.G., Tervo, O.M., Söderkvist, J., 2008. Importance of feeding for egg production in *Calanus finmarchicus* and *C. glacialis* during the Arctic spring. Mar. Ecol. Prog. Ser. 353, 177–190, http://dx.doi.org/10.3354/meps07129.
Magnhagen, C., 1991. Predation risk as a cost of reproduction. Trends Ecol. Evolut. 6, 183–186, http://dx.doi.org/10.1016/0169-5347(91)90210-O.
Marshall, S.M., Orr, A.P., 1972. The Biology of a Marine Copepod: *Calanus finmarchicus* (Gunnerus). Springer Science & Business Media, Berlin, Germany.
Mauchline, J., 1998. The Biology of Calanoid Copepods, vol. 33. Academic Press, San Diego, California, USA.
McLaren, I.A., 1963. Effects of temperature on growth of zooplankton, and the adaptive value of vertical migration. J. Fish. Res. Board Can. 20, 685–727, http://dx.doi.org/10.1139/f63-046.
Melle, W., et al., 2014. The North Atlantic Ocean as habitat for *Calanus finmarchicus*: environmental factors and life history traits. Prog. Oceanogr. 129, 244–284, http://dx.doi.org/10.1016/j.pocean.2014.04.026.
Miller, B.L., Goldberg, D.E., 1995. Genetic algorithms, tournament selection, and the effects of noise. Complex Syst. 9, 193–212.

Miller, C.B., Cowles, T.J., Wiebe, P.H., Copley, N.J., Grigg, H., 1991. Phenology in *Calanus finmarchicus*; hypotheses about control mechanisms. Mar. Ecol. Prog. Ser. 72, 79–91.
Miller, C.B., Lynch, D.R., Carlotti, F., Gentleman, W., Lewis, C.V., 1998. Coupling of an individual-based population dynamic model of *Calanus finmarchicus* to a circulation model for the Georges Bank region. Fish. Oceanogr. 7, 219–234, http://dx.doi.org/10.1046/j.1365-2419.1998.00072.x.
Morris, M., Gust, G., Torres, J., 1985. Propulsion efficiency and cost of transport for copepods: a hydromechanical model of crustacean swimming. Mar. Biol. 86, 283–295, http://dx.doi.org/10.1007/BF00397515.
Nival, P., Carlotti, F., Sciandra, A., 1988. Modelling of recruitment of marine species. In: Rothschild, B.J. (Ed.), Toward a Theory on Biological-Physical Interactions in the World Ocean, vol. 239. Kluwer Academic Publishers, Dordrecht, The Netherlands, pp. 321–342.
Ohman, M.D., 1990. The demographic benefits of diel vertical migration by zooplankton. Ecol. Monogr. 60, 257–281, http://dx.doi.org/10.2307/1943058.
Osgood, K.E., Frost, B.W., 1994. Ontogenetic diel vertical migration behaviors of the marine planktonic copepods *Calanus pacificus* and *Metridia lucens*. Mar. Ecol. Prog. Ser., 13–25.
Østvedt, O.J., 1955. Zooplankton investigations from weather ship M in the Norwegian Sea, 1948–49. Hvalrad Skf 40, 1–93.
Pasternak, A., Kosobokova, K., Drits, A., 1994. Feeding, metabolism and body composition of the dominant Antarctic copepods with comments on their life cycles. Russ. J. Aquat. Ecol. 3, 49–62.
Pearre, S., 1979. Problems of detection and interpretation of vertical migration. J. Plankton Res. 1, 29–44, http://dx.doi.org/10.1093/plankt/1.1.29.
Pearre, S., 2003. Eat and run? The hunger/satiation hypothesis in vertical migration: history, evidence and consequences. Biol. Rev. 78, 1–79.
R Core Team, 2016. R: A Language and Environment for Statistical Computing. 3.3.1.
RStudio Team, 2016. RStudio: Integrated Development Environment for R. 1.0.136.
Record, N., Pershing, A., Runge, J., Mayo, C.A., Monger, B.C., Chen, C., 2010. Improving ecological forecasts of copepod community dynamics using genetic algorithms. J. Mar. Syst. 82, 96–110, http://dx.doi.org/10.1016/j.jmarsys.2010.04.001.
Reid, P.C., Planque, B., Edwards, M., 1998. Is observed variability in the long-term results of the Continuous Plankton Recorder survey a response to climate change? Fish. Oceanogr. 7, 282–288, http://dx.doi.org/10.1046/j.1365-2419.1998.00073.x.
Rhode, S.C., Pawlowski, M., Tollrian, R., 2001. The impact of ultraviolet radiation on the vertical distribution of zooplankton of the genus. Daphnia Nat. 412, 69–72, http://dx.doi.org/10.1038/35083567.
Robinson, C.L.K., 1994. Modelling the Trophodynamics of a Coastal Upwelling System. Doctoral Thesis. The University of British Columbia.
Robledo, L., Soler, A., 2000. Luminous efficacy of global solar radiation for clear skies. Energy Convers. Manage. 41, 1769–1779, http://dx.doi.org/10.1016/S0196-8904(00)00019-4.
Roman, M., Smith, S., Wishner, K., Zhang, X., Gowing, M., 2000. Mesozooplankton production and grazing in the Arabian Sea. Deep Sea Res. Part II: Trop. Stud. Oceanogr. 47, 1423–1450, http://dx.doi.org/10.1016/S0967-0645(99)00149-6.
Runge, J., Ingram, R.G., 1991. Under-ice feeding and diel migration by the planktonic copepods *Calanus glacialis* and *Pseudocalanus minutus* in relation to the ice algal production cycle in southeastern Hudson Bay. Can. Mar. Biol. 108, 217–225, http://dx.doi.org/10.1007/BF01344336.
Russell, F.S., 1927. The vertical distribution of plankton in the sea. Biol. Rev. 2, 213–262, http://dx.doi.org/10.1111/j.1469-185X.1927.tb00878.x.
Sømme, J.D., 1934. Animal plankton of the Norwegian Coast Warers and the Open Sea. I—production of *Calanus finmarchicus* (Gunner) and *Calanus hyperboreus* (Krøyer) in the Lofoten Area. Fiskeridir Skr (Havunders) 4, 1–163.
Søreide, J.E., Leu, E., Berge, J., Graeve, M., Falk-Petersen, S., 2010. Timing of blooms, algal food quality and *Calanus glacialis* reproduction and growth in a changing Arctic. Glob Change Biol. 16, 3154–3163, http://dx.doi.org/10.1111/j.1365-2486.2010.02175.x.
Sainmont, J., Andersen, K.H., Varpe, Ø., Visser, A.W., 2014a. Capital versus income breeding in a seasonal environment. Am. Nat. 184, 466–476, http://dx.doi.org/10.1086/677926.
Sainmont, J., Gislason, A., Heuschele, J., Webster, C.N., Sylvander, P., Wang, M., Varpe, Ø., 2014b. Inter-and intra-specific diurnal habitat selection of zooplankton during the spring bloom observed by Video Plankton Recorder. Mar. Biol. 161, 1931–1941, http://dx.doi.org/10.1007/s00227-014-2475-x.
Sainmont, J., Andersen, K.H., Thygesen, U.H., Fiksen, Ø., Visser, A.W., 2015. An effective algorithm for approximating adaptive behavior in seasonal environments. Ecol. Model. 311, 20–30, http://dx.doi.org/10.1016/j.ecolmodel.2015.04.016.
Sakshaug, E., Johnsen, G.H., Kristiansen, S., von Quillfeldt, C., Rey, F., Slagstad, D., Thingstad, F., 2009. Phytoplankton and primary production. In: Sakshaug, E., Johnsen, G., Kovacs, K. (Eds.), Ecosystem Barents Sea. Tapir Academic Press, Trondheim, Norway, pp. 167–209.
Salzen, E., 1956. The density of the eggs of *Calanus finmarchicus*. J. Mar. Biol. Assoc. U. K. 35, 549–554, http://dx.doi.org/10.1017/S0025315400010407.
Sekino, T., Yamamura, N., 1999. Diel vertical migration of zooplankton: optimum migrating schedule based on energy accumulation. Evol. Ecol. 13, 267–282, http://dx.doi.org/10.1023/A:1006797101565.
Spencer, M., 1997. The effects of habitat size and energy on food web structure: an individual-based cellular automata model. Ecol. Model. 94, 299–316.
Stearns, S.C., 1992. The Evolution of Life Histories, vol. 249. Oxford University Press, Oxford, United Kingdom.
Stibor, H., 1992. Predator induced life-history shifts in a freshwater cladoceran. Oecologia 92, 162–165, http://dx.doi.org/10.1007/BF00317358.
Tarling, G., Burrows, M., Matthews, J., Saborowski, R., Buchholz, F., Bedo, A., Mayzaud, P., 2000. An optimisation model of the diel vertical migration of northern krill (*Meganyctiphanes norvegica*) in the Clyde Sea and the Kattegat. Can. J. Fish. Aquat. Sci. 57, 38–50, http://dx.doi.org/10.1139/f00-171.
Thorisson, K., 2006. How are the vertical migrations of copepods controlled? J. Exp. Biol. Ecol. 329, 86–100, http://dx.doi.org/10.1016/j.jembe.2005.08.011.
Threlkeld, S.T., 1976. Starvation and the size structure of zooplankton communities. Freshw. Biol. 6, 489–496, http://dx.doi.org/10.1111/j.1365-2427.1976.tb01640.x.
Unstad, K.H., Tande, K.S., 1991. Depth distribution of *Calanus finmarchicus* and *C. glacialis* in relation to environmental conditions in the Barents Sea. Polar Res. 10, 409–420, http://dx.doi.org/10.3402/polar.v10i2.6755.
Ussing, H.H., 1938. The biology of some important plankton animals in the fjords of East Greenland. In: Gunnar, T. (Ed.), Treaarsexpeditionen til Christian den X's Land 1931/34, vol. 100. Reitzel, Copenhagen, Denmark, pp. 1–20.
Uye, S., Huang, C., Onbe, T., 1990. Ontogenetic diel vertical migration of the planktonic copepod *Calanus sinicus* in the Inland Sea of Japan. Mar. Biol. 104, 389–396, http://dx.doi.org/10.1007/BF00345674.
van Haren, H., Compton, T.J., 2013. Diel vertical migration in deep sea plankton is finely tuned to latitudinal and seasonal day length. PLoS One 8, e64435, http://dx.doi.org/10.1371/journal.pone.0064435.
Varpe, Ø., Fiksen, Ø., 2010. Seasonal plankton–fish interactions: light regime, prey phenology, and herring foraging. Ecology 91, 311–318, http://dx.doi.org/10.1890/08-1817.1.
Varpe, Ø., Jørgensen, C., Tarling, G., Fiksen, Ø., 2007. Early is better: seasonal egg fitness and timing of reproduction in a zooplankton life-history model. Oikos 116, 1331–1342, http://dx.doi.org/10.1111/j.0030-1299.2007.15893.x.
Varpe, Ø., Jørgensen, C., Tarling, G., Fiksen, Ø., 2009. The adaptive value of energy storage and capital breeding in seasonal environments. Oikos 118, 363–370, http://dx.doi.org/10.1111/j. 1600-0706.2008.17036.x.
Varpe, Ø., 2012. Fitness and phenology: annual routines and zooplankton adaptations to seasonal cycles. J. Plankton Res. 34, 267–276, http://dx.doi.org/10.1093/plankt/fbr108.
Visser, A.W., Jónasdóttir, S.H., 1999. Lipids, buoyancy and the seasonal vertical migration of *Calanus finmarchicus*. Fish. Oceanogr. 8, 100–106, http://dx.doi.org/10.1046/j.1365-2419.1999.00001.x.
Vlymen, W.J., 1970. Energy expenditure of swimming copepods. Limnol. Oceanogr. 15, 348–356, http://dx.doi.org/10.4319/lo.1970.15.3.0348.
Williamson, C.E., Fischer, J.M., Bollens, S.M., Overholt, E.P., Breckenridge, J.K., 2011. Toward a more comprehensive theory of zooplankton diel vertical migration: integrating ultraviolet radiation and water transparency into the biotic paradigm. Limnol. Oceanogr. 56, 1603–1623, http://dx.doi.org/10.4319/lo.2011.56.5.1603.
Wroblewski, J.S., 1982. Interaction of currents and vertical migration in maintaining *Calanus marshallae* in the Oregon upwelling zone—a simulation. Deep Sea Res. Part A Oceanogr. Res. Pap. 29, 665–686, http://dx.doi.org/10.1016/0198-0149(82)90001-2.
Zakardjian, B.A., Runge, J., Plourde, S., Gratton, Y., 1999. A biophysical model of the interaction between vertical migration of crustacean zooplankton and circulation in the Lower St. Lawrence Estuary. Can. J. Fish. Aquat. Sci. 56, 2420–2432, http://dx.doi.org/10.1139/f99-095.
Zanakis, S.H., Evans, J.R., 1981. Heuristic optimization: why, when, and how to use it. Interfaces 11, 84–91, http://dx.doi.org/10.1287/inte.11.5.84.
Zaret, T.M., Kerfoot, W.C., 1975. Fish predation on *Bosmina longirostris*: body-size selection versus visibility selection. Ecology 56, 232–237, http://dx.doi.org/10.2307/1935317.
Zaret, T.M., Suffern, J.S., 1976. Vertical migration in zooplankton as a predator avoidance mechanism. Limnol. Oceanogr. 21, 804–813, http://dx.doi.org/10.4319/lo.1976.21.6.0804.
Zink, R.M., 2002. Towards a framework for understanding the evolution of avian migration. J. Avian Biol. 33, 433–436, http://dx.doi.org/10.1034/j.1600-048X.2002.03081.x.

this appendix accompanies additional material for

A high-resolution modeling study on diel and seasonal vertical migrations of high-latitude copepods

APPENDIX

Kanchana Bandara[1], Øystein Varpe[2,3], [4]Rubao Ji, [1]Ketil Eiane

[1]Faculty of Biosciences and Aquaculture, Nord University, 8049, Bodø, Norway

[2]The University Centre in Svalbard, 9171, Longyearbyen, Norway

[3]Akvaplan-niva, Fram Centre, 9296, Tromsø, Norway

[4]Woods Hole Oceanographic Institution, Redfield 2-14, Woods Hole, Massachusetts 02543, USA

Appendix A1: Additional data on environmental parameters

A1.1 The Irradiance sub-model

The solar irradiance incident on the sea surface (I_0, Eq. 1 in main text) was determined using the global horizontal irradiance (GHI) model of Robledo and Soler (2000) assuming clear sky conditions and discounting for Rayleigh scattering and various other measurable atmospheric parameters such as air pressure, temperature, perceptible water, ozone and aerosol concentrations.

$$I_0 = 1159.24 \cdot (cos\theta_z)^{1.179} \cdot \exp(-0.0019 \cdot (90^0 - \theta_z)) \quad \text{A1.1}$$

Here, θ_z is the solar zenith angle, calculated using,

$$cos\theta_z = (cos\phi \cdot cos\theta_d \cdot cos\theta_h) + (sin\phi \cdot sin\theta_d) \quad \text{A1.2}$$

where, φ is the latitude, θ_d is the declination angle (Eq. 3) and θ_h is the hour angle, which is an angular representation of local solar time (T_s, Eq. A1.4, A1.5) in degrees.

$$\theta_d = 23.45 \cdot sin\left(\frac{360}{365}[D - 81]\right) \quad \text{A1.3}$$

$$\theta_h = 15 \cdot (T_S - 12) \quad \text{A1.4}$$

Here, D is the day of the year (as January 1 = day 1). The local solar time T_S was calculated using the local time (T_L), the difference between the local meridian (= longitude: λ) and local standard time meridian (λo: Eq. 6), and the equation of time (E: Eq. A1.7), which is an empirical equation that accounts for the eccentricity of earth's orbit and the tilt.

$$T_S = T_L + \frac{4 \cdot (\lambda - \lambda_0) + E}{60} \quad \text{A1.5}$$

$$\lambda_0 = 15(T_L - T_{GM}) \quad \text{A1.6}$$

$$E = 9.87 \cdot sin\left(\frac{360}{365}[D-81]\right) - 7.53 \cdot cos\left(\frac{360}{365}[D-81]\right) - 1.5 \cdot sin\left(\frac{360}{365}[D-81]\right) \quad \text{A1.7}$$

Modelled irradiance roughly agrees with the field estimates (https://data.met.no/) and presented in Fig. 1 in the main text.

A1.2 Details of the three model environments

Table A1.1 Detailed description of the three model environments (Fig. 1 in main text)

Parameter	Attribute	Environment-L	Environment-M	Environment-H
Irradiance (µmol m^{-2} s^{-1})	Min.	0	0	0
	Max.	1500	1300	1100
	Time of Max.	day 172 (June 21)	day 172 (June 21)	day 172 (June 21)
Temperature (°C)	Min.	4	3	2
	Max. (°C)	18	15	12
	Time of Max.	day 181 (July 1)	day 188 (July 7)	day 195 (July 14)
Food availability (mg m^{-3} Chl.a)	Min.	0	0	0
	Max.	8	8	8
	Time of Max.	day 105 (April 15)	day 121 (May 1)	day 135 (May 15)
	Productive season (duration)	167 d	153 d	137 d

The modeled irradiance is based on the GHI model of Robledo and Soler (2000) and verified by the field estimates of Norwegian Metrological Institute (https://data.met.no/). Modelled temperature ranges were adopted from Unstad and Tande (1991); Bagøien et al. (2000); Ingvaldsen and Loeng (2009); Basedow et al. (2010); and Melle et al. (2014), and field estimates made during the LoVE MarinEco (http://love.arctosresearch.net) and DWARF (http://www.iopan.gda.pl/projects/Dwarf/) projects, obtained via personal communication through Boris Espinasse and Slawek Kwasniwski respectively. Timing and duration of pelagic

bloom were approximations which were adopted from Falk-Petersen et al. (2009); Daase et al. (2013). All modelled environmental variables represent coastal locations along the southern and southeastern Norwegian shoreline (Northeast Atlantic).

Appendix A2: Predicting diel vertical trajectories using a biased random walk

A2.1 Background

Classic random walk models are simple in the sense that the direction of the movement is completely random, and the movement at current time is not dependent on that of the previous time(s). A change in probability of moving in a certain direction can make a global directional bias, and paths that contain a consistent bias towards a preferred direction is called a biased random walk (BRW, Codling 2003). Here, we developed a BRW algorithm to predict copepod's movement in the vertical dimension (1D), in which the bias was introduced by the gradients of environmental variables (e.g. Alt 1980).

A2.2 The model

The copepod's photoreactive behavior is defined by an individual-specific lower irradiance threshold (α, see Table 2 in the main text), beyond which induces a negative phototatic response (Båtnes et al. 2015; Cohen et al. 2015). At any given time, the copepod searches and occupies a position in the water column with an irradiance level below α that maximizes its growth potential. The objective of the BRW algorithm is to predict the copepod's search pattern (direction and moving distance) in each time-step.

The distance that the copepod can cover between each time-step of the model (1 h) is limited by its cruising velocity, which was modelled as a power function of copepod's structural body mass (see Fig. 4a in main text). If the copepod cruises at a vertical velocity of $U_{i,t}$ m h^{-1}, its movement at each 1 h time-step can be predicted using $U_{i,t}$ (≥ 1) no. of vertical moves.

Given $V_{i,t}$ is the no. of moves that copepod has at its disposal between time-step t and $t + 1$ (for example after the first move $V_{i,t} = U_{i,t} - 1$), z the depth, G the growth potential (see Eq.

1–8 in the main text), P_0 the probability of initial movement at time-step t, P_A the probability of advancing along the direction of the previous move, and P_R (= 1 - P_A) the probability of retreating along the opposite direction to the previous movement, the probabilities of vertical movement are given as in Fig. A2.1.

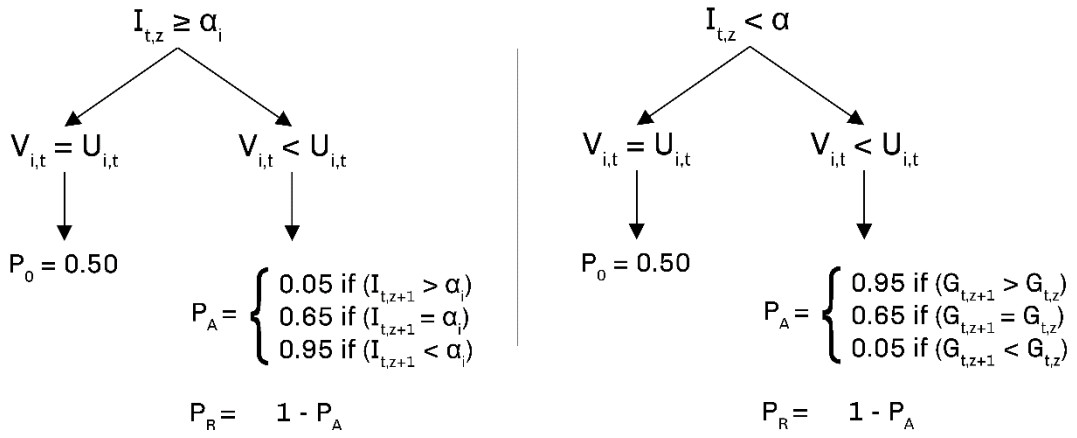

Fig. A2.1 Probabilities of the initial and subsequent vertical movements of the copepod, determined by the Irradiance and the growth potential (which is dependent on food availability and temperature). Decisions are made by drawing uniform random numbers (0–1, with the intervals of 0.01) and checking those against P_0, P_A and/or P_R.

Tuning the decision-making probability cutoffs (0.05, 0.65 and 0.95) changes the influence of stochasticity in the copepod's vertical movement. Using a directionally biased cutoff probability of 0.65 when environmental gradients do not exist is used to avoid the copepod getting stuck in unproductive waters or local food optima.

A2.3 Model predictions and drawbacks

The model predicts the diel vertical trajectories fairly well (Fig. A2.2). Given the growth sub-model (eq. 1–8 in the main text) and lack of starvation tolerance in our model, the predicted optimal diel migrations are restricted to the productive part of the water column (see section 4 in the main text). Constraints of daily feeding or some measure of starvation tolerance measure is needed to accurately predict the DVM amplitude and surface times, especially on older developmental stages.

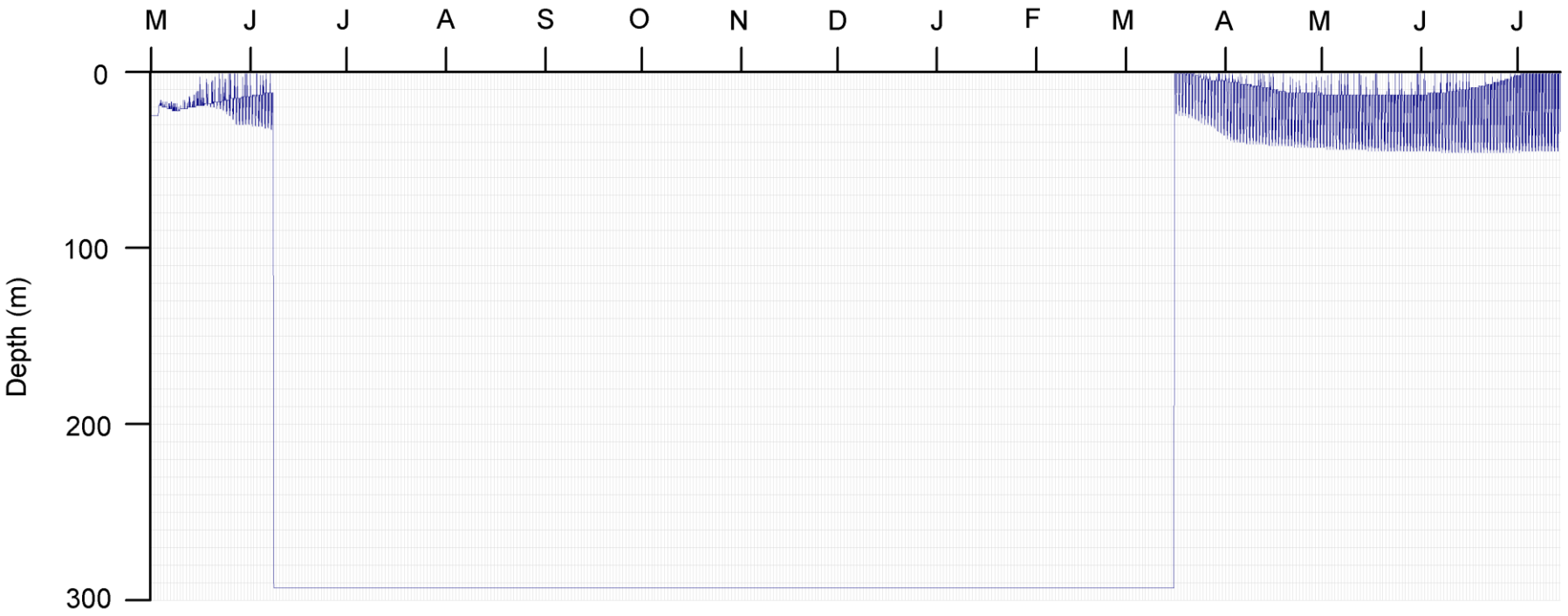

Fig. A2.2 Simulated diel and seasonal vertical trajectory of a copepod with an irradiance sensitivity parameter (α) of 1000 and size-selectivity of α (β) of 2 (see Table 2 and Fig. 4c in main text). Simulation was performed in the Environment-L (Fig. 2 in main text, and Appendix A1).

Appendix A3: Details of the sensitivity analysis

Table A3.1 List of input parameters and environmental variables tested for sensitivity, their relative changes and associated values. Basic run values of these parameters are available in the main text

Input parameter	%Change	Value	Notes
Assimilation coefficient (a)	-25%	0.575	
	+25%	0.875	
Swimming cost	-25%	1.125	Multiplier of basal metabolic cost
	+25%	1.875	
Cruising velocity	-25%	Eq.11	Increase or decrease in the mass-specific cruising velocity (U, Eq. 11)
	+25%	Eq.11	
Body Carbon composition (%)	-25%	30	
	+25%	50	
Visual predation risk (K)	-25%	0.0075	
	+25%	0.0125	
Size dependency of K	-25%	7.5	Changes the slope of the linear model in Fig. 4a in the main text so that the adult female is ca. 7.5 or 12.5 times more vulnerable to visual predators
	+25%	12.5	
Non-visual predation risk (M_n, %)	-25%	0.75	As a percentage of the max. visual predation risk
	+25%	1.25	
Food concentration (F, mg Chl.-a m^{-3})	-25%	10	
	+25%	6	
Temperature (T, °C)	-25%	22.5	Only the maximum temperature. Minimum, i.e. near-bottom temperatures not affected
	+25%	13.5	
Timing of pelagic bloom (d)	–	+15d	In order to maintain the relationship meaningful, the seasonal temperature distribution (Fig. 1 in the main text) was shifted with the algal bloom peak
	–	+15d	
Length of productive season (d)	–	+15d	In order to maintain the relationship meaningful, the seasonal temperature distribution (Fig. 1 in the main text) was expanded/contracted with the productive season expansion/contraction
	–	+15d	
Depth of thermal stratification (m)	–25%	75 m	
	+25%	125 m	
Chl-a vertical distribution (m)	-25%	-0.075	The exponent that scales the vertical scaling of Chl-a distribution (exponential decay with depth) was tuned (default value = -0.06)
	+25%	-0.045	

Appendix A4: Growth rate of the copepod; temperature and food relations

The food-limited growth rate (Eq. 3 in main text) is always lesser than the maximum food-independent growth rate (Eq. 1, 2 in main text). In the model, DVM caused copepods to move away from the regions with maximum food abundance on a daily basis, and resulted in food-limitation, which ultimately caused retardation of growth rates.

The food-limited growth rate increases with temperature and food availability. At any given food concentration, the food-limited growth rate (Eq. 3) decreases and the saturation food concentration (Eq. 8) increased with decreasing temperature (Fig. A4.1–3).

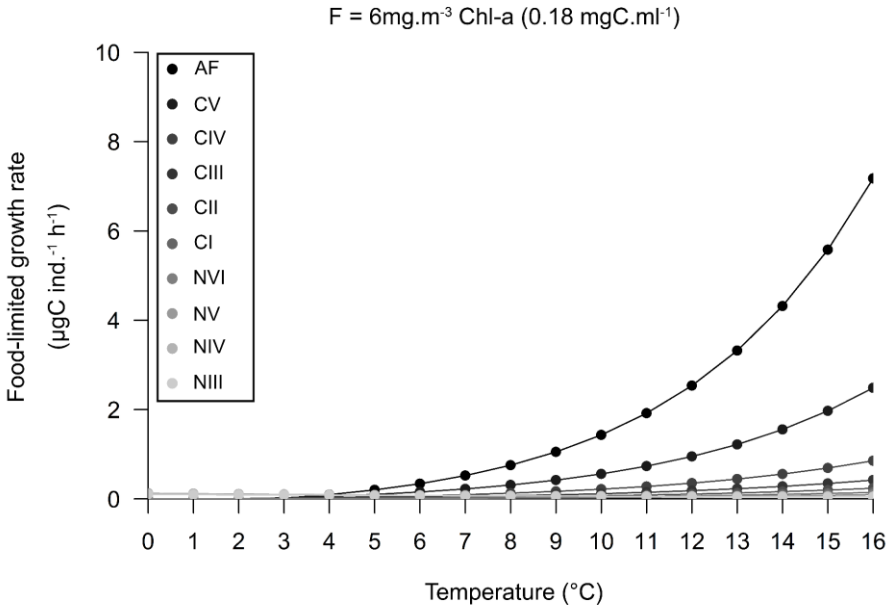

Fig. A4.1 Relationship of the food-limited growth rate and environmental temperature at lower food concentration (6 mg Chl.-a m^{-3})

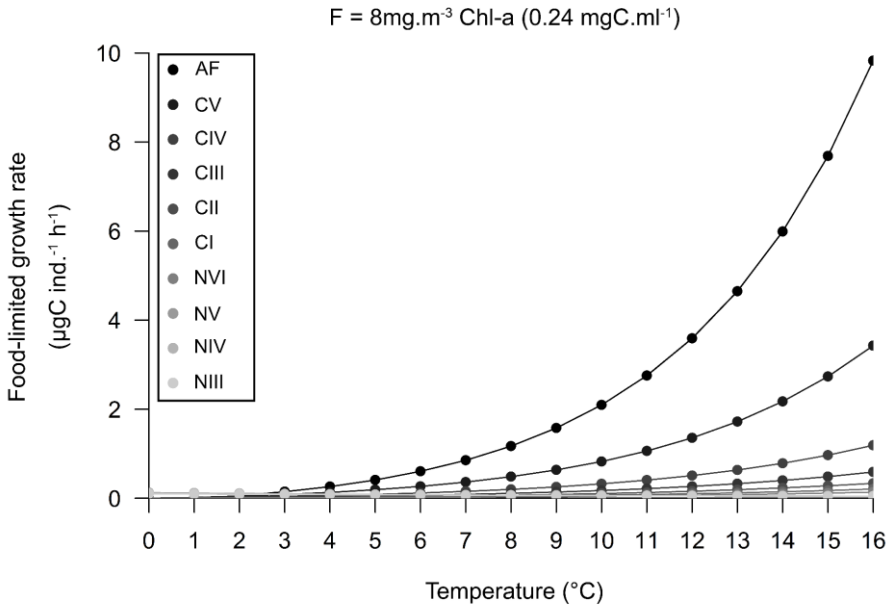

Fig. A4.2 Relationship of the food-limited growth rate and environmental temperature at a higher level of food concentration (8 mg Chl.-a m^{-3})

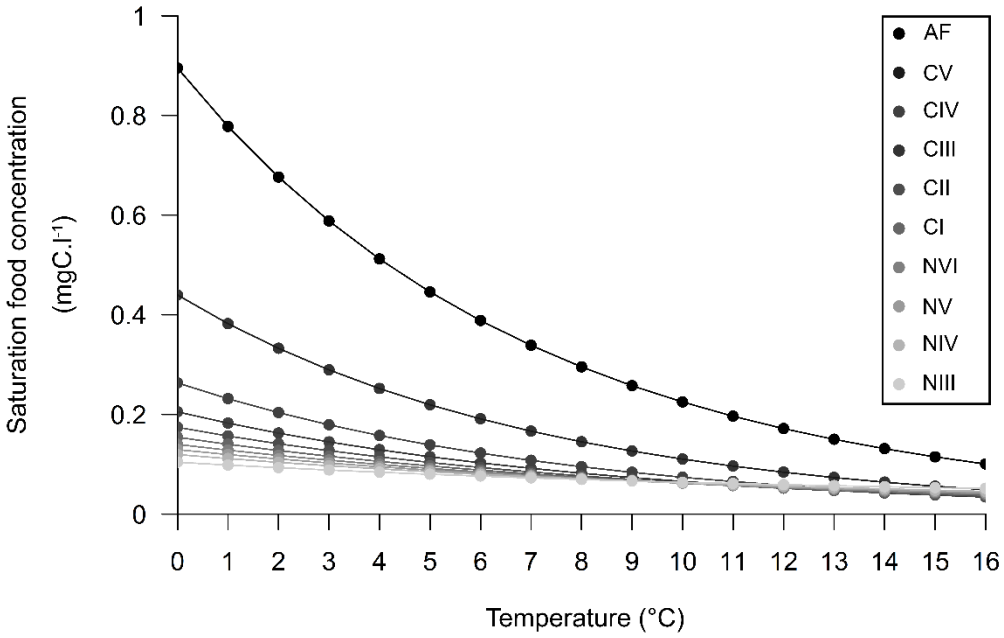

Fig. A4.3 Relationship of the saturation food concentration and environmental temperature at a fixed level of food concentration (8 mg Chl.-a m^{-3})

The Fig. A4.3 above represents the Fig. 5 of Huntley and Boyd (1984). Here, the increase of the saturation food concentration (*f*, see Table 4 in main text) increases due to the exponential relationship between the assimilation coefficient (*b*, see Eq. 4, 8 and Table 4 in main text) and environmental temperature.

Cited Literature

Alt W (1980) Biased random walk models for chemotaxis and related diffusion approximations J Math Biol 9:147-177 doi:https://doi.org/10.1007/BF00275919

Bagøien E, Kaartvedt S, Øverås S (2000) Seasonal vertical migrations of *Calanus* spp. in Oslofjorden Sarsia 85:299-311 doi:http://dx.doi.org/10.1080/00364827.2000.10414581

Basedow SL, Tande KS, Stige LC (2010) Habitat selection by a marine copepod during the productive season in the Subarctic Mar Ecol Prog Ser 416:165-178 doi:https://doi.org/10.3354/meps08754

Båtnes AS, Miljeteig C, Berge J, Greenacre M, Johnsen GH (2015) Quantifying the light sensitivity of *Calanus* spp. during the polar night: potential for orchestrated migrations conducted by ambient light from the sun, moon, or aurora borealis? Polar Biol 38:51-65 doi:https://doi.org/10.1007/s00300-013-1415-4

Codling EA (2003) Biased random walks in biology. Master thesis, The University of Leeds

Cohen JH et al. (2015) Is ambient light during the high Arctic polar night sufficient to act as a visual cue for zooplankton? PloS one 10:e0126247

Daase M et al. (2013) Timing of reproductive events in the marine copepod *Calanus glacialis*: a pan-Arctic perspective Can J Fish Aquat Sci 70:871-884 doi:https://doi.org/10.1139/cjfas-2012-0401

Falk-Petersen S, Mayzaud P, Kattner G, Sargent JR (2009) Lipids and life strategy of Arctic *Calanus* Mar Biol Res 5:18-39 doi:http://dx.doi.org/10.1080/17451000802512267

Huntley M, Boyd C (1984) Food-Limited Growth of Marine Zooplankton Am Nat 124:455-478 doi:https://doi.org/10.1086/284288

Ingvaldsen R, Loeng H (2009) Physical Oceanography. In: Sakshaug E, Johnsen GH, Kovacs K (eds) Ecosystem Barents Sea. Tapir Academic Press, Trondheim, Norway,

Melle W et al. (2014) The North Atlantic Ocean as habitat for *Calanus finmarchicus*: Environmental factors and life history traits Prog Oceanogr 129:244-284 doi:https://doi.org/10.1016/j.pocean.2014.04.026

Robledo L, Soler A (2000) Luminous efficacy of global solar radiation for clear skies Energ Conversat Manag 41:1769-1779 doi:http://dx.doi.org/10.1016/S0196-8904(00)00019-4

Unstad KH, Tande KS (1991) Depth distribution of *Calanus finmarchicus* and *C. glacialis* in relation to environmental conditions in the Barents Sea Polar Res 10:409-420 doi:http://dx.doi.org/10.3402/polar.v10i2.6755

Paper-III

Artificial evolution of behavioral and life history strategies of Arctic *Calanus* spp. in response to bottom-up and top-down selection pressures

Kanchana Bandara[*1,2], Øystein Varpe[2,3], Rubao Ji[4], Ketil Eiane[1]

[1]Faculty of Biosciences and Aquaculture, Nord University, 8049, Bodø, Norway

[2]The University Centre in Svalbard, 9171, Longyearbyen, Norway

[3]Akvaplan-niva, Fram Centre, 9296, Tromsø, Norway

[4]Woods Hole Oceanographic Institution, Redfield 2-14, Woods Hole, Massachusetts 02543, USA

[*] corresponding author: kanchana.bandara@nord.no

Abstract

Strong seasonality of resources and risks act as bottom-up and top-down selection pressures in high-latitudes, under which numerous behavioral and life history strategies evolve. Such seasonal strategies are well-documented for high-latitude marine zooplankton. However, little is known about the separate effects of bottom-up and top-down selection pressures in the shaping up of their seasonal behavioral and life history strategies. Here, we present a model that allows partitioning of bottom-up (i.e. food availability and temperature) and top-down (i.e. visual predation risk) selection pressures to study how behavioral and life history strategies evolve. In the model, differential timing, amplitude and ontogenetic trajectories of diel and seasonal vertical migrations were defined as behavioral strategies. Body size, generation time and birth time comprised the life history strategy. Numerous combinations of behavioral and life history strategies were hardwired to copepods belonging to three model-species representing the Arctic *Calanus* species. In a given model environment, strategies were evaluated for growth, survival and reproductive performances using a fitness estimate, which was heuristically maximized using an evolutionary algorithm. Model simulations were performed in three low- to high-Arctic deterministic seasonal environments at various levels of visual predation risk. At lower visual predation risk, species-specific behavioral and life history strategies were largely influenced by food availability and temperature. However, as visual predation risk increased, the influence of bottom-up selection pressures diminished, and irrespective of the modelled latitude, all model-species employed largely similar strategies under top-down selection pressure. Modest increase of visual predation risk increased the diel vertical migration behavior. Further increase of visual predation risk was associated with the decrease of body size, which created a significant impact on the observed behavioral and life history strategies through allometric processes. We conclude that top-down selection pressures serve a significant role in the evolution of behavioral and life history strategies of high-latitude zooplankton.

Keywords: seasonal strategies, life history evolution, vertical migration, pelagic environments, genetic algorithm, optimization model

1. Introduction

High-latitude pelagic environments are characterized by strong seasonal oscillations of irradiance, which drives seasonal patterns of temperature, primary production and predation risk. These impose strong bottom-up and top-down selection pressures on pelagic inhabitants (Hunter & Price 1992, Power 1992, Varpe 2017) and lead to a wide range of behavioral and life history adaptations (Ohman 1988, Conover 1992, Szulkin et al. 2006, Williams et al. 2017). Seasonal adaptations are usually linked with trade-offs, as all adaptive traits cannot be simultaneously improved without compromising each other, especially in seasonally resource-limited environments with elevated predation risk (Stearns 1989, Fabian & Flatt 2012, Varpe 2017).

Seasonal behavioral and life history adaptations and associated trade-offs are well-documented among marine zooplankton (reviewed in, Conover & Siferd 1993, Hagen & Auel 2001, Varpe 2012). These involve adaptations to cope with both the productive and unproductive parts of the year. During the productive season (spring–summer), zooplankton tend to feed in the warmer, food-rich, near-surface waters to grow and develop rapidly toward attaining sexual maturity (Hopkins et al. 1984, Huntley & Lopez 1992, Lee et al. 2003, Escribano et al. 2014). However, occupation of surface waters elevates the mortality risk through visual predation. This is usually countered by trading off growth potential for survival through diel vertical migration (DVM) (Lampert 1989, Loose & Dawidowicz 1994, Hays 2003). Further, structural growth of late developmental stages (e.g. copepodite III onwards) of many high-latitude zooplankton is traded off to build up energy reserves (Lee et al. 2006). Such trade-offs together with shorter productive season and seasonal peaks of visual predation risk make it usually impossible for zooplankton to attain sexual maturity and reproduce within the same calendar year (Hirche 1996b, Hagen 1999, Kaartvedt 2000, Varpe & Fiksen 2010). Instead, as the unproductive season (autumn–winter) approaches, zooplankton perform seasonal vertical migrations (SVM) to deeper waters and overwinter with minimal biological activity (i.e. diapause, Carlisle & Pitman 1961, Hirche 1996a).

The inability to maintain high biological activity during the unproductive part of the year tends to increase generation times (Conover 1988, Falk-Petersen et al. 2009) and consequently elevates body sizes of most high-latitude zooplankton (Hall et al. 1976, Gillooly et al. 2002). Based on their inverse relationships with temperature, it can also be predicted that generation time and body size of high-latitude zooplankton increase from lower- to higher-Arctic locations (see, Rohde 1992, Blackburn et al. 1999). However, since these two life history traits show plasticity to top-down selection pressures (Brooks & Dodson 1965, Gillooly 2000, Jeppesen et al. 2004), it is interesting to investigate how growth and reproductive advantages of a longer lifespan and larger body size (McLaren 1966) are traded off for survival at elevated levels of size-dependent

predation risk. In addition, as body size changes driven by bottom-up or top-down selection pressures can directly influence physiological and behavioral activity through allometric relationships (Brown et al. 2004), it is crucial to study how these processes influence seasonal behavioral and life history adaptations of high-latitude zooplankton.

Predominantly herbivorous zooplankton occupy a crucial trophic position between primary producers and higher-order consumers, and are well-suited for studying the influences of bottom-up and top-down selection pressures (Hays et al. 2005). In the Arctic, three congeners of *Calanus*, i.e. *C. finmarchicus*, *C. glacialis* and *C. hyperboreus* usually dominate the herbivore biomass (Eiane & Tande 2009). Despite the largely similar morphologies, these three species exhibit diverse behavioral and life history strategies that are plastic to environmental variability (Table 1). These, coupled with latitudinal patterns of species composition and abundance from lower- to higher-Arctic locations (Conover 1988, Daase & Eiane 2007) make *Calanus* an ideal model-species for studying ecological implications of spatio-temporal dynamics of the abiotic and biotic environments (Beaugrand et al. 2002, Hays et al. 2005, Ji et al. 2012, Espinasse et al. 2017). In this study, we present a model of behavioral and life history strategies of Arctic *Calanus* species. In the model, species-specific optimal behavioral and life history strategies are artificially evolved in a deterministic model environment. By performing model simulations along a latitudinal gradient at variable levels of predation risk, we investigate how species-specific behavioral and life history responses of Arctic *Calanus* spp. emerge in response to bottom-up and top-down selection pressures of the environment.

2. Materials and Methods

Although the model is not strictly individual-based, it is described using the Overview, Design concepts and Details (ODD) protocol (Grimm et al. 2006, Grimm et al. 2010) to improve reproducibility.

2.1 Purpose

The purpose of the model is to investigate species-specific behavioral and life history responses of Arctic *Calanus* spp. against bottom-up and top-down selection pressures mediated by the environment.

2.2. Entities, State variable and scales

The model possesses three entities: strategies, model organism and the model environment.

Strategies are of two types: behavioral strategy and life history strategy. The behavioral strategy (or vertical strategy) defines the timing, amplitude and the ontogenetic trajectories of DVM and SVM. These are represented by three evolvable (soft) parameters (Table 2). The life history strategy represents a collection of life history traits (i.e. birth time, body mass, generation length, size at diapause onset, age and size of sexual maturity, onset of spawning, breeding mode and fecundity) and their size- or stage-specific variability. From these, the birth time, body size and generation length are represented by three evolvable parameters (Table 2). Other life history traits emerge as the evolvable parameters are optimized in the model. Strategies are hardwired to the model organism, i.e. copepods belonging to three model-species.

The model organism characterizes hypothetical, semelparous female copepods of species-CF, species-CG and species-CH, that represent the Arctic *Calanus* complex (*C. finmarchicus*, *C. glacialis* and *C. hyperboreus*). Although these species are distributed throughout the Arctic, only *C. glacialis and C. hyperboreus* are considered as species with a true Arctic origin, where *C. finmarchicus* is a boreal species that primarily inhabit the North Atlantic (Fleminger & Hulsemann 1977, Conover 1988). *Calanus* spp. possess a 13-developmental stage ontogeny, which includes an embryonic stage, six naupliar stages (NI–NVI), five copepodite (CI–CV) stages and an adult. Older developmental stages can store lipids, which act as energy reserves that are used to meet the metabolic demands during the diapause (Hirche 1996a, Hagen & Auel 2001). However, overwintering stage composition, size of energy reserves and potential diapause duration varies between species (Table 1 and see also, Falk-Petersen et al. 2009, Maps et al. 2013). Reproduction of *Calanus* spp. usually occur in the spring, but the timing and the sources of energy

allocation vary between the three species (Table 1). *C. hyperboreus* has the longest life cycle duration (usually 3 years) and largest body size, while the relatively small *C. finmarchicus* and *C. glacialis* usually complete their life cycles within 1 or 2 years (Table 1).

The model runs in three 1000-m deep artificial seasonal environments that roughly represent the expected environmental variability along a latitudinal gradient extending from the north Atlantic to the Arctic (ca. 60–80 °N). These model environments do not refer to specific geographic locations, but the modeled environmental parameters were adopted from field measurements taken in this region (Appendix A1). Since water mass characteristics of this region (e.g. Swift 1986) were not modelled for simplicity, the model environments represent typical annual oceanographic characteristics of deep Arctic fjords (reviewed in Cottier et al. 2010). The Environment-L characterizes the lower end of the modelled latitudinal gradient (ca. 60°N). Here, the modelled irradiance, temperature and primary production show pronounced seasonal and vertical variability (Fig. 1A–C), but are assumed constant between years. The modelled sea-surface irradiance follows the global clear-sky horizontal irradiance formulations of Robledo and Soler (2000), and peaks at ca. 1500 µmol m^{-2} s^{-1} (Fig. 1A). The modelled temperature peaks at 15°C in the summer and distributes evenly across the surface mixed layer (Fig. 1B). The depth of surface mixed layer follows the seasonal pattern described by Mann and Lazier (2006), and reaches a maximum of 500 m during the winter. Temperature below the mixed layer decreases with depth and converges to a minimum of 2°C. The pelagic primary production extends from mid-February to late-September, with a chlorophyll-*a* peak (6 mg m^{-3}) in mid-April (Fig. 1C). We manipulated the environmental parameters of Environment-L to formulate two additional seasonal environments, i.e. Environment-M (ca. 70°N, Fig. 1D–F) and Environment-H (ca. 80°N, Fig. 1G–I), representing the mid-point and the higher end of the modelled latitudinal gradient (Appendix A1). For simplicity, we did not model the sea ice dynamics at any of these higher-latitude environments.

Copepods are characterized by four state variables: vertical location (depth), structural body mass, energetic reserve and developmental stage. The model has a temporal coverage of an annual cycle and a unidimensional (vertical) spatial coverage of 1000 m. The time and space consist of 1 h and 1 m discreet intervals.

2.3 Process overview and scheduling

In each timestep, the model follows the evolvable proxies of behavioral and life history strategies hardwired to copepods spawned in different times of the year and simulates their growth, survival and reproduction separately for each model-species.

State variables are updated simultaneously. Strategies are evaluated using a fitness function based on the expected survival and reproductive performances. The fitness is heuristically maximized using a Genetic Algorithm (Holland 1975) to derive species-specific optimal behavioral and life history strategies for a given set of environmental conditions (Fig. 2).

2.4 Design concepts

2.4.1 Basic principles

The modeling framework follows a previous approach from Bandara et al. (2018) to model DVM and SVM over the entire life cycle of a high-latitude copepod in higher spatial and temporal resolution. In the above model, copepod diel and seasonal vertical behavior were modelled as strategies that maximize fitness (hence, the term vertical strategies). Vertical strategies were represented using multiple proxies that define the timing and amplitude (vertical extent) of DVM and SVM. From a large number of vertical strategies seeded at different times of the year, an optimal vertical strategy that maximizes fitness was heuristically estimated for a given set of environmental conditions. The present model was implemented to address a key limitation of the above, which is the lack of species-specific patterns of behavioral and life history strategies (Table 1). We built this to the present model via two design changes: first, the species-specific parameterization of growth survival and reproductive processes (section 2.6), and second, the inclusion of two evolvable parameters to allow the body size and generation time to emerge (Table 2, Fig. 2). The complex multi-dimensional optimization problem ensued was heuristically solved using a Real-Coded Genetic Algorithm (Davis 1989, Lucasius & Kateman 1989, Herrera et al. 1998).

The strategy-oriented construct of the present model shares the same limitations of Bandara et al. (2018). First, sacrificing biological (= individual) resolution to accommodate higher spatial and temporal resolution, and second, the lack of population level responses such as density dependence. Consequently, the modelled behavioral and life history strategies do no show quantitative feedbacks with the model environment (e.g. impact of grazing on food concentration and duration of the productive season).

2.4.2 Emergence

The behavioral and life history strategies emerging from the model are presented in Fig. 2 and described in Table 3.

2.4.3 Adaptation and sensing

Copepods are sensitive to their internal states (i.e. structural body mass, mass of the energetic reserve developmental stage) and external stimuli (i.e. irradiance, temperature, food concentration and depth). Altogether, these determine the size- or stage-specific patterns of growth, survival and reproduction (section 2.6).

2.4.4 Objectives

The model uses a fitness estimate that evaluates the expected reproduction and survival performances rendered by different behavioral and life history strategies (section 2.6.4).

2.4.5 Prediction and stochasticity

The vertical position of eggs within the convective mixed layer and the overwintering depth selection are modelled as stochastic processes (section 2.6.2.4). Further, stochasticity plays a central role in the model initialization (section 2.5) and selection, recombination and mutation operators of the GA (section 2.6.4).

2.4.6 Observations

For a given model environment, the model produces heuristic estimates of the optimal behavioral and life history strategies (Fig. 2, Table 3).

2.5 Initialization

The model initializes with seeding of N (= 2.5 x 10^6) eggs at random times of the year to random depths (< 50 m) of the water column. Each seed represents an embryonic stage of a copepod following a specific behavioral (vertical) strategy, ontogenetic body mass trajectory and a generation time. These are determined by randomly assigning values to the evolvable parameters listed in Table 2.

2.6 Submodels

2.6.1 Growth and development

We modelled species-specific somatic growth in Carbon units following a simple growth formulation, which defines the growth rate (G, µg C ind^{-1} h^{-1}) as the balance between assimilation and metabolic rates (Pütter 1920, Von Bertalanffy 1938) as,

$$G_{i,s,t,z} = a \cdot A_{i,s,t,z} - B_{i,s,t,z} \quad \text{Eq. 1}$$

Here, the assimilation rate is a product of the ingestion rate (A, µg C ind^{-1} h^{-1}) and the assimilation coefficient (a) Huntley and Boyd (1984), where B (µg C ind^{-1} h^{-1}) is the metabolic rate (section 2.6.2.6). Further, i is the individual, s is the species, t is time and z is depth (definitions, units and references of all the terms are listed in Table 4). At a hypothetical reference temperature -2° C, the ingestion rate relates with the structural mass (W_c, µg C) as,

$$A_{i,s,t} = b_s \cdot (W_c)_{i,t}^{m_s} \quad \text{Eq. 2}$$

where b and m are species-specific mass coefficient and exponent of ingestion (Table 5). The ambient temperature (T, °C) elevates the ingestion rate following the exponential function,

$$A_{i,s,t,z} = A_{i,s,t} \cdot c_s \cdot \exp(n_s \cdot T_{t,z}) \quad \text{Eq. 3}$$

where c and n are species-specific temperature coefficient and exponent of ingestion (Table 5). Parameter values for coefficients and exponents of body mass and temperature were estimated following the growth model of Maps et al. (2011) (Table 5, Appendix A2). The temperature-dependent ingestion rate is scaled by the ambient food concentration (F, µg C l^{-1}) into a range of 0–1 following a Holling's type-II (disk) function (Holling 1959) as,

$$A_{i,s,t,z} = A_{i,s,t,z} \cdot \frac{d_{i,t} \cdot F_{t,z}}{1 + d_{i,t} \cdot F_{t,z}} \quad \text{Eq. 4}$$

Here, the parameter d (selected range = 0.1–0.3) defines the food concentration at which the asymptotic value of the above relationship is reached (Fig. 3A, B), and relates with the structural mass (Fig. 3C) as,

$$d_{i,t} = 0.3 \cdot (W_c)_{i,t}^{-0.138} \quad \text{Eq. 5}$$

This produces size-specific satiation food concentrations in the range of 75–125 µg C l^{-1}, (Fig. 3A, B) which are comparable to those estimated by Huntley and Boyd (1984),

Campbell et al. (2001) and Maps et al. (2011). In the above calculations, we used Chl.-*a*:C ratio of 30 (Båmstedt et al. 1991, Sakshaug et al. 2009).

This growth submodel cannot be applied to first and second nauplii stages (NI and NII) which do not feed, but utilize the reserves from the embryo to meet energetic demands (Marshall & Orr 1972, Mauchline 1998). Although catabolization of reserves may lead to loss of body mass of non-feeding stages (Maps et al. 2011), for simplicity, we assumed that the structural masses of NI and NII remain constant during development.

The temperature-dependent development times (h) of eggs and non-feeding NI and NII stages are estimated following a Bělehrádek function (Corkett et al. 1986) as,

$$D_{s,t,z} = 24 \cdot \left[q_s \cdot (T_{t,z} + r_s)^{-2.05}\right] \qquad \text{Eq. 6}$$

Here, species-specific values for the parameters *q* and *r* were adopted from Campbell et al. (2001) and Ji et al. (2012) (Table 5). The development of feeding stages (NIII–Adult, i.e. from stage *j* to *j + 1*, where $4 \le j \le 12$) occurs only if the structural mass (W_c) exceeds a stage-specific critical molting mass (W_j, µg C) as,

$$j_{i,s} = \begin{cases} j_{i,s} + 1 & \text{if} \quad (W_c)_{i,s,t} > (W_j)_{i,s} \\ j_{i,s} & \text{if} \quad (W_c)_{i,s,t} \le (W_j)_{i,s} \end{cases} \qquad \text{Eq. 7}$$

For each model environment, species-specific maximum and minimum estimates of W_j (W_j^{min} and W_j^{max}) were estimated following the growth model of Maps et al. (2011) (Fig. 4, Appendix A2). To maintain the intra-specific plasticity of body sizes in the model, we introduced an evolvable parameter α (body size parameter, range = 0–1, Table 2), which defines the stage-specific critical molting masses of any given copepod as,

$$(W_j)_{i,s} = (W_j^{min})_{i,s} + \left[(W_j^{max})_{i,s} - (W_j^{min})_{i,s}\right] \cdot \alpha_i \qquad \text{Eq. 8}$$

Therefore, based on the parameter value of α, the ontogenetic body mass trajectories of copepods tend to occupy a fixed fraction of the environment- and species-specific ranges (Fig. 4).

288 2.6.2 Survival

289 2.6.2.1 Predation risk

290 We modelled the predation risk (M_v) as a probability function. Here, the depth-
291 specific visual predation risk scales with the downwelling irradiance (I) following Eiane
292 and Parisi (2001) as,

$$I_{t,z} = I_{t,0} \cdot \exp(-\psi \cdot z) \quad \text{Eq. 9}$$

293 where I_z and I_0 are irradiance at depth z and surface at a given time, and ψ (= 0.06 m^{-1})
294 is the attenuation coefficient for downward directed irradiance in the water column. To
295 express this as a probability, we remapped the downwelling irradiance (I) in a range
296 between 0.1–0.9 (I') so that visual predation risk offers non-zero probability of survival
297 at the highest possible irradiance level, and non-zero probability of death at the lowest
298 level, expressed as,

$$(M_v)_{i,t,z} = I'_{t,z} \cdot K_{i,t} \quad \text{Eq. 10}$$

299 Here, K is a parameter that scales the visual predation risk to produce hourly estimates
300 of mortality.

301 The detection efficiency of visually orientating planktivores increases with the
302 size of their prey (Brooks & Dodson 1965, De Robertis 2002, Aljetlawi et al. 2004). Most
303 metrics of detection efficiency, such as predator visual range, reaction distance and
304 electivity index are modelled in a way that it increases rapidly with the initial increase of
305 prey size, while reaching a summit or a plateau as prey size increases further (e.g. Zaret
306 & Kerfoot 1975, Confer et al. 1978, Pastorok 1981, Aksnes & Giske 1993). This is likely
307 due to elevated handling time, prey escape responses and gape-limitations driven by
308 larger prey sizes (Werner 1974, Fields & Yen 1997, Devries et al. 1998, Kiørboe 2011).
309 We followed this logic and modeled the size-dependent visual predation risk as an
310 asymptotic exponential relationship between the body mass (W_c) and K (Fig. 5A),
311 assuming that the largest developmental stage (female of Species-CH) is ca. 25 times
312 more vulnerable to visual predation risk compared to the smallest developmental stage
313 (eggs of species-CF) (Fig. 4, Fig. 5D–E). This scaling accounts for the inclusion of *C.*
314 *hyperboreus* in this model (represented by model-species-CH), compared to a previous
315 model of smaller *C. finmarchicus* and *C. glacialis* (Bandara et al. 2018), which used a
316 maximum 10-fold size-dependent visual predation risk scaling.

317 We modeled the mortality risk imposed by the non-visual predators (M_n) constant
318 over time and depth (Eiane & Parisi 2001), and assumed to account for 10% of the K.

319

2.6.2.2 Diel vertical migration

We used the photoreactive behavior as a proxy to estimate the timing and amplitude of DVM (e.g. Kerfoot 1970, Carlotti & Wolf 1998). Here, an evolvable parameter β (irradiance threshold parameter, Table 2) defines an irradiance threshold, above which a negative phototatic response on the vertical swimming behavior is induced (Båtnes et al. 2015, Cohen et al. 2015). Consequently, at any given time, copepods occupy a depth with an irradiance level ($I_{t,z}$) below β. From all possible depth bins that satisfy the $I_{t,z} < \beta$ condition, we assumed that copepods occupy the depth that maximizes the growth potential (Eq. 1). We predicted this depth deterministically, assuming that copepods are neutrally buoyant and swim vertically in the water column at a constant cruising velocity (U, mh^{-1}) obtained from Bandara et al. (2018) as,

$$U_{i,t} = 8.0116 \cdot (W_c)_{i,t}^{0.4531} \quad \text{Eq. 11}$$

For simplicity, we further assumed that internal state-dependent factors, such as hunger and satiation have a negligible influence on the modelled DVM.

To represent the size- or stage-specific variability of DVM (e.g. Zaret & Kerfoot 1975, Huntley & Brooks 1982, Hays 1995, Eiane & Ohman 2004), we defined an irradiance sensitivity parameter (L, selected range = 1–2.5) that relates positively with structural mass (W_c) following an asymptotic exponential relationship (Fig. 5B). The size-dependent increase of irradiance sensitivity causes the irradiance threshold parameter (β) to decrease as,

$$\beta_{i,t} = \beta_i \cdot \frac{1}{L_{i,t}} \quad \text{Eq. 12}$$

The minimum irradiance sensitivity thresholds produced by this model (i.e. 1.4×10^{-7} µ mol m^{-2} s^{-1} for species-CF, 5.92×10^{-8} µ mol m^{-2} s^{-1} for species-CG and 3.2×10^{-8} µ mol m^{-2} s^{-1} for species-CH) agree with those published for *Calanus* spp. by Båtnes et al. (2015).

2.6.2.3 Energy storage

The developmental stage CIV and CV of species-CF and -CG, and stages CIII, CIV and CV of species-CH can allocate an evolvable fraction γ (energy allocation parameter, Table 2) from surplus growth to build up an energy reserve. The reserve can occupy up to 70% of the structural mass (Fiksen & Carlotti 1998, Jónasdóttir 1999). As a consequence of the body size plasticity allowed in this model, it was observed in the trial runs that copepods always followed the lowest body mass trajectories and overwintered (see below) at a significantly smaller size (W_c ca. 10 µg C for species-CF). This not only

disagrees with the body mass estimates of overwintering *Calanus* spp.(Båmstedt et al. 1991, Pepin & Head 2009), but undermines the concept that a reasonable structural mass should be attained to allow space for lipid sac to be harbored (Miller et al. 2000, Lee et al. 2006). Therefore, we defined a minimal structural mass (W_c, µg C) below which no stores can be maintained as,

$$(W_s)_{i,s,t,z} = \begin{cases} 0 & \text{if} \quad (W_c)_{i,t} < 38 \\ G_{i,s,t,z} \cdot \gamma_i \cdot \left[\frac{1}{1+\exp\left((600-(W_c)_{i,t})/400\right)}\right] & \text{if} \quad 38 < (W_c)_{i,t} < 159 \\ G_{i,s,t,z} \cdot \gamma_i & \text{if} \quad (W_c)_{i,t} \geq 159 \end{cases} \qquad \text{Eq. 13}$$

where W_s (µg C) is the mass of the energy reserve and G is the surplus growth (Eq. 1). Here, energy storage capacity exponentially increases from 38 µg C and reaches a horizontal asymptote at 159 µg C (Fig. 5C). These lower and upper W_c values were estimated from lipid sac volume to body size relationships published by Miller et al. (2000) and Vogedes et al. (2010).

2.6.2.4 Seasonal vertical migration

We used the state of the energetic reserve as a proxy of timing of the SVM (Visser & Jónasdóttir 1999). Here, copepods descend to an overwintering depth when the stores account for an evolvable fraction δ (seasonal descent parameter: Table 2) of the structural mass. For simplicity, we made three general assumptions for selecting overwintering depths. First, copepods always overwinter below the maximum depth of the convective mixed layer (i.e. 500 m) to avoid being circulated back to the surface (Visser & Jónasdóttir 1999, Irigoien 2004). Second, the specific overwintering depth below the mixed layer is selected by a gaussian distribution (mean = 750, SD = 50). Third, internal and external environmental variability has no influence on the overwintering depth selection. Although the third assumption does not hold true in nature (e.g. Hirche 1991, Kaartvedt 1996, Astthorsson & Gislason 2003), we used it here for simplicity, because it was shown by Bandara et al. (2018) that the use of an evolvable overwintering depth parameter had a little influence on the fitness and phenology of the modeled copepod. After descending to overwintering depths, copepods switch to a diapause state (Carlisle & Pitman 1961, Hirche 1996b), where growth, development, vertical movements and reproduction cease (see also section 2.6.2.6). The diapause terminates and copepods ascend from overwintering depths upon exhausting an evolvable fraction ε from the energy reserve (seasonal ascent parameter, Table 2).

382 2.6.2.5 Generation time

383 We introduced an evolvable parameter η (generation time parameter, Table 2) to
384 represent the variability of generation times commonly reported for *Calanus* spp. (Table
385 1). Here, η ranges between 1–3, which indicates the generation time in number of years.
386 This shows species-specific patterns, where η = 1 for species-CF, η ranges between 1–2
387 for species-CG and 1–3 for species-CH (cf. Table 1). Generation times > 1 year are
388 characterized by several subsequent seasonal migrations, which follows the same
389 patterns of energy allocation, and same proxies of ascent and descent described above.
390 After the final diapause, copepods do not allocate surplus growth to maintain energy
391 reserves.

392

393 2.6.2.6 Metabolism

394 The metabolic rate (B, µg C) is the sum of the basal metabolic rate (B_b) and the active
395 metabolic rate (B_a). At the hypothetical reference temperature of -2°C, B_b relates with
396 the total body mass ($W = W_c + W_s$) as,

$$(B_b)_{i,s,t} = f_s \cdot (W)_{i,t}^{o_s} \quad \text{Eq. 14}$$

397 where f and o are mass coefficient and exponent of respiration (Table 5). Ambient
398 temperature elevates B_o following the exponential function,

$$(B_b)_{i,s,t,z} = (B_b)_{i,s,t} \cdot g_s \cdot \exp(p_s \cdot T_{t,z}) \quad \text{Eq. 15}$$

399 where g and p are temperature coefficient and exponent of metabolism (Table 5).
400 Parameter values for above respiration coefficients and exponents were estimated from
401 Maps et al. (2011) (Appendix A2). In the model, B_a consists of swimming costs (i.e.
402 metabolic costs of vertical migrations) and assumed to be 150% of the B_0 (Bandara et al.
403 2018). During diapause, B_a is nullified (since copepods are assumed stagnant) and the B_b
404 is assumed to reduce by 75% in all species (Maps et al. 2010).

405

406 2.6.2.7 Starvation risk

407 Metabolic demands that cannot be sustained by food intake are balanced by energy
408 reserves. In case of an absent or depleted energy reserves, structural mass is
409 catabolized. This induces mortality risk through starvation (starvation risk, M_s).
410 However, we assumed that copepods are tolerant to modest (< 10%) loss of structural
411 mass (Threlkeld 1976). Structural catabolization beyond the above threshold causes the

starvation risk to increase linearly and peaks as 50% of structural mass is lost and causes death (Bandara et al. 2018) as,

$$(M_s)_{i,t} = \begin{cases} 0 & \text{for} \quad (W_x)_{i,t} \leq 0.1 \\ 2 \cdot (W_x)_{i,t} & \text{for} \quad 0.1 < (W_x)_{i,t} \leq 0.5 \\ 1 & \text{for} \quad (W_x)_{i,t} \geq 0.5 \end{cases} \qquad \text{Eq. 16}$$

Here, W_x (µg C) is the catabolized structural mass expressed as a proportion of the maximum structural mass prior to structural catabolization.

2.6.3 Reproduction

In this model, somatic growth of copepods ceases after the final molt (e.g. Fiksen & Giske 1995, Fiksen & Carlotti 1998, Varpe et al. 2007), and the matter gained through feeding and catabolizing energy reserves is only allocated for meeting metabolic demands and reproduction. We modeled the energy input to reproduction as a species-specific process. Here, the reproduction of species-CF represents the pure income breeding strategy of *C. finmarchicus* (Table 1), where the energy input is sourced solely from food intake. Reproduction of species-CH represents the pure capital breeding strategy of *C. hyperboreus* (Table 1), where the energy input is sourced entirely from remaining reserves, by allocating a specific amount of matter (C) equivalent to the temperature-dependent growth rate (Eq. 1–3) from the remaining energetic reserve. Species-CG represents an intermediate reproductive strategy alike *C. glacialis* (Table 1), where energy inputs for reproduction may be sourced from both food-intake and energy reserves. The fecundity (R) from is estimated using the matter allocated to egg production (W_R, µg C) and the species-specific unit egg mass (W_E, µg C) as,

$$R_{i,s,t,z} = \frac{(W_R)_{i,s,t,z}}{(W_E)_s} \qquad \text{Eq. 17}$$

Here, the W_E vary with the species (Table 5), but we assumed that it is not affected by environmental variability.

2.6.4 Fitness function and optimization

To evaluate the performance of behavioral and life history strategies, we used the fitness estimate (Ω) developed by Bandara et al. (2018) as,

$$\Omega_{i,s} = \left(\sum_{t_B}^{t_X} H_{i,t,z} \cdot R_{i,s,t,z} \right) \cdot \omega \qquad \text{Eq. 18}$$

where H is the survivorship, i.e. the probability of survival from birth (t_B) to a given time horizon (t_X), estimated as a function of visual, non-visual and starvation risks (M_v, M_n and M_s) as,

$$H_{i,t,z} = \prod_{t_B}^{t_X} 1 - \left[(M_v)_{i,t,z} + (M_n)_{t,z} + (M_s)_{i,t}\right] \quad \text{Eq. 19}$$

The fitness is adjusted using a binary weight ω (Bandara et al. 2018), as the fitness function is not robust to evaluate generation times less than one year.

We used a Real-Coded Genetic Algorithm to derive environment- and species-specific heuristic estimates of the optimal behavioral and life history strategies that maximize fitness. In the RCGA, the seven proxies of behavioral and life history strategy (Table 2) are considered as genes on a single chromosome. The optimization process begins by selecting a mating pool of N chromosomes (parents) from the initial seeds using a binary (two-way) deterministic tournament (Goldberg & Deb 1991, Miller & Goldberg 1995). Genes of two randomly selected parents from the mating pool are recombined following the Laplace crossover method (LX, Deep & Thakur 2007), which produces two offspring (recombinants). Genes of the recombinants are mutated at a probability of 0.02 per-gene following the Makinen, Periaux and Toivanen mutation (MPTM, Toivanen et al. 1999). The population of strategies resulting from these operations comprises of N parents, whose fitness is known and N offspring, whose fitness is not yet known. Parents with unique gene combinations are selected to construct a reference library, which is updated at each iteration. Each offspring is compared with those in the reference library to assess their fitness. Fitness of the offspring with similar gene combination to those in the reference library are assigned *in-situ*, while the rest goes through the life cycle simulation to determine fitness. Once the fitness of all $2N$ individuals are known, N survivors are selected following a round-robin (all-play-all) tournament of size 10 (Harik et al. 1997, Eiben & Smith 2003). This process is repeated for a minimum of 400 iterations, and terminated when the mean fitness of the population of strategies shows no improvement for a 100 consecutive iterations thenceforth (Eiben & Smith 2003).

2.7 Model development, execution and analysis

The model was developed, executed and analyzed using the R™ v.3.3.1 (R Core Team 2016) and RStudio™ integrated development environment (IDE) v.1.0.136 (RStudio Team 2016), along with the high-performance computing (HPC) packages Rcpp (Eddelbuettel et al. 2011) and bigmemory (Kane et al. 2013).

A basic run (*BR*) with default values for model parameters (Table 4) was performed for each model-species in the Environment-L. To test the influence environmental

variables on the predicted behavioral and life history strategies, we performed a sensitivity analysis following Jørgensen and Bendoricchio (2001), which produces a sensitivity scores (S_x) as,

$$S_x = \frac{(X_{BR} - X_M)/X_{BR}}{(P_{BR} - P_M)/P_{BR}} \quad \text{Eq. 20}$$

where X is the predicted model output of the basic run (X_{BR}) and the modified run (X_M) for a given change (± 25%) of input parameter value between the basic run (P_{BR}) and the modified run (P_M). Sensitivity analysis was performed separately for each model-species.

By performing model runs along the modelled latitudinal gradient at variable levels of visual predation risks we investigated how species-specific behavioral and life history strategies emerge under the influences of bottom-up (i.e. temperature and food availability) and top-down (predation risk) selection pressures (cf. Bandara et al. 2018). Although the modelled food concentration was constant across the model environments, the decreasing duration of the modelled productive season and temperatures ensued a decreasing gradient of growth potential from lower latitude Environment-L to higher latitude Environment-H (Fig. 1, Appendix A1). A gradient of visual predation risks was created by varying the scalar K in between 10^{-6}–10^{-2} (i.e. 10^{-6}, 10^{-5}, 10^{-4}, 5 x 10^{-4}, 10^{-3}, 2.5 x 10^{-3}, 5 x 10^{-3}, 7.5 x 10^{-3} and 10^{-2}). To enhance visualization, we transformed the visual predation risk scalar (K) to its fourth root (K').

As Genetic Algorithms produce heuristic estimates of the maximum fitness, there is no guarantee that it would converge on the global maximum given a potentially diverse fitness landscape (Zanakis & Evans 1981, Rardin & Uzsoy 2001, Strand et al. 2002, Record et al. 2010). Therefore, we replicated each model run 10 times with different starting values for the evolvable parameters (Table 2) to check if the algorithm converges on the same set of solutions. As the optimized parameter values showed little variability between replicate runs (< 7%), we used the mean of the replicates for each parameter for analyses.

3. Results and Discussion

3.1 Emergent strategies of the basic run

An annual life cycle was predicted for all modelled species in the basic run (*BR*). However, the model-predicted optimal behavioral and life history strategy of species-CF was distinctly different from the other model-species.

The predicted optimal birth times for species-CF occurred in mid-June, when the irradiance and the temperature of the model environment (Environment-L) were at its peak, and the food concentration had decreased by ca. 50% compared to its annual maximum (Fig. 6A). This seems counterintuitive, as the optimal birth time coincides the annual maximum of visual predation risk (Eqs. 9 and 10). However, in the model, species-CF possesses the smallest body size (Fig. 4), and hence is the least vulnerable to visual predation risk (Fig. 5A, F). In addition, due to the smaller size, species-CF become satiated at lower food concentrations (Fig. 5C, F) and is less likely to suffer from food-limitation (Fig. 6L). Therefore, it is likely that the smaller body size of species-CF allowed it to utilize higher summertime temperatures to grow and develop faster (Fig. 6P). The higher growth rates of late developmental stages (i.e. copepodite stage IV onwards) likely dampened by two trade-off strategies. First, to minimize the visual predation risk, relatively large developmental stages had to periodically abandon food-rich near-surface waters to perform DVM (down to 50–60 m, Fig. 6D, H). DVM leads to reduced growth and development rates (Houston et al. 1993, Bandara et al. 2018), as growth potential is traded off for survival (Lampert 1989, Hays 2003). Second, in order to survive the winter, CIV and CV stages had to allocate a fraction of surplus growth to build up energy reserves. The optimal energy allocation parameter (γ, Table 2) predicted for species-CF in the *BR* was 0.1, which translates to a 10% decrease in structural growth. Consequently, species-CF grazed toward the end of the productive season and descended to overwintering depths in late-July (Fig. 6A, E) with partly filled energy reserves (W_s/W_c = 0.54, where maximum = 0.70, Fig. 6I). The ascent from overwintering depths occurred in late-January of the following year, before the primary production had commenced, and while the other model-species were still in diapause (Fig. 6A, E–G). This doesn't agree with the well-established notion that the seasonal ascent of *C. finmarchicus* occurs after those of *C. glacialis* and *C. hyperboreus* (e.g. Madsen et al. 2001, Astthorsson & Gislason 2003, Søreide et al. 2008, Bandara et al. 2016). However, the predicted early ascent of species-CF appears to possess an advantage, as it used the post-overwintering surplus energy reserves for structural growth to reach sexual maturity by the time when the pelagic algal bloom had commenced (W_c of overwintering CV ≈ 258 µg C, W_c at sexual maturity ≈ 271 µg C, Fig. 6I). This somewhat resembles the pre-bloom seasonal ascent and spawning patterns observed for *C. finmarchicus* (Diel & Tande 1992, Melle & Skjoldal 1998, Richardson et al. 1999).

These predictions about species-CF in the *BR* points to a life strategy that attempts to elevate structural growth at the expense of energy reserves. This strategy is expected from a species which does not use energy reserves for egg production, such as *C. finmarchicus* (Tande et al. 1985, Niehoff et al. 2002, Madsen et al. 2008). However, it may also be that the optimized strategy for species-CF in the *BR* is an attempt to attain sexual maturity and reproduce within the same productive season. This resembles the life cycle of *C. finmarchicus* in lower latitudes, where it completes several generations per year (e.g. Fish 1936, Lie 1965, Matthews et al. 1978, Gislason & Astthorsson 1996, McLaren et al. 2001, Bagøien et al. 2012). As our model does not allow generation times < 1 year to be simulated, the ability to maintain multiple generations per year and its adaptive significance in the modelled environments remain unclear.

The model-predicted birth times for species-CG and -CH occurred ca. 1 month earlier than species-CF between late-April and May. Unlike species-CF, these two model-species did not employ early birth as a strategy to utilize the seasonal temperature peak to attain higher growth rates. This was likely caused by the increased vulnerability to visual predation risk and the higher satiation food concentrations associated with their relatively large body sizes (Figs. 3, 5A, E and F). Consequently, species-CG and -CH were characterized by slower growth rates, pronounced food limitation and 1.5–2 times longer development times compared to species-CF (Fig. 6L and P). Possibly due to occupying a time of the year with lower growth potential, their DVM did not increase much compared to species-CF (Fig. 6D and H), in line with observations made by numerous other empirical and modeling work (e.g. Hardy & Gunther 1935, Huntley & Brooks 1982, Andersen & Nival 1991, Fiksen & Giske 1995, Tarling et al. 2000, Bandara et al. 2018). However, irrespective of the lower growth rates, species-CG and -CH descended to overwintering depths with maximum possible energy reserves (W_s/W_c = 0.70, Fig. 6J, K). To attain such large reserve loads, older developmental stages (CIII, CIV and CV) allocated up to 40% of the surplus growth to reserve build-up, while grazing until the very end of the productive season (Fig. 6F, G).

It appears that species-CG and -CH are adopting a more conservative strategy that prepares themselves for an upcoming overwintering period, than pushing themselves toward attaining sexual maturity. We interpret this conservative life strategy as a classic adaptation to seasonality in the Arctic pelagic environments (Conover & Siferd 1993, Hagen & Auel 2001). The decision to store more and overwinter possesses a significant pay-off in the following year, where surplus reserves can be allocated to egg production. Species-CG and -CH ascended in mid-February, with the commencement of pelagic primary production (Fig. 6F, G). As the food-availability until mid-April (peak bloom) was relatively low, species-CG used the post-overwintering surplus energy reserves as a capital for egg production (Fig. 6B, C, J, K), which agrees well with the egg production strategy described for *C. glacialis* (Swift 1986, Melle & Skjoldal 1998, Niehoff et al. 2002,

Søreide et al. 2010). The profitability of the mixed income and capital breeding strategy of species-CG was such that its total fecundity was higher compared to the other model-species (Fig. 6M–O). The egg production of species-CH ceased ca. 10 d before the peak pelagic bloom, as the reserves were spent on producing nearly 1700 eggs (equivalent to capital input of ca. 950 µgC, Fig. 6K, O). This agrees with the capital breeding strategy described for *C. hyperboreus* (Dawson 1978, Matthews et al. 1978, Smith 1990, Hirche 1997, Scott et al. 2000, Niehoff et al. 2002, Hirche & Kosobokova 2003). After spawning, the species-CH females lived toward the end of the productive season, without serving any adaptive benefit (Fig. 6G, K, O). This hints at a possibility that if not constrained by our model, these females could have acquired energy reserves and probably spawned again in the following year. Such iteroparous breeding has been commonly reported for *C. hyperboreus* (Hirche & Kwasniewski 1997, Arnkværn et al. 2005, Hirche 2013).

3.2 Sensitivity of emergent strategies to environmental variability

3.2.1 Food concentration

At a 25% higher food concentration (F = 225 µg C l^{-1} ≈ 7.5 mg Chl.-a m^{-3}), the predicted optimal birth time of species-CF occurred ca. 2 days later compared to *BR* on June 18 (Fig. 7A, Table 6). It seems that species-CF used the higher food concentrations and temperatures later in the year to speed-up structural growth, but allocated less for energy reserves and entered diapause with 3% less energy reserves compared to *BR* (W_s/W_c = 0.52). The timing of seasonal descent did not change much from the *BR*, mainly because of late birth time, slightly elevated DVM (which tend to reduce growth potential) and ca. 2% larger size of the overwintering CVs (Table 6). However, higher food concentration influenced the income breeding egg production of species-CF, which was elevated by ca. 15% compared to the *BR*.

The influence of elevated food concentration on the species-CG and -CH was notably different from that of species-CF. The predicted birth times of species-CG and -CH occurred ca. 2 days earlier (Fig. 7B, C, Table 6), and the growth allocation parameter was ca. 11% higher at 25% higher food concentration compared to the *BR*. Thus, it seems that these two model-species used the higher growth potential resulted from elevated food concentration to develop energy reserves rather than structural growth. This was achieved by two means: firstly, through rapid accumulation of reserves, shown by the 2–4 days earlier timing of seasonal descent, and secondly, by elevating the size of the overwintering CVs by ca. 2% compared to the *BR* (Table 6), which allows a little extra space for energy storage at the maximum W_s/W_c ratio of 0.7 (cf. Fig. 5C). Consequently, the number of capital breeding eggs increased for both model-species, atop of which,

species-CG produced more income breeding eggs, using the higher food concentrations (Fig. 7B, and Table 6).

These findings point to how a small improvement in growth potential was differentially utilized by the three model-species. This was largely driven by their breeding modes. Since there is no added advantage of carrying extra energy reserves for the purely income breeding species-CF, it directed the higher growth potential towards accelerating structural growth, which likely reflect a short-term motivation toward attaining sexual maturity within the same calendar year (Jönsson 1997, Sainmont et al. 2014, Barta 2016). However, since the duration of the productive season remained the same as *BR*, SVM and diapause yet appeared to be inevitable for this species (Fig. 1A–C). On the other hand, the capital breeding strategy of species-CG and -CH made them use the elevated growth potential as a long-term investment (Varpe et al. 2009, Ejsmond et al. 2015) that increased fecundity in the following year (Table 6).

At a 25% lower food concentration (F = 135 µg C l^{-1} = 4.5 mg Chl.-a m^{-3}), the differences between the two emergent strategies of the *BR* appeared to diminish. Here, the predicted optimal birth times of all species occurred ca. 12–15 d earlier in the year (Fig. 7A–C, Table 6). Due to lowered growth potential, they occupied more time in food-rich near-surface waters with reduced DVM, and grazed later into the productive season before descending to diapause in late-August. Further, ca. 40% of the surplus growth was allocated to building up of energy reserves. Irrespective of the breeding mode, fecundity of all model-species decreased by 5–11% (Table 6). The attempt to elevate energy reserves by the purely income breeding species-CF indicates a shift towards a more conservative strategy. Storing additional reserves compared to *BR* reflects the difference in the structural masses of the overwintering CV and the adult, which was spanned by allocating the reserves to structural growth in the following year. This plasticity of life strategy of species-CF reflects that of *C. finmarchicus* in Arctic locations, which can maintain viable populations in cold and food-limited environments (e.g. Hirche & Kwasniewski 1997, Madsen et al. 2001, Arnkværn et al. 2005, Hirche & Kosobokova 2007, Bandara et al. 2016).

3.2.2 Temperature

Temperature had the highest influence on the strategies emerging from the *BR* (Fig. 7D–F). A 25% temperature increase throughout the water column (i.e. T_{max} = 18.75 °C, T_{min} = 2.5 °C) caused the birth times of all model-species to delay by 2–35 days (Table 6). This delay became more pronounced in species-CG and -CH, which reflects their motivation to utilize the higher growth potential by allowing their younger developmental stages to thrive in warmer, food-rich waters of the late-spring and

summer. Here, the elevated visual predation risk was countered by performing pronounced DVM (Table 6). In all model-species, the predicted development times and sizes of the overwintering stages and females decreased (Table 6). Instead of prioritizing structural growth, all model-species allocated more of the surplus growth to building up of energy reserves and entered diapause with nearly full lipid reserves (W_s/W_c > 0.69). This seems to be a driven by the elevated temperature at overwintering depths, which tends to exhaust energy reserves faster than those used in the *BR* (2.5 °C vs 2.0 °C, cf. Eq. 15). Consequently, the number of capital breeding eggs decreased in species-CG and -CH. However, due to the elevated assimilation efficiency at higher temperatures (Eq. 3), income breeding appeared more profitable for species-CF and -CG, which is shown by 15%–20% increase of fecundity (Table 6). This suggests that in a warmer ocean, *C. finmarchicus* would use the elevated fecundity as an advantage to increase their populations in the high-Arctic (see also, Beaugrand et al. 2002, Chust et al. 2014). Under similar circumstances, the purely income breeding strategy of *C. hyperboreus* could become disadvantageous, as energy requirements at diapause elevates, and leaves less reserves for egg production (Hirche 1991, 1997, Maps et al. 2013). However, the flexible breeding strategy of *C. glacialis* will enable it to cope with either warming or cooling scenarios, as loss of fecundity through decreased capital breeding would be compensated from income breeding and vice versa (Falk-Petersen et al. 2007, Daase et al. 2013, Grote et al. 2015).

At lower temperatures (i.e. T_{max} = 11.25 °C, T_{min} = 1.5 °C), all species were born 2–27 days earlier in the year and occupied more time in near-surface waters with reduced DVM (Fig. 7, Table 6). This reflects the longer time it takes to develop to diapause stage due to lower growth potential attained in colder waters (Eqs. 1–3). Further, grazing continued toward the very end of the productive season (late August in most cases), and the overwintering CVs of all model-species were ca. 2–4% larger than predicted in the *BR* (Table 6). At the time of seasonal descent, CVs of species-CF had partly filled energy reserves (W_s/W_c ≈ 0.51). This reflects the decreased diapause metabolic costs at lower temperatures (1.5 °C vs 2.0 °C, cf. Eq. 15). In contrast, species-CG and -CH entered diapause with full energy reserves (W_s/W_c ≈ 0.70), and used the post-overwintering surplus reserves to elevate capital breeding (Table 6). However, only the purely income breeding species-CH had a ca. 10% fecundity gain, while species-CF and -CG suffered a 12%–15% loss of income breeding potential (and hence the total fecundity, Table 6), due to decreased assimilation efficiency rendered at lower temperatures (Eq. 3).

683 3.2.3 Predation risk

684 Compared to food concentration and temperature, a 25% change in non-visual and
685 visual predation risks had a negligible influence on the emergent behavioral and life
686 history strategies of the *BR* (Fig. 7G–L). low sensitivity to non-visual predation risk has
687 also been observed by (Bandara et al. 2018). The low sensitivity to visual predation risk
688 may be due to that it operates on a larger range than manifested in the sensitivity
689 analysis (see below).

690

691 3.3 Emergent strategies under bottom-up and top-down selection pressures

692 3.3.1 Emergent strategies at low visual predation risk

693 At the lowest level of visual predation risk ($K' = 0.032$), the species-specific behavioral
694 and life history strategies emerging from the model appear to be heavily influenced by
695 the patterns of food availability and temperature. Here, in each model environment, the
696 predicted optimal birth times of all model-species occurred the earliest (Fig. 8C1–C9).
697 The DVM was less pronounced (Fig. 9A1–A9), and hence they suffered least from food-
698 limitation (Fig. 9B1–B9). All model-species developed relatively slowly due to lower
699 temperatures that occurred earlier in the season (Fig. 1B, E and H), and developed to CV
700 stage with the highest structural and energy reserve masses possible (Fig. 8B1–B9).
701 These large CVs descended to overwintering depths earlier in the year (Fig. 8A1–A8) for
702 diapause. This was followed by an earlier seasonal ascent and reproduction (Fig. 8C1–
703 C8). At the onset of reproduction, females were older compared to higher predation risk
704 levels (Fig. 8D1–D8) and their body masses were the highest (Fig. 8E1–E8). The larger
705 females of species-CF and -CG could assimilate more efficiently (Eqs. 1 and 2), and
706 produced the highest number of eggs (Fig. 8F1–F6). The extensive energy reserves of
707 larger overwintering CVs of species-CG and -CH were used for higher capital breeding
708 output (Fig. 8F4–F8).

709 Al the lowest level of visual predation risk, environment and species-specific patterns
710 were also apparent. In species-CF, the birth times shifted ca. 45 days later into the year
711 from mid-April to early-June along the modelled latitudinal gradient (Fig. 8C1–C3). These
712 match the exact times at which the peak pelagic bloom occurred in these model
713 environments (Fig. 1C, F and I). Because of the decreasing gradient of growth potential
714 encountered along the modelled latitudinal gradient and the ca. 20% increase of the size
715 of the overwintering CVs (Fig. 8B1–B3), the timing of seasonal descent shifted by ca. 78
716 days from late-June to early-September (Fig. 8A1–A3). The timing of seasonal ascent and
717 onset of reproduction also followed an increasing trend along the modelled latitudinal
718 gradient, and aligned with the time of the onset of pelagic algal bloom (Figs. 1C, F and I,
719 and 8C1–C3). Because of delayed birth times and elevated development times

720 associated with lower temperatures, the age of sexual maturity increased along the
721 modelled latitudinal gradient (Fig. 8D1–D3). Further, the size at sexual maturity also
722 increased by ca. 20% (Fig. 8E1–E3). However, the increased size of female could not
723 compensate for the decreased assimilation rates induced by lower temperature at
724 higher latitude model environments, as the fecundity decreased by ca. 30% (Fig. 8F1–
725 F3). These findings suggest that species-CF timed its reproduction to match the timing
726 of the pelagic algal bloom along the modeled latitudes. This has been a common
727 observation for *C. finmarchicus*, and reflects the strong dependency of its reproduction
728 on the food availability (Tande & Hopkins 1981, Aksnes & Magnesen 1983, Hirche &
729 Kosobokova 2003, Madsen et al. 2008).

730 Unlike species-CF, the birth times of species-CG and -CH did not change much along
731 the modelled latitudinal gradient (Fig. 8C4–C9). At the lower latitude Environment-L,
732 predicted birth times of species-CG and -CH roughly aligned with the timing of the peak
733 pelagic algal bloom (Figs. 1C, 8C4 and C7). At higher latitude environments, their birth
734 times were predicted ca. 7–25 days ahead of the peak algal bloom (Figs. 1F, I, 8C5, C6,
735 C8 and C9). These temporal offsets roughly align with the cumulative development times
736 estimated from eggs to first feeding NIII stage estimated from Bělehrádek temperature
737 functions (Eq. 6, Table 5), and thus reflect the classical descriptions of capital breeding
738 strategies of Arctic *Calanus* species (reviewed in, Falk-Petersen et al. 2009, Søreide et al.
739 2010, Daase et al. 2013), where egg production is timed so that first feeding stages can
740 feed under non-limiting food concentrations.

741 In species-CG, the size of the overwintering CVs increased by ca. 25% along the
742 modelled latitudinal gradient (Fig. 8B4–B6). Given the lower temperatures modelled at
743 higher latitude environments (Fig. 1B, E and H) these larger CVs had to graze toward the
744 end of the productive season to gain energy reserves required for overwintering (Fig.
745 8A4–A6). The timing of seasonal ascent and reproduction of species-CG showed a delay
746 of ca. 60 days along the modelled latitudinal gradient (Fig. 8A4–A6 and C4–C6), and
747 reflects the coupling of its reproduction with the timing of the pelagic bloom (Fig. 1C, F
748 and I) despite being a partly a capital breeder (Fig. 8G4–G6). Although capital breeding
749 of species-CG accounted for an increasing fraction of the total egg production along the
750 modelled latitudinal gradient (7%–11%), the total fecundity decreased by ca. 21% due
751 to the reduced income breeding potential ensued by lower growth potential sustained
752 in higher latitude model environments (Fig. 8F4–F6).

753 The variability in the timing of SVM and reproduction was least apparent for species-
754 CH. Its timing of seasonal descent showed the least variability along the modelled
755 latitudinal gradient (i.e. ca. 30 days from late-August to late-September, Fig. 8A7–A9),
756 while the timing of seasonal ascent and the onset of reproduction did not change (Fig.
757 8C7–C9). This reflects the decoupling of species-CH's reproduction from the timing of

pelagic bloom, which was driven by the purely capital breeding strategy. The early-January seasonal ascent and the onset of reproduction predicted by our model for the highest latitude model environment may be doubtful since it occurs in the midst of the Arctic polar night with the pelagic algal bloom ca. 5–6 months away (Fig. 1G, I). However, this aligns with recent field observations on the timing of seasonal ascent and reproduction in several high-Arctic fjords in the Svalbard archipelago between 78°–80° N (Daase et al. 2014, Błachowiak-Samołyk et al. 2015, Bandara et al. 2016). Given the strict herbivory of the modelled copepods, the viability of these early eggs remains questionable, as NIII emerges within ca. 15 days (at -1.5 °C) after being spawned, which precedes the pelagic bloom by several months. However, in nature, these early born copepods may survive, as they can feed on alternative food, such as microzooplankton and ice algae (Runge & Ingram 1991, Søreide et al. 2008, Campbell et al. 2016).

Although we assumed $K´$ = 0.032 as a reference value for extremely low visual predation risk, it had a notable influence on species-CH at the Environment-H. Here, unlike other model-species, the species-CH did not follow the maximum potential stage-specific body mass trajectory (W_j^{max}, Fig. 4G–I). Consequently, the size of the overwintering CV and the size at sexual maturity predicted for species-CH was ca. 11% smaller compared to that predicted for Environment-M (Fig. 8B8, B9, E8 and E9). As the size of the energy reserve was modelled as a fixed (yet, evolvable) fraction of the structural mass, the decreased structural mass translated to a ca. 15% decrease of fecundity (Fig. 8F8 and F9). This finding points to the fact that the adaptive advantage of a larger body size at higher latitudes can be highly sensitive to top-down environmental selection pressures (see below).

3.3.2 Emergent strategies at elevated visual predation risk

As the visual predation risk increased from its baseline level of $K´$ = 0.032 toward 0.32, the bottom-up influences described above diminished, and all model-species reacted to visual predation risk in more or less the same manner. Altogether, two behavioral and life history strategies were manifested to counter the elevated visual predation risk.

3.3.1.1 Plasticity of behavior: diel vertical migration

DVM was used to counter relatively modest levels of visual predation risk, i.e. $0.032 \leq K´ \leq 0.15$. Here, feeding stages (NII and onwards) of all model-species reduced the time spent in warmer, food-rich near-surface waters by descending to depths typically exceeding 100 m (Fig. 9A1–A9 and B1–B9). As reduced surface time decreases feeding opportunities, diel migrants suffered from increased food limitation (Fig. 9C1–C9), which led to reduced growth rates that ultimately elevated development times (Fig. 9D1–D9).

To compensate for the DVM-induced loss of growth potential, birth times of all model-species were shifted later into the year (Fig. 8C1–C6), possibly to utilize the higher temperatures that occur later in the season (Fig. 1B, E and H) and attain higher growth. Consequently, they had to feed later into the productive season to fulfil the energy requirements needed to survive the forthcoming unproductive winter, and descended to overwintering depths in late-autumn (Fig. 8A1–A9). This late-birth strategy was such successful that, despite the elevated DVM, fecundity of all model species remained largely unchanged (Fig. 8F1–F9). An exception to the above-mentioned phenological shifts was observed for species-CH at the Environment-H. Here, timing of birth, SVM, reproduction did not change for the initial increase of visual predation risk despite its larger body size (Fig. 8A9, B9 and C9). At Environment-H, younger developmental stages (up to NVI) of species-CH did not perform notable DVM (Fig. 9A9, B). This was caused by the early seasonal ascent and reproduction of this species, which allowed its younger developmental stages to elevate foraging efforts in near-surface waters in a period with minimal irradiance, that reduces the risks imposed by visually orientating planktivores (Fig. 1G).

Although DVM is the most immediate response against elevated visual predation (reviewed in, Lampert 1989, Hays 2003, Brierley 2014), the associated phenological shifts were brought into prominence in the recent work of Bandara et al. (2018). Findings of the above study and those of this investigation agrees well, but do not align with the belief that increased visual predation risk drives earlier seasonal descents in *Calanus* spp.(Kaartvedt 2000, Varpe & Fiksen 2010).

3.3.1.2 Plasticity of body size

As the visual predation risk increased further ($0.15 \leq K' \leq 0.22$), the trading-off of growth potential for survival became unprofitable. This was caused by the inability to further delay the birth times (Fig. 8C1–C9) in response to elevated DVM, as the growth and development of later developmental stages became constrained by the duration of the productive season. At this point, model-species began to adjust the size (i.e. structural and energy reserve masses, W_c and W_s) of overwintering stages. Here, instead of overwintering as larger CV stages with full energy reserves, all species entered diapause as CIV and CIII stages with 50%–90% lesser structural and energy reserve masses. This strategy did not notably reduce the DVM nor the food limitation effects ensued (Fig. 9), but allowed the model-species to reduce visual predator-induced mortality risk during the ca. 200–350 days long diapause, as in this model, visual predation risk was not nullified even at greater depths (Eqs. 9 and 10). Similar predictions have been made previous models (e.g. Fiksen & Carlotti 1998, Varpe et al. 2007, Bandara et al. 2018). The timing of reproduction of all species were significantly

delayed by this strategy, as the smaller overwintering stages must use the post-overwintering residual energy reserves or gains from food intake to elevate their structural mass to attain sexual maturity. This reduced the capital breeding potential of species-CG and -CH. Further, at $K' \geq 0.18$, species-CG could not produce any capital breeding eggs, and switched its reproductive strategy to pure income breeding (Fig. 8G4–G6).

Further increase of visual predation risk, i.e. $0.22 < K' \leq 0.32$ was dealt with the reduction of body masses at each developmental stage. In the model, this was achieved by evolving smaller values for the body size parameter α (Table 2). Modelled copepods with smaller body masses could reduce the vulnerability of younger developmental stages to visual predation, and hence the DVM was restored back to the levels observed at lowest level of visual predation risk (Fig. 9A1–A9, and B1–B9). As the copepods could occupy more time on the food-rich near-surface waters, the food limitation of younger developmental stages also decreased (Fig. 9C1–C9). However, birth times did not shift back in time to occur earlier in the year, probably reflecting the need for the smaller size copepods to occupy warmer waters to elevate their assimilation efficiency (Eqs. 1–3). Consequently, adult females attained sexual maturity at smaller body sizes, and the expected fecundity decreased dramatically by 20%–60% among income breeding species-CF and -CG (Fig. 8F1–F6). As the capacity to carry energy reserves decreases with body size (Fig. 5C), the capital breeding capacity of species-CH was severely hampered, and its fecundity decreased by ca. 40% at the lower latitude Environment-L, and ca. 96% at the higher latitude Environment-H (Fig. 8F7–F9).

3.4 Concluding remarks

The artificial evolution of body sizes observed in this study resembles the classic field observations of rapid evolution of zooplankton body sizes in response to size-selective predation by planktivorous fish in smaller freshwater lakes (e.g. Brooks & Dodson 1965, Wells 1970, Zaret & Kerfoot 1975). Although such observations are rare in the Arctic marine realm, recent hypotheses suggest that the evolution of differential body size pattern among *Calanus* spp. is largely due to extensive size-selective predation induced by mega planktivores (Berge et al. 2012, Falk-Petersen et al. 2015). A key difference between the above studies and our model is that body size plasticity evolves as the 'last resort', when the increasing visual predation risk could not be countered with behavioral strategies. However, if visual predation risk elevates beyond the limits of behavioral toleration, it can have dramatic consequences on zooplankton life strategies which can easily outweigh those induced in the bottom-up (Figs. 8 and 9).

Further, elevated visual predation risk obscured the apparent south to north trends in ontogenetic body size patterns observed under the minimum visual predation risk (Fig. 8E1–E9, cf. Fig. 4), leading to increased overlap of body size ranges (especially between species-CF and -CG) irrespective of the modelled latitude. Therefore, top-down selection pressures, such as the presence of resident or seasonally migrating populations of planktivorous fish (e.g. Varpe et al. 2005, Renaud et al. 2012) should be considered as an important factor when assessing the potential for misidentifying coexisting *C. finmarchicus* and *C. glacialis* populations using morphometric methods (e.g. Parent et al. 2011, Gabrielsen et al. 2012).

At all scenarios tested, the annual life cycle was the only generation time emerged in this model. Upon further testing we found that > 1 year generation times do emerge when the duration of pelagic productive season is cut down by ca. 40% under lower levels of visual predation risk modelled here ($K < 5x10^{-3}$). Therefore, it is likely that the influences of bottom-up selection pressures become more apparent in higher-latitude seasonal environments where resource limitation and year to year stochastic environmental variability is more pronounced (Roff 1980, Fiksen 2000, Ji 2011).

Bottom-up and top-down environmental variability acts as selection pressures that operates interactively to drive seasonal adaptations of high-latitude pelagic inhabitants (Varpe 2017). There is often a discrepancy in views about which selective force holds the primacy (Hunter & Price 1992, Power 1992, Baum & Worm 2009). Using a model that allows partitioning the two selection pressures and artificial evolution of seasonal strategies, we argue that top-down selective forces are more significant in shaping up of behavioral and life history strategies of Arctic *Calanus* species. However, the influences of alternative food sources, sea-ice, and spatio-temporal heterogeneity of the environment should be considered toward drawing stronger conclusions.

Acknowledgements

This project was funded by VISTA (project no. 6165), a basic research program in collaboration between The Norwegian Academy of Science and Letters and Statoil. ØV received funding from the Fulbright Arctic Initiative and thanks the Woods Hole Oceanographic Institution for hosting during the Fulbright exchange.

900 **Table 1** The inter-and intra-specific diversity of some life history traits/attributes of
901 *Calanus* spp. Body mass estimates are from prosome length (PL) to dry mass (DM)
902 relationships published by Robertson (1968). Cited literature only serve as examples.
903 See Falk-Petersen et al. (2009), and Bandara (2014) for an extensive review on some of
904 these life history traits.

Trait/attribute	*C. finmarchicus*	*C. glacialis*	*C. hyperboreus*
Center of distribution	North Atlantic[5,11]	Arctic (shelf) [5,11]	Arctic (oceanic) [11]
Body size			
Length (mm PL)	2.2[4]–3.2[14,30,17]	3.2[14,17,25]–4.6[17,28]	3.9[17]–6.7[28]
Mass (µg DM)	204–557[3]	533–1742[3]	1016–5947[3]
Timing of reproduction	In synchrony with pelagic bloom[8,16,31]	Before or in synchrony with pelagic bloom[12,22,26,32]	Before the pelagic bloom[6,7,12,26]
Reproductive strategy	Income breeding[18]	Income or capital breeding[32]	Capital breeding[2,19]
Most common overwintering stages	CIV[8,31,33] CV[15,22,28]	CIV[23,17,29] CV[13,21,24]	CIII[13,27] CIV[6,7,29] CV[20,25,28] Females[13,21,29]
Most common generation times (years)	1[9,21,29]	1–2[10,23,24,29]	1–3[1,13,20,23,25]

[1] Conover (1965), [2] Conover (1967), [3] Robertson (1968), [4] Jaschnov (1972), [5] Fleminger and Hulsemann (1977), [6] Dawson (1978), [7] Matthews et al. (1978), [8] Tande and Hopkins (1981), [9] Aksnes and Magnesen (1983), [10] Tande et al. (1985), [11] Conover (1988), [12] Smith (1990), [13] Hirche (1991), [14] Unstad and Tande (1991), [15] Diel and Tande (1992), [16] Plourde and Runge (1993), [17] Hirche et al. (1994), [18] Hirche (1996b), [19] Hirche and Niehoff (1996), [20] Hirche (1997), [21] Hirche and Kwasniewski (1997), [22] Melle and Skjoldal (1998), [23] Falk-Petersen et al. (1999), [24] Scott et al. (2000), [25] Madsen et al. (2001), [26] Niehoff et al. (2002), [27] Astthorsson and Gislason (2003), [28] Hirche and Kosobokova (2003), [29] Arnkværn et al. (2005), [30] Daase and Eiane (2007), [31] Madsen et al. (2008), [32] Søreide et al. (2010), [33] Hirche and Kosobokova (2011)

905

Table 2 List of evolvable (soft) parameters optimized by the Genetic Algorithm. The parameters β, γ, δ and ε are proxies that define the behavioral strategy (vertical strategy), while the rest are proxies that define some key aspects of the life history strategy. These proxies (parameters 1–6) of behavioral and life history strategies are hardwired to copepods spawned in different times of the year (t_B).

Term	Definition	Range	Interval	Unit
α	Body size parameter	0–1	0.01	dim. less
β	Irradiance threshold parameter	10^{-7}–1	*	µmol m^{-2} s^{-1}
γ	Energy allocation parameter	0–1	0.01	dim. less
δ	Seasonal descent parameter	0–1	0.01	dim. less
ε	Seasonal ascent parameter	0–1	0.01	dim. less
η	Generation time parameter	1–3	1	years
t_B	Birth time	1–8760	1	h

*Intervals = 10^{-7}, 10^{-6}, 10^{-5}, 10^{-4}, 10^{-3}, 10^{-2}, 10^{-1}, 1

912 **Table 3** Description of the emergent behavioral and life history strategies of the model.
913 Note that unlike Bandara et al. (2018), the amplitude of the SVM (overwintering depth)
914 is not an emergent property of this model.

Trait/attribute	Units	Description
Time of birth	Day of the year	Time of being spawned
Surface time	h	Unified estimate representing the timing of DVM, i.e. the stage-specific mean no. of hours per day occupied in waters with highest growth potential (usually the surface waters)
Amplitude of diel vertical migration	m	The vertical range corresponding to the above
Time of seasonal descent and ascent	Day of the year	Separate estimates representing the timing of SVM (ascent and descent)
Size at seasonal descent	µg C	Structural and energetic reserve mass at the onset of diapause
Age of sexual maturity	d	Time since birth to the first egg production
Size at sexual maturity	µgC	Structural mass at first egg production
Onset of spawning	Day of the year	Time of first egg production
Fecundity	No. of eggs	No. of eggs produced during the lifetime
Breeding mode index	dim.less	Proportion of capital breeding eggs (0 = pure income breeding, 1 = pure capital breeding)
Food limitation index	dim.less	Stage-specific total no. hours with food-limited growth (Eq. 3) as a fraction of stage duration (0 = no food limitation, 1 = total food limitation)
Development time	d	From egg to a given stage
Longevity	d	Duration of the life cycle, from birth to death

915

916 **Table 4** Definitions, values and units of the non-evolvable (hard) parameters used in the
917 model. See Table 2 for a description of evolvable parameters

Term	Definition	Value/Reference	Units
a	Assimilation coefficient	0.6[3]	–
$A_{i,s,t,z}$	Ingestion rate	Eqs. 2–4	µg C ind.$^{-1}$ h^{-1}
b_s	mass coefficient of ingestion	Eq. 2, Table 5	–
$B_{i,s,t,z}$	Metabolic rate	Eqs. 14–15	µg C ind.$^{-1}$ h^{-1}
$(B_a)_{i,s,t,z}$	Active metabolic rate	$1.5 \cdot B_b$	µg C ind.$^{-1}$ h^{-1}
$(B_b)_{i,s,t,z}$	Basal metabolic rate	Eqs. 6–7	µg C ind.$^{-1}$ h^{-1}
c_s	Temperature coefficient of ingestion	Eq. 3, Table 5	–
$d_{i,t}$	Parameter for satiation food concentration	0.1–0.3	–
$D_{s,t,z}$	Development time	Eq. 6	h
$F_{t,z}$	Ambient food concentration	Fig. 1	µg C l^{-1}
f_s	mass coefficient of metabolism	Table 5	–
$G_{i,s,t,z}$	Growth rate	Eq. 1	µg C ind.$^{-1}$ h^{-1}
g_s	temperature coefficient of metabolism	Table 5	–
$H_{i,t,z}$	Survivorship	Eq. 19	–
i	Individual	–	–
$I_{t,0}$	Irradiance incident on sea surface	Fig. 1	µmol m^{-2} s^{-1}
$I_{t,z}$	Irradiance at depth z	Eq. 9	µmol m^{-2} s^{-1}
$I'_{t,z}$	Remapped $I_{t,z}$	0.1–0.9	–
j	Developmental stage	0–12	Egg–Adult
$K_{i,t}$	Scalar for visual predation risk	10^{-6}–10^{-2}	–
$L_{i,t}$	Irradiance sensitivity parameter	1–2.5	–
m_s	Mass exponent of ingestion	Eq. 2, Table 5	–
$(M_n)_{i,t,z}$	Non-visual predation risk	$0.1 \cdot K$	–
$(M_s)_{i,t}$	Starvation risk	Eq. 16	–
$(M_v)_{i,t,z}$	Visual predation risk	Eq. 10	–
n_s	Temperature exponent of ingestion	Eq. 3, Table 5	–
N	No. of initial seeds	2.5 x 10^6	strategies
o_s	mass exponent of metabolism	Table 5	–
p_s	temperature exponent of metabolism	Table 5	–
q_s	Development time parameter-1	Table 5[1, 4]	–
r_s	Development time parameter-2	Table 5[1, 4]	–
$R_{i,s,t,z}$	Fecundity	Eq. 17	No. of eggs
s	Species	CF, CG, CH	–
$T_{t,z}$	Ambient temperature	Fig. 1	°C
t	Time	1–8760	h
t_R	Time of sexual maturity	1–8760	hour
t_X	Time horizon	1–8760	hour
$U_{i,t}$	Cruising velocity	Eq. 11	m h^{-1}
W_c	Structural body mass	–	µg C

continued…

continued…

$(W_E)_s$	Species-specific unit egg mass	Table 5	µg C
W_j	Stage-specific critical molting mass	Fig. 3	µg C
$(W_j^{max})_{i,s}$	Stage-specific minimum W_j	Fig. 3	µg C
$(W_j^{min})_{i,s}$	Stage-specific minimum W_j	Fig. 3	µg C
$(W_R)_{i,s,t,z}$	Matter allocated for egg production	Eq. 17	µg C
W_s	Mass of the energy reserve	–	µg C
$(W_x)_{i,s}$	Catabolized structural mass (proportion of the maximum lifetime structural mass)	0.1–0.5	–
z	Depth	1–1000	m
φ	Termination condition of GA	Section 2.6.3	–
ψ	Water column light attenuation coefficient	0.06[2]	m^{-1}
$\Omega_{i,s}$	Fitness	Eq. 18	–
ω	Weight for fitness	0 or 1[5]	–

[1] Campbell et al. (2001), [2] Eiane and Parisi (2001), [3] Maps et al. (2011), [4] Ji et al. (2012), [5] Bandara et al. (2018)

Table 5 Species-specific values parameter values for coefficients and exponents of ingestion and respiration (estimated from Maps et al. 2011, Appendix A2), along with species-specific egg masses and development time parameters. See Table 4 for term definitions.

Parameter	Species-CF	Species-CG	Species-CH
b_s	0.009283	0.01656	0.01319
m_s	0.7524	0.7518	0.7516
c_s	1.2382	1.1606	1.1833
n_s	0.0966	0.0673	0.0761
f_s	0.0008487	0.003292	0.001153
o_s	0.75	0.75	0.75
g_s	1.2956	1.1382	1.2065
p_s	0.1170	0.0585	0.0849
$(W_E)_s$	0.23 µg C[2]	0.40 µg C[3]	0.56 µg C[4]
q_s (eggs)	595[5]	839[6]	1495[6]
q_s (NI)	388[5]	548[6]	974[6]
q_s (NIII)	581[5]	819[6]	1461[6]
r_s (eggs, NI, and NII)	9.11[1]	13.04[1]	13.66[1]

[1] Corkett et al. (1986), [2] Hirche and Bohrer (1987), [3] Hirche (1990), [4] Smith (1990), [5] Campbell et al. (2001), [6] Ji et al. (2012)

Table 6 Influence of ±25% changes in food concentration (*F*) and temperature (*T*) changes on the behavioral and life history strategies emergent from the basic run (*BR*) for the three model-species. Variations of food concentration ranges between *F* –: 135 µg C l^{-1}, *F* +: 225 µg C l^{-1}, and temperature between *T*–: 11.25 °C max and 1.5 °C min, and *T*+: 18.75 °C max and 2.5 °C min. Influences of predation risk are not tabulated due to their lesser significance (cf. Fig. 7).

Species	Scenario tested	Absolute Fitness	Surface time (h)[1]	DVM amplitude (m)[1]	Food-limitation (dim. less)[1]	Development Time (d)[2]	Time of seasonal descent	Time of seasonal ascent	Size at seasonal descent (µg C)	Size at sexual maturity (µg C)	Age at sexual maturity (d)	Onset of spawning (d)	Birth time	Fecundity	Breeding mode index (dim. less)
	BR	12227.31	19.63	16.12	0.96	44.13	Jul.30	Jan.24	258.31	271.65	244	Feb.16	Jun.16	12628	0.00
	F +	12870.88	19.40	16.36	0.97	40.19	Jul.28	Jan.29	274.12	276.94	242	Feb.15	Jun.18	13111	0.00
CF	*F* –	11253.92	19.77	16.02	0.94	63.16	Aug.03	Jan.14	249.21	264.43	261	Feb.15	Jun.01	11621	0.00
	T +	14739.06	19.58	16.09	0.97	32.60	Jul.20	Jan.31	260.55	262.21	242	Feb.15	Jun.18	15239	0.00
	T –	10337.61	19.56	16.22	0.95	69.75	Aug.13	Jan.14	272.41	283.22	254	Feb.14	Jun.04	10686	0.00
	BR	12100.56	18.53	21.87	0.95	76.21	Aug.10	Feb.16	554.38	554.38	266	Feb.16	May.26	13031	0.07
	F +	12941.16	18.46	21.89	0.97	80.17	Aug.12	Feb.15	563.85	563.85	267	Feb.15	May.24	13947	0.07
CG	*F* –	10838.82	18.82	21.23	0.94	85.08	Aug.05	Feb.16	537.29	537.29	278	Feb.16	May.12	11649	0.06
	T +	13732.62	18.01	22.47	0.96	59.83	Aug.09	Feb.14	530.66	530.66	248	Feb.14	Jun.11	14727	0.05
	T –	10797.90	18.67	21.64	0.95	100.91	Aug.07	Feb.14	579.93	579.93	291	Feb.14	Apr.29	11683	0.08
	BR	1450.29	18.05	29.51	0.93	135.46	Aug.28	Feb.16	1918.04	1918.04	308	Feb.16	Apr.15	1690	1.00
	F +	1479.60	17.80	30.13	0.95	133.01	Aug.24	Feb.16	1957.79	1957.79	309	Feb.16	Apr.13	1721	1.00
CH	*F* –	1376.78	18.19	28.69	0.93	141.62	Aug.21	Feb.16	1860.71	1860.71	319	Feb.16	Apr.02	1609	1.00
	T +	1366.20	17.77	30.12	0.94	96.25	Aug.25	Feb.17	1852.35	1852.35	272	Feb.17	May.21	1583	1.00
	T –	1516.58	18.21	28.92	0.93	152.38	Aug.23	Feb.14	1994.31	1994.31	328	Feb.14	Mar.24	1781	1.00

[1]Mean for all developmental stages, [2]From egg to adult excluding the overwintering duration

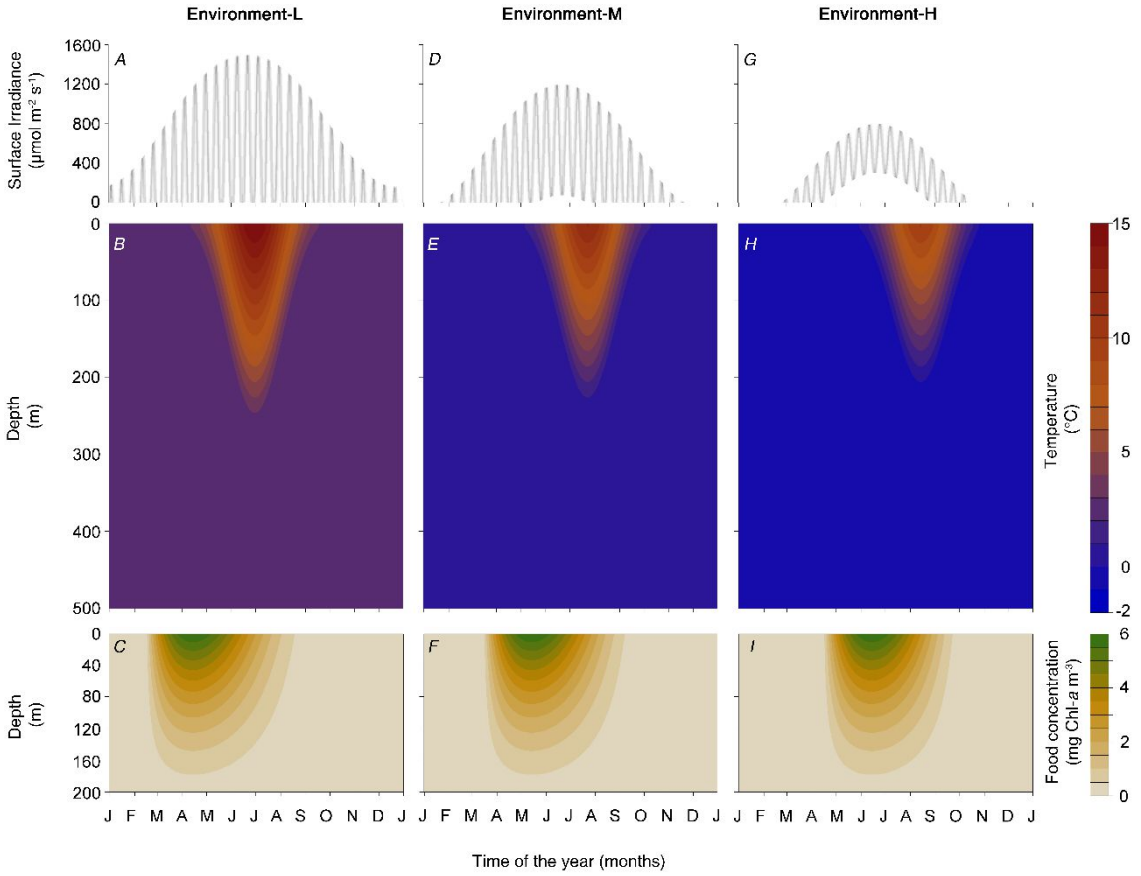

931

932 **Fig.1** Dynamics of modeled sea-surface irradiance (A, D, G), temperature (B, E, H) and
933 food availability (C, F, I, as Chlorophyll-*a* biomass) in the three model environments. The
934 bottom depth is 1000 m, but the ordinates of lower panels are cropped due to the
935 vertical homogeneity of those parameters. See Appendix A1 for a detailed comparison.

936

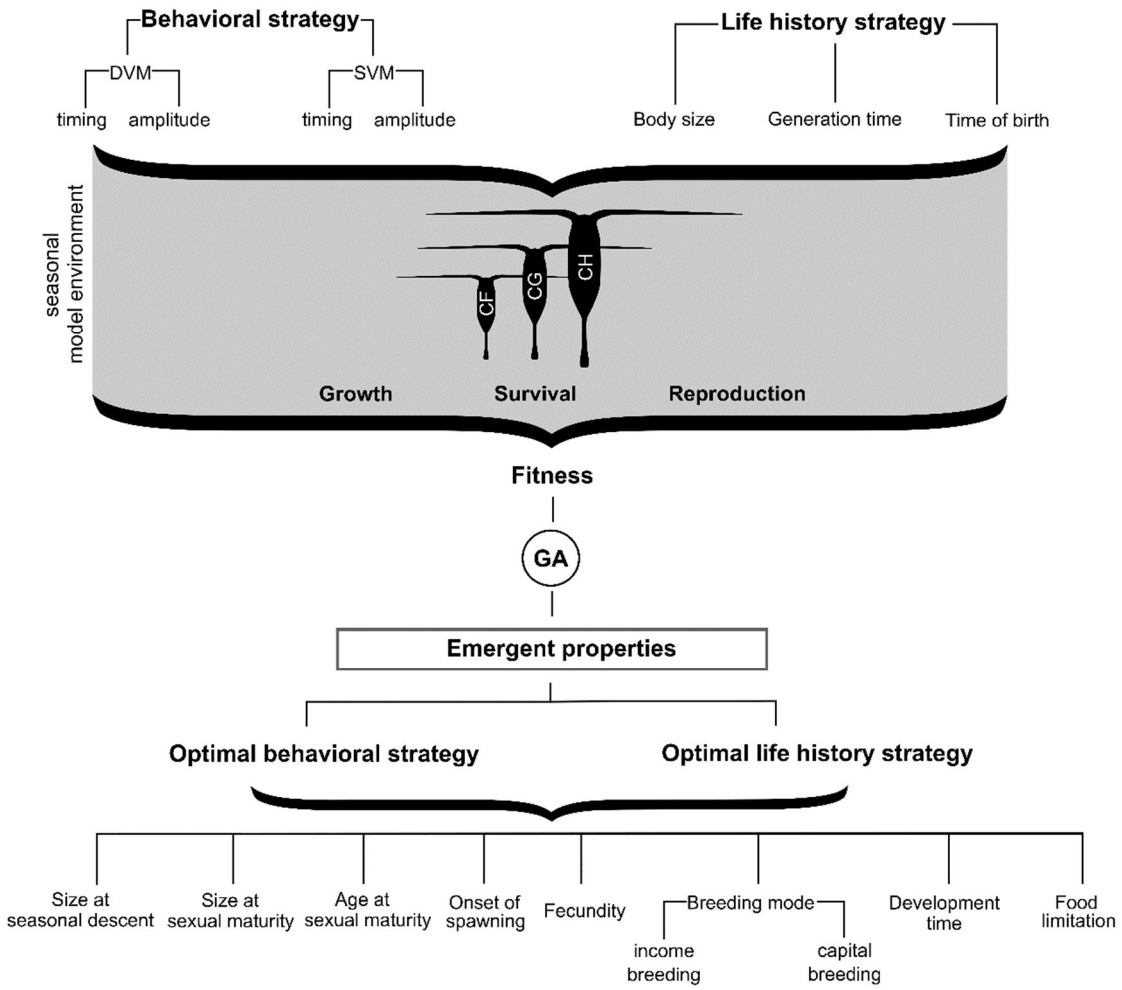

937 **Fig. 2** The model overview. The behavioral strategy (vertical strategy) and some key
938 aspects of the life history strategy are defined by seven evolvable free parameters (cf.
939 Table 2). These are hardwired to model copepods of three different species representing
940 *C. finmarchicus*, *C. glacialis* and *C. hyperboreus*. For a given model environment, a
941 Genetic Algorithm heuristically finds the optimal combination for these parameters
942 through a fitness function of growth, survival and reproduction, and predicts the
943 environment- and species-specific optimal behavioral and life history strategies.

944

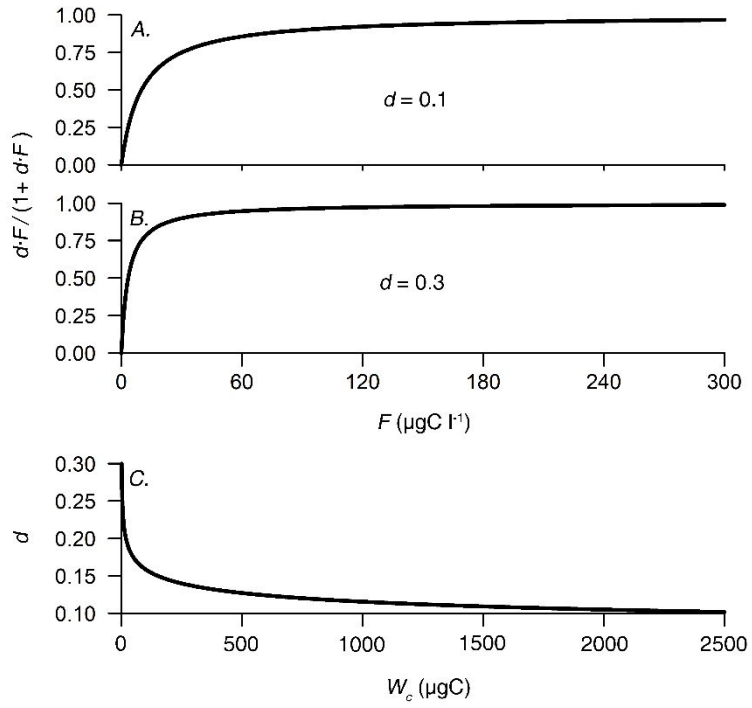

945 **Fig. 3** (A–B) The shape of the Holling's type-II (disk) function (Eq. 4) at the higher (0.3)
946 and lower (0.1) ends of parameter *d*, which describes the dependency of ingestion rate
947 on the ambient food concentration. (C) The power function (Eq. 5) through which
948 parameter *d* relates with the structural mass (W_c). In panels A and B, the y-intercept of
949 the horizontal asymptote is ca. 75 µgC l^{-1} for d = 0.3 and 125 µgC l^{-1} for d = 0.1. This is
950 the satiation food concentration, above which ingestion rate becomes solely
951 temperature-dependent (Eq. 3).

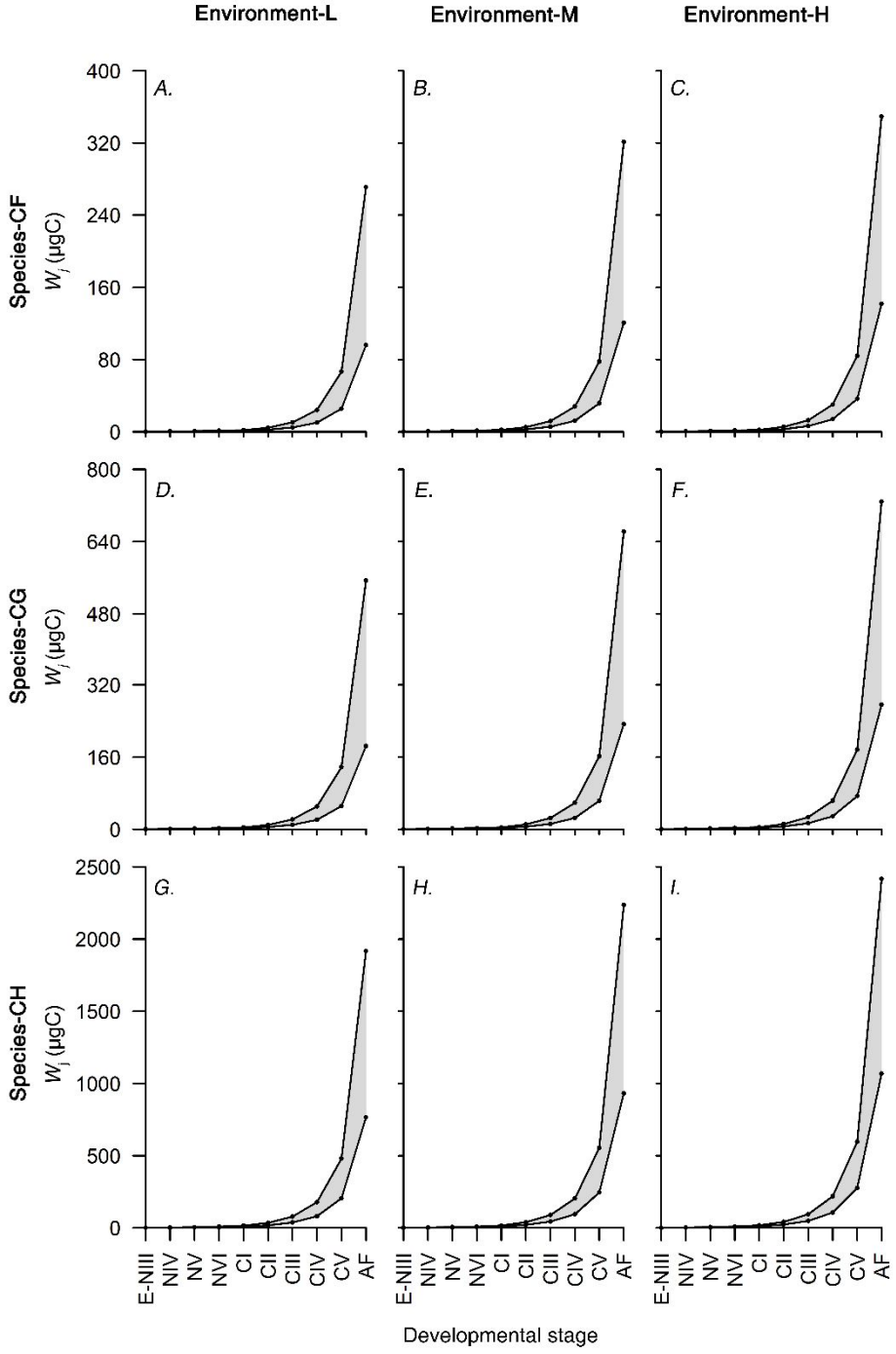

952 **Fig. 4** The species-specific maximum (W_j^{max}: upper line and points in each panel) and
953 minimum (W_j^{min}: lower line and points in each panel) critical molting masses estimated
954 for each model environment. Based on the value of the evolvable body size parameter
955 (α), stage-specific critical molting masses for a given copepod occupies a fixed fraction
956 between the minima and maxima, i.e. within the shaded area. See Appendix A2 for
957 tabulated values.

958

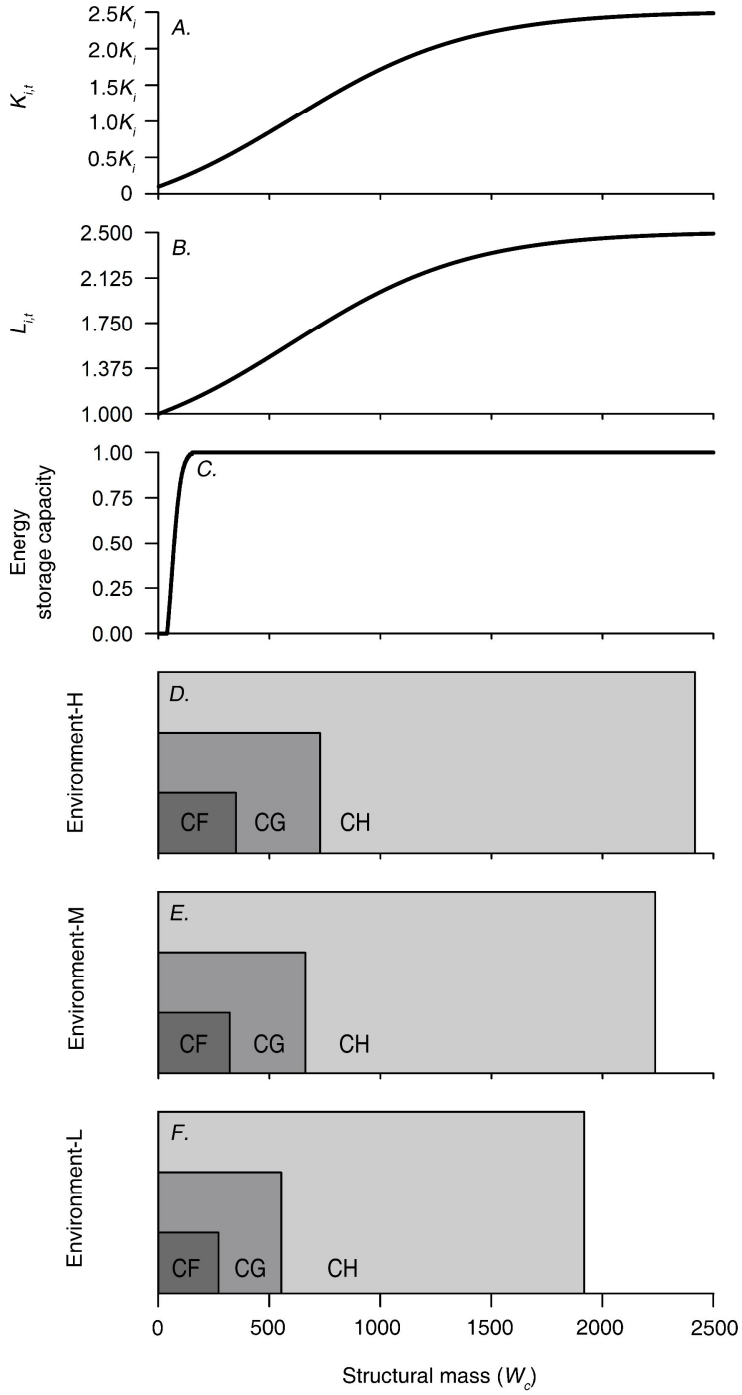

959 **Fig. 5** Size-dependent relationships of (A) visual predation risk scalar *K*, (B) irradiance
960 sensitivity parameter *L*, and (C) the energy storage capacity (Eq. 13). Panels D–F provide
961 a rough reference to how these size-specific patterns can influence species-specific
962 processes in different model environments. Vertical axes of D–F have no dimensions,
963 but the height of the boxes is to show the overlap of inter-specific size ranges.

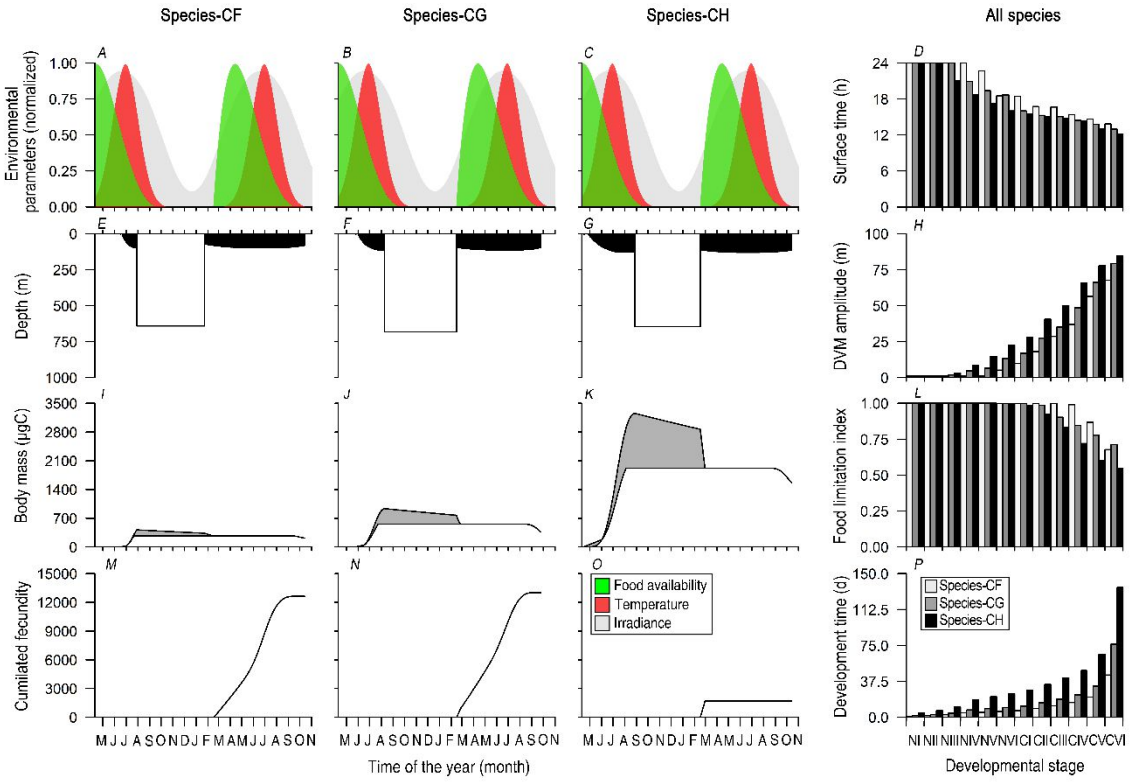

964 **Fig. 6** Some behavioral and life history traits/attributes of the three model-species
965 traced in the basic run at Environment-L (A–C). To the left are predicted lifetime
966 variability of the vertical trajectories (E–G), structural and energetic reserve masses (I–
967 K) and fecundity (M–O). To the right are stage-specific attributes (D, H, L and P). Shaded
968 regions of panels I–K represent the mass of energy reserve.

969

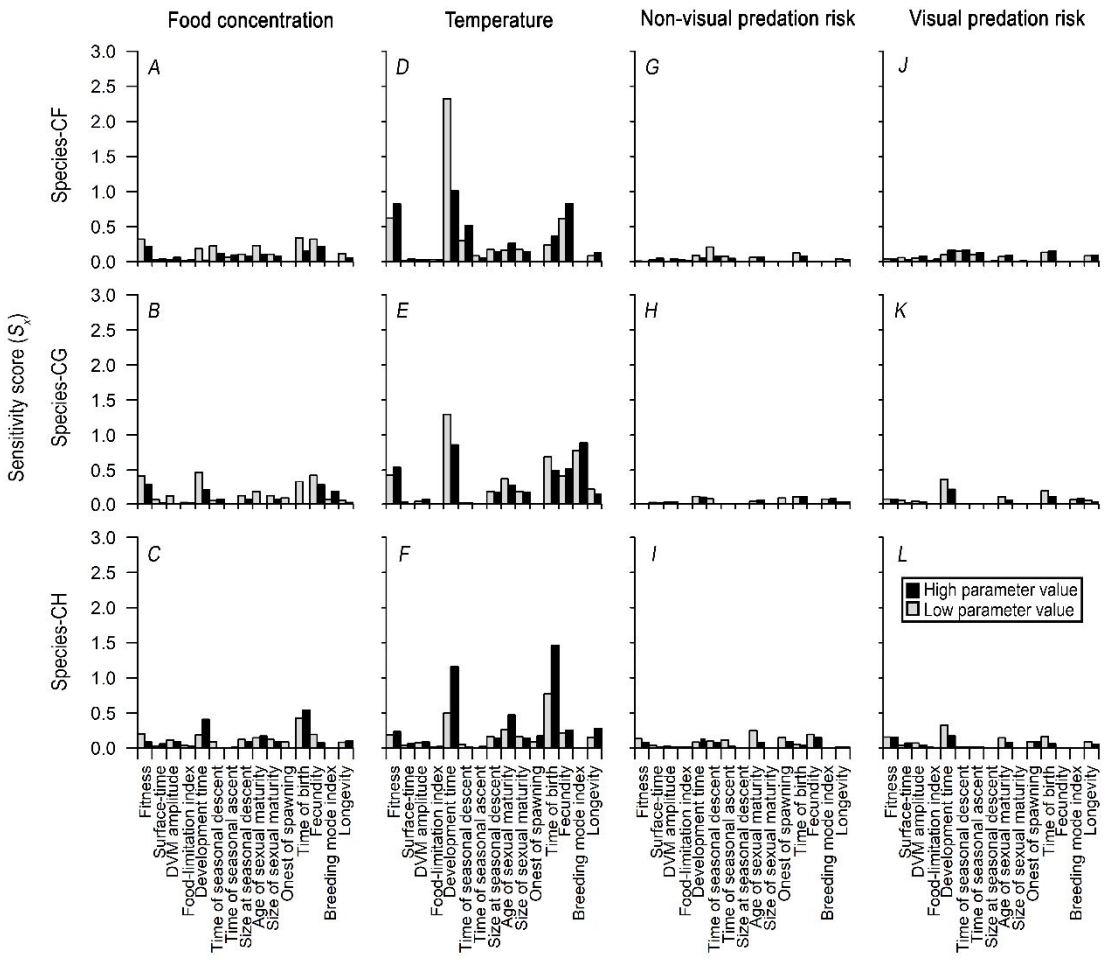

970 **Fig. 7** Graphical summary of the sensitivity analysis. Plotted as bars are absolute
971 sensitivity scores, the height of which indicating the degree of sensitivity. Further details
972 are provided in Table 6.

973

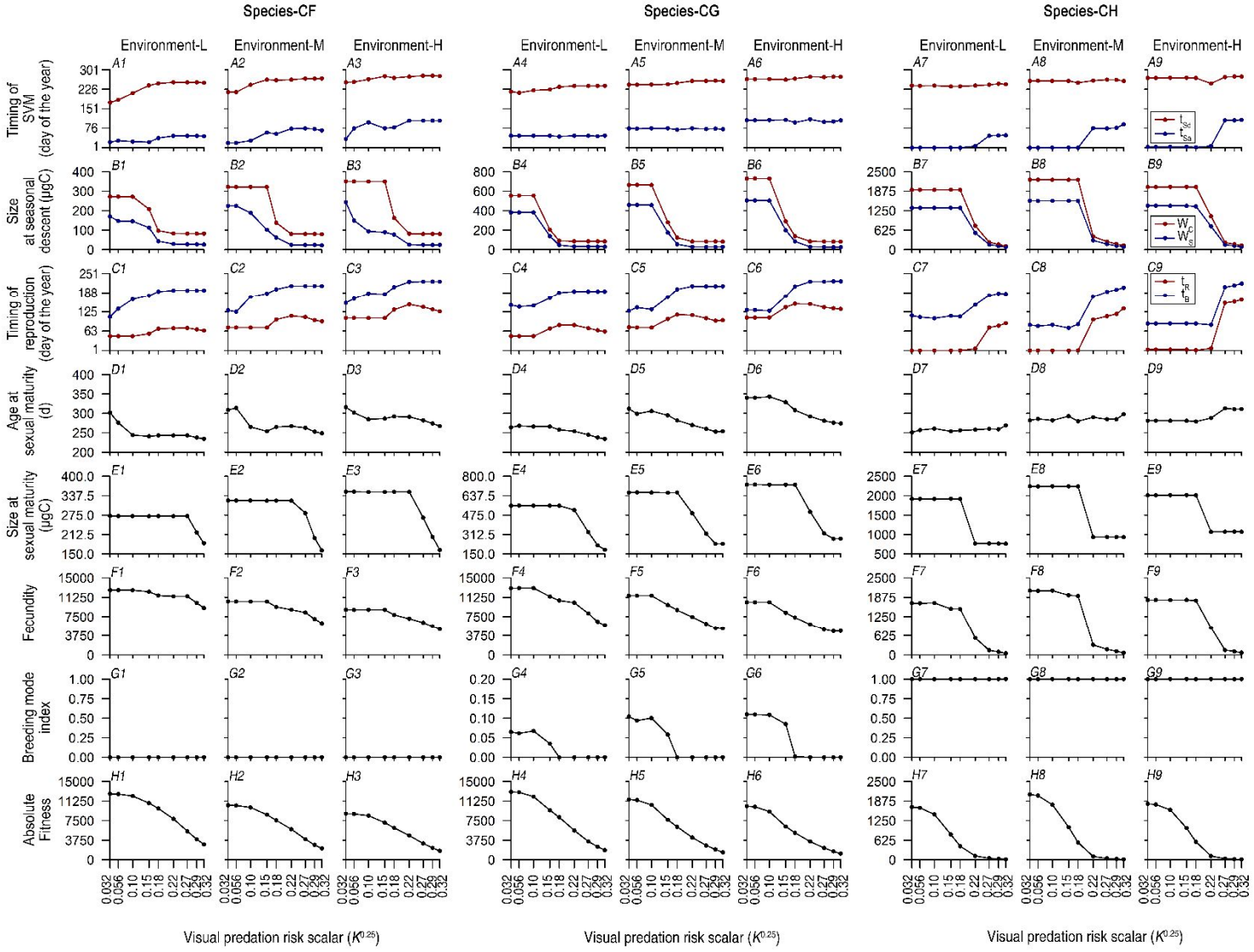
Species-CF
Species-CG
Species-CH
Environment-L
Environment-M
Environment-H
Timing of SVM (day of the year)
Size at seasonal descent (μgC)
Timing of reproduction (day of the year)
Age at sexual maturity (d)
Size at sexual maturity (μgC)
Fecundity
Breeding mode index
Absolute Fitness
Visual predation risk scalar ($K^{0.25}$)

974 **Fig. 8** Predicted variability of species-specific life history traits along the modelled latitudinal gradient under variable levels of visual
975 predation risk. t_{sd}: time of seasonal descent, t_{sa}: time of seasonal ascent, W_c: structural mass, W_s: mass of energy reserve, t_B: optimal birth
976 time, t_R: time of first reproduction

977

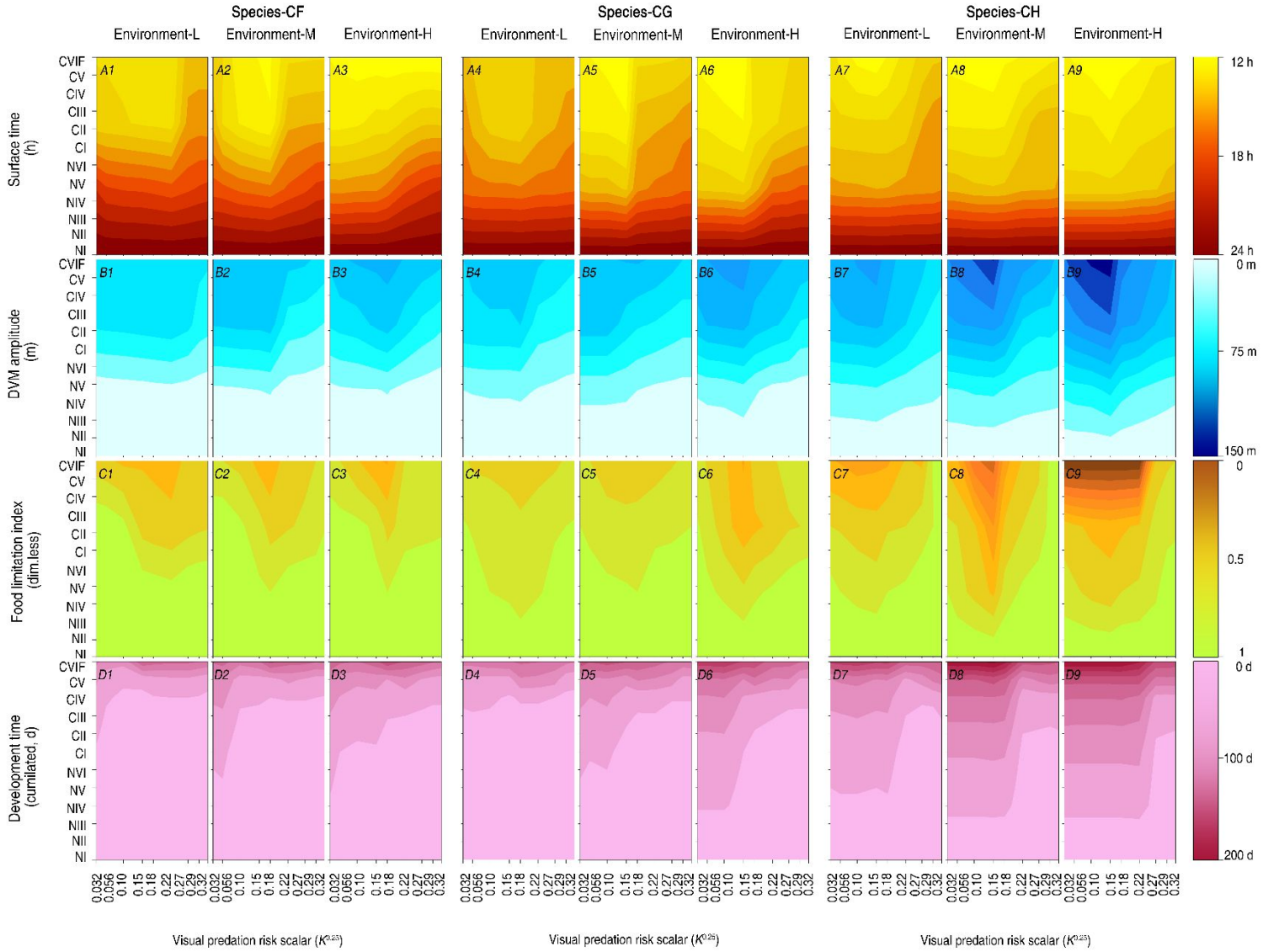
Species-CF
Species-CG
Species-CH
Environment-L
Environment-M
Environment-H
Surface time (h)
DVM amplitude (m)
Food limitation index (dim.less)
Development time (cumulated, d)
CVIF
CV
CIV
CIII
CII
CI
NVI
NV
NIV
NIII
NII
NI
A1
A2
A3
A4
A5
A6
A7
A8
A9
B1
B2
B3
B4
B5
B6
B7
B8
B9
C1
C2
C3
C4
C5
C6
C7
C8
C9
D1
D2
D3
D4
D5
D6
D7
D8
D9
12 h
18 h
24 h
0 m
75 m
150 m
0
0.5
1
0 d
100 d
200 d
0.032
0.056
0.10
0.15
0.18
0.22
0.27
0.29
0.32
Visual predation risk scalar ($K^{0.25}$)

978 **Fig. 9** Predicted stage-specific variability of (A1–A9) surface time, (B1–B9) DVM amplitude, (C1–C9) food limitation index and (D1–D9) the
979 development times (excluding overwintering duration) of each model-species along the modelled latitudinal gradient at variable levels of
980 visual predation risk. See table 3 for descriptions of the above variables.

981

982 **Literature Cited**

983 Aksnes DL, Giske J (1993) A theoretical model of aquatic visual feeding. Ecological
984 Modelling 67:233-250

985 Aksnes DL, Magnesen T (1983) Distribution, development, and production of *Calanus*
986 *finmarchicus* (Gunnerus) in Lindåspollene, western Norway, 1979. Sarsia 68:195-
987 207

988 Aljetlawi AA, Sparrevik E, Leonardsson K (2004) Prey – predator size - dependent
989 functional response: derivation and rescaling to the real world. Journal of Animal
990 Ecology 73:239-252

991 Andersen V, Nival P (1991) A model of the diel vertical migration of zooplankton based
992 on euphausiids. Journal of Marine Research 49:153-175

993 Arnkværn G, Daase M, Eiane K (2005) Dynamics of coexisting *Calanus finmarchicus*,
994 *Calanus glacialis* and *Calanus hyperboreus* populations in a high-Arctic fjord.
995 Polar Biology 28:528-538

996 Astthorsson OS, Gislason A (2003) Seasonal variations in abundance, development and
997 vertical distribution of *Calanus finmarchicus*, *C. hyperboreus* and *C. glacialis* in
998 the East Icelandic Current. Journal of Plankton Research 25:843-854

999 Bagøien E, Melle W, Kaartvedt S (2012) Seasonal development of mixed layer depths,
1000 nutrients, chlorophyll and *Calanus finmarchicus* in the Norwegian Sea – A basin-
1001 scale habitat comparison. Progress in Oceanography 103:58-79

1002 Båmstedt U, Eilertsen HC, Tande KS, Slagstad D, Skjoldal HR (1991) Copepod grazing and
1003 its potential impact on the phytoplankton development in the Barents Sea. Polar
1004 Research 10:339-354

1005 Bandara K (2014) Mesozooplankton community dynamics in a high arctic fjord. Nord
1006 University

1007 Bandara K, Varpe Ø, Ji R, Eiane K (2018) A high-resolution modeling study on diel and
1008 seasonal vertical migrations of high-latitude copepods. Ecological Modelling
1009 368C:357-376

1010 Bandara K, Varpe Ø, Søreide JE, Wallenschus J, Berge J, Eiane K (2016) Seasonal vertical
1011 strategies in a high-Arctic coastal zooplankton community. Marine Ecology
1012 Progress Series 555:49-64

1013 Barta Z (2016) Behavioural change over the annual cycle: optimal annual routines.
1014 Current Opinion in Behavioral Sciences 12:138-141

1015 Båtnes AS, Miljeteig C, Berge J, Greenacre M, Johnsen GH (2015) Quantifying the light
1016 sensitivity of *Calanus* spp. during the polar night: potential for orchestrated

migrations conducted by ambient light from the sun, moon, or aurora borealis? Polar Biology 38:51-65

Baum JK, Worm B (2009) Cascading top-down effects of changing oceanic predator abundances. Journal of Animal Ecology 78:699-714

Beaugrand G, Reid PC, Ibanez F, Lindley JA, Edwards M (2002) Reorganization of North Atlantic marine copepod biodiversity and climate. Science 296:1692-1694

Berge J, Gabrielsen TM, Moline MA, Renaud PE (2012) Evolution of the Arctic *Calanus* complex: an Arctic marine avocado? Journal of Plankton Research 34:191-195

Błachowiak-Samołyk K, Wiktor JM, Hegseth EN, Wold A, Falk-Petersen S, Kubiszyn AM (2015) Winter Tales: the dark side of planktonic life. Polar Biology 38:23-36

Blackburn TM, Gaston KJ, Loder N (1999) Geographic gradients in body size: a clarification of Bergmann's rule. Diversity and distributions 5:165-174

Brierley AS (2014) Diel vertical migration. Current Biology 24:R1074-R1076

Brooks JL, Dodson SI (1965) Predation, body size, and composition of plankton. Science 150:28-35

Brown JH, Gillooly JF, Allen AP, Savage VM, West GB (2004) Toward a metabolic theory of ecology. Ecology 85:1771-1789

Campbell RG, Ashjian CJ, Sherr EB, Sherr BF and others (2016) Mesozooplankton grazing during spring sea-ice conditions in the eastern Bering Sea. Deep Sea Research Part II: Topical Studies in Oceanography 134:157-172

Campbell RG, Wagner MM, Teegarden GJ, Boudreau CA, Durbin EG (2001) Growth and development rates of the copepod *Calanus finmarchicus* reared in the laboratory. Marine Ecology Progress Series 221:161-183

Carlisle DB, Pitman WJ (1961) Diapause, neurosecretion and hormones in Copepoda. Nature 190:827-828

Carlotti F, Wolf KU (1998) A Lagrangian ensemble model of *Calanus finmarchicus* coupled with a 1D ecosystem model. Fisheries Oceanography 7:191-204

Chust G, Castellani C, Licandro P, Ibaibarriaga L, Sagarminaga Y, Irigoien X (2014) Are *Calanus* spp. shifting poleward in the North Atlantic? A habitat modelling approach. ICES Journal of Marine Science 71:241-253

Cohen J, Berge J, Moline MA, Sørensen AJ and others (2015) Is ambient light during the high Arctic polar night sufficient to act as a visual cue for zooplankton? PloS one 10:e0126247

Confer JL, Howick GL, Corzette MH, Kramer SL, Fitzgibbon S, Landesberg R (1978) Visual Predation by Planktivores. Oikos 31:27-37

1052 Conover DO (1992) Seasonality and the scheduling of life history at different latitudes.
1053 Journal of Fish Biology 41:161-178

1054 Conover RJ (1965) Notes on the molting cycle, development of sexual characters and sex
1055 ratio in *Calanus hyperboreus*. Crustaceana 8:308-320

1056 Conover RJ (1967) Reproductive Cycle, Early Development, and Fecundity in Laboratory
1057 Populations of the Copepod *Calanus Hyperboreus*. Crustaceana 13:61-72

1058 Conover RJ (1988) Comparative life histories in the genera *Calanus* and *Neocalanus* in
1059 high latitudes of the northern hemisphere. In: Biology of Copepods. Springer, p
1060 127-142

1061 Conover RJ, Siferd TD (1993) Dark-Season Survival Strategies of Coastal Zone
1062 Zooplankton in the Canadian Arctic. Arctic 46:303-311

1063 Corkett CJ, McLaren IA, Sevigny JM (1986) The rearing of the marine calanoid copepods
1064 *Calanus finmarchicus* (Gunnerus), *C. glacialis* Jaschnov and *C. hyperboreus*
1065 Krøyer with comment on the equiproportional rule. Syllogeus 58:539-546

1066 Cottier FR, Nilsen F, Skogseth R, Tverberg V, Skarðhamar J, Svendsen H (2010) Arctic
1067 fjords: a review of the oceanographic environment and dominant physical
1068 processes. Geological Society, London, Special Publications 344:35-50

1069 Daase M, Eiane K (2007) Mesozooplankton distribution in northern Svalbard waters in
1070 relation to hydrography. Polar Biology 30:969-981

1071 Daase M, Falk-Petersen S, Varpe Ø, Darnis G and others (2013) Timing of reproductive
1072 events in the marine copepod *Calanus glacialis*: a pan-Arctic perspective.
1073 Canadian journal of fisheries and aquatic sciences 70:871-884

1074 Daase M, Varpe Ø, Falk-Petersen S (2014) Non-consumptive mortality in copepods:
1075 occurrence of *Calanus* spp. carcasses in the Arctic Ocean during winter. Journal
1076 of Plankton Research 36:129-144

1077 Davis L (1989) Adapting operator probabilities in genetic algorithms Proceedings of the
1078 third international conference on Genetic algorithms. Morgan Kaufmann
1079 Publishers Inc., George Mason University, USA, p 61-69

1080 Dawson JK (1978) Vertical distribution of *Calanus hyperboreus* in the central Arctic
1081 Ocean. Limnology and Oceanography 23:950-957

1082 De Robertis A (2002) Size‐dependent visual predation risk and the timing of vertical
1083 migration: An optimization model. Limnology and Oceanography 47:925-933

1084 Deep K, Thakur M (2007) A new crossover operator for real coded genetic algorithms.
1085 Applied Mathematics and Computation 188:895-911

Devries DR, Stein RA, Bremigan MT (1998) Prey selection by larval fishes as influenced by available zooplankton and gape limitation. Transactions of the American Fisheries Society 127:1040-1050

Diel S, Tande KS (1992) Does the spawning of *Calanus finmarchicus* in high latitudes follow a reproducible pattern? Marine Biology 113:21-31

Eddelbuettel D, François R, Allaire J, Chambers J, Bates D, Ushey K (2011) Rcpp: Seamless R and C++ integration. Journal of Statistical Software 40:1-18

Eiane K, Ohman MD (2004) Stage-specific mortality of *Calanus finmarchicus*, *Pseudocalanus elongatus* and *Oithona similis* on Fladen Ground, North Sea, during a spring bloom. Marine Ecology Progress Series 268:183-193

Eiane K, Parisi D (2001) Towards a robust concept for modelling zooplankton migration. Sarsia 86:465-475

Eiane K, Tande KS (2009) Meso and Macrozooplankton. In: Sakshaug E, Johnsen GH, Kovacs KM (eds) Ecosystem Barents Sea. Tapir Academic Press, Trondheim, Norway, p 209-234

Eiben AE, Smith JE (2003) Introduction to evolutionary computing. Springer, Berlin, Germany

Ejsmond MJ, Varpe Ø, Czarnoleski M, Kozłowski J (2015) Seasonality in offspring value and trade-offs with growth explain capital breeding. The American Naturalist 186:E111-E125

Escribano R, Hidalgo P, Valdés V, Frederick L (2014) Temperature effects on development and reproduction of copepods in the Humboldt Current: the advantage of rapid growth. Journal of Plankton Research 36:104-116

Espinasse M, Halsband C, Varpe Ø, Gislason A, Gudmundsson K, Falk-Petersen S, Eiane K (2017) The role of local and regional environmental factors for *Calanus finmarchicus* and *C. hyperboreus* abundances in the Nordic Seas. Polar Biology 40:2363–2380

Fabian D, Flatt T (2012) Life history evolution. Nature Education Knowledge 3:10-24

Falk-Petersen S, Mayzaud P, Kattner G, Sargent JR (2009) Lipids and life strategy of Arctic *Calanus*. Marine Biology Research 5:18-39

Falk-Petersen S, Pavlov V, Berge J, Cottier FR, Kovacs KM, Lydersen C (2015) At the rainbow's end: high productivity fueled by winter upwelling along an Arctic shelf. Polar Biology 38:5-11

Falk-Petersen S, Pavlov V, Timofeev S, Sargent JR (2007) Climate variability and possible effects on arctic food chains: the role of *Calanus*. In: Ørbæk JB, KallenbornIngunn

R, Tombre I, Hegseth EN, Falk-Petersen S, Hoel AH (eds) Arctic alpine ecosystems and people in a changing environment. Springer, Berlin, Germany, p 147-166

Falk-Petersen S, Pedersen G, Kwasniewski S, Hegseth EN, Hop H (1999) Spatial distribution and life-cycle timing of zooplankton in the marginal ice zone of the Barents Sea during the summer melt season in 1995. Journal of Plankton Research 21:1249-1264

Fields DM, Yen J (1997) The escape behavior of marine copepods in response to a quantifiable fluid mechanical disturbance. Journal of Plankton Research 19:1289-1304

Fiksen Ø (2000) The adaptive timing of diapause–a search for evolutionarily robust strategies in *Calanus finmarchicus*. ICES Journal of Marine Science 57:1825-1833

Fiksen Ø, Carlotti F (1998) A model of optimal life history and diel vertical migration in *Calanus finmarchicus*. Sarsia 83:129-147

Fiksen Ø, Giske J (1995) Vertical distribution and population dynamics of copepods by dynamic optimization. ICES Journal of Marine Science 52:483-503

Fish CJ (1936) The biology of *Calanus finmarchicus* in the Gulf of Maine and Bay of Fundy. The Biological Bulletin 70:118-141

Fleminger A, Hulsemann K (1977) Geographical range and taxonomic divergence in North Atlantic *Calanus* (*C. helgolandicus*, *C. finmarchicus* and *C. glacialis*). Marine Biology 40:233-248

Gabrielsen TM, Merkel B, Søreide JE, Johansson-Karlsson E and others (2012) Potential misidentifications of two climate indicator species of the marine arctic ecosystem: *Calanus glacialis* and *C. finmarchicus*. Polar Biology 35:1621-1628

Gillooly JF (2000) Effect of body size and temperature on generation time in zooplankton. Journal of Plankton Research 22:241-251

Gillooly JF, Charnov EL, West GB, Savage VM, Brown JH (2002) Effects of size and temperature on developmental time. Nature 417:70-73

Gislason A, Astthorsson OS (1996) Seasonal development of *Calanus finmarchicus* along an inshore-offshore gradient southwest of Iceland. Ophelia 44:71-84

Goldberg DE, Deb K (1991) A Comparative Analysis of Selection Schemes Used in Genetic Algorithms. In: Rawlins GJE (ed) Foundations of Genetic Algorithms. Elsevier, p 69-93

Grimm V, Berger U, Bastiansen F, Eliassen S and others (2006) A standard protocol for describing individual-based and agent-based models. Ecological Modelling 198:115-126

1156 Grimm V, Berger U, DeAngelis DL, Polhill JG, Giske J, Railsback SF (2010) The ODD
1157 protocol: a review and first update. Ecological Modelling 221:2760-2768

1158 Grote U, Pasternak A, Arashkevich E, Halvorsen E, Nikishina A (2015) Thermal response
1159 of ingestion and egestion rates in the Arctic copepod *Calanus glacialis* and
1160 possible metabolic consequences in a warming ocean. Polar Biology 38:1025-
1161 1033

1162 Hagen W (1999) Reproductive strategies and energetic adaptations of polar
1163 zooplankton. Invertebrate Reproduction & Development 36:25-34

1164 Hagen W, Auel H (2001) Seasonal adaptations and the role of lipids in oceanic
1165 zooplankton. Zoology 104:313-326

1166 Hall DJ, Threlkeld ST, Burns CW, Crowley PH (1976) The size-efficiency hypothesis and
1167 the size structure of zooplankton communities. Annual Review of Ecology and
1168 Systematics 7:177-208

1169 Hardy AC, Gunther ER (1935) The plankton of the South Georgia whaling grounds and
1170 adjacent waters, 1926-1927. Discovery Reports 11:1-456

1171 Harik GR, Lobo FG, Goldberg DE (1997) The compact genetic algorithm. Urbana
1172 51:61801

1173 Hays GC (1995) Ontogenetic and seasonal variation in the diel vertical migration of the
1174 copepods *Metridia lucens* and *Metridia longa*. Limnology and Oceanography
1175 40:1461-1465

1176 Hays GC (2003) A review of the adaptive significance and ecosystem consequences of
1177 zooplankton diel vertical migrations. In: Jones MB, Ingólfsson A, Ólafsson E,
1178 Helgason GV, Gunnarsson K, Svavarsson J (eds) Migrations and Dispersal of
1179 Marine Organisms Developments in hydrobiology. Springer, Dordrecht, The
1180 Netherlands, p 163-170

1181 Hays GC, Richardson AJ, Robinson C (2005) Climate change and marine plankton. Trends
1182 in ecology & evolution 20:337-344

1183 Herrera F, Lozano M, Verdegay JL (1998) Tackling real-coded genetic algorithms:
1184 Operators and tools for behavioural analysis. Artificial Intelligence Review
1185 12:265-319

1186 Hirche H-J (1990) Egg production of *Calanus finmarchicus* at low temperature. Marine
1187 Biology 106:53-58

1188 Hirche H-J (1991) Distribution of dominant calanoid copepod species in the Greenland
1189 Sea during late fall. Polar Biology 11:351-362

1190 Hirche H-J (1996a) Diapause in the marine copepod, *Calanus finmarchicus*—a review.
1191 Ophelia 44:129-143

Hirche H-J (1996b) The reproductive biology of the marine copepod, *Calanus finmarchicus*—a review. Ophelia 44:111-128

Hirche H-J (1997) Life cycle of the copepod *Calanus hyperboreus* in the Greenland Sea. Marine Biology 128:607-618

Hirche H-J (2013) Long-term experiments on lifespan, reproductive activity and timing of reproduction in the Arctic copepod *Calanus hyperboreus*. Marine Biology 160:2469-2481

Hirche H-J, Bohrer RN (1987) Reproduction of the Arctic copepod *Calanus glacialis* in Fram Strait. Marine Biology 94:11-17

Hirche H-J, Hagen W, Mumm N, Richter C (1994) The Northeast Water Polynya, Greenland Sea. Polar Biology 14:491-503

Hirche H-J, Kosobokova KN (2003) Early reproduction and development of dominant calanoid copepods in the sea ice zone of the Barents Sea—need for a change of paradigms? Marine Biology 143:769-781

Hirche H-J, Kosobokova KN (2007) Distribution of *Calanus finmarchicus* in the northern North Atlantic and Arctic Ocean—expatriation and potential colonization. Deep Sea Research Part II: Topical Studies in Oceanography 54:2729-2747

Hirche H-J, Kosobokova KN (2011) Winter studies on zooplankton in Arctic seas: the Storfjord (Svalbard) and adjacent ice-covered Barents Sea. Marine Biology 158:2359

Hirche H-J, Kwasniewski S (1997) Distribution, reproduction and development of *Calanus* species in the Northeast Water in relation to environmental conditions. Journal of Marine Systems 10:299-317

Hirche H-J, Niehoff B (1996) Reproduction of the Arctic copepod *Calanus hyperboreus* in the Greenland Sea-field and laboratory observations. Polar Biology 16:209-219

Holland JH (1975) Adaptation in natural and artificial systems. An introductory analysis with application to biology, control, and artificial intelligence. Ann Arbor, MI: University of Michigan Press, Michigan, USA

Holling CS (1959) Some Characteristics of Simple Types of Predation and Parasitism. The Canadian Entomologist 91:385-398

Hopkins CCE, Tande KS, Grønvik S, Sargent JR (1984) Ecological investigations of the zooplankton community of balsfjorden, Northern Norway: An analysis of growth and overwintering tactics in relation to niche and environment in *Metridia longa* (Lubbock), *Calanus finmarchicus* (Gunnerus), *Thysanoessa inermis* (Krøyer) and *T. raschi* (M. Sars). Journal of Experimental Marine Biology and Ecology 82:77-99

Houston AI, McNamara JM, John MCH (1993) General Results concerning the Trade-Off between Gaining Energy and Avoiding Predation. Philosophical Transactions: Biological Sciences 341:375-397

Hunter MD, Price PW (1992) Playing chutes and ladders: heterogeneity and the relative roles of bottom‐up and top‐down forces in natural communities. Ecology 73:724-732

Huntley ME, Boyd C (1984) Food-Limited Growth of Marine Zooplankton. The American Naturalist 124:455-478

Huntley ME, Brooks ER (1982) Effects of age and food availability on diel vertical migration of *Calanus pacificus*. Marine Biology 71:23-31

Huntley ME, Lopez MDG (1992) Temperature-dependent production of marine copepods: a global synthesis. The American Naturalist 140:201-242

Irigoien X (2004) Some ideas about the role of lipids in the life cycle of *Calanus finmarchicus*. Journal of Plankton Research 26:259-263

Jaschnov WA (1972) On the systematic status of *Calanus glacialis*, *Calanus finmarchicus* and *Calanus helgolandicus*. Crustaceana 22:279-284

Jeppesen E, Jensen JP, Søndergaard M, Fenger‐Grøn M and others (2004) Impact of fish predation on cladoceran body weight distribution and zooplankton grazing in lakes during winter. Freshwater Biology 49:432-447

Ji R (2011) *Calanus finmarchicus* diapause initiation: new view from traditional life history-based model. Marine Ecology Progress Series 440:105-114

Ji R, Ashjian CJ, Campbell RG, Chen C and others (2012) Life history and biogeography of Calanus copepods in the Arctic Ocean: an individual-based modeling study. Progress in Oceanography 96:40-56

Jónasdóttir SH (1999) Lipid content of *Calanus finmarchicus* during overwintering in the Faroe–Shetland Channel. Fisheries Oceanography 8:61-72

Jönsson KI (1997) Capital and income breeding as alternative tactics of resource use in reproduction. Oikos:57-66

Jørgensen SE, Bendoricchio G (2001) Fundamentals of ecological modelling. Elsevier Science Ltd., Oxford, UK

Kaartvedt S (1996) Habitat preference during overwintering and timing of seasonal vertical migration of *Calanus finmarchicus*. Ophelia 44:145-156

Kaartvedt S (2000) Life history of *Calanus finmarchicus* in the Norwegian Sea in relation to planktivorous fish. ICES Journal of Marine Science 57:1819-1824

Kane MJ, Emerson JW, Weston S (2013) Scalable Strategies for Computing with Massive Data. Journal of Statitical Software 55:1-19

Kerfoot WB (1970) Bioenergetics of Vertical Migration. The American Naturalist 104:529-546

Kiørboe T (2011) What makes pelagic copepods so successful? Journal of Plankton Research 33:677-685

Lampert W (1989) The Adaptive Significance of Diel Vertical Migration of Zooplankton. Functional Ecology 3:21-27

Lee H-W, Ban S, Ikeda T, Matsuishi T (2003) Effect of temperature on development, growth and reproduction in the marine copepod *Pseudocalanus newmani* at satiating food condition. Journal of Plankton Research 25:261-271

Lee RF, Hagen W, Kattner G (2006) Lipid storage in marine zooplankton. Marine Ecology Progress Series 307:273-306

Lie U (1965) Quantities of zooplankton and propagation of *Calanus finmarchicus* at permanent stations on the Norwegian coast and at Spitsbergen, 1959 1962. Fiskeridirektoratets skrifter, Serie Havundersøkelser 13:5-19

Loose CJ, Dawidowicz P (1994) Trade‐offs in diel vertical migration by zooplankton: the costs of predator avoidance. Ecology 75:2255-2263

Lucasius CB, Kateman G (1989) Application of genetic algorithms in chemometrics Proceedings of the third international conference on Genetic algorithms. Morgan Kaufmann Publishers Inc., p 170-176

Madsen SJ, Nielsen TG, Hansen BW (2001) Annual population development and production by *Calanus finmarchicus*, *C. glacialis* and *C. hyperboreus* in Disko Bay, western Greenland. Marine Biology 139:75-93

Madsen SJ, Nielsen TG, Tervo OM, Söderkvist J (2008) Importance of feeding for egg production in *Calanus finmarchicus* and *C. glacialis* during the Arctic spring. Marine Ecology Progress Series 353:177-190

Mann KH, Lazier JRN (2006) Dynamics of Marine Ecosystems: Biological-Physical Interactions in the Oceans. Blackwell Publishing, Oxford, United Kingdom

Maps F, Pershing AJ, Record NR (2011) A generalized approach for simulating growth and development in diverse marine copepod species. ICES journal of marine science 69:370-379

Maps F, Plourde S, Zakardjian B (2010) Control of dormancy by lipid metabolism in *Calanus finmarchicus*: a population model test. Marine Ecology Progress Series 403:165-180

Maps F, Record NR, Pershing AJ (2013) A metabolic approach to dormancy in pelagic copepods helps explaining inter-and intra-specific variability in life-history strategies. Journal of Plankton Research 36:18-30

Marshall SM, Orr AP (1972) The biology of a marine copepod: *Calanus finmarchicus* (Gunnerus). Springer Science & Business Media, Berlin, Germany

Matthews JBL, Hestad L, Bakke JLW (1978) Ecological-studies in korsfjorden, western norway-generations and stocks of *Calanus hyperboreus* and *Calanus finmarchicus* in 1971-1974. Oceanologica acta 1:277-284

Mauchline J (1998) The biology of calanoid copepods. Academic Press, San Diego, California, USA

McLaren IA (1966) Adaptive significance of large size and long life of the chaetognath *Sagitta elegans* in the arctic. Ecology 47:852-855

McLaren IA, Head EJH, Sameoto DD (2001) Life cycles and seasonal distributions of *Calanus finmarchicus* on the central Scotian Shelf. Canadian Journal of Fisheries and Aquatic Sciences 58:659-670

Melle W, Skjoldal HR (1998) Reproduction and development of *Calanus finmarchicus*, *C. glacialis* and *C. hyperboreus* in the Barents Sea. Marine Ecology Progress Series 169:211-228

Miller BL, Goldberg DE (1995) Genetic algorithms, tournament selection, and the effects of noise. Complex systems 9:193-212

Miller CB, Crain JA, Morgan CA (2000) Oil storage variability in *Calanus finmarchicus*. ICES Journal of Marine Science 57:1786-1799

Niehoff B, Madsen SJ, Hansen B, Nielsen TG (2002) Reproductive cycles of three dominant *Calanus species* in Disko Bay, West Greenland. Marine Biology 140:567-576

Ohman MD (1988) Behavioral Responses of Zooplankton to Predation. Bulletin of Marine Science 43:530-550

Parent GJ, Plourde S, Turgeon J (2011) Overlapping size ranges of *Calanus* spp. off the Canadian Arctic and Atlantic Coasts: impact on species' abundances. Journal of Plankton Research 33:1654-1665

Pastorok RA (1981) Prey vulnerability and size selection by *Chaoborus* larvae. Ecology 62:1311-1324

Pepin P, Head EJH (2009) Seasonal and depth-dependent variations in the size and lipid contents of stage 5 copepodites of *Calanus finmarchicus* in the waters of the Newfoundland Shelf and the Labrador Sea. Deep Sea Research Part I: Oceanographic Research Papers 56:989-1002

Plourde S, Runge JA (1993) Reproduction of the planktonic copepod *Calanus finmarchicus* in the Lower St. Lawrence Estuary: relation to the cycle of phytoplankton production and evidence for a *Calanus* pump. Marine Ecology Progress Series:217-227

Power ME (1992) Top‐down and bottom‐up forces in food webs: do plants have primacy. Ecology 73:733-746

Pütter A (1920) Studies on physiological similarity VI. growth similarities (*in German*). Pflüger's Archiv für die Gesamte Physiologie des Menschen und der Tiere 180:298-340

R Core Team (2016) R: A Language and Environment for Statistical Computing 3.3.1 https://www.R-project.org/

Rardin RL, Uzsoy R (2001) Experimental evaluation of heuristic optimization algorithms: A tutorial. Journal of Heuristics 7:261-304

Record NR, Pershing AJ, Runge JA, Mayo C, Monger BC, Chen C (2010) Improving ecological forecasts of copepod community dynamics using genetic algorithms. Journal of Marine Systems 82:96-110

Renaud PE, Berge J, Varpe Ø, Lønne OJ, Nahrgang J, Ottesen C, Hallanger I (2012) Is the poleward expansion by Atlantic cod and haddock threatening native polar cod, *Boreogadus saida*? Polar Biology 35:401-412

Richardson K, Jónasdóttir SH, Hay SJ, Christoffersen A (1999) *Calanus finmarchicus* egg production and food availability in the Faroe–Shetland Channel and northern North Sea: October–March. Fisheries Oceanography 8:153-162

Robertson A (1968) Continuous plankton recorder: a method for studying the biomass of calanoid copepods. Bulletins of marine ecology VI:185–223

Robledo L, Soler A (2000) Luminous efficacy of global solar radiation for clear skies. Energy Conversion and Management 41:1769-1779

Roff D (1980) Optimizing development time in a seasonal environment: The 'ups and downs' of clinal variation. Oecologia 45:202-208

Rohde K (1992) Latitudinal gradients in species diversity: the search for the primary cause. Oikos 65:514-527

RStudio Team (2016) RStudio: Integrated Development Environment for R 1.0.136 http://www.rstudio.com/

Runge JA, Ingram RG (1991) Under-ice feeding and diel migration by the planktonic copepods *Calanus glacialis* and *Pseudocalanus minutus* in relation to the ice algal production cycle in southeastern Hudson Bay, Canada. Marine Biology 108:217-225

Sainmont J, Andersen KH, Varpe Ø, Visser AW (2014) Capital versus income breeding in a seasonal environment. The American Naturalist 184:466-476

Sakshaug E, Johnsen GH, Kristiansen S, von Quillfeldt C, Rey F, Slagstad D, Thingstad F (2009) Phytoplankton and Primary Production. In: Sakshaug E, Johnsen GH, Kovacs KM (eds) Ecosystem Barents Sea. Tapir Academic Press, Trondheim, Norway, p 167-209

Scott CL, Kwasniewski S, Falk-Petersen S, Sargent JR (2000) Lipids and life strategies of *Calanus finmarchicus*, *Calanus glacialis* and *Calanus hyperboreus* in late autumn, Kongsfjorden, Svalbard. Polar Biology 23:510-516

Smith SL (1990) Egg production and feeding by copepods prior to the spring bloom of phytoplankton in Fram Strait, Greenland Sea. Marine Biology 106:59-69

Søreide JE, Falk-Petersen S, Hegseth EN, Hop H, Carroll ML, Hobson KA, Błachowiak-Samołyk K (2008) Seasonal feeding strategies of *Calanus* in the high-Arctic Svalbard region. Deep Sea Research Part II: Topical Studies in Oceanography 55:2225-2244

Søreide JE, Leu E, Berge J, Graeve M, Falk-Petersen S (2010) Timing of blooms, algal food quality and *Calanus glacialis* reproduction and growth in a changing Arctic. Global Change Biology 16:3154-3163

Stearns SC (1989) Trade-Offs in Life-History Evolution. Functional Ecology 3:259-268

Strand E, Huse G, Giske J (2002) Artificial evolution of life history and behavior. The American Naturalist 159:624-644

Swift JH (1986) The Arctic Waters. In: Hurdle BG (ed) The Nordic Seas. Springer, New York, USA, p 129-154

Szulkin M, Dawidowicz P, Dodson SI (2006) Behavioural uniformity as a response to cues of predation risk. Animal Behaviour 71:1013-1019

Tande KS, Hassel A, Slagstad D (1985) Gonad maturation and possible life cycle strategies in *Calanus finmarchicus* (Gunnerus) and *C. glacialis* (Jaschnov) in the northwestern part of the Barents Sea. In: Christiensen ME (ed) Marine biology of polar regions and effects of stress on marine organisms. Wiley, Chichester, UK, p 141-155

Tande KS, Hopkins CCE (1981) Ecological investigations of the zooplankton community of Balsfjorden, northern Norway: the genital system in *Calanus finmarchicus* and the role of gonad development in overwintering strategy. Marine Biology 63:159-164

Tarling GA, Burrows M, Matthews J, Saborowski R, Buchholz F, Bedo A, Mayzaud P (2000) An optimisation model of the diel vertical migration of northern krill

(*Meganyctiphanes norvegica*) in the Clyde Sea and the Kattegat. Canadian Journal of Fisheries and Aquatic Sciences 57:38-50

Threlkeld ST (1976) Starvation and the size structure of zooplankton communities. Freshwater Biology 6:489-496

Toivanen J, Makinen RE, Périaux J, Cloud Cedex F (1999) Multidisciplinary shape optimization in aerodynamics and electromagnetics using genetic algorithms. International Journal of Numerical Methods in Fluids 30:149-159

Unstad KH, Tande KS (1991) Depth distribution of *Calanus finmarchicus* and *C. glacialis* in relation to environmental conditions in the Barents Sea. Polar Research 10:409-420

Varpe Ø (2012) Fitness and phenology: annual routines and zooplankton adaptations to seasonal cycles. Journal of Plankton Research 34:267-276

Varpe Ø (2017) Life History Adaptations to Seasonality. Integrative and Comparative Biology 57:943–960

Varpe Ø, Fiksen Ø (2010) Seasonal plankton–fish interactions: light regime, prey phenology, and herring foraging. Ecology 91:311-318

Varpe Ø, Fiksen Ø, Slotte A (2005) Meta-ecosystems and biological energy transport from ocean to coast: the ecological importance of herring migration. Oecologia 146:443

Varpe Ø, Jørgensen C, Tarling GA, Fiksen Ø (2007) Early is better: seasonal egg fitness and timing of reproduction in a zooplankton life‐history model. Oikos 116:1331-1342

Varpe Ø, Jørgensen C, Tarling GA, Fiksen Ø (2009) The adaptive value of energy storage and capital breeding in seasonal environments. Oikos 118:363-370

Visser AW, Jónasdóttir SH (1999) Lipids, buoyancy and the seasonal vertical migration of *Calanus finmarchicus*. Fisheries Oceanography 8:100-106

Vogedes D, Varpe Ø, Søreide JE, Graeve M, Berge J, Falk-Petersen S (2010) Lipid sac area as a proxy for individual lipid content of arctic calanoid copepods. Journal of Plankton Research 32:1471-1477

Von Bertalanffy L (1938) A quantitative theory of organic growth (inquiries on growth laws. II). Human Biology 10:181-213

Wells L (1970) Effects of alewife predation on zooplankton populations in Lake Michigan. Limnology and Oceanography 15:556-565

Werner EE (1974) The fish size, prey size, handling time relation in several sunfishes and some implications. Journal of the Fisheries Board of Canada 31:1531-1536

1439 Williams CM, Ragland GJ, Betini G, Buckley LB and others (2017) Understanding
1440 evolutionary impacts of seasonality: an introduction to the symposium.
1441 Integrative and Comparative Biology 57:921-933

1442 Zanakis SH, Evans JR (1981) Heuristic “optimization”: Why, when, and how to use it.
1443 Interfaces 11:84-91

1444 Zaret TM, Kerfoot WC (1975) Fish Predation on *Bosmina longirostris*: Body-Size Selection
1445 Versus Visibility Selection. Ecology 56:232-237

1446

APPENDIX

Artificial evolution of behavioral and life history strategies of Arctic *Calanus* spp. in response to bottom-up and top-down selection pressures

Kanchana Bandara[*1,2], Øystein Varpe[2,3], Rubao Ji[4], Ketil Eiane[1]

[1]Faculty of Biosciences and Aquaculture, Nord University, 8049, Bodø, Norway

[2]The University Centre in Svalbard, 9171, Longyearbyen, Norway

[3]Akvaplan-niva, Fram Centre, 9296, Tromsø, Norway

[4]Woods Hole Oceanographic Institution, Redfield 2-14, Woods Hole, Massachusetts 02543, USA

[*] corresponding author: kanchana.bandara@nord.no

A1: Summary environmental parameters of the model environments

The modeled irradiance was estimated following the global clear-sky horizontal irradiance model of Robledo and Soler (2000). A comprehensive account of the irradiance submodel is provided in Bandara et al. (2018). Estimated irradiance over the modeled environments roughly agree with the field estimates. Field estimates of temperature were adopted from Swift (1986), Ingvaldsen and Loeng (2009), Daase and Eiane (2007), Daase et al. (2013), Bandara (2014), Bandara et al. (2016). Further, temperature and Chlorophyll-a biomass data collected during the UNIS AB820 (2012-2016) cruise from Van Mijenfjorden, Isfjorden, Billefjorden, Kongsfjorden, and offshore stations around 78–81°N were used via Paul E. Renaud (course coordinator 2016). Year-round field data (temperature and Chlorophyll-a biomass observations) from Lofoten and Vesterålen regions were also obtained from mooring data via Boris Espinasse (http://love.arctosresearch.net). Finally, temperature data from southern and southeastern Norwegian fjords (60–70°N) were also obtained following communications with Slawek Kwasniweski. These data were considered when deciding the seasonal maxima, minima of temperature and maximum Chlorophyll-a biomass parameterizations.

Table A1: Comparison between model environments. Cf. Fig. 1 in main text

Parameter	Attribute	Env-L	Env-M	Env-H
Irradiance (µmol m^{-2} s^{-1})	Min.	0	0	0
	Max.	1500	1200	800
	Time of Max.	day 172 (June 21)	day 172 (June 21)	day 172 (June 21)
Temperature (°C)	Min.	2	0	-1.5
	Max. (°C)	15	12	10
	Time of Max.	day 181 (July 1)	day 203 (July 21)	day 212 (Aug 1)
Food availability (mg m^{-3} Chl.a)	Min.	0	0	0
	Max.	6	6	6
	Time of Max.	day 105 (April 15)	day 135 (May 15)	day 165 (Jun 15)
	Productive season (duration)	229 d	208 d	180 d

A2: Growth and development submodel

Maps et al. (2011) have formulated a mechanistic model to describe growth and development of several high-latitude calanoid copepod species. Their predictions include *Calanus finmarchicus*, *C. glacialis* and *C. hyperboreus*. At constant food concentration and constant temperatures, this growth model performs well. However, in their model, growth (µg C) emerges as a function of development.

In this model, when temperature and food concentration varies over time, the development times tend to shift. For example, a copepod performing DVM would encounter variable temperature and food concentrations on daily if not hourly basis. This variability of development times causes large amounts of Carbon to be assimilated between the development stage *j* and *j + 1*. We observed that copepods performing DVM attaining unrealistic structural masses as a result (e.g. females with structural masses ca. 4 x 10^4 µg C at -1–10 °C and 0–180 µg C l^{-1}). Due to this limitation, we could not implement Maps et al. (2011) growth model as the growth submodel in our work.

However, given the usefulness of the above model at constant temperature and food concentrations, we used it to parameterize a simple growth model that we formulated (Eqs. 1–8 and 14–15). The temperature and mass coefficients and exponents of our model were estimated from the temperature and mass specific growth predictions (at satiation food concentrations) simulated by Maps et al. (2011)'s model. Predicted development times of the above model and those predicted by ours at constant temperatures and food concentrations are identical. However, at variable temperatures and food concentrations (such experienced by diel migrating copepods) our model produces more meaningful estimates, as development is a function of growth (the concept of critical molting masses, e.g. Fiksen & Giske 1995, Fiksen & Carlotti 1998). The only down side to this is that we had to adopt a new evolvable parameter to describe the body mass trajectory.

The critical molting masses (W_j) were calculated from running the Maps et al. (2011) at minimum and maximum environmental specific temperatures (see Table A1 above) under the minimum and maximum food concentration. Here, the W_j^{max} is given by running the above model at minimum temperature at maximum food concentration. W_j^{min} was extracted in vice versa scenario (Table A2).

Table A2: Minimum and maximum stage-specific critical molting masses (µg C) for each model-species for the three environments. Estimates are derived following the method described above. These are presented in Fig. 4 in the main text. Egg to NIII mass was assumed to remain constant during the development.

	Species-CF						Species-CG						Species-CH					
	Env.-L		Env.-M		Env.-H		Env.-L		Env.-M		Env.-H		Env.-L		Env.-M		Env.-H	
	W_j^{min}	W_j^{max}	W_j^{min}	W_j^{max}	W_j^{min}	W_j^{max}	W_j^{min}	W_j^{max}	W_j^{min}	W_j^{max}	W_j^{min}	W_j^{max}	W_j^{min}	W_j^{max}	W_j^{min}	W_j^{max}	W_j^{min}	W_j^{max}
E-NIII	0.23	0.23	0.23	0.23	0.23	0.23	0.40	0.40	0.40	0.40	0.40	0.40	0.56	0.56	0.56	0.56	0.56	0.56
NIV	0.44	0.59	0.47	0.62	0.49	0.63	0.90	1.15	0.95	1.21	0.98	1.23	1.94	2.70	2.07	2.86	2.17	2.96
NV	0.61	0.91	0.66	0.97	0.70	1.01	1.31	1.87	1.42	1.98	1.49	2.04	3.36	5.20	3.68	5.63	3.89	5.86
NVI	0.80	1.31	0.89	1.43	0.95	1.49	1.83	2.80	2.01	3.00	2.14	3.11	5.30	8.85	5.89	9.70	6.31	10.17
CI	1.08	1.94	1.23	2.15	1.34	2.26	2.62	4.30	2.92	4.65	3.14	4.87	8.55	15.29	9.62	16.95	10.42	17.90
CII	2.31	4.61	2.66	5.20	2.94	5.51	5.18	9.99	5.97	11.10	6.58	11.77	17.98	35.19	20.72	39.55	22.79	42.09
CIII	4.78	10.49	5.62	12.00	6.35	12.82	10.27	22.37	12.09	25.35	13.66	27.21	37.44	78.37	43.85	88.99	48.54	95.13
CIV	10.18	24.27	12.27	28.10	13.96	30.20	21.11	51.05	25.50	58.91	29.26	63.77	80.48	178.08	95.12	204.15	106.75	219.04
CV	25.68	66.59	31.63	77.94	36.58	84.36	51.54	138.08	63.56	162.21	74.01	177.05	204.98	480.14	244.94	554.96	277.95	597.47
Adult	96.16	271.08	120.91	321.26	141.84	349.34	184.57	553.57	233.59	662.52	276.49	728.69	766.22	1917.90	932.82	2237.50	1068.91	2416.83

Cited Literature

Bandara K (2014) Mesozooplankton community dynamics in a high arctic fjord. Nord University

Bandara K, Varpe Ø, Ji R, Eiane K (2018) A high-resolution modeling study on diel and seasonal vertical migrations of high-latitude copepods. Ecological Modelling 368C:357-376

Bandara K, Varpe Ø, Søreide JE, Wallenschus J, Berge J, Eiane K (2016) Seasonal vertical strategies in a high-Arctic coastal zooplankton community. Marine Ecology Progress Series 555:49-64

Daase M, Eiane K (2007) Mesozooplankton distribution in northern Svalbard waters in relation to hydrography. Polar Biology 30:969-981

Daase M, Falk-Petersen S, Varpe Ø, Darnis G and others (2013) Timing of reproductive events in the marine copepod *Calanus glacialis*: a pan-Arctic perspective. Canadian journal of fisheries and aquatic sciences 70:871-884

Fiksen Ø, Carlotti F (1998) A model of optimal life history and diel vertical migration in *Calanus finmarchicus*. Sarsia 83:129-147

Fiksen Ø, Giske J (1995) Vertical distribution and population dynamics of copepods by dynamic optimization. ICES J Mar Sci 52:483-503

Ingvaldsen R, Loeng H (2009) Physical Oceanography. In: Sakshaug E, Johnsen GH, Kovacs K (eds) Ecosystem Barents Sea. Tapir Academic Press, Trondheim, Norway, p 33-64

Maps F, Pershing AJ, Record NR (2011) A generalized approach for simulating growth and development in diverse marine copepod species. ICES journal of marine science 69:370-379

Robledo L, Soler A (2000) Luminous efficacy of global solar radiation for clear skies. Energy Conversion and Management 41:1769-1779

Swift JH (1986) The Arctic Waters. In: Hurdle BG (ed) The Nordic Seas. Springer, New York, USA, p 129-154